Dissertation

Renormalization group analysis of order parameter fluctuations in fermionic superfluids

Benjamin Obert

Max-Planck-Institut für Festkörperforschung
Stuttgart 2014

Renormalization group analysis of order parameter fluctuations in fermionic superfluids

Von der Fakultät Mathematik und Physik der Universität Stuttgart
zur Erlangung der Würde eines Doktors der Naturwissenschaften
(Dr. rer. nat.) genehmigte Abhandlung

Vorgelegt von

Benjamin Obert

aus Bad Saulgau

Hauptberichter:	Prof. Dr. Walter Metzner
Mitberichter:	Prof. Dr. Alejandro Muramatsu

Tag der mündlichen Prüfung: 10.02.2014

Max-Planck-Institut für Festkörperforschung
Stuttgart 2014

For my family

Abstract

In this work fluctuation effects in two interacting fermion systems exhibiting fermionic s-wave superfluidity are analyzed with a modern renormalization group method. A description in terms of a fermion-boson theory allows an investigation of order parameter fluctuations already on the one-loop level. In the first project a quantum phase transition between a semimetal and a s-wave superfluid in a Dirac cone model is studied. The interplay between fermions and quantum critical fluctuations close to and at the quantum critical point at zero and finite temperatures are studied within a coupled fermion-boson theory. At the quantum critical point non-Fermi liquid and non-Gaussian behaviour emerge. Close to criticality several quantities as the susceptibility show a power law behaviour with critical exponents. We find an infinite correlation length in the entire semimetallic ground state also away from the quantum critical point. In the second project, the ground state of an s-wave fermionic superfluid is investigated. Here, the mutual interplay between fermions and order parameter fluctuations is studied, especially the impact of massless Goldstone fluctuations, which occur due to spontaneous breaking of the continuous U(1)-symmetry. Fermionic gap and bosonic order parameter are distinguished. Furthermore, the bosonic order parameter is decomposed in transverse and longitudinal fluctuations. The mixing between transverse and longitudinal fluctuations is included in our description. Within a simple truncation of the fermion-boson RG flow, we describe the fermion-boson theory for the first time in a consistent manner. Several singularities appear due the Goldstone fluctuations, which partially cancel due to symmetry. Our RG flow captures the correct infrared asymptotics of the system, where the collective excitations act as an interacting Bose gas. Lowest order Ward identities and the massless Goldstone mode are fulfilled in our truncation.

Contents

CHAPTER 1

Introduction

1.1 Introduction and overview

The importance of fluctuations in correlated fermion systems is well-known. Fluctuation effects lead to deviations compared to the standard mean-field picture. In particular, massless fluctuations have a drastic impact on the behaviour of the system. In quantum critical systems massless critical fluctuations lead to a breakdown of the Fermi-liquid theory accompanied by the appearance of anomalous critical exponents and the emergence of universality. In charge-neutral superfluid systems spontaneous symmetry breaking of the continuous charge symmetry occurs and massless Goldstone excitations emerge. There, the order parameter fluctuations, especially the massless Goldstone fluctuations, affect strongly the behaviour of the system, and lead to different results compared to the mean-field theory. To cope with these fascinating physical systems, a plethora of many-body techniques has been developed during the decades in condensed matter research, to tackle the many body-problem of interacting Fermi systems. Among other methods, renormalization group (RG) techniques have been established as valuable tools to analyze divergencies often caused by massless fluctuations in various physical contexts, ranging from high-energy physics down to low-temperature condensed matter physics.

In this thesis fluctuation effects in two different interacting fermion systems exhibiting s-wave superfluidity are analyzed with a modern renormalization group method. The first project deals with a quantum phase transition between a semimetal and a superfluid in

a Dirac cone model. Quantum critical fluctuations close to and at the quantum critical point. The mutual interplay between fermions and critical fluctuations is analyzed with a coupled fermion-boson functional renormalization group approach. Non-Fermi liquid and non-Gaussian behaviour emerge. Several quantities, as the correlation length and the susceptibility, show a power law behaviour close to the quantum critical point. We will also find an unusual behaviour of the correlation length in the semimetallic ground state. In the second project, the ground state of a s-wave fermionic superfluid is investigated. The interplay of fermions and order parameter fluctuation will be analyzed, especially the spectacular impact of massless Goldstone fluctuations. Here, for the first time a truncation for the fermion-boson theory is employed that captures the correct infrared asymptotics of the system. The collective excitations behave as an interacting Bose gas. Lowest order Ward identities are fulfilled and the linearly dispersing Goldstone mode is preserved within the truncation. In both projects the RG flow of fermions and bosonic fluctuations is analyzed by the coupled fermion-boson functional renormalization group approach, which captures order parameter fluctuations properly already on the one-loop level. In the rest of the introduction, we give a brief overview over the functional RG method, followed by an introduction of both research projects.

The functional renormalization group is a further development of the early Wilson renormalization group theory originally applied to critical phenomena. For his achievement, Wilson was honoured with the Nobel prize in 1982. It is an ideal tool to analyze systems where perturbation theory is plagued with divergences. The RG method treats different energy scales not in one shot but scale after scale. This is implemented by reducing a cutoff during the RG flow in a controlled way. A pedagogical introduction to the Wilson RG with applications to fermionic systems can be found in Shankar (1991, 1994) and Polchinski (1993). In early days in condensed matter physics, fermionic systems were only analyzed in one dimension with renormalization group concepts. The renormalization group method was applied mainly to purely bosonic theories to describe phase transitions and critical phenomena in $O(N)$-models. Then, new formulations of renormalization group ideas in terms of the functional flow equations were developed. First steps towards the functional RG were undertaken by Polchinski (1984), who laid a foundation for simple renormalizability proofs for the ϕ^4-theory. Then, Wieczerkowski (1988) developed the Wick-ordered scheme, which proved to be appropriate for mathematical estimates, and Wetterich (1993) suggested a formulation of the flow equation in the form of a one-particle-irreducible (1PI) scheme, which turned out to be the most convenient for practical calculations.

The heart of the formulation in the 1PI formalism is a flow equation for the regu-

larized effective action. The regulator introduces a cutoff scale, which is sent to zero in the infrared limit. The functional RG then smoothly connects the microscopic action in the ultraviolet limit with the full effective action in the infrared limit, which contains the entire thermodynamics and correlation functions. The first applications of the functional renormalization group to correlated Fermi systems were stability analyzes of the two dimensional Hubbard model, pioneered by Zanchi and Schulz (1998, 2000), Halboth and Metzner (2000) and Honerkamp et al. (2001a). By the introduction of an infinitesimal symmetry breaking field in the bare microscopic action, Salmhofer et al. (2004) paved the way towards symmetry-breaking in the purely fermionic functional RG approach. They employed a truncation scheme for the flow, suggested by Katanin (2004), which yields an exact description of symmetry breaking for mean-field models. Over the years, especially the attractive Hubbard model served as a prototype model to analyze the functional RG flow in the context of spontaneous symmetry-breaking. For instance, Gersch et al. (2008) analyzed the model within the so-called N-patch scheme. Here, three fermionic momenta are discretized in the Brillouin zone. Recently, this work was extended by Eberlein and Metzner (2013). They employed a channel-decomposition of the Nambu vertex and calculated the RG flow of its singular dependencies. In that work, the singular dependencies of the vertex were expressed in terms of two fermionic and one bosonic-like momenta. A more detailed historical overview on the (functional) renormalization group in fermionic systems and a broad range of applications can be found in the comprehensive review by Metzner et al. (2012).

The functional renormalization group for coupled fermion-boson theories was developed only later. Baier et al. (2004) calculated for the first time a coupled fermion-boson functional RG flow to analyze antiferromagnetism in the two-dimensional repulsive Hubbard model. Friederich et al. (2011) improved this work, by decoupling the Hubbard interaction not only in a single but in three different channels, and computed a phase diagram. Other studies focused on the analysis of the ground state of a fermionic superfluid, where the particle-particle channel is the most dominant one (Birse et al. (2005), Krippa (2007), Diehl et al. (2007), Strack et al. (2008), Kopietz et al. (2010)). The advantage of the coupled fermion-boson RG approach is its ease to analyze the interplay between fermions and order-parameter fluctuations in rather simple truncations. Only a small number of couplings parametrizing the effective action is necessary to capture the essential physics of the investigated models, thus leading to a reduction of the numerical effort compared to the purely fermionic approach. The impact of order parameter fluctuations is already captured on a one-loop level and their interplay with the fermions can be tracked in a transparent way. Technically, the fermionic two-particle interaction

is decoupled by a Hubbard-Stratonovich transformation and bosonic degrees of freedom are introduced (Popov (1987)). Afterwards, both fermions and bosons are integrated out step by step under renormalization. Thus, order parameter fluctuations are naturally implemented in this approach. In the context of quantum criticality, such coupled fermion-boson theories have also been used to analyze the quantum critical fluctuations in situations where the standard theory for quantum criticality given by the Hertz and Millis paradigm is not applicable (Löhneysen (2007)). Since then, several works appeared investigating a fermion-boson system with the functional RG approach. For instance, Strack et al. (2010) analyzed the impact of quantum critical fluctuations close to a semimetallic-superfluid quantum phase transition in a Dirac cone model. At the quantum critical point non-Fermi liquid and non-Gaussian behaviour emerges. In this thesis, we follow that spirit of the coupled fermion-boson functional RG approach and study the interplay between fermions and bosonic fluctuations in two different systems with attractively interacting fermions. First, we will discuss a project, where we extend the previous work by Strack et al. (2010) and analyze the Dirac cone model, which undergoes a quantum phase transition between a semimetal and a superfluid. Afterwards, we will present the second project, where we analyze the impact of order parameter fluctuations, especially the impact of the massless Goldstone fluctuations on the ground state of an s-wave superfluid. We now motivate both systems and explain our research goals in the rest of this introduction.

Non-Fermi liquid behaviour occurs in several materials. One example is the strange metal behaviour above the superconducting dome in the phase diagram of high-T_c cuprates. There, the resistance shows a linear temperature dependence instead of a quadratic dependence as one would expect from the Landau-Fermi-liquid paradigm. Here, scenarios have been proposed with a hidden quantum critical point under the superconducting dome, where this quantum critical point is expected to induce the strange metal behaviour (Moon and Sachdev (2010)). Another material class is given by the heavy-fermion systems exhibiting a rich phase diagram, where a quantum critical point induces non-Fermi liquid behaviour close to an ordered (magnetic) phase (for reviews, see Si et al. (2010) and Löhneysen et al. (2007)). Hence, quantum criticality is one of the main scenarios to explain non-Fermi liquid behaviour in itinerant electron systems. In general, criticality is accompanied by the phenomenon of universality (Cardy (1996) and Goldenfeld (1992)), where different systems obey the same universal critical behaviour close to the transition. At a continuous phase transition order parameter fluctuations become important, and the correlation length diverges. Thermodynamical quantities show a power-law behaviour with critical exponents, which are related by several scaling laws. As mentioned above, mean-field approaches are no more appropriate at the transition and more sophisticated methods

such as the renormalization group have to be applied for treating the critical behaviour of the transition properly. In contrast to classical critical systems, quantum critical systems have a quantum critical point at zero temperature, where quantum fluctuations dominate. The standard description of quantum criticality in Fermi systems is given by the Hertz-Millis theory (Hertz (1976) and Millis (1993)). Starting from a fermionic microscopic theory, the fermionic interaction is decoupled by a Hubbard-Stratonovich transformation and bosonic fields are introduced. Afterwards the fermions are integrated out and an effective bosonic theory is obtained. Several years ago many systems were found in which this paradigm for quantum criticality fails, since no local bosonic theory can be found, due to gapless fermionic excitations in metals (for reviews see Belitz et al. (2005) and Löhneysen et al. (2007)). Thus, other approaches for such models were investigated, where both fermionic and order parameter fluctuations are treated on the same footing within a coupled fermion-boson theory. First research in that direction was undertaken by Vojta et al. (2000a, 2000b), Belitz et al. (2001a, 2001b) and Abanov et al. (2003), who investigated quantum criticality close to an ordered phase of itinerant magnetism. Since then several models were analyzed with the fermion-boson functional RG method (Gies and Jaeckel (2004), Gies et al. (2009), Strack et al. (2010) and Scherer et al. (2013)).

In 2010, Strack et al. introduced the Dirac cone model as a prototype model for the phase transition between a semimetal and a superfluid. Intensive research on semimetallic systems was triggered by the fabrication of graphene sheets by Novoselov and Geim, which was honoured with the Nobel prize in 2010. The vanishing density of states at only one point lead to peculiar features of this material in contrast to metals or insulators. The purpose of the work by Strack et al. (2010) was to calculate quantum critical properties close to a quantum critical point in a semimetal with one Dirac cone. Here the ordered phase is not an itinerant magnetic phase, but to an s-wave fermionic superfluid phase. Hence, a simple attractive interaction was proposed, which allows the analysis of a quantum critical point between a fermionic superfluid and a semimetal in a simple setup. The Dirac cone model was analyzed in two dimensions at zero temperature in a simple truncation. Due to the massless fermions in the semimetal, a local expansion in the bosonic fields is not possible and a fermion-boson RG was employed. The critical exponent of the susceptibility close to criticality was determined by a numerical solution of the RG flow. The critical exponent for the correlation length was indirectly determined by a putative scaling law. At the critical point anomalous dimensions appeared below three dimensions, signalling non-Fermi liquid and non-Gaussian behaviour. Identical renormalization factors for the momentum and frequency dependence were assumed, implying that the Fermi velocity does not renormalize during the flow. At the quantum

critical point the spectral weight of fermionic quasi-particles disappeared. This result naturally inspires new questions: What is the scaling behaviour of the susceptibility and the correlation length at finite temperatures above the quantum critical point, and how do the momentum and frequency renormalization factors scale in that regime? Can the critical exponent for the correlation length at zero temperature also be extracted from a numerical solution of the RG flow as the critical exponent for the susceptibility? Do the critical exponents fulfill scaling laws? Does the Fermi velocity remain invariant in a refined ansatz for the fermionic self-energy, if different renormalization factors for the frequency and momentum dependence are introduced? This thesis gives answers to all these questions. The results were already published (Obert et al. (2011)).

In our second project, we investigate the ground state of a fermionic superfluid. Superfluidity has a long tradition in condensed matter physics, starting with the discovery of He^4 superfluidity in 1937 by Kapitsa, Allen and Misener. The discovery of fermionic superfluidity in He^3 by Lee, Osheroff and Richardson was honoured with the Nobel prize in 1996. It turned out that in contrast to conventional superconductors, which exhibit an s-wave singlet order parameter and are described by BCS-theory from Bardeen, Cooper and Schrieffer (Nobel prize 1972), the order parameter of He^3 exhibits a p-wave-triplet symmetry (Vollhardt and Wölfle (1990)). The phenomenological Landau liquid theory describes the system properties in the normal state. Nowadays, also other forms of fermionic superfluids, especially s-wave superfluidity, can be realized in ultra-cold atoms in optical lattices (Bloch et al. 2008). Since a few years, experiments with ultra-cold gases allow the simulation of many-body models and the simulation of the BCS-BEC crossover in experiments with fermionic atoms where the interaction strength is tuned by a Feshbach resonance (Bloch et al. (2008)). Systems undergoing that crossover are strongly correlated at the unitary point of the crossover, where fluctuations become particularly important. Hence, the theoretical understanding of fluctuation effects in prototype models for fermionic superfluidity is of high relevance. Continuum models of attractively interacting fermions and lattice models as the attractive Hubbard model serve as prototype models for fermionic superfluidity with s-wave singlet pairing. During the years both kinds of models have been investigated (Griffin et al. (1995)). In contrast to superconductors, charge-neutral superfluids have a linearly dispersing Goldstone mode due to the absence of the Anderson-Higgs mechanism (Nobel prize 2013). Phenomena like the BCS-BEC crossover were analyzed numerically and analytically within these models.

In the framework of the functional RG method several approaches have been applied to analyze the attractive Hubbard model in two dimensions. Both Gersch et al. (2008) and Eberlein and Metzner (2013) studied the fermionic RG flow into the broken-symmetry

phase. Gersch et al. (2008) used the N-patch scheme, while Eberlein and Metzner (2013) applied a channel-decomposition of the vertex. The merit of these approaches lies in its unbiased treatment of the pairing, magnetic and density channel. But to capture the infrared asymptotic behaviour of the longitudinal order parameter fluctuations, terms beyond a fermionic one-loop order are required (Eberlein (2013)). Several groups analyzed fermionic superfluidity in a coupled fermion-boson setup with the functional RG. Birse et al. (2005) pioneered this route by the introduction of a simple truncation for the fermionic superfluid. Some years later, the BCS-BEC crossover was analyzed in the superfluid ground state by Diehl et al. (2007) and Krippa (2007). Flörchinger et al. (2008) additionally considered particle-hole fluctuations in their functional RG study of the BEC-BCS crossover. Another truncation was investigated by Bartosch et al. (2009), who combined the Schwinger-Dyson equations and the functional RG flow with Ward identities, and distinguished between fermionic gap and bosonic order parameter. Strack et al. (2008) also implemented a coupled fermion-boson functional renormalization group flow for the ground state of the fermionic superfluid, where they distinguished also the fermionic gap and bosonic order parameter. As in previous studies they employed a local ansatz for the bosonic potential. However, in contrast to the previous works they decomposed the order parameter fluctuations in a longitudinal and transverse direction. They showed that Goldstone fluctuations lead to a singular behaviour of the longitudinal degrees of freedom of the fermionic superfluid, as an interacting Bose gas (Castellani et al. (1997), Pistolesi et al. (2004)). However, the Goldstone theorem and the linear dispersion of the Goldstone modes had to be implemented by hand. Furthermore, they neglected a linear frequency dependence in the bosonic effective action, which leads to a mixing between transverse and longitudinal bosonic fluctuations. Hence, several questions remained open and inspire fresh research: Is a local ansatz for the bosonic potential justified, as suggested by power counting arguments, or is a non-local bosonic potential necessary for an appropriate description due to symmetry? Are the fermionic single-particle gap and the bosonic order parameter linked by a simple connection? Is it possible to find a simple truncation, where the linearly dispersing massless Goldstone mode is preserved within a coupled fermion-boson theory? How does the mixing between transverse and bosonic fluctuations affect the RG flow? What can be said about the fulfillment of Ward identities within a truncated coupled fermion-boson ansatz? In total, what is a consistent minimal truncation of the fermion-boson functional RG flow to describe the ground state of an s-wave fermion superfluid? This thesis answers these questions. The results were already published (Obert et al. (2013)).

Summing up, this work investigates fluctuation effects in two different interacting

fermion systems with the functional renormalization group in the 1PI-scheme. Quantum critical fluctuations are studied in the Dirac cone model, which is a prototype model for a quantum phase transition between a semimetal and a superfluid. Secondly, the impact of order parameter fluctuations is investigated in the ground state of a fermionic s-wave superfluid, where the attractive Hubbard model serves as a prototype model for the numerical evaluation of the functional RG flow. The effect of order parameter fluctuations is analyzed in both projects within a coupled fermion-boson renormalization group approach.

1.2 Outline

The thesis is structured as follows: Chapter 2 provides the derivation of the flow equation of the fermion-boson functional RG method and its formulation for situations with spontaneous symmetry breaking. In Chapter 3 the functional renormalization group is applied to the Dirac cone model and deals with quantum criticality close to and at the quantum critical point at zero temperature and finite temperatures in two dimensions. In chapter 4 the ground state of an s-wave fermionic superfluid is investigated and the impact of order parameter fluctuations is studied. The last chapter, Chapter 5, concludes the thesis with a summary and an outlook. The appendices present an explicit derivation of the flow equations presented in Chapter 3 and 4, and the derivation of the Ward identities for a coupled fermion-boson system.

CHAPTER 2

Method: Functional renormalization group

Here, we will derive the functional RG equations for a coupled fermion-boson system. The central result of this chapter is the renormalization group equation for the scale-dependent effective action, which connects the bare microscopic action in the ultraviolet limit with the full effective action in the infrared limit. The scale-dependence Λ will be introduced by a regulator term for both fermions and bosons. We will present functional RG equations applicable for the symmetric regime Eq. (2.33) and for the symmetry-broken regime Eq. (2.48).

The chapter is structured as follows: Section 2.1 gives a short overview over the historical developments and introduces the general concept of the method. Afterwards a derivation of the functional renormalization group equations for a mixed boson-fermion theory is presented in section 2.2. Finally, section 2.3 addresses briefly the functional RG equations in the context of spontaneous symmetry breaking.

2.1 Introduction and overview

In this section, we give a short overview over the historical developments and applications of the functional renormalization group method. We follow the review article of Metzner et al. (2012). The functional renormalization group is a further development of Wilson's RG idea (Nobel prize 1982). Polchinski (1984) pointed out the first step towards functional flow equations within the formalism of generating functionals, which was followed by

the Wick ordered RG scheme, see Wieczerkowski (1988) and the one-particle-irreducible (1PI)-scheme, see Wetterich (1993). In this work, we are interested in fermionic models, which we analyze within the 1PI renormalization group scheme.

The heart of the functional renormalization group consists of a flow equation for the scale-dependent effective action, which connects the microscopic action $S[\psi, \bar{\psi}]$ at scales $\Lambda = \infty$ with the full effective action $\Gamma[\psi, \bar{\psi}]$ at low scales $\Lambda = 0$. Thermodynamical information as well as correlation functions can be extracted from the effective action. The scale Λ is introduced through a regulator term, which regularizes low-energy modes of the theory. For instance, these may be single-particle excitations around the Fermi surface in a metallic phase.

The regulator is chosen in such a way that the microscopic action matches the scale-dependent effective action $\Gamma^{\Lambda=\infty} = S$ in the ultraviolet limit. The regularization can be implemented in the form of a multiplicative or an additive regulator, by a smooth or sharp cutoff, and momentum or frequency regularization. The regulator should not explicitly break the symmetry of the underlying model. Also other parameters have been used as cutoffs and flow parameters, for instance temperature, see Honerkamp and Salmhofer (2001b) as well as interaction, see Honerkamp et al. (2004). Due to the complexity of the renormalization group equation, several approximation schemes exist. The effective action is truncated at a certain order by an expansion in fields and gradients, that is governed by power counting arguments and symmetry reasons. Due to such truncations conservation laws such as Ward identities are broken or only fulfilled to a certain order, see Katanin (2004) for a discussion of local Ward identities and Eberlein (2013) for a discussion of global Ward identities. Hence, they are often implemented by hand, see for instance Kopietz et al. (2010) and Strack et al. (2008). In these works the Goldstone theorem in a fermionic superfluid was implemented by hand.

Models of different dimensionalities have been analyzed by the functional RG throughout the years, from transport in a Luttinger liquid in one dimension, over two dimensional systems, for instance the attractive and repulsive Hubbard model, up to three and more dimensional system, as the bosonic $O(N)$ models. A plethora of different physical concepts have also been studied, e.g. systems with competing instabilities, spontaneous symmetry breaking, quantum criticality, quantum wires, quantum dots, and more recently transport in non-equilibrium systems. For a comprehensive review see Metzner et al. (2012).

The purely fermionic functional RG is an unbiased approach, which is ideally suited to cope with competing order instabilities until one or more channels diverge at the critical scale. On the other hand, for the interplay between fermions and order parameter fluctuations a coupled fermion-boson RG approach seems to be more appropriate. A mixed

fermion-boson theory can be obtained from a purely fermionic model by decoupling the fermionic interaction by a Hubbard-Stratonovich transformation in one or several bosonic channels, see Popov (1987) and Altand and Simons (2010). In this thesis we will use a fermion-boson renormalization group approach in the 1PI scheme, where the fermionic interaction is decoupled in the particle-particle channel. For the regulator a sharp Litim momentum cutoff (Dirac cone model) and frequency cutoff (fermionic superfluid) will be applied and a numerical solution of the flow will be presented for two dimensions.

2.2 Derivation of the renormalization group equation

Here, we will derive the functional RG equations for a coupled fermion-boson system. The central result of this chapter is the flow equation for the scale-dependent effective action, which connects the bare microscopic action with the full effective action. The scale-dependence Λ will be included by a regulator term for fermions and bosons. Starting form the partition function with external source fields, we introduce the generating functionals for connected Green's functions and the 1PI vertex functions. Finally, the renormalization group equation for the scale-dependent effective action is derived. An introduction to the functional integral formalism, which we use here, can be found in the textbooks of Negele and Orland (1998) and Zinn-Justin (2002).

The point of departure for our derivation is given by the microscopic action of a coupled fermion-boson system

$$S[\tilde{\psi},\tilde{\phi}] = S_{\tilde{\psi}^2+\tilde{\phi}^2}[\tilde{\psi},\tilde{\phi}] + V[\tilde{\psi},\tilde{\phi}], \tag{2.1}$$

where $\tilde{\phi}_Q$ denotes bosonic (complex-valued) fields and $\tilde{\psi}_K$ fermionic (Grassmann) fields.[1] We will not specify the interaction term $V[\tilde{\psi},\tilde{\phi}]$ here, which typically includes coupling terms between bosons and fermions. The quadratic part in fermionic and bosonic fields of this action reads

$$S_{\tilde{\psi}^2+\tilde{\phi}^2}[\tilde{\psi},\tilde{\phi}] \;=\; \frac{1}{2}\int_{Q,Q'} \tilde{\phi}_Q \mathcal{G}_b^{-1}(Q,Q')\tilde{\phi}_{Q'} + \frac{1}{2}\int_{K,K'} \tilde{\psi}_K \mathcal{G}_f^{-1}(K,K')\tilde{\psi}_{K'}, \tag{2.2}$$

with the shorthand notation for the integrals $\int_{Q,Q'}$ and $\int_{K,K'}$ depending on the details of the system. For instance, the variable $Q = (q_0, \mathbf{q}, c)$ collects bosonic Matsubara fre-

[1] The fields $\tilde{\psi}_K$ and $\tilde{\phi}_Q$ denote microscopic bosonic and fermionic degrees of freedom over which is integrated in the path integral formalism. Later, the fields $\psi_K = \langle\tilde{\psi}_K\rangle$ and $\phi_Q = \langle\tilde{\phi}_Q\rangle$ are introduced as averages over these microscopic fields.

quencies q_0, momenta $\mathbf{q}$ and and an index c. The latter index distinguishes between the bosonic field ϕ and its complex-conjugate partner ϕ^* and we will refer to it as c-index. The variable $K = (k_0, \mathbf{k}, \sigma, \alpha, c)$ collects Matsubara frequencies k_0, momenta $\mathbf{k}$, spins σ, bands α and also a c-index, distinguishing now fermionic fields ψ and their conjugate partners $\bar{\psi}$. For illustration, a possible basis in fermionic and bosonic fields in this notation is given by

$$\psi_K = \left(\psi_{k\uparrow}, \psi_{k\downarrow}, \bar{\psi}_{k\uparrow}, \bar{\psi}_{k\downarrow}\right), \quad \phi_Q = \left(\phi_q, \phi_q^*\right), \tag{2.3}$$

where the variables $q = (q_0, \mathbf{q})$ and $k = (k_0, \mathbf{k})$ include bosonic and fermionic frequencies and momenta, respectively.

The bosonic propagator is symmetric $\mathcal{G}_b^{-1}(Q, Q') = \mathcal{G}_b^{-1}(Q', Q)$, while the fermionic propagator is antisymmetric in its arguments, $\mathcal{G}_f^{-1}(K, K') = -\mathcal{G}_f^{-1}(K', K)$. The second derivative of the bare action with respect to fermionic and bosonic fields yields the bare boson and fermion propagator

$$\frac{\delta^2 S}{\delta\tilde{\phi}_Q \delta\tilde{\phi}_{Q'}} = \mathcal{G}_b^{-1}(Q, Q'), \quad \frac{\delta^2 S}{\delta\tilde{\psi}_K \delta\tilde{\psi}_{K'}} = -\mathcal{G}_f^{-1}(K, K'). \tag{2.4}$$

A scale-dependent regulator of the form

$$\Delta S_\Lambda[\tilde{\psi}, \tilde{\phi}] = \frac{1}{2}\int_{Q,Q'} \tilde{\phi}_Q \mathcal{R}_b^\Lambda(Q, Q')\tilde{\phi}_{Q'} + \frac{1}{2}\int_{K,K'} \tilde{\psi}_K \mathcal{R}_f^\Lambda(K, K')\tilde{\psi}_{K'} \tag{2.5}$$

is added to the microscopic action and regularizes both boson and fermion propagators through the functions $\mathcal{R}_b^\Lambda(Q, Q')$ and $\mathcal{R}_f^\Lambda(K, K')$ at low energies through a cutoff Λ. The partition function with external source field J_Q and η_K for bosons and fermions is defined as

$$Z^\Lambda[\eta, J] = \int \mathcal{D}\tilde{\psi}\mathcal{D}\tilde{\phi} \exp\left(-S[\tilde{\psi}, \tilde{\phi}] - \Delta S_\Lambda[\tilde{\psi}, \tilde{\phi}] + \int_{Q'} J_{Q'}\tilde{\phi}_{Q'} + \int_{K'} \eta_{K'}\tilde{\psi}_{K'}\right), \tag{2.6}$$

where J and η denote external bosonic and fermionic source fields. The functional integral measure $\mathcal{D}\tilde{\psi}$ sums over all fermionic degrees of freedom and $\mathcal{D}\tilde{\phi}$ sums over all bosonic degrees of freedom.

Then, the generating functional for connected correlation functions can be defined as

the logarithm of the partition function with external source fields

$$W_\Lambda[\eta, J] = \ln Z^\Lambda[\eta, J] \tag{2.7}$$

$$= \ln \int \mathcal{D}\tilde{\psi}\mathcal{D}\tilde{\phi} \exp\left(-S[\tilde{\psi}, \tilde{\phi}] - \Delta S_\Lambda[\tilde{\psi}, \tilde{\phi}] + \int_{Q'} J_{Q'}\tilde{\phi}_{Q'} + \int_{K'} \eta_{K'}\tilde{\psi}_{K'}\right). \tag{2.8}$$

By successively applying functional derivatives with respect to the external bosonic J and fermionic η source fields correlations of arbitrary order can be calculated. For instance the expectation values of the bosonic and fermionic field read

$$\phi_Q \equiv \langle\tilde{\phi}_Q\rangle = \frac{\delta W_\Lambda[\eta, J]}{\delta J_Q} \tag{2.9}$$

$$= \frac{1}{Z^\Lambda[\eta, J]} \int \mathcal{D}\tilde{\psi}\mathcal{D}\tilde{\phi}\, \tilde{\phi}_Q \exp\left(-S[\tilde{\psi}, \tilde{\phi}] - \Delta S_\Lambda[\tilde{\psi}, \tilde{\phi}] + \int_{Q'} J_{Q'}\tilde{\phi}_{Q'} + \int_{K'} \eta_{K'}\tilde{\psi}_{K'}\right)$$

and

$$\psi_K \equiv \langle\tilde{\psi}_K\rangle = \frac{\delta W_\Lambda[\eta, J]}{\delta \eta_K} \tag{2.10}$$

$$= \frac{1}{Z^\Lambda[\eta, J]} \int \mathcal{D}\tilde{\psi}\mathcal{D}\tilde{\phi}\, \tilde{\psi}_K \exp\left(-S[\tilde{\psi}, \tilde{\phi}] - \Delta S_\Lambda[\tilde{\psi}, \tilde{\phi}] + \int_{Q'} J_{Q'}\tilde{\phi}_{Q'} + \int_{K'} \eta_{K'}\tilde{\psi}_{K'}\right).$$

A second functional derivative with respect to fermionic and bosonic external source fields leads to the correlation functions

$$G_b(Q, Q') \equiv \frac{\delta^2 W_\Lambda[\eta, J]}{\delta J_Q \delta J_{Q'}} = \langle\tilde{\phi}_Q\tilde{\phi}_{Q'}\rangle - \langle\tilde{\phi}_Q\rangle\langle\tilde{\phi}_{Q'}\rangle, \tag{2.11}$$

$$G_f(K, K') \equiv \frac{\delta^2 W_\Lambda[\eta, J]}{\delta \eta_K \delta \eta_{K'}} = \langle\tilde{\psi}_K\tilde{\psi}_{K'}\rangle - \langle\tilde{\psi}_K\rangle\langle\tilde{\psi}_{K'}\rangle$$

for bosons and fermions in the limit of vanishing source fields η and J. The correlation functions enter the full effective action in the quadratic part. Now we will introduce the scale-dependent regularized effective action as Legendre transformation of the generating functional of the connected Green's function Eq. (2.8)

$$\tilde{\Gamma}^\Lambda[\psi, \phi] = -W_\Lambda[\eta, J] + \int_{Q'} J_{Q'}\phi_{Q'} + \int_{K'} \eta_{K'}\psi_{K'}, \tag{2.12}$$

and also the non-regularized effective action as

$$\Gamma^\Lambda[\psi, \phi] = -W_\Lambda[\eta, J] + \int_{Q'} J_{Q'}\phi_{Q'} + \int_{K'} \eta_{K'}\psi_{K'} - \Delta S_\Lambda[\psi, \phi]. \tag{2.13}$$

where the regulator term in its definition $\Gamma^\Lambda = \tilde{\Gamma}^\Lambda - \Delta S_\Lambda[\psi, \phi]$ is added to the regularized effective action. The effective action is the generating functional for the one-particle-irreducible (1PI) vertex functions. The corresponding direct and inverse Legendre relations are

$$\frac{\delta\tilde{\Gamma}^\Lambda[\psi,\phi]}{\delta\phi_Q} = J_Q, \qquad \frac{\delta\tilde{\Gamma}^\Lambda[\psi,\phi]}{\delta\psi_K} = -\eta_K, \tag{2.14}$$

$$\frac{\delta W_\Lambda[\eta,J]}{\delta J_Q} = \phi_Q, \qquad \frac{\delta W_\Lambda[\eta,J]}{\delta\eta_K} = \psi_K, \tag{2.15}$$

which transform the arguments of the Schwinger functional Eq. (2.8) and the scale-dependent effective action Eq. (2.12) into each other $(\eta, J) \longleftrightarrow (\psi, \phi)$.

Now, we focus on the derivation of the central result of this section: The RG flow equation for the scale-dependent effective action. To this end, we apply a scale derivative to the effective action and obtain

$$\frac{d}{d\Lambda}\tilde{\Gamma}^\Lambda[\psi,\phi] = -\frac{\partial W_\Lambda[\eta,J]}{\partial\Lambda} - \int_{Q'}\frac{dJ_{Q'}}{d\Lambda}\frac{\delta W_\Lambda[\eta,J]}{\delta J_{Q'}} - \int_{K'}\frac{d\eta_{K'}}{d\Lambda}\frac{\delta W_\Lambda[\eta,J]}{\delta\eta_{K'}} \tag{2.16}$$

$$+ \int_{Q'}\frac{dJ_{Q'}}{d\Lambda}\phi_{Q'} + \int_{K'}\frac{d\eta_{K'}}{d\Lambda}\psi_{K'}, \tag{2.17}$$

which reduces to

$$\frac{d}{d\Lambda}\tilde{\Gamma}^\Lambda[\psi,\phi] = -\frac{\partial}{\partial\Lambda}W_\Lambda[\eta,J] = \langle\partial_\Lambda\Delta S_\Lambda[\psi,\phi]\rangle \tag{2.18}$$

with the Legendre relations Eq. (2.14) and (2.15). The last equation is obtained by inserting the definition of the Schwinger functional Eq. (2.8). Applying the definition of the boson and fermion correlation functions yields

$$\frac{d}{d\Lambda}\tilde{\Gamma}^\Lambda[\psi,\phi] = \frac{1}{2}\int_{Q,Q'}\partial_\Lambda\mathcal{R}_b^\Lambda(Q,Q')\langle\phi_Q\phi_{Q'}\rangle + \frac{1}{2}\int_{K,K'}\partial_\Lambda\mathcal{R}_f^\Lambda(K,K')\langle\psi_K\psi_{K'}\rangle \tag{2.19}$$

$$= \frac{1}{2}\int_{Q,Q'}\partial_\Lambda\mathcal{R}_b^\Lambda(Q,Q')\frac{\delta^2 W_\Lambda[\eta,J]}{\delta J_Q\delta J_{Q'}} + \frac{1}{2}\int_{K,K'}\partial_\Lambda\mathcal{R}_f^\Lambda(K,K')\frac{\delta^2 W_\Lambda[\eta,J]}{\delta\eta_K\delta\eta_{K'}} \tag{2.20}$$

$$+ \frac{1}{2}\int_{Q,Q'}\partial_\Lambda\mathcal{R}_b^\Lambda(Q,Q')\langle\phi_Q\rangle\langle\phi_{Q'}\rangle + \frac{1}{2}\int_{K,K'}\partial_\Lambda\mathcal{R}_f^\Lambda(K,K')\langle\psi_K\rangle\langle\psi_{K'}\rangle$$

and finally

$$\frac{d}{d\Lambda}\tilde{\Gamma}^{\Lambda}[\psi,\phi] = \frac{1}{2}\int_{Q,Q'}\partial_\Lambda \mathcal{R}_b^\Lambda(Q,Q')\frac{\delta^2 W_\Lambda[\eta,J]}{\delta J_Q \delta J_{Q'}} + \frac{1}{2}\int_{K,K'}\partial_\Lambda \mathcal{R}_f^\Lambda(K,K')\frac{\delta^2 W_\Lambda[\eta,J]}{\delta \eta_K \delta \eta_{K'}} + \partial_\Lambda \Delta S_\Lambda[\psi,\phi]. \tag{2.21}$$

Subtracting the regulator term on both sides, one obtains for the flow of the effective action

$$\frac{d}{d\Lambda}\Gamma^{\Lambda}[\psi,\phi] = \frac{1}{2}\int_{Q,Q'}\partial_\Lambda \mathcal{R}_b^\Lambda(Q,Q')\frac{\delta^2 W_\Lambda[\eta,J]}{\delta J_Q \delta J_{Q'}} + \frac{1}{2}\int_{K,K'}\partial_\Lambda \mathcal{R}_f^\Lambda(K,K')\frac{\delta^2 W_\Lambda[\eta,J]}{\delta \eta_K \delta \eta_{K'}}. \tag{2.22}$$

After switching fermionic and bosonic field derivatives $\frac{\delta^2 W_\Lambda[\eta,J]}{\delta\eta_K\delta\eta_{K'}} = -\frac{\delta^2 W_\Lambda[\eta,J]}{\delta\eta_{K'}\delta\eta_K}$ and $\frac{\delta^2 W_\Lambda[\eta,J]}{\delta J_Q \delta J_{Q'}} = \frac{\delta^2 W_\Lambda[\eta,J]}{\delta J_{Q'}\delta J_Q}$, one can use the Trace symbol Tr as shorthand notation for the circular integrals

$$\frac{d}{d\Lambda}\Gamma^{\Lambda}[\psi,\phi] = \int_{Q,Q'}\frac{1}{2}\partial_\Lambda \mathcal{R}_b^\Lambda(Q,Q')\frac{\delta^2 W_\Lambda[\eta,J]}{\delta J_Q \delta J_{Q'}} - \int_{K,K'}\frac{1}{2}\partial_\Lambda \mathcal{R}_f^\Lambda(K,K')\frac{\delta^2 W_\Lambda[\eta,J]}{\delta \eta_{K'} \delta \eta_K} \tag{2.23}$$

$$= \frac{1}{2}\mathrm{Tr}\left[\partial_\Lambda \mathcal{R}_b \frac{\delta^2 W}{\delta J^2}\right] - \frac{1}{2}\mathrm{Tr}\left[\partial_\Lambda \mathcal{R}_f \frac{\delta^2 W}{\delta \eta^2}\right], \tag{2.24}$$

where the compact matrix notation

$$\partial_\Lambda \mathcal{R}_b = \Big(\partial_\Lambda \mathcal{R}_b^\Lambda(Q,Q')\Big), \quad \partial_\Lambda \mathcal{R}_f = \Big(\partial_\Lambda \mathcal{R}_f^\Lambda(K,K')\Big), \tag{2.25}$$

$$\frac{\delta^2 W}{\delta J^2} = \Big(\frac{\delta^2 W_\Lambda[\eta,J]}{\delta J_Q \delta J_{Q'}}\Big), \quad \frac{\delta^2 W}{\delta \eta^2} = \Big(\frac{\delta^2 W_\Lambda[\eta,J]}{\delta J_K \delta J_{K'}}\Big) \tag{2.26}$$

was introduced with Q and Q' or K and K' denoting rows and columns. We will use this notation until the end of this section. Later, the scale and field dependence of the effective action will also be suppressed and we will use the abbreviation $\Gamma = \Gamma^\Lambda[\psi,\phi]$. In the next step, the second derivatives of the Schwinger functional are expressed in terms of the effective action. To this end, one applies functional derivatives with respect to external source fields to the Legendre relations, see Eq. (2.14) and (2.15) and obtains

$$\frac{\delta\eta}{\delta\psi}\frac{\delta^2 W}{\delta\eta^2} + \frac{\delta J}{\delta\psi}\frac{\delta^2 W}{\delta J\delta\eta} = 1, \qquad \frac{\delta\eta}{\delta\phi}\frac{\delta^2 W}{\delta\eta^2} + \frac{\delta J}{\delta\phi}\frac{\delta W}{\delta J\delta\eta} = 0 \tag{2.27}$$

and

$$\frac{\delta\eta}{\delta\psi}\frac{\delta^2 W}{\partial\eta\delta J} + \frac{\delta J}{\delta\psi}\frac{\delta^2 W}{\delta J\delta J} = 0, \qquad \frac{\delta\eta}{\delta\phi}\frac{\delta^2 W}{\partial\eta\delta J} + \frac{\delta J}{\delta\phi}\frac{\delta^2 W}{\delta J\delta J} = 1. \tag{2.28}$$

In the next step, insertion of the Legendre relations, see Eq. (2.14) and (2.15), results in

$$-\frac{\delta^2\tilde{\Gamma}}{\delta\psi^2}\frac{\delta^2 W}{\delta\eta^2}+\frac{\delta^2\tilde{\Gamma}}{\delta\psi\delta\phi}\frac{\delta^2 W}{\delta J\delta\eta}=1, \qquad -\frac{\delta^2\tilde{\Gamma}}{\delta\phi\delta\psi}\frac{\delta^2 W}{\delta\eta^2}+\frac{\delta^2\tilde{\Gamma}}{\delta\phi^2}\frac{\delta W}{\delta J\delta\eta}=0 \tag{2.29}$$

and

$$-\frac{\delta^2\tilde{\Gamma}}{\delta\psi^2}\frac{\delta^2 W}{\partial\eta\delta J}+\frac{\delta^2\tilde{\Gamma}}{\delta\phi\delta\psi}\frac{\delta^2 W}{\delta J\delta J}=0, \qquad -\frac{\delta^2\tilde{\Gamma}}{\delta\phi\delta\psi}\frac{\delta^2 W}{\delta\eta\delta J}+\frac{\delta^2\tilde{\Gamma}}{\delta\phi^2}\frac{\delta^2 W}{\delta J^2}=1, \tag{2.30}$$

which facilitate the replacement of the second derivatives of the Schwinger functional by the second derivative of the effective action

$$\frac{\delta^2 W}{\delta\eta^2}=-\left(\frac{\delta^2\tilde{\Gamma}}{\delta\psi^2}\right)^{-1}\left(1-\frac{\delta^2\tilde{\Gamma}}{\delta\psi\delta\phi}\left(\frac{\delta^2\tilde{\Gamma}}{\delta\phi^2}\right)^{-1}\left(\frac{\delta^2\tilde{\Gamma}}{\delta\phi\delta\psi}\right)\left(\frac{\delta^2\tilde{\Gamma}}{\delta\psi^2}\right)^{-1}\right)^{-1} \tag{2.31}$$

and

$$\frac{\delta^2 W}{\delta J^2}=\left(\frac{\delta^2\tilde{\Gamma}}{\delta\phi^2}\right)^{-1}\left(1-\frac{\delta^2\tilde{\Gamma}}{\delta\phi\delta\psi}\left(\frac{\delta^2\tilde{\Gamma}}{\delta\psi^2}\right)^{-1}\left(\frac{\delta^2\tilde{\Gamma}}{\delta\psi\delta\phi}\right)\left(\frac{\delta^2\tilde{\Gamma}}{\delta\phi^2}\right)^{-1}\right)^{-1}. \tag{2.32}$$

Inserting both relations into the flow equation for the effective action we obtain the central result of this chapter, the functional renormalization group equation for a coupled fermion and boson theory

$$\begin{aligned}\frac{d}{d\Lambda}\Gamma=&\frac{1}{2}\mathrm{Tr}\left[\partial_\Lambda\mathcal{R}_b\left(\frac{\delta^2\tilde{\Gamma}}{\delta\phi^2}\right)^{-1}\left(1-\frac{\delta^2\tilde{\Gamma}}{\delta\phi\delta\psi}\left(\frac{\delta^2\tilde{\Gamma}}{\delta\psi^2}\right)^{-1}\left(\frac{\delta^2\tilde{\Gamma}}{\delta\psi\delta\phi}\right)\left(\frac{\delta^2\tilde{\Gamma}}{\delta\phi^2}\right)^{-1}\right)^{-1}\right]\\&+\frac{1}{2}\mathrm{Tr}\left[\partial_\Lambda\mathcal{R}_f\left(\frac{\delta^2\tilde{\Gamma}}{\delta\psi^2}\right)^{-1}\left(1-\frac{\delta^2\tilde{\Gamma}}{\delta\psi\delta\phi}\left(\frac{\delta^2\tilde{\Gamma}}{\delta\phi^2}\right)^{-1}\left(\frac{\delta^2\tilde{\Gamma}}{\delta\phi\delta\psi}\right)\left(\frac{\delta^2\tilde{\Gamma}}{\delta\psi^2}\right)^{-1}\right)^{-1}\right].\end{aligned} \tag{2.33}$$

This functional RG equation is identical to the equation derived within the superfield formalism in the review by Metzner et al. (2012), see Eq. (99), by calculating the inverse of the supermatrix. Another equivalent formulation can be found in Berges et al. (2002).

The right hand side consists of two terms with a similar structure. The first term contains a scale derivative of the bosonic regulator, while the second one contains a scale derivative of the fermionic regulator. The scale derivatives of these regulators are constituent parts of the bosonic and fermionic single-scale propagators, which are defined in Eq. (2.37) and (2.39) below. The regularized effective action $\tilde{\Gamma}=\Gamma+\Delta S$ only appears on

the right hand side of the flow equation, while on the left hand side only the unregularized effective action appears. When expanding the flow equation, regularized fermionic and bosonic propagators will appear on the right hand side

$$\mathcal{G}_b(Q,Q') = \left(\frac{\delta^2\tilde{\Gamma}^\Lambda[\psi,\phi]}{\delta\phi_{\tilde{Q}}\delta\phi_{\tilde{Q}'}}\right)^{-1}_{Q,Q'} = \left(\frac{\delta^2\Gamma^\Lambda[\psi,\phi]}{\delta\phi_{\tilde{Q}}\delta\phi_{\tilde{Q}'}} + \mathcal{R}_b^\Lambda(\tilde{Q},\tilde{Q}')\right)^{-1}_{Q,Q'}, \tag{2.34}$$

$$\mathcal{G}_f(K,K') = -\left(\frac{\delta^2\tilde{\Gamma}^\Lambda[\psi,\phi]}{\delta\psi_{\tilde{K}}\delta\psi_{\tilde{K}'}}\right)^{-1}_{K,K'} = -\left(\frac{\delta^2\Gamma^\Lambda[\psi,\phi]}{\delta\psi_{\tilde{K}}\delta\psi_{\tilde{K}'}} - \mathcal{R}_f^\Lambda(\tilde{K},\tilde{K}')\right)^{-1}_{K,K'}, \tag{2.35}$$

where the external indices Q, Q' and K, K' depend on the external indices $\tilde{Q}, \tilde{Q}'$ and $\tilde{K}, \tilde{K}'$ through a non-trival connection due to the matrix inversion. For clarity reasons we explicitly write out the internal structure of the inverse matrix. The bosonic regulator $\mathcal{R}_b^\Lambda(K,K') = \mathcal{R}_b^\Lambda(K',K) = \frac{\delta^2\Delta S_\Lambda[\psi,\phi]}{\delta\phi_K\delta\phi_{K'}}$ is symmetric in its argument, whereas the fermionic regulator $\mathcal{R}_f^\Lambda(K',K) = -\mathcal{R}_f^\Lambda(K,K') = \frac{\delta^2\Delta S_\Lambda[\psi,\phi]}{\delta\psi_K\delta\psi_{K'}}$ has an internal antisymmetric structure. The so-called single scale propagators are defined as scale derivatives of the fermion and boson propagators with fixed self-energy

$$\mathcal{S}_f = \frac{\partial\mathcal{G}_f}{\partial\Lambda}\Big|_\Sigma = -\frac{\partial}{\partial\Lambda}\left(\frac{\delta^2\Gamma}{\delta\psi^2} - \mathcal{R}_f\right)^{-1} = -\left(\frac{\delta^2\Gamma}{\delta\psi^2} - \mathcal{R}_f\right)^{-1}\partial_\Lambda\mathcal{R}_f\left(\frac{\delta^2\Gamma}{\delta\psi^2} - \mathcal{R}_f\right)^{-1} \tag{2.36}$$

$$= -\mathcal{G}_f(\partial_\Lambda\mathcal{R}_f)\mathcal{G}_f, \tag{2.37}$$

$$\mathcal{S}_b = \frac{\partial\mathcal{G}_b}{\partial\Lambda}\Big|_\Sigma = \frac{\partial}{\partial\Lambda}\left(\frac{\delta^2\Gamma}{\delta\phi^2} + \mathcal{R}_b\right)^{-1} = -\left(\frac{\delta^2\Gamma}{\delta\phi^2} + \mathcal{R}_b\right)^{-1}\partial_\Lambda\mathcal{R}_b\left(\frac{\delta^2\Gamma}{\delta\phi^2} + \mathcal{R}_b\right)^{-1} \tag{2.38}$$

$$= -\mathcal{G}_b(\partial_\Lambda\mathcal{R}_b)\mathcal{G}_b. \tag{2.39}$$

Here, we used the shorthand notation $\mathcal{G}_f = (\mathcal{G}_f(K,K'))$ and $\mathcal{G}_b = (\mathcal{G}_b(K,K'))$ for the fermionic and bosonic propagators. Further, the relation $\partial_\Lambda A^{-1} = -A^{-1}\left(\partial_\Lambda A\right)A^{-1}$ was applied, which holds for general matrices A with scale-dependent entries.

For an explicit evaluation of the flow equations, the basis for fermionic and bosonic fields has to be specified. In the case of the first project (Dirac cone model) we will work in the basis

$$\psi_K = \left(\psi_{k+\uparrow}, \psi_{k+\downarrow}, \bar{\psi}_{k+\uparrow}, \bar{\psi}_{k+\downarrow}, \psi_{k-\uparrow}, \psi_{k-\downarrow}, \bar{\psi}_{k-\uparrow}, \bar{\psi}_{k-\downarrow}\right), \tag{2.40}$$

where the general variable is specified as $K = (k, \alpha, \sigma, c)$ with fermionic momenta $\mathbf{k}$ and Matsubara frequencies k_0 collected in $k = (k_0, \mathbf{k})$. The second index of the fermionic fields denotes a band index $\alpha = \pm$ which allocates fermions to the upper and lower Dirac cone,

and the third index corresponds to the spin $\sigma = \downarrow, \uparrow$. Finally, the fourth index c denotes the index for conjugated and non-conjugated fermionic fields, $\bar{\psi}$ and ψ, respectively. In the case of the second project (fermionic superfluid) there is no band index α and the basis is

$$(\psi_K) = \left(\psi_{k\uparrow}, \psi_{k\downarrow}, \bar{\psi}_{k\uparrow}, \bar{\psi}_{k\downarrow}\right), \tag{2.41}$$

where $K = (k, c, \sigma)$. The bosonic degrees of freedom will be described by a complex-valued field

$$(\phi_Q) = \left(\phi_q, \phi_q^*\right) \tag{2.42}$$

in the Dirac cone model and in the symmetric regime of the fermionic superfluid, where the variable $Q = (q, c)$ collects bosonic momenta $\mathbf{q}$ and Matsubara frequencies q_0 in $q = (q_0, \mathbf{q})$ and conjugated fields $c = \phi, \phi^*$ in the index c. In the symmetry-broken regime of the fermionic superfluid, the bosonic field will be decomposed in real-valued transverse and longitudinal fields

$$(\phi_Q) = (\sigma_q, \pi_q), \tag{2.43}$$

where now the index $Q = (q, c)$ includes again bosonic momenta and Matsubara frequencies as above, but $c = \sigma, \pi$ distinguishes now between longitudinal σ and transverse π field species.

2.3 Spontaneous symmetry breaking

Here, we derive the flow equations for situations with spontaneous symmetry breaking. During the flow the bosonic sector of the effective action develops a Mexican hat shape with degenerate minima. The order parameter in the broken-phase can be defined as the location of one of those minima. For our discussion we choose a real-valued order parameter denoted as α^Λ, which grows from zero to a finite value α during the renormalization procedure. The value of the order parameter is then determined by the minimum condition

$$\frac{\delta\Gamma[\phi, \phi^*]}{\delta\phi}\Big|_{\phi=\phi^*=\alpha^\Lambda} = \frac{\delta\Gamma[\phi, \phi^*]}{\delta\phi^*}\Big|_{\phi=\phi^*=\alpha^\Lambda} = 0. \tag{2.44}$$

Decomposing the bosonic fields

$$\phi(x) = \alpha^{\Lambda} + \sigma(x) + i\pi(x), \tag{2.45}$$

$$\phi^*(x) = \alpha^{\Lambda} + \sigma(x) - i\pi(x) \tag{2.46}$$

into longitudinal $\sigma(x)$ and transverse $\pi(x)$ fluctuations around the scale-dependent order parameter α^{Λ}, the corresponding minimum condition for the new effective action in terms of longitudinal and transverse bosonic fields reads

$$\frac{\delta\Gamma[\sigma + \alpha^{\Lambda}, \pi]}{\delta\sigma}\Big|_{\sigma=\pi=0} = 0. \tag{2.47}$$

In the next step, the renormalization group equation for situations with a developing finite order parameter α^{Λ} are derived. The total scale derivative of the scale-dependent effective action

$$\frac{d}{d\Lambda}\Gamma^{\Lambda}[\psi, \bar{\psi}, \sigma + \alpha^{\Lambda}, \pi] = \frac{\partial}{\partial\Lambda}\Gamma^{\Lambda}[\psi, \bar{\psi}, \sigma + \alpha^{\Lambda}, \pi] + \frac{\delta\Gamma^{\Lambda}}{\delta\sigma}[\psi, \bar{\psi}, \sigma + \alpha^{\Lambda}, \pi]\frac{d}{d\Lambda}\,\alpha^{\Lambda} \tag{2.48}$$

has two parts. The first part is given by the expression for the flow equation

$$\begin{aligned}\frac{\partial}{\partial\Lambda}\Gamma = &\frac{1}{2}\mathrm{Tr}\left[\partial_{\Lambda}\mathcal{R}_b\left(\frac{\delta^2\tilde{\Gamma}}{\delta\phi^2}\right)^{-1}\left(1 - \frac{\delta^2\tilde{\Gamma}}{\delta\phi\delta\psi}\left(\frac{\delta^2\tilde{\Gamma}}{\delta\psi^2}\right)^{-1}\left(\frac{\delta^2\tilde{\Gamma}}{\delta\psi\delta\phi}\right)\left(\frac{\delta^2\tilde{\Gamma}}{\delta\phi^2}\right)^{-1}\right)^{-1}\right] \\ &+ \frac{1}{2}\mathrm{Tr}\left[\partial_{\Lambda}\mathcal{R}_f\left(\frac{\delta^2\tilde{\Gamma}}{\delta\psi^2}\right)^{-1}\left(1 - \frac{\delta^2\tilde{\Gamma}}{\delta\psi\delta\phi}\left(\frac{\delta^2\tilde{\Gamma}}{\delta\phi^2}\right)^{-1}\left(\frac{\delta^2\tilde{\Gamma}}{\delta\phi\delta\psi}\right)\left(\frac{\delta^2\tilde{\Gamma}}{\delta\psi^2}\right)^{-1}\right)^{-1}\right],\end{aligned} \tag{2.49}$$

which was derived in the previous part. We use the short-hand notation

$$\frac{\partial}{\partial\Lambda}\Gamma = \frac{\partial}{\partial\Lambda}\Gamma^{\Lambda}[\psi, \bar{\psi}, \sigma + \alpha, \pi], \quad \tilde{\Gamma} = \tilde{\Gamma}^{\Lambda}[\psi, \bar{\psi}, \sigma + \alpha, \pi]. \tag{2.50}$$

Here, we work in the basis of longitudinal and transverse bosonic fields $\phi = (\sigma, \pi)$. Hence, the second derivative of the effective action with respect to bosonic fields is given by

$$\frac{\delta^2\tilde{\Gamma}^{\Lambda}[\psi, \bar{\psi}, \sigma + \alpha^{\Lambda}, \pi]}{\delta\phi^2} = \begin{pmatrix} \frac{\delta^2\tilde{\Gamma}^{\Lambda}[\psi,\bar{\psi},\sigma+\alpha^{\Lambda},\pi]}{\delta\sigma\delta\sigma} & \frac{\delta^2\tilde{\Gamma}^{\Lambda}[\psi,\bar{\psi},\sigma+\alpha^{\Lambda},\pi]}{\delta\sigma\delta\pi} \\ \frac{\delta^2\tilde{\Gamma}^{\Lambda}[\psi,\bar{\psi},\sigma+\alpha^{\Lambda},\pi]}{\delta\pi\delta\sigma} & \frac{\delta^2\tilde{\Gamma}^{\Lambda}[\psi,\bar{\psi},\sigma+\alpha^{\Lambda},\pi]}{\delta\pi\delta\pi} \end{pmatrix}. \tag{2.51}$$

The second part of the renormalization group equation Eq. (2.48) is proportional to the flow of the order parameter. The following recipe illustrates how the RG equation is solved

with an ansatz for the scale-dependent effective action.[2] First an ansatz for $\Gamma^\Lambda[\psi, \bar{\psi}, \sigma + \alpha^\Lambda, \pi]$ is stated. The prefactors of this expansion correspond to couplings parametrizing the bosonic and fermionic self-energies and interactions, which will renormalize during the flow. This whole ansatz is then inserted into the flow equations. Functional field differentiation on both sides of the flow equations leads directly to the flow for bosonic and fermionic self-energies and other couplings.

The flow of the order parameter can easily be determined by considering the flow of the minimum of the effective action. Applying a functional derivative with respect to the longitudinal fields yields

$$0 = \frac{d}{d\Lambda}\frac{\delta}{\delta\sigma}\Gamma^\Lambda[\psi, \bar{\psi}, \sigma + \alpha^\Lambda, \pi]\Big|_{\sigma=\pi=0} \tag{2.52}$$

$$= \frac{\delta}{\delta\sigma}\frac{\partial}{\partial\Lambda}\Gamma^\Lambda[\psi, \bar{\psi}, \sigma + \alpha^\Lambda, \pi]\Big|_{\sigma=\pi=0} + \frac{d\alpha^\Lambda}{d\Lambda}\frac{\delta^2}{\delta\sigma^2}\Gamma^\Lambda[\psi, \bar{\psi}, \sigma + \alpha^\Lambda, \pi]\Big|_{\sigma=\pi=0}, \tag{2.53}$$

which directly leads to

$$\frac{d\alpha^\Lambda}{d\Lambda} = -\left(\frac{\delta^2\Gamma[\psi, \bar{\psi}, \sigma + \alpha^\Lambda, \pi]}{\delta\sigma\delta\sigma}\right)^{-1} \cdot \frac{\delta}{\delta\sigma}\frac{\partial}{\partial\Lambda}\Gamma^\Lambda[\psi, \bar{\psi}, \sigma + \alpha^\Lambda, \pi]\Big|_{\sigma=\pi=0}. \tag{2.54}$$

The evolution of the order parameter is determined by bosonic and fermionic tadpole diagrams. In the following chapters we will apply the functional renormalization group method to the Dirac cone model and to the fermionic superfluid.

[2] Apart from the present scheme also other truncation schemes exist, for instance the full potential RG analysis. There, the full field dependence is taken into account in terms of a local bosonic potential and only a gradient expansion is applied. We refer to the review by Metzner et al. (2012) and to the work by Jackubczyk et al. (2009) for further details.

CHAPTER 3

Project 1: Superfluid-semimetallic quantum phase transition

In this chapter we analyze a quantum phase transition between a superfluid and a semimetal in the Dirac cone model. We analyze the quantum critical behaviour close to and at the quantum critical point, which separates both phases, at zero and finite temperatures. The system is studied within a coupled fermion-boson functional renormalization group approach. At the quantum critical point non-Gaussian and non-Fermi liquid behaviour emerge, due to the appearance of anomalous dimensions. At finite temperatures, close to criticality, critical exponents for the susceptibility and the correlation length are determined. The critical exponents obey several scaling laws. An infinite correlation length occurs not only at the quantum critical point, but also in the entire semimetallic ground state.

The chapter is structured as follows: After a short overview over quantum criticality in section 3.1, the Dirac cone model is introduced in section 3.2. Afterwards, in section 3.3 our truncation and parametrization for the scale-dependent effective action is presented. This will be used to analyze the interplay between fermions and order parameter fluctuations close to the quantum critical point within the functional RG formalism. For that truncation section 3.4 presents the functional RG flow in terms of rescaled variables at zero and finite temperatures. In section 3.5, the analytic structure of the particle-particle bubble gives us insights about the low-energy behaviour of the bosonic propagator and will lead us to an unexpected power law decay. This will imply an infinite correlation length and time in the entire ground state away from the critical point. Finally, the renormalization group equations are solved numerically in two dimensions at zero and at

finite temperatures in section 3.6 and conclusions are drawn in section 3.7.

3.1 Introduction

In general quantum phase transitions occur at zero temperature by varying a non-thermal control parameter. In the case of a continuous quantum phase transition, a quantum critical point separates the symmetric and symmetry-broken phase. Although located at zero temperature, and therefore not experimentally reachable, the quantum critical point can strongly affect the finite temperature regime, within the so-called quantum critical region above the critical point. In this regime quantum and thermal fluctuations have a mutual interplay so that a description in terms of classical criticality breaks down and non-Fermi liquid properties emerge.

The standard approach for dealing with quantum criticality in correlated electron systems was introduced by Hertz (1976) and Millis (1993) and is known as the Hertz-Millis theory. Here, the fermionic interaction is decoupled by introducing an order parameter field via Hubbard-Stratonovich transformation. Afterwards the fermionic degrees of freedom are integrated out and an effective bosonic theory is obtained. It was shown later that this procedure of integrating fermions out may lead to divergent coefficients for the effective bosonic theory and render the approximation with a local quartic term invalid. This occurs due to the existence of gapless fermionic excitations around the Fermi surface especially in low dimensionality (for review see Belitz et al. (2005) and Löhneysen et al. (2007)).

The need for other routes towards quantum criticality leads to several approaches with coupled fermion-boson theories, where both fermions and order parameter fluctuations are treated on the same footing (Altshuler et al. (1994, 1995), Vojta et al. (2000a, 2000b), Abanov et al. (2000), Abanov et al. (2003), Rech et al. (2006), Kaul et al. (2008), Huh and Sachdev (2008) and Strack et al. (2010).

Coupled fermion-boson theories were also studied within the functional renormalization group framework (see Berges et al. (2002), Baier et al. (2004), Schütz et al. (2005) and Metzner et al. (2012). The interplay between gapless fermions and massless bosons was analyzed within the functional renormalization group scheme in different physical systems: in quantum electrodynamics, see Gies and Jaeckel (2004), non-abelian gauge theory, see Pawlowski et al. (2004), the Gross-Neveu model, see Rosa et al. (2001), Höfling et al. (2002) and Scherer et al. (2013), and the Dirac cone model, see Strack et al. (2010).

The Dirac cone model was introduced and analyzed in the last work and undergoes a quantum phase transition between superfluid and semimetal. Nowadays it is hard to

imagine not coming into contact with Dirac cones in condensed matter physics. First, due to the groundbreaking experiments by Geim and Novoselov on graphene, which was honoured by the Nobel prize in 2010 and triggered intensive research in that field. In this two-dimensional material, two Dirac cones appear in the honeycomb band structure at two nonequivalent sites in the Brillouin-zone. In contrast to graphene the Dirac cone model has no entanglement of the momentum dependence with the pseudo-spin degree of freedom, which is related to the 2-atom structure of the unit cell of graphene. To analyze interaction effects in graphene, the Hubbard model is often employed, see for instance Meng et al. (2010). Second, the introduction of the symmetry-protected Dirac cones in the field of topological insulators, where Dirac fermions describe surface states in some of these three dimensional systems. Here, the spin orientation is also correlated with momenta, in contrast to the Dirac cone model.

Although seemingly similar to the Gross-Neveu model, the Dirac cone model was proven to fall in another universality class. Strack et al. (2010) pointed out that the model exhibits a quantum phase transition from a semimetal to a superfluid. Due to gapless fermions the Hertz-Millis theory fails in this regime and a coupled fermion-boson renormalization group method was applied at zero temperature. Within a simple truncation a breakdown of the Fermi-liquid concept and a non-Gaussian behaviour was observed at the quantum critical point, due to the appearance of anomalous dimensions below three dimensions. The critical exponent for the susceptibility and a scaling law was determined by the explicit solution in two dimensions.

We extend this existing truncation of the RG flow in several directions. First, we distinguish between momentum and frequency renormalization, which will lead to a vanishing Fermi velocity in the infrared. Furthermore, the work is extended to finite temperatures and critical exponents and anomalous dimensions are determined. We revisit the ground state of the model and find a non-analytic behaviour of the fermionic particle-particle bubble which leads to a diverging correlation length also away from the quantum critical point. This indicates that the entire semimetal phase at zero temperature is in some sense 'critical'. This resembles the situation in graphene, where the Dirac point which separates the hole-doped and electron-doped phase may be interpreted as a critical point (Sheehy and Schamlian (2007)). The next section gives a detailed introduction to the Dirac cone model.

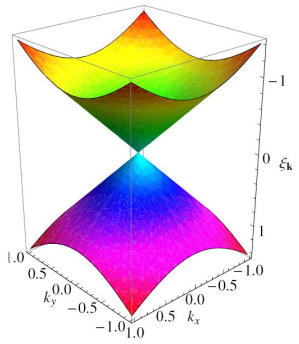

Figure 3.1: Visualization of the dispersion relation $\epsilon_{\mathbf{k}\alpha} = \alpha v_f |\mathbf{k}|$ of the Dirac cone model in two dimensions. The chemical potential μ is set to zero, so that only the states in the lower cone are occupied and the Fermi surface consists of only one point (Picture from Strack et al. (2010)).

3.2 Model

The Dirac cone model was introduced by Strack et al. (2010) as a prototype model for a quantum phase transition between a semimetal and a superfluid. The model consists of spinful fermions with a linear dispersion relation $\epsilon_{\mathbf{k}\alpha} = \alpha v_f |\mathbf{k}|$, where v_f denotes the Fermi velocity, α the band index of the lower and upper Dirac cone and $\sigma = \uparrow, \downarrow$ the spin configuration. Figure 3.1 shows the dispersion relation in two dimensions. The chemical potential μ is set to zero to obtain a point-like Fermi surface, where only the states of the lower cone are occupied. The contact interaction is attractive ($U < 0$) and includes inter- and intra-band processes. In total the microscopic action reads

$$S[\psi, \bar{\psi}] = \int_{k\alpha\sigma} \bar{\psi}_{k\alpha\sigma}(-ik_0 + \epsilon_{\mathbf{k}\alpha})\, \psi_{k\alpha\sigma} + U \int_{k\alpha} \int_{k'\alpha'} \int_{q} \bar{\psi}_{-k,\alpha\downarrow} \bar{\psi}_{k+q,\alpha\uparrow} \psi_{k'+q,\alpha'\uparrow} \psi_{-k',\alpha'\downarrow} + \int_{k\alpha\sigma} m_\alpha \bar{\psi}_{k\alpha\sigma} \psi_{k\alpha\sigma}, \tag{3.1}$$

where $\psi_{k\alpha\sigma}$ and $\bar{\psi}_{k\alpha\sigma}$ denote anticommuting fermionic fields. The short-hand notation for the integral $\int_{k\alpha\sigma} = T \sum_{k_0} \int_{\mathbf{k}} \frac{d^d k}{(2\pi)^d} \sum_{\alpha} \sum_{\sigma}$ includes integrations over fermionic Matsubara frequencies $k_0 = (2n+1)\pi T$ with integer n, integrations over momenta $\mathbf{k}$, which are restricted by an ultraviolet cutoff $|\epsilon_{\mathbf{k}\alpha}| < \Lambda_0$ and summations over both band indices $\alpha = \pm 1$ and spin configurations $\sigma = \uparrow, \downarrow$. Additionally, a finite counterterm mass m_α is added to the bare microscopic action which preserves a gapless dispersion during the flow and which will be discussed in section 3.3.

The fermionic interaction term can be decoupled with a Hubbard-Stratonovich trans-

formation in the s-wave spin-singlet pairing channel by introducing a complex bosonic auxiliary field which is conjugated to the fermionic bilinear $U \int_{k\alpha} \psi_{k+q,\alpha\uparrow}\psi_{-k,\alpha\downarrow}$. The resulting coupled fermion-boson microscopic action reads

$$\begin{aligned} S[\psi,\bar{\psi},\phi] = &\int_{k\alpha\sigma} \bar{\psi}_{k\alpha\sigma}(-ik_0 + \epsilon_{\mathbf{k}\alpha} + m_\alpha)\,\psi_{k\alpha\sigma} - \int_q \phi_q^* \frac{1}{U}\,\phi_q \\ &+ \int_{k\alpha}\int_q \left(\bar{\psi}_{-k,\alpha\downarrow}\bar{\psi}_{k+q,\alpha\uparrow}\,\phi_q + \psi_{k+q,\alpha\uparrow}\psi_{-k,\alpha\downarrow}\,\phi_q^*\right) , \end{aligned} \tag{3.2}$$

where ϕ_q and ϕ_q denote the complex valued bosonic fields. The integration $\int_q = \sum_{q_0} \int_{\mathbf{q}} \frac{d^d q}{(2\pi)^d}$ runs over bosonic Matsubara frequencies $q_0 = 2n\pi T$ with integer n and bosonic transfer momenta $\mathbf{q}$. The Hubbard Stratonovich transformation replaces the fermionic interaction through a quadratic bosonic part with a bosonic mass of strength $-1/U$ and through a normal Yukawa coupling between bosonic and fermionic degrees of freedom with strength one.

A saddle-point analysis of the theory leads to a BCS-like gap equation

$$\Delta_{MF} = -U \int_{k\alpha} \frac{\Delta_{MF}}{k_0^2 + \epsilon_{\mathbf{k}\alpha}^2 + \Delta_{MF}^2} \tag{3.3}$$

with the mean-field gap Δ_{MF}, which signals a phase transition to a superfluid phase at a finite coupling strength. The vanishing density of states at the (point-like) Fermi surface $N(E) \propto E^{3-d}$ prevents a weak-pairing instability and a finite interaction U_{qc} becomes necessary to reach the superfluid state. The upper critical dimension is given by $d_c^+ = 3$. Figure 3.2 visualizes the quantum phase transition between semimetallic and superfluid phases, which are separated by a quantum critical point at a finite interaction strength U_{qc}.

As mentioned in the introduction section 3.1, the standard approach for analyzing quantum criticality is given by the Hertz-Millis theory, where the fermions in the coupled fermion-boson theory would be integrated out and the resulting purely bosonic theory is analyzed within a renormalization group scheme. It was shown by Strack et al. (2010) that this approach fails here, because of a linear divergence in the local bosonic self-interaction due to fermionic loop diagrams. Hence, they approached the critical point with a coupled fermion-boson theory where both degrees of freedom are treated on the same footing. We follow this route and analyze the coupled fermion-boson theory. In the next section we will present our truncation of the scale-dependent effective action for a functional renormalization group analysis beyond a mean-field study.

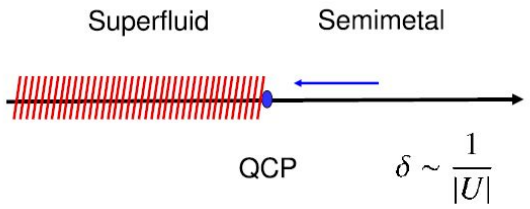

Figure 3.2: At zero temperature the superfluid and the semimetallic phase are separated by a quantum critical point (QCP). In the superfluid phase s-wave spin singlet pairing occurs, while in the semimetallic phase a massless Dirac cone remains. The transition is controlled by the non-thermal parameter $m_b^2 = -\frac{1}{U}$, given by the inverse interaction strength (Picture from Strack et al. (2010)).

3.3 Truncation and parametrization of the effective action

In the following, our truncation and parametrization for the scale-dependent effective action Γ^Λ are presented. The leading low energy terms will be kept to capture the quantum critical behaviour close to and at the phase transition. We will analyze the critical behaviour within a coupled fermion-boson approach, approaching the QCP from the symmetric phase at zero and finite temperature.

As we saw in chapter 2, the full effective action $\Gamma^{\Lambda=0}$ includes the complete thermodynamics and all correlation functions of the system. We now make an ansatz for the scale-dependent effective action Γ^Λ in powers of fields and gradients. The scale-dependent action will be truncated at fourth order in the bosonic fields. Scale-dependent renormalization factors parametrize the momentum and frequency dependence for the fermionic and bosonic propagator during the flow. The flow of the renormalization factors and local terms is calculated by inserting the ansatz in the renormalization group equation Eq. (2.33), and expanding the right hand side in powers of fields.

Our ansatz for the scale-dependent effective action consists of four terms

$$\Gamma^\Lambda = \Gamma_{\bar{\psi}\psi} + \Gamma_{\phi^*\phi} + \Gamma_{|\phi|^4} + \Gamma_{\psi^2\phi^*}. \tag{3.4}$$

The quadratic term in fermionic fields

$$\Gamma_{\bar{\psi}\psi} = \int_{k\alpha\sigma} \bar{\psi}_{k\alpha\sigma}(-iZ_f k_0 + A_f \epsilon_{\mathbf{k}\alpha} + m_\alpha)\,\psi_{k\alpha\sigma} \tag{3.5}$$

includes the renormalization factors Z_f and A_f, which parametrize the frequency and

momentum dependence and start both with initial value one. Further a fermionic mass term is parametrized by m_α, which is generated during the flow due to the fermionic two-particle interaction. Hence, a finite counterterm mass is added to the microscopic action, see Eq. (3.1) and (3.2), and is fine-tuned in such a way that the generated fermionic mass is cancelled out. This preserves a massless dispersion relation and keeps a fermionic band gap closed. A finite fermionic band gap would correspond to a finite fermionic mass. The value of the counterterm mass does not need to be specified, but would be given by the value of the fermionic band gap in the infrared regime without a counterterm.

The quadratic bosonic term

$$\Gamma_{\phi^*\phi} = \int_q \phi_q^* \left(Z_b q_0^2 + A_b \mathbf{q}^2 + m_b^2 \right) \phi_q \tag{3.6}$$

is parametrized by a mass term m_b^2 which is initially given by the $m_b^2 = -\frac{1}{U}$, and Z_b and A_b, which parametrize the quadratic frequency and momentum dependence. Both quadratic dependencies will only be generated in the course of the flow and are not present in the original microscopic action. During the flow, a vanishing bosonic mass, $m_b^2 = 0$, signals the occurrence of spontaneous symmetry breaking and is used to determine the location of the quantum critical point. Further a local bosonic self-interaction is introduced

$$\Gamma_{|\phi|^4} = \frac{u}{8} \int_{q,q',p} \phi^*_{q+p} \phi^*_{q'-p} \phi_{q'} \phi_q \ , \tag{3.7}$$

which is parametrized through the running coupling u^Λ and which stabilises the boson theory close to criticality. The Yukawa vertex

$$\Gamma_{\psi^2\phi^*} = g \int_{k\alpha} \int_q \left(\bar{\psi}_{-k,\alpha\downarrow} \bar{\psi}_{k+q,\alpha\uparrow} \phi_q + \psi_{k+q,\alpha\uparrow} \psi_{-k,\alpha\downarrow} \phi_q^* \right) \tag{3.8}$$

will not be renormalized in the symmetric phase, so that $g^\Lambda = 1$. The vertex correction of order g^3 vanishes due to particle conservation, see Strack et al. (2008). For this theory the fermionic and bosonic propagators are given by

$$G_{f\alpha}(k) = -\langle \psi_{k\alpha\sigma} \bar{\psi}_{k\alpha\sigma} \rangle = \frac{1}{i Z_f k_0 - A_f \epsilon_{\mathbf{k}\alpha} - m_\alpha} \ , \tag{3.9}$$

$$G_b(q) = -\langle \phi_q \phi_q^* \rangle = \frac{-1}{Z_b q_0^2 + A_b \mathbf{q}^2 + m_b^2} \ . \tag{3.10}$$

In contrast to the previous truncation by Strack et al. (2010), different renormalization factors for the frequency and momentum dependence are considered for both fermion,

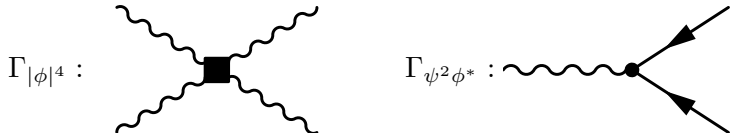

Figure 3.3: Vertices of the bosonic self-interaction and the Yukawa coupling.

$Z_f \neq A_f$, and boson fields, $Z_b \neq A_b$. Further, the opening of a fermionic gap due to the fermion interaction is prevented by implementing a counterterm mass term, as mentioned above. Diagrams for both bosonic self-interaction and the Yukawa vertex are illustrated in figure 3.3.

The renormalization group flow starts in the ultraviolet limit with the condition

$$\Gamma^{\Lambda_0} = S, \tag{3.11}$$

where the (scale-dependent) effective action matches the bare microscopic action.

For our analysis, we will start with the following initial values for the flowing couplings

$$Z_f^{\Lambda_0} = 1, \quad A_f^{\Lambda_0} = 1, \quad m_\alpha^{\Lambda_0} = m_\alpha, \qquad g^{\Lambda_0} = 1 \tag{3.12}$$

$$Z_b^{\Lambda_0} = 1, \quad A_b^{\Lambda_0} = 1, \quad m_b^{\Lambda_0} = \sqrt{\frac{1}{|U|}}, \quad u^{\Lambda_0} = 0. \tag{3.13}$$

In our truncation, we assume a finite value for the bosonic renormalization factors $Z_b^{\Lambda_0} = 1$, $A_b^{\Lambda_0} = 1$ already in the microscopic action. However, due to a local fermionic two-particle interaction of our model, the bosonic renormalization factors Z_b and A_b should be zero at the beginning of the flow.

We motivate briefly our choice of the finite initial values for the bosonic renormalization factors: In the case of zero initial values both bosonic renormalization factors are generated by fermions at early stages of the flow accompanied with high anomalous dimensions. This leads to a somewhat pathological behaviour for the bosonic regulator. Since the regulator is directly proportional to A_b, it immediately reacts on a change in A_b. Already at the beginning of the flow the fermions generate notables values A_b due to high bosonic anomalous dimensions. Hence, the bosonic regulator is switched on at the same scale regularizing the theory. Finally, in the infrared limit it vanishes again. Therefore, a finite choice of the renormalization factors Z_b and A_b suggests itself to avoid this pathological off-on-off behaviour of the bosonic regulator. Furthermore, this also simplifies the numerical treatment in the beginning of the flow, where we can neglect the scale derivative of the bosonic renormalization factor. Then, a term of the form $\int \phi_q^*(q_0^2 + \mathbf{q}^2)\phi_q$ appears

already in the microscopic action, which suppresses the interaction at low frequency and momentum transfers.

3.4 Renormalization group equations

The functional renormalization group equations for a coupled fermion-boson theory were derived in chapter 2. In this chapter, we derive the flow equation for the various couplings within our truncation, presented in the previous section. The truncation is plugged into the flow equation and the flow for the couplings are determined by expanding the right hand side of the flow equation in powers of the fields. To extract the frequency and momentum dependence of the fermionic and bosonic propagator, external frequency and momentum derivatives have to be applied.

The scale-dependence Λ is implemented by a sharp Litim momentum cutoff

$$R_f(\mathbf{k}) = A_f(-\Lambda \operatorname{sgn}(\epsilon_{\mathbf{k}\alpha}) + \epsilon_{\mathbf{k}\alpha})\,\Theta(\Lambda - |\epsilon_{\mathbf{k}\alpha}|) + \delta \mathrm{m}_\alpha^\Lambda, \tag{3.14}$$

$$R_b(\mathbf{q}) = A_b(-\Lambda^2 + \mathbf{q}^2)\,\Theta(\Lambda^2 - \mathbf{q}^2), \tag{3.15}$$

which regularizes both fermionic and bosonic propagators

$$G_{f\alpha}(k) = \frac{1}{iZ_f k_0 - \alpha A_f|\mathbf{k}| - m_\alpha + R_f(\mathbf{k})}, \tag{3.16}$$

$$G_b(q) = \frac{-1}{Z_b q_0^2 + A_b\mathbf{q}^2 + m_b^2 - R_b(\mathbf{q})}\,, \tag{3.17}$$

where $-\alpha A_f|\mathbf{k}|$ is replaced by $-\alpha A_f\Lambda$ in the fermionic propagator and $A_b\mathbf{q}^2$ by $A_b\Lambda^2$ in the bosonic propagator if $v_f|\mathbf{k}| < \Lambda$ and $|\mathbf{q}| < \Lambda$ is fulfilled. We choose the value of δm_α^Λ in such a way that it cancels out the scale-dependent mass m_α in Eq. (3.5) at each scale.

This choice of the regulator simplifies the expressions on the right hand side of the flow equation, and all frequency and momentum integrations and sums, respectively, can be executed explicitly in both the zero and finite temperature regime.

3.4.1 General flow equations

Expanding the renormalization group equation in fields and gradients, the flow for the couplings reads

$$\frac{d}{d\Lambda} Z_f = -g^2 \frac{\partial}{i\partial k_0}\Big|_{k=0} \int_q D_\Lambda \left[G_{f\alpha}(q-k) G_b(q) \right], \tag{3.18}$$

$$\frac{d}{d\Lambda} A_f = 0, \tag{3.19}$$

$$\frac{d}{d\Lambda} m_b^2 = -g^2 \int_{k\alpha} D_\Lambda \left[G_{f\alpha}(k) G_{f\alpha}(-k) \right] - \frac{u}{2} \int_q D_\Lambda \, G_b(q), \tag{3.20}$$

$$\frac{d}{d\Lambda} Z_b = -\frac{1}{2} \frac{\partial^2}{\partial p_0^2}\Big|_{p=0} g^2 \int_{k\alpha} D_\Lambda \left[G_{f\alpha}(k+p) G_{f\alpha}(-k) \right], \tag{3.21}$$

$$\frac{d}{d\Lambda} A_b = -\frac{1}{2} \frac{\partial^2}{\partial p_x^2}\Big|_{p=0} g^2 \int_{k} D_\Lambda \left[G_{f\alpha}(k+p) G_{f\alpha}(-k) \right], \tag{3.22}$$

$$\frac{d}{d\Lambda} u = 4g^4 \int_{k\alpha} D_\Lambda \left[G_{f\alpha}(-k) \right]^2 \left[G_{f\alpha}(k) \right]^2 - \frac{5}{4} u^2 \int_q D_\Lambda \left[G_b(q) \right]^2, \tag{3.23}$$

$$\frac{d}{d\Lambda} g = 0, \tag{3.24}$$

where $D_\Lambda = \frac{d}{d\Lambda}\Big|_{\Sigma^\Lambda} = \sum_{s=f,b} \left(\frac{d}{d\Lambda} R_s \right) \partial_{R_s}$ denotes a scale derivative acting only on fermionic and bosonic regulators, while keeping the self-energy of both propagators constant. In the zero temperature case, $T = 0$, the shorthand notation for the integrals $\int_q = \int_{q_0} \int_{\mathbf{q}}$ and $\int_k = \int_{k_0} \int_{\mathbf{k}}$ includes integration over continuous frequencies and momenta and the symbols $\frac{\partial}{\partial_{k_0}}$ and $\frac{\partial}{\partial_{p_0}}$ denote standard continuous derivatives.

A finite temperature, $T > 0$, the shorthand notation for the integrals $\int_k = T \sum_{k_0} \int_{\mathbf{k}}$ and $\int_q = T \sum_{q_0} \int_{\mathbf{q}}$ consists of sums over discrete fermionic $k_0 = (2n+1)\pi T$ and bosonic $q_0 = 2n\pi T$ Matsubara frequencies, respectively. The continuous frequency derivatives are then replaced by discrete derivatives

$$\frac{\partial}{\partial k_0} f_f(k_0) \overset{T>0}{\to} \frac{f_f(\pi T) - f_f(-\pi T)}{2\pi T}, \tag{3.25}$$

$$\frac{\partial^2}{\partial q_0^2} f_b(q_0) \overset{T>0}{\to} \frac{f_b(2\pi T) + f_b(-2\pi T) - 2 f_b(0)}{(2\pi T)^2}, \tag{3.26}$$

with the general functions $f_f(k_0)$ and $f_b(q_0)$. Figure 3.4 to 3.6 show diagrammatic contributions to the flow for the fermionic self-energy, the bosonic self-energy and the bosonic

Figure 3.4: Diagrammatic contribution to the fermionic self-energy.

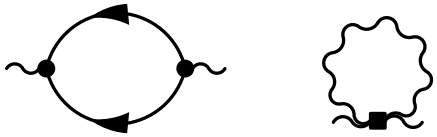

Figure 3.5: Diagrammatic contributions to the bosonic self-energy.

self-interaction.

In the flow equations Eq. (3.18)-(3.24), the prefactors in front of the integrals are identical to the prefactors obtained from an renormalization group analysis of the fermionic superfluid in the symmetric regime, which will be discussed later in chapter 4. Here, due to the interaction, several summations over band indices appear which address fermions in the lower and the upper Dirac cone.

When calculating the integrals on the right hand side explicitly, scale and external momentum derivatives of the regulators appear. For the scale derivative of the fermionic regulator the exact expression $\partial_\Lambda R^\Lambda_{f\alpha}(\mathbf{k}) = -A_f \mathrm{sgn}\left(\epsilon_{\mathbf{k}\alpha}\right)\Theta\left(\Lambda - |\epsilon_{\mathbf{k}\alpha}|\right)$ will be used, while we approximate the scale derivative of the bosonic regulator as in previous work by $\partial_\Lambda R^\Lambda_b(\mathbf{q}) \approx -2A_b\Lambda\Theta\left(\Lambda^2 - \mathbf{q}^2\right)$, where the scale derivative of the bosonic renormalization factor $\frac{d}{d\Lambda}A_b$ was neglected.

3.4.2 Rescaled flow equations at zero temperature $T = 0$

Previously, the flow equation were presented in a general form. As mentioned above, due to an appropriate choice of the sharp Litim momentum cutoff, integrands appearing on the right side of the flow become momentum independent, up to bosonic contributions to the flow of $\frac{d}{d\Lambda}A_b$. Hence, both frequency and momentum integrations can be performed analytically for all integrals and only the differential equation system for the flow has to be solved numerically.

We present the flow equation in a rescaled form, which is convenient to analyze

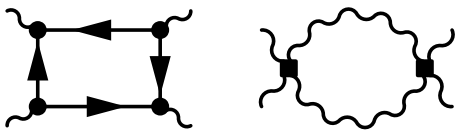

Figure 3.6: Diagrammatic contributions to the bosonic self-interaction.

the behaviour of the system close to criticality and its fix point structure. Close to the quantum critical point, several quantities show a scaling behaviour. Therefore, we introduce the rescaled variables

$$\tilde{m}_b^2 = \frac{m_b^2}{A_b \Lambda^2}, \quad \tilde{u} = \frac{u(K_d/d)}{\Lambda^{3-d}\sqrt{Z_b A_b^3}}, \quad \tilde{g} = \frac{g\sqrt{K_d/d}}{\Lambda^{\frac{3-d}{2}}\sqrt{Z_f A_f A_b}}, \quad \tilde{\lambda} = \frac{A_f}{Z_f}\sqrt{\frac{Z_b}{A_b}} \tag{3.27}$$

with the abbreviation $K_d = d\pi^{\frac{d}{2}}/(\Gamma(\frac{d}{2}+1)(2\pi)^d)$ defined as the surface of the d-dimensional unit sphere multiplied by the factor $\frac{1}{(2\pi)^d}$. We also introduce anomalous dimensions,

$$\eta_f^Z = -\frac{\partial \log Z_f}{\partial \log \Lambda}, \quad \eta_f^A = -\frac{\partial \log A_f}{\partial \log \Lambda}, \quad \eta_b^Z = -\frac{\partial \log Z_b}{\partial \log \Lambda}, \quad \eta_b^A = -\frac{\partial \log A_b}{\partial \log \Lambda}, \tag{3.28}$$

defined by the logarithmic scale derivative of the bosonic and fermionic renormalization factors. They determine the scaling behaviour of the fermionic and bosonic propagator in the infrared and indicate non-Fermi liquid behaviour and non-Gaussian behaviour, respectively.

At zero temperature the flow for the rescaled couplings reads

$$\frac{\partial \tilde{m}_b^2}{\partial \log \Lambda} = \left(\eta_b^A - 2\right)\tilde{m}_b^2 - \frac{\tilde{u}}{4}\frac{1}{(1+\tilde{m}_b^2)^{3/2}} + \tilde{g}^2 \tag{3.29}$$

$$\frac{\partial \tilde{u}}{\partial \log \Lambda} = \left(\frac{3}{2}\eta_b^A + \frac{1}{2}\eta_b^Z + d - 3\right)\tilde{u} + \frac{15}{16}\tilde{u}^2\frac{1}{(1+\tilde{m}_b^2)^{5/2}} - 6\frac{\tilde{g}^4}{\tilde{\lambda}} \tag{3.30}$$

$$\frac{\partial \tilde{g}}{\partial \log \Lambda} = \left(\frac{\eta_f^A}{2} + \frac{\eta_f^Z}{2} + \frac{\eta_b^A}{2} + \frac{d-3}{2}\right)\tilde{g} \tag{3.31}$$

$$\frac{\partial \tilde{\lambda}}{\partial \log \Lambda} = \left(-\eta_f^A + \eta_f^Z - \frac{1}{2}\eta_b^Z + \frac{1}{2}\eta_b^A\right)\tilde{\lambda} \tag{3.32}$$

and

$$\eta_f^Z = \tilde{g}^2\tilde{\lambda}^2\frac{1}{\sqrt{1+\tilde{m}_b^2}(\tilde{\lambda}+\sqrt{1+\tilde{m}_b^2})^3} + \frac{1}{2}\tilde{g}^2\tilde{\lambda}\frac{\tilde{\lambda}+3\sqrt{1+\tilde{m}_b^2}}{(1+\tilde{m}_b^2)^{3/2}(\tilde{\lambda}+\sqrt{1+\tilde{m}_b^2})^3} \tag{3.33}$$

$$\eta_f^A = 0 \tag{3.34}$$

$$\eta_b^Z = \frac{3}{4}\frac{\tilde{g}^2}{\tilde{\lambda}^2} \tag{3.35}$$

$$\eta_b^A = \frac{1}{2}\tilde{g}^2. \tag{3.36}$$

In the case of identical frequency and momentum renormalization, $Z_f \to A_f$ and $Z_b \to A_b$, implying $\tilde{\lambda} \to 1$, all flows reduce to the previous result by Strack et al. (2010).

3.4.3 Rescaled flow equations at finite temperatures $T > 0$

At finite temperatures, the execution of the Matsubara sums and the replacement of the continuous derivatives by finite difference quotients, Eq. (3.25) and (3.26), of the renormalization group equations Eq. (3.18)-(3.24), lead us to the rescaled flow equations

$$\frac{\partial \tilde{m}_b^2}{\partial \log \Lambda} = (\eta_b^A - 2)\tilde{m}_b^2 + \tilde{g}^2 \left(\tanh(\frac{1}{2T_f}) - \frac{1}{2T_f} \frac{1}{\cosh^2(\frac{1}{2T_f})} \right) \tag{3.37}$$
$$- \frac{\tilde{u}}{4} \frac{1}{(1+\tilde{m}_b^2)^{3/2}} \left[-\frac{\sqrt{1+\tilde{m}_b^2}}{2T_b} + \frac{\sqrt{1+\tilde{m}_b^2}}{2T_b} \coth^2\left(\frac{\sqrt{1+\tilde{m}_b^2}}{2T_b}\right) + \coth\left(\frac{\sqrt{1+\tilde{m}_b^2}}{2T_b}\right) \right]$$

$$\frac{\delta \tilde{u}}{\partial \log \Lambda} = \left(d - 3 + \frac{3}{2}\eta_b^A + \frac{1}{2}\eta_b^Z \right) \tilde{u} \tag{3.38}$$
$$+ 4\frac{\tilde{g}^4}{\tilde{\lambda}} \left[-\frac{3}{2}\tanh\left(\frac{1}{2T_f}\right) + \frac{3}{2}\frac{1}{2T_f}\frac{1}{\cosh^2\left(\frac{1}{2T_f}\right)} + \frac{1}{(2T_f)^2}\frac{\tanh\left(\frac{1}{2T_f}\right)}{\cosh^2\left(\frac{1}{2T_f}\right)} \right]$$
$$+ \frac{5}{8}\frac{\tilde{u}^2}{(1+\tilde{m}_b^2)^{5/2}} \left[\left(\frac{\sqrt{1+\tilde{m}_b^2}}{2T_b}\right)^2 \frac{\coth(\frac{\sqrt{1+\tilde{m}_b^2}}{2T_b})}{\sinh^2(\frac{\sqrt{1+\tilde{m}_b^2}}{2T_b})} \right.$$
$$\left. + \frac{3}{2}\left(\frac{\sqrt{1+\tilde{m}_b^2}}{2T_b}\right) \frac{1}{\sinh^2(\frac{\sqrt{1+\tilde{\delta}}}{2T_b})} + \frac{3}{2}\coth\left(\frac{\sqrt{1+\tilde{\mathrm{m}}_\mathrm{b}^2}}{2\mathrm{T_b}}\right) \right]$$

$$\eta_b^A = -\tilde{g}^2 \frac{\cosh^{-3}\left(\frac{1}{2T_f}\right)}{16T_f^2} \left[4T_f \cosh\left(\frac{1}{2T_f}\right) \right.$$
$$\left. + \sinh\left(\frac{1}{2T_f}\right)\left(1 - 4T_f^2 - 4T_f^2\cosh\left(\frac{1}{T_f}\right)\right) \right] \tag{3.39}$$

$$\eta_b^Z = -\frac{1}{8}\frac{\tilde{g}^2}{\tilde{\lambda}^2} \frac{\cosh^{-2}\left(\frac{1}{2T_f}\right)\left(1 + \pi^2 T_f^2 - \sinh\left(\frac{1}{T_f}\right)\left(3T_f + 3\pi^2 T_f^3\right)\right)}{T_f\left(1+\pi^2 T_f^2\right)^2} \tag{3.40}$$

$$\eta_f^A = 0 \tag{3.41}$$

$$
\begin{aligned}
\eta_f^Z = \frac{\tilde{g}^2}{\tilde{\lambda}^2} & \frac{1}{2\tilde{x}\tilde{T}_f\left(1-2\left(\tilde{x}^2-\pi^2\tilde{T}_f^2\right)+\left(\tilde{x}^2+\pi^2\tilde{T}_f^2\right)^2\right)^2} \\
& \cdot\Bigg\{2T_f\coth\left(\frac{\sqrt{1+\tilde{m}_b^2}}{2\tilde{T}_b}\right)\left[1-3\tilde{x}^4-2\pi^2\tilde{x}^2\tilde{T}_f^2+\pi^4\tilde{T}_f^4+2\left(\tilde{x}^2+\pi^2\tilde{T}_f^2\right)\right] \\
& \quad +\ \tilde{x}\cosh^{-2}\left(\frac{1}{2\tilde{T}_f}\right)\left[1-2\left(\tilde{x}^2-\pi^2\tilde{T}_f^2\right)+\left(\tilde{x}^2+\pi^2\tilde{T}_f^2\right)^2\right] \\
& \quad +\tilde{x}T_f\cosh^{-2}\left(\frac{1}{2\tilde{T}_f}\right)\sinh\left(\frac{1}{\tilde{T}_f}\right)\left[-3+2\left(\tilde{x}^2-\pi^2\tilde{T}_f^2\right)+\left(\tilde{x}^2+\pi^2\tilde{T}_f^2\right)^2\right)\Bigg]\Bigg\} \\
& -\frac{\tilde{g}^2}{\tilde{\lambda}^4}\frac{1}{4\tilde{x}^3\tilde{T}_f\left(1-2\left(\tilde{x}^2-\pi^2\tilde{T}_f^2\right)+\left(\tilde{x}^2+\pi^2\tilde{T}_f^2\right)^2\right)^2} \\
& \cdot\Bigg\{-2\tilde{T}_f\coth\left(\frac{\sqrt{1+\tilde{m}_b^2}}{2\tilde{T}_b}\right)\Bigg[\left(1+\left(\tilde{x}^2+\pi^2\tilde{T}_f^2\right)^2\left(3\tilde{x}^2+\pi^2\tilde{T}_f^2\right)\right) \\
& \qquad\qquad +3\tilde{x}^4-7\tilde{x}^2+3\pi^2\tilde{T}_f^2-2\pi^2\tilde{x}^2\tilde{T}_f^2+3\pi^4\tilde{T}_f^4\Bigg] \\
& \quad -\frac{\tilde{x}}{\sinh^2\left(\frac{\sqrt{1+\tilde{m}_b^2}}{2\tilde{T}_b}\right)}\left[1-\tilde{x}^2+3\pi^2\tilde{T}_f^2+(\tilde{x}^2+\pi^2\tilde{T}_f^2)^3-\tilde{x}^4-2\pi^2\tilde{x}^2\tilde{T}_f^2+3\pi^4\tilde{T}_f^4\right] \\
& \quad -16\tilde{x}^3\tilde{T}_f\tanh\left(\frac{1}{2\tilde{T}_f}\right)\left[1-\tilde{x}^2-\pi^2\tilde{T}_f^2\right]\Bigg\},
\end{aligned}
\tag{3.42}
$$

where rescaled fermionic and bosonic temperatures are introduced to eliminate an explicit scale dependence in the flow equations

$$
\tilde{T}_f \;=\; \frac{T}{\Lambda}\frac{Z_f}{A_f},\quad \tilde{T}_b=\frac{T}{\Lambda}\sqrt{\frac{Z_b}{A_b}},\quad \tilde{x}=\frac{\sqrt{1+\tilde{m}_b^2}}{\tilde{\lambda}}. \tag{3.43}
$$

In the zero temperature limit $T \to 0$, these equations reduce to the previous result Eq. (3.29)-(3.36).

In the next section 3.5, we analyze the analytic structure of the fermionic particle-particle bubble, which will justify our quadratic ansatz of the bosonic propagator in the renormalization group flow. Finally, in section 3.6, the flow equations at zero and finite temperatures are solved numerically in two dimensions, to analyze the behaviour of the system close to and at the quantum critical point.

3.5 Fermionic particle-particle bubble and correlation decay

In general, when dealing with an ansatz for the effective action, the random phase approximation (RPA) serves as a guideline, how to parametrize the frequency and momentum dependence of the bosonic propagator. The main building block for RPA-propagators in our theory, that was decoupled in the particle-particle-channel, is given by the fermionic particle-particle bubble. Therefore, we will discuss the low frequency and momentum behaviour of the fermionic particle-particle bubble in presence of and without a cutoff in subsection 3.5.1. In presence of a cutoff we will find a regular quadratic frequency and momentum dependence, which justifies our ansatz for the scale-dependent effective action Γ^{Λ}. By contrast, the analysis of the fermionic particle-particle bubble without a cutoff gives us a hint of what we possibly encounter in the infrared limit of the RG flow. Here, linear non-analytic terms will dominate the low frequency and momentum dependence, which will have a drastic impact on the correlation decay in the whole semimetallic ground state. We will discuss the real space and real time behaviour of the correlation function in the subsection 3.5.2.

3.5.1 Bare fermionic particle-particle bubble

The fermionic particle-particle bubble

$$\Pi(q_0, \mathbf{q}) = \int_{k\alpha} G_{f\alpha}(-k) G_{f\alpha}(k+q), \tag{3.44}$$

with $q = (q_0, \mathbf{q})$ enters the RPA solution of the bosonic propagator as

$$G_b^{RPA}(q) = \frac{U}{1 - U\Pi(q_0, \mathbf{q})}. \tag{3.45}$$

At zero external frequencies and momenta the bubble remains finite

$$\Pi(0,0) = \frac{K_d}{v_f^d} \frac{\Lambda_0^{d-1}}{d-1} \quad \text{for} \quad d \geq 2, \tag{3.46}$$

while it diverges below two dimensions. The density of states vanishes in dimensions $d > 1$

$$N(E) = \int_{\mathbf{k}} \delta(E - |\xi_{\mathbf{k}\alpha}|) = \begin{cases} \frac{E^{d-1}}{v_f^d} K_d & \text{if} \quad 0 < E < \Lambda_0 \\ 0 & \text{else} \end{cases} \tag{3.47}$$

at the Dirac point. Hence, a finite interaction strength is necessary to reach the superfluid state for $d \geq 2$. The constant K_d is defined as $\int \frac{d^d\mathbf{k}}{(2\pi)^d} = K_d \int d|\mathbf{k}||\mathbf{k}|^{d-1}$. Inserting the fermionic propagator and making the denominator real-valued, the bubble Eq. (3.44) reads

$$\Pi(q_0, \mathbf{q}) = \int_{k\alpha} \left(\frac{ik_0(\xi_{\mathbf{k}\alpha} - \xi_{\mathbf{k}+\mathbf{q}\alpha}) + iq_0\xi_{\mathbf{k}\alpha}}{(k_0^2 + \xi_{\mathbf{k}\alpha}^2)((k_0+q_0)^2 + \xi_{\mathbf{k}+\mathbf{q}\alpha}^2)} + \frac{k_0^2 + k_0q_0 + \xi_{\mathbf{k}\alpha}\xi_{\mathbf{k}+\mathbf{q}\alpha}}{(k_0^2 + \xi_{\mathbf{k}\alpha}^2)((k_0+q_0)^2 + \xi_{\mathbf{k}+\mathbf{q}\alpha}^2)} \right) \tag{3.48}$$

due to inflection symmetry $\xi_{-\mathbf{k}\alpha} = \xi_{\mathbf{k}\alpha}$ and band symmetry $\xi_{\mathbf{k}-\alpha} = -\xi_{\mathbf{k}\alpha}$. The external frequency and momentum dependence, respectively, of the fermionic particle-particle bubble, is given by

$$\Pi(0, \mathbf{q}) = \int_{k\alpha} \frac{k_0^2 + \xi_{\mathbf{k}\alpha}\xi_{\mathbf{k}+\mathbf{q}\alpha}}{(k_0^2 + \xi_{\mathbf{k}\alpha}^2)(k_0^2 + \xi_{\mathbf{k}+\mathbf{q}\alpha}^2)} \tag{3.49}$$

and

$$\Pi(q_0, 0) = \int_{k\alpha} \frac{k_0^2 + k_0q_0 + \xi_{\mathbf{k}\alpha}^2}{(k_0^2 + \xi_{\mathbf{k}\alpha}^2)((k_0+q_0)^2 + \xi_{\mathbf{k}\alpha}^2)}. \tag{3.50}$$

After performing frequency and momentum integrations, one finally obtains

$$\Pi(0, \mathbf{q}) = \int_{\mathbf{k}} \frac{2}{|\xi_{\mathbf{k}+}| + |\xi_{\mathbf{k}+\mathbf{q}+}|}, \quad \Pi(q_0, 0) = \int_0^{\Lambda_0} dE \frac{4EN(E)}{(q_0^2 + 4E^2)}, \tag{3.51}$$

where the band summation has already been performed.

Now we will analyze the small frequency and momentum dependence separately in two dimensions ($d = 2$). First, we begin with the frequency dependence of the bubble in situations both with and without an infrared cutoff. In the absence of a cutoff, the pure frequency dependence of the particle-particle bubble reads

$$\Pi(q_0, 0) = \frac{\Lambda_0}{2\pi v_f^2} \left[1 - \left(\frac{q_0}{2\Lambda_0} \right) \arctan\left(\frac{2\Lambda_0}{q_0} \right) \right]. \tag{3.52}$$

Expanding in $|q_0|$ leads to a linear non-analytic frequency dependence

$$\Pi(q_0,0) \overset{q_0\ll\Lambda_0}{\approx} \frac{\Lambda_0}{2\pi v_f^2}\left[1-\frac{\pi}{2}\frac{|q_0|}{2\Lambda_0}+\left(\frac{q_0}{2\Lambda_0}\right)^2+\mathcal{O}\left(\frac{|q_0|}{2\Lambda_0}\right)^3\right]. \tag{3.53}$$

Otherwise, in presence of a cutoff, the pure frequency dependence is given by

$$\Pi^\Lambda(q_0,0)=\frac{\Lambda_0}{2\pi v_f^2}\left[1-\frac{\Lambda}{\Lambda_0}-\left(\frac{q_0}{2\Lambda_0}\right)\arctan\left(\frac{2\Lambda_0}{q_0}\right)+\frac{q_0}{2\Lambda_0}\arctan\left(\frac{2\Lambda}{\mathrm{q}_0}\right)\right], \tag{3.54}$$

which yields a regular analytic expression

$$\Pi^\Lambda(q_0,0) \overset{q_0\ll\Lambda_0,\Lambda}{\approx} \frac{\Lambda_0}{2\pi v_f^2}\left[1-\frac{\Lambda}{\Lambda_0}+\frac{\Lambda-\Lambda_0}{\Lambda}\left(\frac{q_0}{2\Lambda_0}\right)^2+\mathcal{O}\left(\left(\frac{q_0}{2\Lambda_0}\right)^4\right)\right] \tag{3.55}$$

after expansion in small frequencies q_0. The non-analytic behaviour of the bubble in the infrared $\Lambda = 0$, see Eq. (3.53), is signalled by the prefactor of the quadratic term in Eq. (3.55), which diverges linearly in the limit $\Lambda \to 0$. As we will see later, this is consistent with a diverging renormalization factor Z_b in the infrared regime of the renormalization group flow. Therefore, we obtain

$$\frac{\partial}{\partial q_0}\Pi^\Lambda(q_0,0)\Big|_{q=0}=0, \quad \frac{\partial^2}{\partial q_0^2}\Pi^\Lambda(q_0,0)\Big|_{q=0}\propto\frac{1}{\Lambda}, \tag{3.56}$$

which justifies our quadratic ansatz of the frequency dependence in the bosonic propagator. In figure 3.7 the frequency dependence of the particle-particle bubble with and without cutoff is plotted, where we choose $\Lambda = 0.1\Lambda_0$.

In dimension $d = 1$ the fermionic particle-particle bubble diverges logarithmically at zero momenta and frequencies, which would signal an instability towards fermionic superfluidity for an arbitrary interaction strength if particle-hole fluctuations are neglected. In $d = 3$ the fermionic particle-particle bubble remains finite at zero frequencies and momenta and the low frequency dependence is dominated by a $q_0^2\log(|q_0|)$ term. Hence, a finite interaction strength becomes necessary to obtain a fermionic superfluid.

In the next step we analyze the small momentum dependence of the fermionic particle-particle bubble at vanishing external frequencies. Switching to polar coordinates $\mathbf{k} = (k_x, k_y) = (k_r\cos\phi, k_r\sin\phi)$ for the internal momentum integrations and for the external momenta $\mathbf{q} = (q_x, q_y) = (q_r\cos\Theta, q_r\sin\Theta)$, the bare fermionic particle-particle bubble

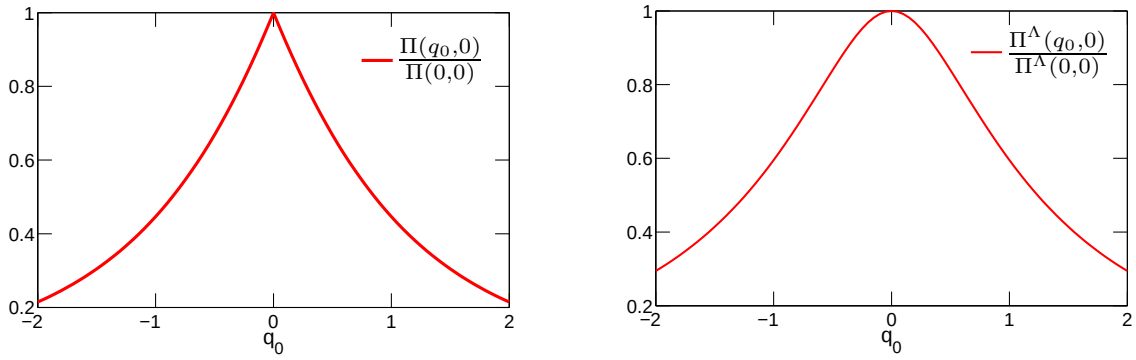

Figure 3.7: Plot of the external frequency dependence of the normalized particle-particle bubble $\Pi(q_0, 0)$ in absence and in presence of a cutoff Λ. In presence of a cutoff ($\Lambda > 0$) the fermionic particle-particle bubble exhibits a quadratic frequency dependence, while in absence of a cutoff ($\Lambda = 0$) a linear non-analytic frequency dependence appears for small scales.

reads

$$\Pi(0, \mathbf{q}) \overset{d=2}{=} \frac{2}{(2\pi)^2 v_f} \int_0^{\Lambda_0/v_f} \int_0^{2\pi} \frac{d\phi dk_r}{1 + \sqrt{1 + 2\frac{q_r}{k_r}\cos\phi + \left(\frac{q_r}{k_r}\right)^2}} \tag{3.57}$$

The regularized fermionic-particle-particle bubble reads

$$\Pi^{\Lambda}(0, \mathbf{q}) \overset{d=2}{=} \frac{2}{(2\pi)^2 v_f} \int_{\Lambda/v_f}^{\Lambda_0/v_f} \int_0^{2\pi} \frac{d\phi dk_r}{1 + \sqrt{1 + 2\frac{q_r}{k_r}\cos\phi + \left(\frac{q_r}{k_r}\right)^2}}, \tag{3.58}$$

where a sharp infrared cutoff Λ gaps out the low energy modes. The first derivative of Eq. (3.58) with respect to q_r vanishes at $q_r = 0$ and only the second derivative of Eq. (3.58) remains finite,

$$\frac{\partial}{\partial q_r}\Pi^{\Lambda}(q_0, \mathbf{q})\Big|_{q=0} = 0, \quad \frac{\partial^2}{\partial q_r^2}\Pi^{\Lambda}(0, \mathbf{q})\Big|_{q=0} \propto \frac{1}{\Lambda}, \tag{3.59}$$

but again diverges linearly in the infrared limit $\Lambda \to 0$, similar to the frequency dependence discussed above.

The analytic expression for the fermionic particle-particle bubble Eq. (3.57) with no cutoff involves lengthy expressions in terms of elliptic integrals, which indicate a non-analytic frequency dependence. A numerical integration of this expressions reveals a non-

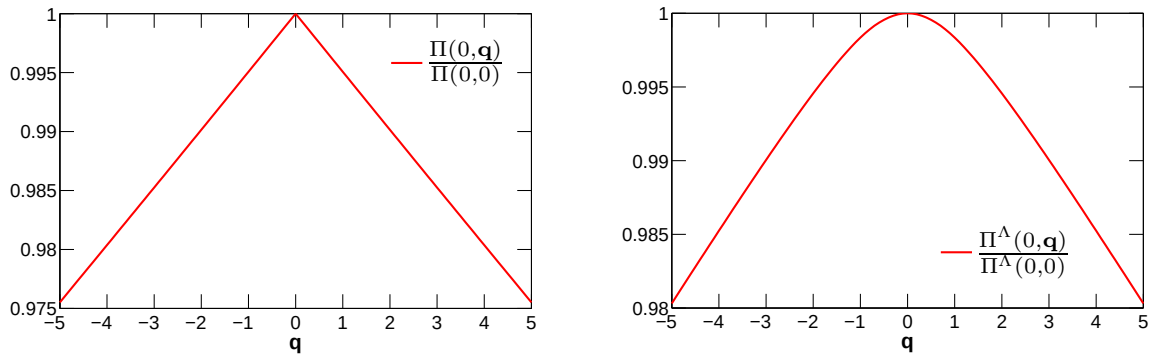

Figure 3.8: Plot of the external momentum dependence of the particle-particle bubble $\Pi(0, \mathbf{q})$ in absence and in presence of a cutoff Λ. In presence of a cutoff ($\Lambda > 0$) the fermionic particle-particle bubble exhibits a quadratic momentum dependence, while in absence of a cutoff ($\Lambda = 0$) a linear non-analytic momentum dependence appears.

analytic linear behaviour in absence of a cutoff ($\Lambda = 0$) in two dimensions and confirms this conjecture. Figure 3.8 shows the numerical results for the normalized fermionic particle-particle bubble in absence and in presence of a cutoff, $\Pi(0, \mathbf{q})$ and $\Pi^{\Lambda}(0, \mathbf{q})$.

In summary, the fermionic particle-particle bubble of the Dirac cone model develops a non-analytic behaviour for low frequencies and momenta. In presence of a cutoff scale, ($\Lambda > 0$) this non-analytic behaviour disappears, and only a quadratic frequency and momentum dependence dominates the low energy regime. The prefactor of this quadratic behaviour diverges linearly with the scale Λ^{-1} in the infrared limit $\Lambda \to 0$. This indicates the presence of non-analytic terms $|q_r|$ and $|q_0|$ for $\Lambda = 0$. Since there is a regulator throughout the renormalization group flow, which provides a cutoff scale to the theory, a quadratic ansatz in frequencies and momenta for the bosonic propagator is justified, see Eq. (3.6). Next, we will analyze the impact of these non-analytic terms on the decay of correlations in real space and time.

3.5.2 Diverging correlation length

In the previous subsection we discovered that the unregularized fermionic particle-particle bubble shows a linear non-analytic behaviour for small frequencies and momenta. Now, we will show that this feature is responsible for a diverging correlation length and time not only at the quantum critical point, but also in the entire semimetallic ground state at zero temperature. Typically, away from the quantum phase transition we would have expected a regular quadratic momentum and frequency dependence, which would immediately lead to a well-defined finite correlation length. Due to the above non-analyticities it is not

obvious how a correlation length can be defined. Therefore, we study the impact of these non-analytic terms on the long distance and long time behaviour of the correlation function. First, we revisit the well-known result for the correlation length for a system without non-analytic terms. Second, we explicitly calculate the spatial and temporal correlation decay and show that the linear non-analytic term in two dimensions leads to a power law decay, which implies infinite correlation length and time in the whole semimetallic phase.

We start with the analysis of a regular quadratic momentum and frequency dependence of the bosonic propagator, which is parametrized by finite Z and A factors,

$$\langle \phi_q^* \phi_q \rangle = G_b(q_0, \mathbf{q}) = \frac{1}{Z q_0^2 + A\mathbf{q}^2 + m_b^2}, \tag{3.60}$$

and include a mass term m_b^2, which measures the distance to the phase transition. In this subsection all three quantities are scale-independent. The spatial correlations decay exponentially

$$\langle \phi^*(\mathbf{r})\phi(0)\rangle = \int_{\mathbf{q}} G_b(0,\mathbf{q}) e^{i\mathbf{q}\cdot|\mathbf{r}|\mathbf{e}_r} = \frac{2}{A(2\pi)^2}\int_0^\infty \int_0^\pi d\phi dq_r \frac{e^{i|\mathbf{r}|q_r\cos\phi}}{q_r^2 + \frac{m_b^2}{A}} q_r \tag{3.61}$$

$$= \frac{1}{A(2\pi)}\int_0^\infty dq_r \frac{J_0(|\mathbf{r}|q_r)q_r}{q_r^2 + \frac{m_b^2}{A}} = \frac{K_0\left(\sqrt{\frac{m_b^2}{A}}|\mathbf{r}|\right)}{(2\pi)A} \overset{|\mathbf{r}|\to\infty}{\propto} e^{-\sqrt{\frac{m_b^2}{A}}|\mathbf{r}|}, \tag{3.62}$$

with the unit vector $\mathbf{e}_r = \frac{\mathbf{r}}{|\mathbf{r}|}$ in radial direction. The asymptotic behaviour is given by

$$\langle \phi^*(\mathbf{r})\phi(0)\rangle \overset{|\mathbf{r}|\to\infty}{\propto} e^{-\frac{|\mathbf{r}|}{\xi}}, \tag{3.63}$$

where in the last line the correlation length $\xi = \sqrt{A/m_b^2}$ is introduced. $J_0(x)$ denotes the Bessel function of the first kind and $K_0(x)$ the modified Bessel function of second kind. A similar result can be obtained for the temporal correlations, which also decay exponentially

$$\langle \phi^*(t)\phi(0)\rangle = \int_{q_0} G_b(q_0,0)e^{-iq_0 t} = \frac{1}{Z}\int_{-\infty}^\infty \frac{dq_0}{2\pi}\frac{e^{-iq_0 t}}{q_0^2 + \frac{m_b^2}{Z}} \tag{3.64}$$

$$\langle \phi^*(t)\phi(0)\rangle \propto e^{-\frac{|t|}{\xi_\tau}}. \tag{3.65}$$

with the correlation time defined as $\xi_\tau = \sqrt{Z/m_b^2}$. Hence, a regular quadratic frequency and momentum dependence of the bosonic propagator leads to a finite correlation time

and length $\xi, \xi_\tau < \infty$ away from criticality ($m_b^2 \neq 0$).

We now move on to the case of a non-analytic term in the bosonic propagator

$$G_b^{-1}(q) = Zq_0^2 + A\mathbf{q}^2 + Z_l|q_0| + A_l|\mathbf{q}| + m_b^2, \tag{3.66}$$

where Z and A again parametrize the regular quadratic frequency and momentum dependence. Additionally, linear non-analytic frequency and momentum dependencies are added to the propagator and parametrized by Z_l and A_l, respectively.

First, we analyze the spatial correlation decay

$$\begin{aligned}\langle\phi^*(\mathbf{r})\phi(0)\rangle &= \frac{1}{(2\pi)}\int_0^\infty dq_r \frac{J_0(|\mathbf{r}|q_r)q_r}{Aq_r^2 + A_l|q_r| + m_b^2} = \frac{1}{(2\pi)A}\int_0^\infty \frac{J_0(|\mathbf{r}|q_r)q_r}{(q_r+a)(q_r+b)} \\ &= \frac{1}{(2\pi)A}\left[\frac{\pi}{2}\frac{b}{b-a}\left(H_0(b|\mathbf{r}|) - N_0(b|\mathbf{r}|)\right) - \frac{\pi}{2}\frac{a}{b-a}\left(H_0(a|\mathbf{r}|) - N_0(a|\mathbf{r}|)\right)\right],\end{aligned} \tag{3.67}$$

which can be easily expressed in a sum of Struve functions $H_0(x)$ and Bessel functions of second kind (also called Neumann functions) $N_0(x)$, by a partial fraction decomposition with the zeros

$$a = \frac{A_l}{2A} + \sqrt{\left(\frac{A_l}{2A}\right)^2 - \frac{m_b^2}{A}}, \quad b = \frac{A_l}{2A} - \sqrt{\left(\frac{A_l}{2A}\right)^2 - \frac{m_b^2}{A}}. \tag{3.68}$$

Using the formula for the asymptotic behaviour for the difference between Struve and Neumann functions, see Gradshteyn and Ryzhik (1965) formula 8.554,

$$H_0(a|\mathbf{r}|) - N_0(a|\mathbf{r}|) \overset{|\mathbf{r}|\to\infty}{\approx} \frac{1}{\pi}\sum_{n=0} c_n \left(\frac{a|\mathbf{r}|}{2}\right)^{-2n-1} \tag{3.69}$$

with the expansion coefficient $c_n = \frac{\Gamma(n+\frac{1}{2})}{\Gamma(\frac{1}{2}-n)}$, the long distance behaviour of the correlation function is given by a power law decay

$$\langle\phi^*(\mathbf{r})\phi(0)\rangle \propto \frac{1}{|\mathbf{r}|^3} \tag{3.70}$$

with exponent three, which indicates an infinite correlation length in the whole semimetal phase at zero temperature. The weaker decay of order $\frac{1}{|\mathbf{r}|}$ in the asymptotic behaviour Eq. (3.69) cancels out, due to the structure of the coefficients in Eq. (3.68). The double logarithmic plot in figure 3.9 of the spatial correlation confirms this analytic result.

In the limit of a vanishing linear non-analyticity $A_l = 0$ the coefficients Eq. (3.68)

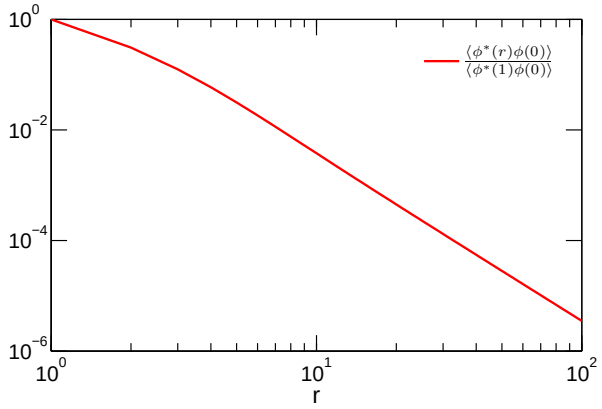

Figure 3.9: Decay of spatial correlation $\langle\phi^*(\mathbf{r})\phi(0)\rangle$ reveals a power law $\propto \frac{1}{|\mathbf{r}|^3}$ at long distances.

reduce to

$$a = i\sqrt{\frac{m_b^2}{A}}, \quad b = -i\sqrt{\frac{m_b^2}{A}}, \tag{3.71}$$

and we obtain for the spatial correlation the expression

$$\begin{aligned}\langle\phi^*(\mathbf{r})\phi(0)\rangle &= \frac{1}{(2\pi)A}\int_0^\infty dq_r \frac{J_0(|\mathbf{r}|q_r)q_r}{q_r^2 + \frac{m_b^2}{A}} \\ &= \frac{1}{(2\pi)A}\frac{\pi}{4}\left[H_0(a|\mathbf{r}|) + H_0(-a|\mathbf{r}|) - N_0(a|\mathbf{r}|) - N_0(-a|\mathbf{r}|)\right] \\ &= \frac{-1}{(2\pi)A}\frac{\pi}{4}\Big[N_0(a|\mathbf{r}|) + N_0(-a|\mathbf{r}|)\Big] = \frac{K_0\left(\sqrt{\frac{m_b^2}{A}}|\mathbf{r}|\right)}{(2\pi)A}.\end{aligned} \tag{3.72}$$

Hence, an exponential decay for the spatial correlation

$$\langle\phi^*(\mathbf{r})\phi(0)\rangle \overset{|\mathbf{r}|\to\infty}{\propto} e^{-\frac{|\mathbf{r}|}{\xi}} \tag{3.73}$$

reappears with a finite correlation length $\xi = \sqrt{A/m_b^2}$.

In a similar way, the temporal correlations

$$\langle \phi^*(t)\phi(0)\rangle = \int_{-\infty}^{\infty} \frac{\exp(-iq_0 t)}{Zq_0^2 + Z_l|q_0| + m_b^2} \frac{dq_0}{2\pi} \tag{3.74}$$

$$= \frac{2}{Z}\int_0^{\infty} \frac{\cos(q_0 t)}{(q_0+a)(q_0+b)} \frac{dq_0}{2\pi} \tag{3.75}$$

$$= \frac{2}{2\pi Z(b-a)} \Big[-\cos(a|t|)\,\mathrm{Ci(a|t|)} + \sin(\mathrm{a|t|})\left(\frac{\pi}{2} - \mathrm{Si(a|t|)}\right) + \cos(b|t|)\,\mathrm{Ci(b|t|)} - \sin(\mathrm{b|t|})\left(\frac{\pi}{2} - \mathrm{Si(b|t|)}\right)\Big] \tag{3.76}$$

can be studied, where $\mathrm{Ci}(x) = -\int_x^{\infty} \frac{\cos(t)}{t}$ and $\mathrm{Si}(x) = \int_0^x \frac{\sin(t)}{t}$ denote the cosine integral and the sine integral. Here, one obtains a power law decay in time with a quadratic exponent for the temporal correlation function

$$\langle \phi^*(t)\phi(0)\rangle \propto \frac{1}{t^2}. \tag{3.77}$$

Again a partial fraction decomposition is performed with the coefficients

$$a = \frac{1}{2}\frac{Z_l}{Z} + \sqrt{\left(\frac{Z_l}{Z}\frac{1}{2}\right)^2 - \left(\frac{m_b^2}{Z}\right)}, \quad b = \frac{1}{2}\frac{Z_l}{Z} - \sqrt{\left(\frac{Z_l}{Z}\frac{1}{2}\right)^2 - \left(\frac{m_b^2}{Z}\right)}, \tag{3.78}$$

which in the limit $Z_l = 0$ reduce to

$$a = i\sqrt{\frac{m_b^2}{Z}}, \quad b = -i\sqrt{\frac{m_b^2}{Z}}, \tag{3.79}$$

and lead to an exponential decay of the temporal correlations

$$\langle \phi^*(t)\phi(0)\rangle \overset{t\gg 1}{=} e^{-\frac{|t|}{\xi_\tau}} \tag{3.80}$$

with the correlation time $\xi_\tau = \sqrt{Z/m_b^2}$. Figure 3.10 confirms the analytic result with a double logarithmic plot of the bosonic correlation function versus time.

In summary, due to the non-analytic momentum and frequency structure of the fermionic particle-particle bubble Eq. (3.44) at zero temperature in two dimensions, both temporal and spatial correlations decay with power laws in the entire semimetallic phase

$$\langle \phi^*(t)\phi(0)\rangle \propto \frac{1}{t^2}, \quad \langle \phi^*(\mathbf{r})\phi(0)\rangle \propto \frac{1}{|\mathbf{r}|^3}, \tag{3.81}$$

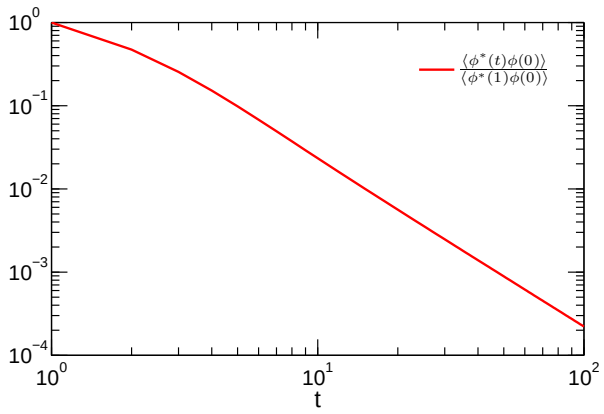

Figure 3.10: Decay of temporal correlation $\langle\phi^*(t)\phi(0)\rangle$ reveals a power law $\propto \frac{1}{t^2}$ at long timescales.

which implies an infinite correlation length and correlation time

$$\xi, \xi_\tau = \infty. \tag{3.82}$$

These RPA-like results will be confirmed by the numerical solution of the functional RG flow in the next section 3.6. In the infrared, the renormalization factors A_b^Λ and Z_b^Λ, which parametrize the quadratic momentum and frequency dependencies, diverge linearly with the cutoff scale $\propto \Lambda^{-1}$, which implies an infinite correlation length and correlation time even away from the quantum critical point at $T = 0$.

3.6 Numerical results

In this section, the numerical solution of the renormalization group equations is presented. The program for the renormalization group flow is implemented with the Mathematica software package and runs on a single double-core CPU. The system of differential equations is solved with a standard Runge-Kutta solver of fourth order. The flow is solved in two dimensions ($d = 2$), at zero and finite temperatures and with an ultraviolet cutoff $\Lambda_0 = 1$. First, the behaviour at the quantum critical point is discussed in subsection 3.6.1. Second, the semimetallic ground state will be analyzed in subsection 3.6.2, and finally the quantum critical regime above the quantum critical point is studied in subsection 3.6.3.

3.6.1 Quantum critical point: $T = 0$, $U = U_{qc}$

To determine the location of the quantum critical point at zero temperature, the fermionic two-particle interaction U is fine-tuned in such a way that the bosonic mass renormalizes down to zero ($m_b^2 \to 0$) in the infrared limit $\Lambda \to 0$. We find a critical interaction of $U_{qc} = -15.646$. Compared to the mean-field value, the critical interaction is larger by a factor of 2.5, so that the symmetry-broken phase shrinks due to the impact of fluctuations, as expected.

Due to the vanishing mass ($m_b^2 \to 0$) the pairing susceptibility χ diverges at the critical point. The correlation length ξ and the correlation time ξ_τ are also infinite, since the bosonic renormalization factors $Z_b, A_b \to \infty$ diverge in the infrared, see figure 3.12, at the quantum critical point. As expected, at criticality scaling occurs and the rescaled variables in Eq. (3.27) show a scaling behaviour at intermediate scales down to the infrared. Figure 3.13 shows the scaling of the rescaled bosonic mass $\tilde{m}_b^2$, the bosonic self-interaction $\tilde{u}$ and the Yukawa vertex $\tilde{g}$. As mentioned, the bosonic renormalization factors Z_b, A_b and the fermionic renormalization factor Z_f diverge as power laws in terms of the vanishing scale $\Lambda \to 0$, which is illustrated on the left side of figure 3.12. By contrast, the fermionic renormalization factor parametrizing the momentum dependence A_f does not renormalize at all. The right hand side of figure 3.12 shows the finite fermionic and bosonic anomalous dimensions, Eq. (3.28), corresponding to the diverging renormalization factors, which signal non-Gaussian and non-Fermi liquid behaviour at the quantum critical point. A fixpoint analysis of the equations Eq. (3.29)-(3.36) leads to similar results for the anomalous dimensions.

The fixpoint equations $\frac{\partial \log \tilde{g}}{\partial \log \Lambda} = 0$ and $\frac{\partial \log \tilde{\lambda}}{\partial \log \Lambda} = 0$ lead to scaling equations

$$\eta_b^A + \eta_f^Z + \eta_f^A = 3 - d, \qquad \eta_b^Z - \eta_b^A = 2(\eta_f^Z - \eta_f^A). \tag{3.83}$$

between fermionic and bosonic anomalous dimensions. Since the fermionic renormalization factor for the momentum dependence remains constant during the flow, $\eta_f^A = 0$, and the scaling equations reduce to

$$\eta_b^A + \eta_f^Z = 3 - d, \qquad \eta_b^Z - \eta_b^A = 2\eta_f^Z. \tag{3.84}$$

The numerical values for the anomalous dimensions read

$$\eta_b^A \approx 0.75, \quad \eta_b^Z \approx 1.25, \quad \eta_f^Z \approx 0.25 \tag{3.85}$$

in two dimensions at the quantum critical point. They are obtained by the numerical solution of the flow, if one approaches the quantum critical point from the semimetallic phase, see figure 3.15 or from the finite temperature regime above the critical point, see figure 3.16.

The divergence of the fermionic Z_f renormalization factor indicates a breakdown of the quasi-particle picture and the occurrence of non-Fermi liquid behaviour, which is common in quantum critical interacting fermion systems.[1] The fermionic renormalization factor A_f, parametrizing the momentum dependence does not renormalize at all, which leads together with $Z_f \to \infty$ to a vanishing Fermi velocity $v_f = 0$ at the quantum critical point. This was missed in the previous work by Strack et al. (2010), since a common renormalization factor for the frequency and momentum dependence of the fermionic propagator was used there.

As mentioned, due to the finite bosonic anomalous dimensions, the order parameter shows non-Gaussian critical behaviour with different scaling of momentum and frequency dependence.[2] This unequal scaling between momenta and frequencies leads to an anomalous dynamical exponent of

$$z_f = 1 + \eta_f^Z - \eta_f^A = z_b = 1 + \frac{\eta_b^Z - \eta_b^A}{2} \approx 1.25. \tag{3.86}$$

in contrast to the bare value $z_f = z_b = 1$ of the bare action. The critical dynamical exponents for fermions and bosons are identical due to the scaling relation in Eq. (3.84).

[1] For instance, the fermionic self-energy exhibits an anomalous frequency scaling $\propto \omega^{2/3}$ at the quantum critical point associated with a d-wave Pomeranchuk instability, which was studied by Metzner et al. (2003) and Dell'Anna and Metzner (2006).

[2] It was shown by Abanov et al. (2000, 2003, 2004) that at an antiferromagnetic QCP of the spin-fermion model, the spin susceptibility also exhibits anomalous scaling behaviour in the momentum $\propto |\mathbf{q}|^{-1.75}$.

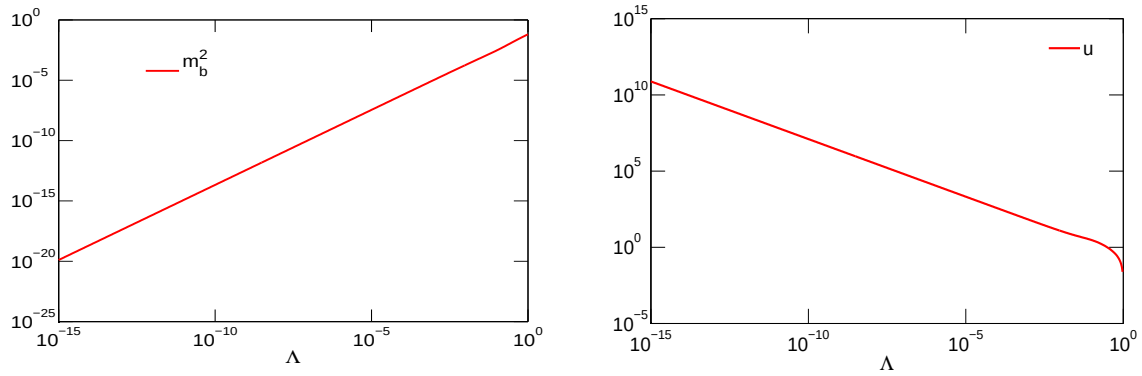

Figure 3.11: At the quantum critical point, the bosonic mass renormalizes down to zero m_b^2 and the local bosonic self-interaction u diverges in the infrared limit $\Lambda \to 0$.

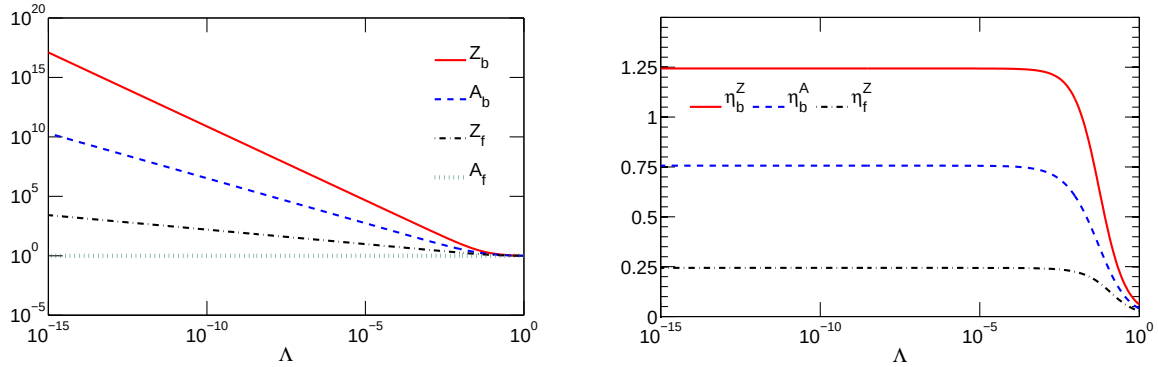

Figure 3.12: The bosonic renormalization factors A_b and Z_b and the fermionic renormalization factor Z_f diverge at the quantum critical point in the infrared, implying finite anomalous dimensions and therefore non-Gaussian and non-Fermi liquid behaviour. Several scaling laws are satisfied. The fermionic renormalization factor A_f, which parametrizes the momentum dependence, does not renormalize at all.

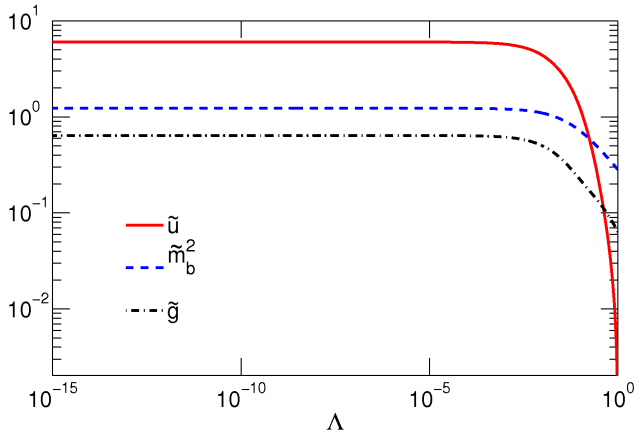

Figure 3.13: The rescaled bosonic mass $\tilde{m}_b^2$, bosonic self-interaction $\tilde{u}$ and Yukawa coupling $\tilde{g}$ start scaling at intermediate scales down to the infrared $\Lambda \to 0$ at the quantum critical point.

3.6.2 Semimetallic phase: $T = 0$, $|U| < |U_{qc}|$

In the semimetallic phase, at zero temperature and away from the quantum critical point, the bosonic mass saturates in the infrared ($m_b^2 > 0$). The susceptibility χ is finite, but diverges when approaching the quantum critical point as a power law

$$\chi \propto (|U_{qc}| - |U|)^{-\gamma_0} \tag{3.87}$$

with an exponent $\gamma_0 \approx 1.725$, see figure 3.14.

One would expect a similar behaviour for the correlation length. In our case it turns out that the renormalization factors Z_b^Λ and A_b^Λ, parametrizing the frequency and momentum dependence in the bosonic propagator do not saturate in the infrared $\Lambda \to 0$, but diverge as a power law $\propto 1/\Lambda$, see left side of figure 3.15. Thus, finite anomalous dimensions $\eta_b^A = \eta_b^Z = 1$ appear in the entire semimetallic phase and not only at the quantum critical point, as illustrated on the right side of figure 3.15. This indicates a non-analytic linear scaling of the bosonic propagator in the infrared in the frequency and momentum dependence, and a diverging correlation length and time

$$\xi, \xi_\tau = \infty \tag{3.88}$$

due to $\xi = \sqrt{\frac{A_b^{\Lambda=0}}{m_b^2}}$ and $\xi_\tau = \sqrt{\frac{Z_b^{\Lambda=0}}{m_b^2}}$. Both results are consistent with the RPA-like analysis from section 3.5. There, the regularized fermionic particle-particle bubble showed a quadratic momentum and frequency dependence, but with a prefactor which diverges

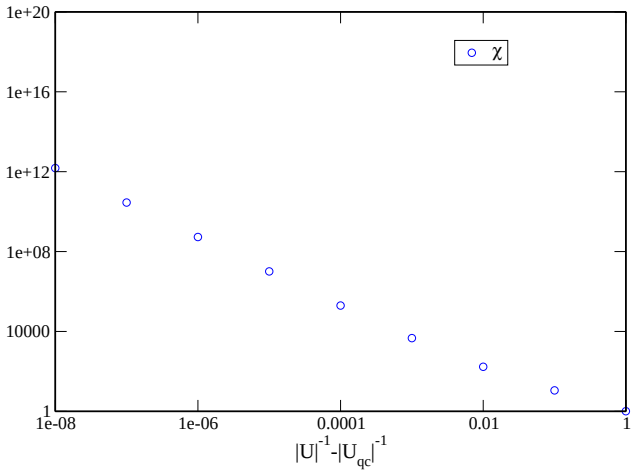

Figure 3.14: Approaching the quantum critical point at zero temperature, the susceptibility diverges as a power law in the interaction strength U.

linearly in the infrared $\propto 1/\Lambda$, indicating a non-analytic linear momentum and frequency dependence. Second, the Fourier transformation of the non-analytic propagator leads to a power law decay of spatial and temporal correlations, implying an infinite correlation time and length $\xi_\tau = \infty$ and $\xi = \infty$. Both results are reproduced within our functional renormalization group approach. In theories discussing interactions in graphene, the Dirac point is seen as a quantum phase transition between a hole-doped and a electron-doped Fermi liquid (Sheehy and Schmalian (2007)). This resembles the situation we encounter, however in their work the diamagnetic susceptibility also diverges at the quantum critical point. Thermodynamical properties, as in Sheehy and Schmalian (2007) or transport properties as discussed in Fritz et al. (2008), can then be calculated with scaling concepts from the critical theory.

As can be seen from figure 3.15, both fermionic renormalization factors Z_f and A_f remain finite at the end of the flow, leading to a vanishing fermionic anomalous dimension $\eta_Z^f, \eta_A^f = 0$. At intermediate scales finite anomalous dimensions appear, which correspond to the critical behaviour at the critical point, since we are close to the QCP but still in the semimetallic ground state. Hence, finite fermionic quasi-particle excitations remain with a finite Fermi velocity $v_f \neq 0$.

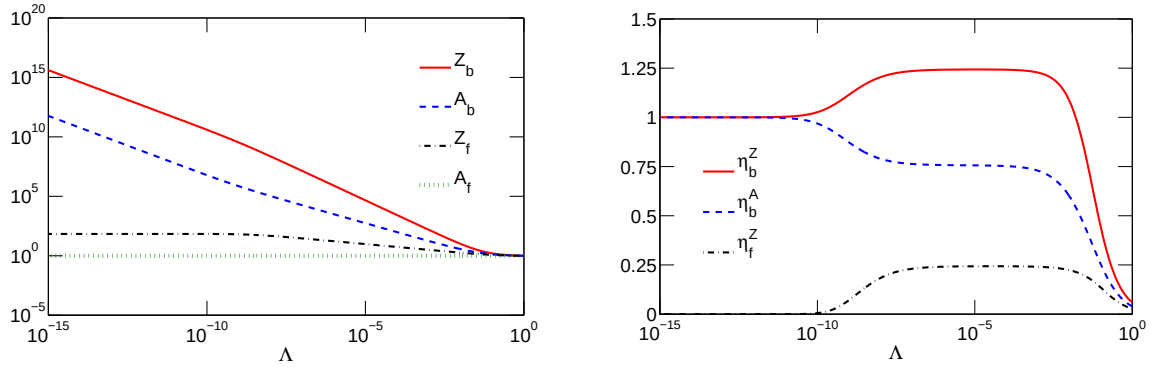

Figure 3.15: In the semimetallic ground state, the bosonic renormalization factors Z_b and A_b do not saturate, but diverge with a power law $\propto \Lambda^{-1}$. Therefore, finite bosonic anomalous dimensions are found, which indicate a non-analytic linear behaviour in frequency and momentum dependence of the bosonic propagator leading to an infinite correlation length in the entire semimetallic ground state. We emphasize that in both figures the system is in the semimetallic phase, however close to the quantum critical point. Hence, on intermediate scales also other anomalous dimensions are visible, which coincide with the values for the anomalous dimensions at the quantum critical point.

3.6.3 Quantum critical region: $T > 0$, $U = U_{qc}$

In the finite temperature regime above the quantum critical point, the temperature T acts naturally as a cutoff, since no modes exist below frequencies $k_0 \leq \pi T$ in the fermionic particle-particle bubble. Hence, all renormalization factors for the fermionic and bosonic frequency and momentum dependence saturate in the infrared limit $\Lambda \to 0$. Thus, no finite anomalous dimensions exist above the quantum critical point, see left and right side of figure 3.16. Again at intermediate scales anomalous dimensions are visible, which correspond to the quantum critical behaviour, since we are close to but still above the QCP. The renormalization factors diverge as a power law in the temperature

$$A_b \propto T^{-\bar{\eta}_b^A}, \quad Z_b \propto T^{-\bar{\eta}_b^Z}, \quad Z_f \propto T^{-\bar{\eta}_f^Z} \tag{3.89}$$

with the exponents $\bar{\eta}_b^A \approx 0.60$, $\bar{\eta}_b^Z \approx 1.00$ and $\bar{\eta}_f^Z \approx 0.20$.

As illustrated in figure 3.17 the susceptibility and the correlation length remain finite in the finite temperature region and only diverge at the quantum critical point. They obey a power law behaviour close to the quantum critical point

$$\chi \propto T^{-\gamma}, \quad \xi \propto T^{-\nu}, \quad \xi_\tau \propto T^{-\nu_\tau}, \tag{3.90}$$

which are derived from $\chi \propto (T - T_c)^{-\gamma}$ and $\xi \propto (T - T_c)^{-\nu}$ with the critical temperature

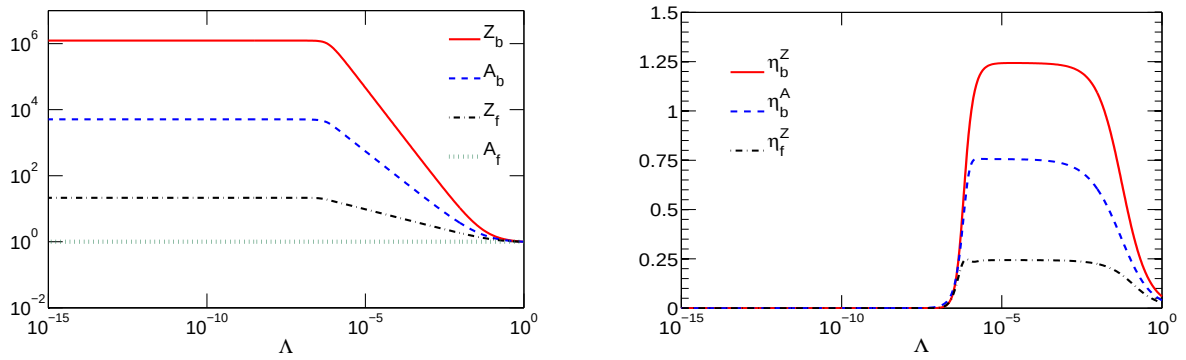

Figure 3.16: The quantum critical point is approached from finite temperatures. Bosonic and fermionic renormalization factors (Z_b, A_b and Z_f) scale and finite anomalous dimensions are found on intermediate scales. They coincide with the anomalous dimensions at the quantum critical point, since we are close to QCP but still in the finite temperature regime. In the infrared limit the temperature acts as an cutoff and leads to finite renormalization factors and vanishing anomalous dimensions.

$T_c = 0$. The corresponding critical exponents read

$$\gamma \approx 1.00, \quad \nu \approx 0.80, \quad \nu_\tau \approx 1.00 \tag{3.91}$$

We find that the dynamical exponent is the inverse of the critical exponent of the correlation length $z_b = \frac{1}{\nu}$, which is consistent with the scaling of the correlation time $\xi_\tau \propto T^{-1}$. Finally, the critical exponents obey the classical scaling law, see Goldenfeld (1992)

$$\gamma = (2 - \eta_b^A)\nu. \tag{3.92}$$

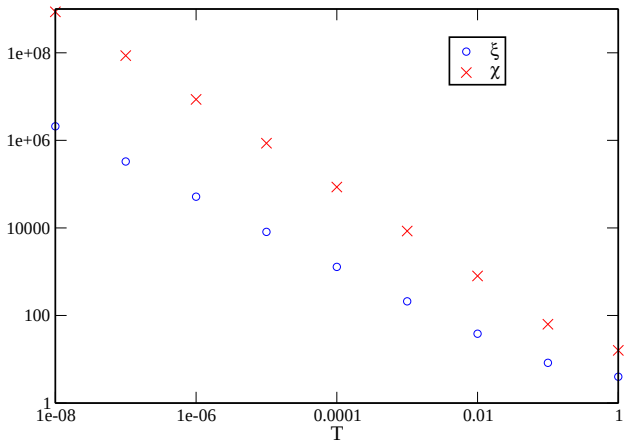

Figure 3.17: Approaching the quantum critical point from finite temperatures leads to a power law divergence of both the susceptibility and the correlation length.

3.7 Conclusion

This chapter was devoted to a study of the Dirac cone model, which exhibits a quantum phase transition between semimetal and superfluid. The analysis of the zero and finite temperature regime around the quantum critical point in two dimensions was performed within a fermion-boson functional renormalization group method. At the quantum critical point non-Fermi liquid and non-Gaussian behaviour occurred. A different renormalization of the frequency and momentum dependence led to a vanishing Fermi-velocity. In the semimetallic ground state away from the quantum critical point the fermionic particle-particle bubble showed a non-analytic behaviour in the absence of a cutoff. This leads to a power law decay of temporal and spatial correlations, which was confirmed within our functional RG approach. Hence, the semimetallic ground state seems to be critical, due to the infinite correlation time and correlation length, while the pairing susceptibility remains finite. Approaching the quantum critical point from the finite temperature region, both correlation length and pairing susceptibility diverge as a power law behaviour with critical exponents, as expected. The critical exponents and anomalous dimensions obey several scaling laws.

CHAPTER 4

Project 2: Low-energy singularities in fermionic superfluids

In this chapter we analyze the ground state of a fermionic superfluid with functional renormalization group methods in the 1PI formulation. Due to the attractive interaction between the fermionic particles, spontaneous symmetry breaking occurs towards s-wave superfluidity. The absence of the Anderson-Higgs mechanism[1] in charge-neutral fermionic superfluids leads to the emergence of massless Goldstone excitations. Several divergences occur due to the massless character of these excitations in the infrared, requiring an RG treatment. To investigate the mutual interplay between fermions and order parameter fluctuations, we analyze the low-energy physics of the fermionic superfluid by a coupled fermion-boson theory. The order parameter fluctuations, described by the bosonic field, are decomposed into transverse and longitudinal components. We then study the infrared asymptotics of the flow, where bosonic fluctuations decouple from the fermions and especially the Goldstone boson dominates the behaviour of the flow. The non-locality of the bosonic self-interaction plays a major role. Several cancellations of divergencies will occur. We show that the spectral weight of the Goldstone mode is preserved and the Goldstone theorem is explicitly fulfilled within our truncation. Lowest order Ward identities are respected by our truncation. The collective excitations behave as an interacting Bose gas. In this work we achieve a consistent treatment of the fermionic and bosonic sector in a minimal truncation of the functional RG flow equations.

This chapter is structured as follows. We begin with a brief historical overview of

[1] For the discovery of the Anderson-Higgs mechanism P. W. Higgs and F. Englert were honoured with the Nobel prize 2013, see Higgs (1964), Anderson (1958, 1963) and Englert and Brout (1964).

fermionic superfluidity and a short review about spontaneous symmetry breaking in the functional RG literature, see section 4.1. Section 4.2 introduces the attractive Hubbard model as a prototype model for fermionic superfluidity and presents mean-field results. The truncation and ansatz of the scale-dependent effective action for the coupled fermion-boson theory is presented in section 4.3. We distinguish between the symmetric regime above and the symmetry-broken regime below the critical scale Λ_c. The RG flow for self-energies and couplings parametrizing the effective action can be found in section 4.4. In section 4.5 Ward identities and the Goldstone theorem are discussed. Subsequently, analytic results for the asymptotic behaviour of the flow in the infrared limit are presented in section 4.6. Section 4.7 discusses the low frequency behaviour of the fermionic particle-particle bubble and numerical results of a mean-field flow of our RG equations. Finally, section 4.8 shows numerical results for the RG equation in two dimensions. The chapter closes with a conclusion in section 4.9.

4.1 Introduction

Due to their s-wave superfluid ground state the attractive Hubbard model and continuum models for attractively interacting fermions are often applied as prototype models for fermionic superfluidity on the lattice and in the continuum, respectively. Hence, they are of high interest in the area of ultracold atom gases. Nowadays, sophisticated experimental setups facilitate the simulation of many-body models in the laboratory. For reviews concerning bosonic atoms see Jaksch and Zoller (2005) and for fermionic and bosonic atoms see Bloch et al. (2008). Thereby, ultracold bosonic and fermionic atoms, respectively, are loaded in an atomic trap and the interactions between them are tuned by Feshbach resonances. Hofstetter et al. (2002) proposed such a setup for fermionic atoms and Chin et al. (2006) found for the first time evidence for superfluidity of ultracold fermionic atoms in an optical lattice. An interesting phenomenon occurring in such fermionic systems with attractive interaction is given by the so-called BEC-BCS crossover, see Griffin et al. (1995) and Keller et al. (1999, 2001). For every finite interaction strength Cooper pairs are formed by fermions with opposite spin direction. For weak interactions only weakly bound pairs exist, whereas for strong interactions tightly bound pairs exist which can undergo a Bose-Einstein condensation. Both regimes are connected by a smooth crossover. Even in the weak-coupling limit particle-hole fluctuations lead to a reduction of the superconducting gap compared to the mean-field result, see Gorkov and Melik-Barkhudarov (1961) and Martin-Rodero and Flores (1992).

Several approaches have been used to analyze fluctuation effects in these systems.

Continuous models for interacting fermionic atoms in three dimensions were intensively investigated by functional RG methods, for reviews see Diehl et al. (2010) and Scherer et al. (2010). Three dimensional continuous models and the attractive Hubbard model often serves as a testbed for new methods and approximations. We now briefly review two distinct technical routes towards spontaneous symmetry breaking in interacting Fermi systems within the functional RG method. The RG flow in systems with spontaneous symmetry breaking is characterized by a divergence of the two-particle vertex at a critical scale, where anomalous fermionic expectation values appear, see Metzner et al. (2012) for a detailed review.

The first route is given by a purely fermionic approach and was pioneered by Salmhofer et al. (2004). By adding a small symmetry breaking field to the bare microscopic action the divergence of the two-particle vertex is regularized at the critical scale. Therefore, the RG flow can be continued to the symmetry-broken phase. Only at the end of the flow the symmetry breaking field is sent to zero. The truncation proposed by Katanin (2004) solves mean-field models exactly, see Salmhofer et al. (2004), Gersch et al. (2005) and Gersch et al. (2006). The attractive Hubbard model was investigated by Gersch et al. (2008) as a non-mean-field model within the so-called N-patch approach in the Katanin scheme. The Fermi surface is split into several segments which are called patches. Irrelevant frequency and momentum dependencies were neglected. Reasonable values for the fermionic single-particle gap were found in this rather crude parametrization. Eberlein (2013) and Eberlein and Metzner (2013) examined the attractive Hubbard model by a comprehensive numerical analysis of the functional RG flow. Extending the channel decomposition proposed by Husemann et al. (2009) to the symmetry-broken phase, they continued the RG flow into the symmetry-broken phase within a fermionic functional RG approach and considered the full frequency dependence of the vertex. Previous results for the superconducting gap were confirmed for weak and intermediate interaction strength. However, it turned out that global Ward identities are not captured within the Katanin truncation. Ward identities and the Goldstone theorem had to be enforced by a projection method. A one-loop truncation of the flow treats order parameter fluctuations rather poorly, important terms capturing the correct renormalization behaviour of the longitudinal mass are only included on two-loop level.

The second route towards symmetry breaking was pioneered by Baier et al. (2004) in a study of antiferromagnetism in the repulsive Hubbard model. An order parameter field is introduced in the original purely fermionic theory via a Hubbard-Stratonovich transformation, see Popov (1987). Afterwards, the coupled theory with both fermionic and bosonic degrees of freedom is analyzed with the functional RG method. Over the

years, different studies have been performed. Krahl and Wetterich (2007) discussed the Kosterlitz-Thouless transition in two dimensional superfluids and Diehl et al. (2007) analyzed the BEC-BCS crossover. The ground state of a fermionic superfluid was investigated by several authors: Birse et al. (2005), Diehl et al. (2007), Krippa (2007), Strack et al. (2008), Flörchinger et al. (2008) and Bartosch et al. (2009).

The importance of fluctuations on fermionic superfluids is well-known. Feldman et al. (1993) studied mathematically rigorously the impact of fluctuations on fermionic superfluids and proved the pertubative renormalizability of singularities caused by the Goldstone mode. Several singularities cancel out due to symmetry and conservation laws as Ward identities are fulfilled. Other singularities require a renormalization group analysis. Diener et al. (2008) studied the impact of Gaussian fluctuations on such a system. As mentioned above, several authors analyzed the ground state of the system with a functional RG analysis in simple truncations. Birse et al. (2005) proposed the first truncation of the fermion-boson functional RG flow to describe the fermionic superfluid. Other truncations followed, which also discussed the BCS-BEC crossover (Krippa (2007) and Diehl et al. (2007)). Flörchinger et al. (2008) additionally took particle-hole fluctuations into account. Bartosch et al. (2009) analyzed the fermionic superfluid with a combined approach of functional RG and Dyson-Schwinger equations. They distinguished between the fermionic gap and the bosonic order parameter, which were connected by a Yukawa coupling. One year earlier, a distinction between both quantities was already considered by Strack et al. (2008) in a truncation of the fermion-boson functional RG approach, where they analyzed the interplay between fermions and order parameter fluctuations in the attractive Hubbard model. In contrast to other authors, they distinguished longitudinal and transverse directions of bosonic fluctuations in the symmetry-broken regime. They found the correct infrared asymptotic for the longitudinal bosonic mode consistent with the behaviour of an interacting Bose gas. This is expected since the fermionic excitations are totally gapped in a fermionic s-wave superfluid. Singularities were driven by the massless Goldstone mode. The interacting Bose gas was analyzed in early works in a perturbative approach by Nepomnyashchy (1992) and later in a comprehensive work by Castellani et al. (1997) and Pistolesi et al. (2004) within a field-theoretical RG approach.[2]

However, Strack et al. (2008) did not capture the correct infrared behaviour of the Goldstone mode within the truncation. The Goldstone theorem and the finiteness of the transverse renormalization factor were implemented by hand.[3] Moreover, a subleading

[2]Dupuis et al. (2009) and Sinner et al. (2009, 2010) analyzed the interacting Bose gas behaviour within an functional RG approach.

[3]The Goldstone theorem was also implemented by hand in the study by Bartosch et al. (2009), where the fermionic superfluid was analyzed within a combined approach with Schwinger Dyson equations and

linear imaginary frequency dependence, which would lead to a mixing between transverse and longitudinal fluctuations, was neglected in the truncation.

In our approach we extend this work of Strack et al. (2008) in several directions. We follow the spirit of analyzing a coupled fermion-boson theory within the functional RG approach. The bosonic field will also be decomposed in transverse and longitudinal direction. We introduce in addition a linear frequency dependence in the bosonic propagator leading to the mixing of transverse and longitudinal modes. We introduce a non-local bosonic self-interaction, where the quadratic frequency and momentum dependence is parametrized by a so-called Y-term. In total, we propose a minimal truncation for a fermion-boson theory describing fermionic superfluidity, which captures the correct infrared behaviour of the interacting Bose gas for both transverse and longitudinal excitations. Lowest order Ward identities are respected by our truncation. Furthermore the Goldstone theorem is fulfilled and a finite spectral weight for the Goldstone mode is obtained within our truncation.

4.2 The model

The Hamiltonian of the attractive Hubbard model is given by

$$H = \sum_{i,j} \sum_{\sigma} t_{ij} c^{\dagger}_{i\sigma} c_{j\sigma} + U \sum_{i} c^{\dagger}_{i\uparrow} c_{i\uparrow} c^{\dagger}_{i\downarrow} c_{i\downarrow} \tag{4.1}$$

with an attractive on-site interaction $U < 0$ between fermionic particles with opposite spin. Fermionic creation and annihilation operators $c^{\dagger}_{i\sigma}$ and $c_{i\sigma}$ obey the anticommuting relation $[c_{i\sigma'}, c^{\dagger}_{j\sigma}]_{-} = \delta_{i,j}\delta_{\sigma,\sigma'}$. The kinetic term, given by a hopping term t_{ij} between different sites, competes with the on-site interaction. A review of the attractive Hubbard model and its extensions can be found in Micnas et al. (1990). At zero temperature the model has a superfluid ground state with a broken $U(1)$-charge symmetry. At half-filling the superconducting order mixes with charge density wave order. In two dimensions a Kosterlitz-Thouless-like transition is expected at finite temperatures.

As mentioned in the introduction, the model was already studied in several works within the functional RG method. Gersch et al. (2008) and Eberlein and Metzner (2013) investigated the model with an N-patch approach and with a channel-decomposition of the Nambu vertex, respectively. The strength of those purely fermionic fRG studies relies on the unbiased treatment of different channels and is therefore ideally suited for the

a vertex expansion of the functional RG equation.

analysis of competing instabilities. Particle-hole and particle-particle fluctuations were both taken into account in a unbiased manner. Reasonable results were found for the fermionic single-particle gap for weak to intermediate interaction strengths. Particle-hole fluctuations and order parameter fluctuations reduce the fermionic single-particle gap compared to the mean-field gap. Eberlein (2013) pointed out that global Ward identities are not compatible with the Katanin scheme in general. Thus, the Goldstone theorem has to be enforced by a projection method.

The mutual interplay between fermions and order parameter fluctuations is more easily treated in a coupled fermion-boson functional RG approach. Here, the fermionic interaction is decoupled by a Hubbard-Stratonovich transformation into one (or several) bosonic fields while the fermions are not integrated out. During the coupled RG flow the bosonic potential is deformed from a symmetric parabola-like potential to a Mexican-hat-like potential. The transition between both regimes, the symmetric and symmetry-broken one, occurs at the so-called critical scale, where symmetry breaking occurs and finite anomalous fermionic expectation values appear. An order parameter is naturally implemented by the bosonic field after the decoupling of the fermionic two-particle interaction. Strack et al. (2008) analyzed the impact of order parameter fluctuations in the attractive Hubbard model. The singular behaviour of the longitudinal mass and renormalization factors was found to be consistent with the behaviour of an interacting Bose gas. However, the Goldstone theorem and the linear dispersion of the Goldstone mode were fixed by hand.

Since the fermionic particle-particle channel is the most dominant channel in the ground state of the fermionic superfluid, it is natural to decouple the fermionic interaction by a Hubbard-Stratonovich transformation in the s-wave pairing channel. The microscopic action for the coupled fermion-boson theory then reads

$$\begin{aligned} S[\bar{\psi},\psi,\phi^*,\phi] = &\int_{k\sigma} \bar{\psi}_{k\sigma}\left(ik_0 - \xi_{\mathbf{k}}\right)\psi_{k\sigma} - \int_q \frac{1}{U}\phi_q^*\phi_q \\ &+ \int_{k,q}\left(\bar{\psi}_{-k+q\downarrow}\bar{\psi}_{k\uparrow}\phi_q + \psi_{k\uparrow}\psi_{-k+q\downarrow}\phi_q^*\right), \end{aligned} \tag{4.2}$$

where $\bar{\psi}_{k\sigma}$ and $\psi_{k\sigma}$ denote fermionic fields with spin $\sigma = \uparrow, \downarrow$ and ϕ_q^* and ϕ_q complex-valued bosonic fields. The dispersion relation is given by $\xi_{\mathbf{k}} = -2t(\cos k_x + \cos k_y) - \mu$, where μ represents the chemical potential and t_{ij} next-nearest neighbour hopping specified as $t_{ij} = -t$. The action consists of three parts, a quadratic fermionic, a quadratic bosonic part and a normal Yukawa coupling. Here, the bosonic mass is given by the relation $m_b^2 = -\frac{1}{U}$.

At the beginning of the flow the scale-dependent effective action is identical to the microscopic action

$$\Gamma^{\Lambda=\Lambda_0}[\bar{\psi}, \psi, \phi^*, \phi] = S[\bar{\psi}, \psi, \phi^*, \phi] \tag{4.3}$$

and serves as the starting point for the RG flow, see chapter 2.

We now repeat the central results of previous mean-field considerations. Applying a saddle point approximation to Eq. (4.2) one finds the BCS gap equation

$$\Delta = -U \int_k \frac{\Delta}{E_{\mathbf{k}}^2 + k_0^2}, \tag{4.4}$$

where Δ denotes the fermionic single-particle gap, and $E_{\mathbf{k}} = \sqrt{\xi_{\mathbf{k}}^2 + \Delta^2}$ the energies of fermionic excitations, see Popov (1987) and Strack et al. (2008). Neglecting bosonic fluctuations and running only a fermionic mean-field flow, Salmhofer et al. (2004) obtained the correct mean-field result for the superconducting gap, since the Katanin scheme solves mean-field models exactly. However, in the work by Strack et al. (2008), the solution of the RG flow without bosonic fluctuations leads to a reduced gap compared to mean-field result. This issue could be traced back to the ansatz for the bosonic self-interaction, which is not identical to the exact bosonic mean-field potential, see Strack et al. (2008) and Popov (1987). An analysis of the pole structure of the bosonic mean-field propagators shows the existence of a massless collective excitation with a linear dispersion, the Goldstone mode, as expected.

4.3 Truncation and parametrization

In this section we introduce the ansätze for the scale-dependent effective action for both the symmetric and symmetry-broken regime parametrized by several renormalization factors and coupling constants. The effective action is truncated at fourth order in bosonic fields, further a gradient expansion is employed. For the fermions we consider a quadratic term in fermionic fields and a Yukawa vertex, which couples fermions to the bosonic degrees of freedom. We will not consider renormalizations of the fermionic frequency and momentum dependence in the quadratic fermionic term. Renormalization factors parametrize the frequency and momentum dependence of the bosonic self-energy. Furthermore, a non-local bosonic self-interaction is taken into account, which will induce the fulfillment of Goldstone's theorem and lowest order Ward identities. A transverse-longitudinal basis is chosen for the description of the complex bosonic fields in the

symmetry-broken regime. Transverse modes represent phase or Goldstone fluctuations, respectively, whereas longitudinal modes describe fluctuations in radial or amplitude direction in the superfluid state. Furthermore, we distinguish between bosonic order parameter and fermionic single-particle gap.

Subsection 4.3.1 introduces the ansatz for the scale-dependent effective action in the symmetric and subsection 4.3.2 for the scale-dependent effective action in the symmetry-broken regime.

4.3.1 Symmetric regime

In both the symmetric and symmetry-broken regime the effective action is invariant under U(1)-symmetry. Our ansatz for the scale-dependent effective action reads

$$\Gamma^{\Lambda} = \Gamma_{\bar{\psi}\psi} + \Gamma_{\phi^*\phi} + \Gamma_{\phi^4} + \Gamma_{\psi^2\phi^*}, \tag{4.5}$$

and consists of several terms which are discussed below. In general, the action includes a purely bosonic and a purely fermionic sector linked by a Yukawa coupling in our truncation. The quadratic part in fermionic fields reads

$$\Gamma_{\bar{\psi}\psi} = \int_{k\sigma} \bar{\psi}_{k\sigma} \left(ik_0 - \xi_{\mathbf{k}} \right) \psi_{k\sigma} \tag{4.6}$$

with the dispersion relation $\xi_{\mathbf{k}} = -2t(\cos k_x + \cos k_y) - \mu$. We will not consider renormalization effects of the fermionic self-energy receiving only a finite renormalization. In principle, a fermionic two-particle interaction term is regenerated during the flow due to fourth order contributions in the fermion-boson vertex. We discard these contributions, since they only lead to finite renormalizations.[4]

Before we introduce the bosonic ansatz in frequency and momentum space, we first discuss the bosonic ansatz in real space for clarity. The ansatz reads

$$\Gamma_b = \frac{Z_b}{2} \int dx |\nabla \phi(x)|^2 + \frac{W}{2} \int dx \phi(x)^* \partial_\tau \phi(x) \tag{4.7}$$

$$+ \frac{u}{8} \int dx \left(|\phi(x)|^2 \right)^2 + \frac{Y}{8} \int dx \left(\nabla |\phi(x)|^2 \right)^2, \tag{4.8}$$

where the variable $x = (\tau, \mathbf{r})$ collects imaginary time τ and space coordinates $\mathbf{r}$. The quadratic part in bosonic fields includes a spatial gradient term and a temporal derivative.

[4] By a dynamical decoupling of the interaction at each scale, one could implement this term into our truncation, see Gies et al. (2002, 2004) and Flörchinger et al. (2009).

These terms are generated during the flow. Second, a non-local bosonic self-interaction is generated, where the local interaction is parametrized by u and a non-local dependence is parametrized by the so-called Y-term. This non-local term is necessary to preserve the $U(1)$-symmetry, if transverse and longitudinal fluctuations of the bosonic order parameter fluctuations are distinguished in the symmetry-broken regime.

We move on to the frequency and momentum representation of the bosonic ansatz. The quadratic part in bosonic fields is then given by

$$\Gamma_{\phi^*\phi} = \frac{1}{2}\int_q \phi_q^* \left(-iWq_0 + Z_b(q_0^2 + \omega_{\mathbf{q}}^2) + m_b^2\right)\phi_q. \tag{4.9}$$

The renormalization factor Z_b parametrizes the quadratic frequency and momentum dependence of the propagator.[5] The imaginary linear frequency dependence is parametrized by the renormalization factor W.[6] The bosonic mass m_b^2 vanishes at the critical scale $\Lambda = \Lambda_c$ signalling spontaneous symmetry breaking. In principle, a real-valued linear momentum dependence is also generated due to a sharp frequency regularization, see section 4.7. However, it is an artefact due to our frequency regulator and vanishes in the infrared, so that we neglect it. The bosonic dispersion relation is approximated by $\omega_{\mathbf{q}}^2 = 4 - 2\cos q_x - 2\cos q_y$ and describes an isotropic quadratic momentum dependence for small q and is periodic in the Brillouin zone. In general, the prefactors of the frequency and momentum dependence are described by different renormalization factors. For simplicity, we assume here that both renormalization factors renormalize in the same way.

The bosonic self-interaction reads

$$\Gamma_{\phi^4} = \frac{1}{8}\int_{k,k',q} U(q)\phi_k\phi_{k-q}^*\phi_{k'}\phi_{k'+q}^* \tag{4.10}$$

with the function $U(q) = Y(q_0^2 + \omega_{\mathbf{q}}^2) + u$. It is parametrized by the local term u and by the so-called Y term describing a quadratic frequency and momentum dependence of the non-local bosonic self-interaction.[7] Figure 4.1 shows the frequency and momentum resolved non-local bosonic self-interaction. Later, when we present the RG flow for the

[5] The quadratic frequency dependence was neglected in previous works by Birse et al. (2005), Diehl et al. (2007) and Krippa (2007).

[6] An imaginary frequency dependence of the bosonic propagator was discussed previously in the fRG literature in the context of the interacting Bose see Flörchinger et al. (2008, 2009a, 2009b).

[7] The Y-term parametrizing a quadratic momentum dependence of the non-local bosonic self-interaction was already discussed in the context of $O(N)$ models, see Tetradis and Wetterich (1994) and Strack et al. (2008). It is crucial to preserve the symmetry, if transverse and longitudinal bosonic fluctuations are distinguished.

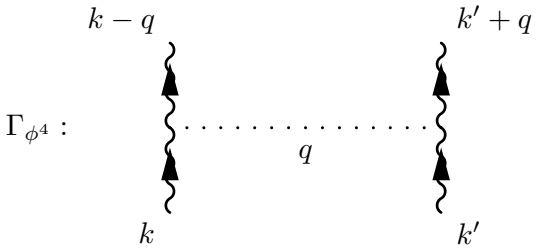

Figure 4.1: Resolved frequency and momentum transfer q in the non-local bosonic self-interaction.

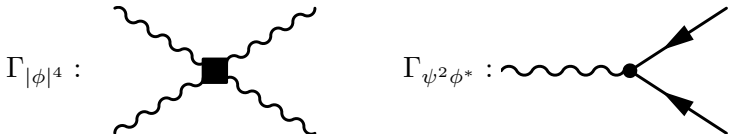

Figure 4.2: Bosonic self-interaction and normal Yukawa vertex.

couplings in the symmetric regime, we will explicitly show the resolved frequency and momentum transfers in the diagrams contributing to the RG flow.

The last term in the ansatz for the effective action Eq. (4.5) describes the Yukawa coupling connecting the fermionic and bosonic sector of the theory. In the symmetric regime only the so-called normal Yukawa vertex appears

$$\Gamma_{\psi^2\phi^*} = g \int_{k,q} \left(\bar{\psi}_{-k+q\downarrow} \bar{\psi}_{k\uparrow} \phi_q + \psi_{k\uparrow} \psi_{-k+q\downarrow} \phi_q^* \right), \tag{4.11}$$

which is given by that term in the microscopic action, which couples fermionic and bosonic fields after the application of the Hubbard-Stratonovich transformation. In the symmetry-broken regime also an anomalous Yukawa vertex appears, which includes terms with two incoming fermionic fields and one incoming bosonic field.

We assume a frequency and momentum independent coupling g. This coupling is not renormalized in the symmetric phase in our truncation. The one-loop corrections to the normal Yukawa vertex of order g^3 vanish in the symmetric regime owing to particle conservation. Since it is initialized with strength one in the microscopic action, the normal Yukawa remains $g = 1$ during the RG flow. Diagrams for the bosonic self-interaction and the Yukawa vertex are illustrated in figure 4.2. Solid lines correspond to fermionic propagators and wiggly lines to bosonic propagators.

4.3.2 Symmetry-broken regime

Now, we introduce the ansatz for the scale-dependent effective action describing the RG flow of the attractive Hubbard model in the symmetry-broken phase. In contrast to the symmetric case, where we worked in the basis $\phi_Q = (\phi_q, \phi_q^*)$ for the description of the bosons, we now switch to the transverse and longitudinal basis $\phi_Q = (\pi_q, \sigma_q)$ around the bosonic order parameter α. The explicit transformations between both representations read

$$\phi_q = \alpha\delta_{q,0} + \sigma_q + i\pi_q, \tag{4.12}$$

$$\phi_q^* = \alpha\delta_{q,0} + \sigma_{-q} - i\pi_{-q}. \tag{4.13}$$

The total ansatz for the effective action

$$\Gamma^\Lambda = \Gamma_{\bar{\psi}\psi} + \Gamma_{\psi\psi} + \Gamma_b + \Gamma_{\psi^2\sigma+\psi^2\pi} \tag{4.14}$$

consists of several terms. The purely fermionic sector is given by the first and second term. The third term denotes the purely bosonic sector of the effective action given by

$$\Gamma_b = \Gamma_{\sigma^2} + \Gamma_{\pi^2} + \Gamma_{\pi\sigma} + \Gamma_{\sigma^4} + \Gamma_{\pi^4} + \Gamma_{\sigma^2\pi^2} + \Gamma_{\sigma^3} + \Gamma_{\sigma\pi^2}, \tag{4.15}$$

where the single terms will be discussed below. Finally, the last term $\Gamma_{\psi^2\sigma+\psi^2\pi}$ in Eq. (4.14) describes couplings between longitudinal and transverse bosonic fields, respectively, to fermionic fields.

The quadratic part in fermionic fields

$$\Gamma_{\bar{\psi}\psi} = \int_{k\sigma} \bar{\psi}_{k\sigma} \left(ik_0 - \xi_{\mathbf{k}}\right) \psi_{k\sigma} \tag{4.16}$$

is identical to the expression in the symmetric phase. In the symmetry-broken phase anomalous fermionic expectation values appear, which are parametrized by

$$\Gamma_{\psi\psi} = \int_k \left(\Delta\bar{\psi}_{-k\downarrow}\bar{\psi}_{k\uparrow} + \Delta^*\psi_{k\uparrow}\psi_{-k\downarrow}\right). \tag{4.17}$$

Here, the fermionic single-particle gap is denoted as Δ.

In real space the purely bosonic part of the effective reads

$$\Gamma_b = \frac{Z_b}{2}\int dx|\nabla\phi(x)|^2 + \frac{W}{2}\int dx\phi(x)^*\partial_\tau\phi(x) \\ + \frac{u}{8}\int dx\left(|\phi(x)|^2 - |\alpha|^2\right)^2 + \frac{Y}{8}\int dx\left(\nabla|\phi(x)|^2\right)^2 \tag{4.18}$$

with a finite order parameter α generated during the flow in the symmetry-broken phase. In momentum and frequency representation the quadratic part in bosonic fields consists of three parts: A quadratic part in longitudinal bosonic fields

$$\Gamma_{\sigma^2} = \frac{1}{2}\int_q \sigma_q\left(Z_\sigma(q_0^2+\omega_{\mathbf{q}}^2) + m_\sigma^2\right)\sigma_{-q}, \tag{4.19}$$

a quadratic part in transverse bosonic fields

$$\Gamma_{\pi^2} = \frac{1}{2}\int_q \pi_q\left(Z_\pi(q_0^2+\omega_{\mathbf{q}}^2) + m_\pi^2\right)\pi_{-q}, \tag{4.20}$$

and a mixing term between longitudinal and transverse fluctuations

$$\Gamma_{\pi\sigma} = \int_q \pi_q(m_{\sigma\pi}^2 + Wq_0)\sigma_{-q} \tag{4.21}$$

due to a linear frequency dependence of the bosonic propagator parametrized by W. The renormalization factors Z_π and Z_σ parametrize the quadratic frequency and momentum dependence of the bosonic propagators. The longitudinal mass is denoted by m_σ^2. We set the transverse mass m_π^2 zero, which is consistent with the fulfillment of Goldstone's theorem in our truncation, as we will see later in section 4.5. The mixed mass term $m_{\sigma\pi}^2 = 0$ vanishes due to symmetry. Renormalizations for the longitudinal mass m_σ^2, and both the transverse and longitudinal renormalization factor are considered.

In longitudinal and transverse representation the bosonic self-interaction is split into

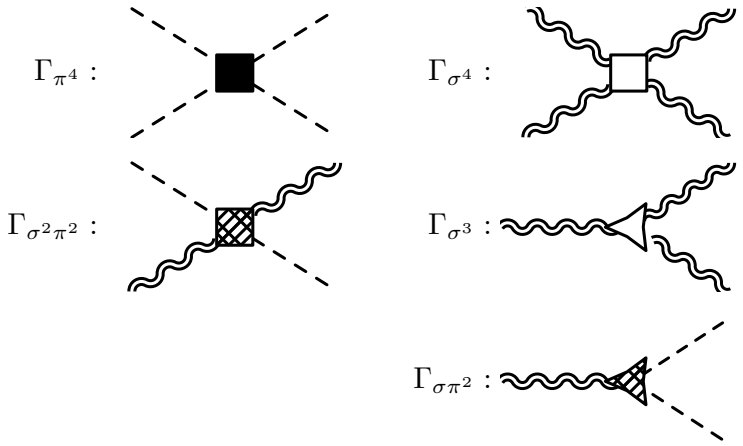

Figure 4.3: Bosonic vertices in the symmetry-broken regime.

several interaction processes between transverse and longitudinal modes

$$\Gamma_{\sigma^3} = \frac{1}{2}\int_{q,p} U(q)\alpha\sigma_p\sigma_{-q-p}\sigma_q, \tag{4.22}$$

$$\Gamma_{\sigma^4} = \frac{1}{8}\int_{p,p',q} U(q)\sigma_p\sigma_{q-p}\sigma_{p'}\sigma_{-q-p'}, \tag{4.23}$$

$$\Gamma_{\pi^4} = \frac{1}{8}\int_{p,p',q} U(q)\pi_p\pi_{q-p}\pi_{p'}\pi_{-q-p'}, \tag{4.24}$$

$$\Gamma_{\sigma^2\pi^2} = \frac{1}{4}\int_{p,p',q} U(q)\sigma_p\sigma_{q-p}\pi_{p'}\pi_{-q-p'}, \tag{4.25}$$

$$\Gamma_{\sigma\pi^2} = \frac{1}{2}\int_{p,q} U(q)\alpha\sigma_q\pi_p\pi_{-p-q}. \tag{4.26}$$

The function $U(q) = Y(q_0^2 + \omega_{\mathbf{q}}^2) + u$ parametrizes the non-local bosonic self-interaction as in the symmetric regime.[8] A finite Y-term is decisive when distinguishing between longitudinal and transverse renormalization factors. Figure 4.3 shows the diagrams corresponding to the bosonic vertices.

Local bosonic self-interaction u and Y-term are determined indirectly by the relations

$$u = \frac{m_\sigma^2}{|\alpha|^2}, \quad Y = \frac{Z_\sigma - Z_\pi}{\alpha^2}, \tag{4.27}$$

which follow straight from the ansatz of the bosonic effective action in the representation from Eq. (4.18) by inserting the transformations Eq. (4.12) and (4.13). The local bosonic

[8]The contributions to the bosonic self-interaction are the same as in a $O(2)$ model, see Tetradis and Wetterich (1994) and Strack et al. (2008).

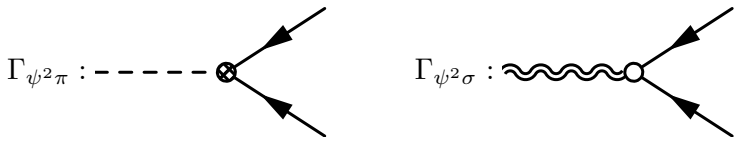

Figure 4.4: Yukawa vertices in the symmetry-broken regime.

self-interaction is calculated by the ratio between longitudinal mass and order parameter squared. The Y-term is determined by the difference between longitudinal and transverse renormalization factor divided by the order parameter squared. The relations are in full agreement with Ward identities in a linear sigma model, as we will see in section 4.5. In the limit $Y = 0$ both longitudinal and transverse renormalization factors are thus enforced to be identical, $Z_\sigma = Z_\pi$.

In the symmetry-broken regime, besides the normal Yukawa vertex also an anomalous Yukawa vertex of the form

$$\Gamma_{\psi^2\phi} = \tilde{g} \int_{k,q} \left(\bar{\psi}_{-k+q\downarrow} \bar{\psi}_{k\uparrow} \phi^*_{-q} + \psi_{k\uparrow} \psi_{-k+q\downarrow} \phi_{-q} \right), \tag{4.28}$$

appears, where $\tilde{g}$ denotes the corresponding coupling strength. In the longitudinal transverse basis the Yukawa terms

$$\Gamma_{\psi^2\sigma} = g_\sigma \int_{k,q} \left(\bar{\psi}_{-k+q/2\downarrow} \bar{\psi}_{k+q/2\uparrow} \sigma_q + \psi_{k+q/2\uparrow} \psi_{-k+q/2\downarrow} \sigma_{-q} \right), \tag{4.29}$$

$$\Gamma_{\psi^2\pi} = i g_\pi \int_{k,q} \left(\bar{\psi}_{-k+q/2\downarrow} \bar{\psi}_{k+q/2\uparrow} \pi_q - \psi_{k+q/2\uparrow} \psi_{-k+q/2\downarrow} \pi_{-q} \right) \tag{4.30}$$

then couple transverse and longitudinal bosonic fields to fermionic fields. In general, the transverse Yukawa coupling, $g_\pi = g - \tilde{g}$, and longitudinal Yukawa coupling, $g_\sigma = g + \tilde{g}$, are different. However, we will set both couplings equal, $g_\pi = g_\sigma$, to be consistent with Ward identities, which we will discuss in section 4.5. Finally, this leads to a natural fulfillment of Goldstone's theorem in our truncation as we will see later. In figure 4.4 both Yukawa vertices are shown diagrammatically.

4.4 RG flow equations

In this section we present the functional RG equations, which we use for the analysis of the attractive Hubbard model. We solve the functional RG equation for our ansätze of the scale-dependent effective action, discussed in section 4.3. RG equations for the couplings and self-energies parametrizing the effective action are presented for the symmetric and

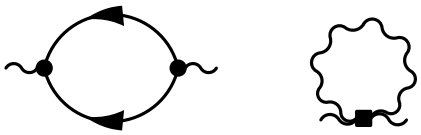

Figure 4.5: Diagrammatic contributions to the bosonic self-energy.

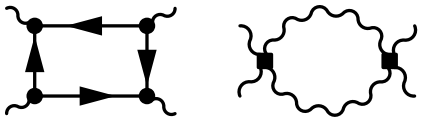

Figure 4.6: Diagrammatic contributions to the bosonic self-interaction.

symmetry-broken regime. Subsection 4.4.1 presents flow equations for the symmetric regime and subsection 4.4.2 presents flow equations for the symmetry-broken regime.

4.4.1 Symmetric regime: Flow equations

Here we present the flow equations for the couplings parametrizing the scale-dependent effective action in the symmetric regime, see section 4.3.1. By expanding the RG equations for the effective action Eq. (2.33) in fields and gradients, the flow equations for the couplings are determined by comparison of coefficients. Contributions to the flow are given in terms of 1PI Feynman diagrams. Figure 4.5 and 4.6 illustrate the diagrammatic contributions to the flow of the bosonic self-energy and self-interaction, respectively. Details of the derivation of the functional RG equations for the couplings can be found in the appendix A. There, the couplings are extracted by functional differentiation with respect to bosonic and fermionic fields.

We regularize the theory by a sharp Litim frequency cutoff[9] for fermions and bosons

$$R_f(k) = i(\Lambda \mathrm{sgn}(\mathrm{k}_0) - \mathrm{k}_0)\Theta(\Lambda - |\mathrm{k}_0|), \tag{4.31}$$

$$R_b(q) = Z_b(\Lambda^2 - q_0^2)\Theta(\Lambda^2 - q_0), \tag{4.32}$$

which are added to the inverse propagators. The frequency dependence of the fermionic and bosonic propagator is then replaced by the cutoff scale for small frequencies $|k_0|, |q_0| < \Lambda$, $Z_b q_0^2 \to Z_b \Lambda^2$ and $ik_0 \to i\Lambda \mathrm{sgn}(k_0)$, respectively. After the evaluation of the functional

[9] Often a Litim cutoff significantly simplifies the expressions on the right hand side of the flow equation, see Litim (2001). Strack et al. (2008) applied a sharp multiplicative frequency cutoff.

Figure 4.7: Fermionic and bosonic propagators in the symmetic regime.

RG equation for our ansatz, the regularized fermionic propagator

$$G_f(k) = \frac{1}{ik_0 - \xi_{\mathbf{k}} + R_f(k)}, \tag{4.33}$$

and bosonic propagator

$$G_b(q) = \frac{2}{-iWq_0 + Z_b(q_0^2 + \mathbf{q}^2) + m_b^2 + R_b(q)}, \tag{4.34}$$

will appear on the right side of the flow equation. Corresponding fermionic and bosonic single-scale propagators

$$S_f(k) = D_\Lambda G_f(k) = \frac{\partial}{\partial\Lambda}\Big|_\Sigma G_f(k), \quad S_b(k) = D_\Lambda G_b(q) = \frac{\partial}{\partial\Lambda}\Big|_\Sigma G_b(q) \tag{4.35}$$

are obtained by the scale derivative of the regularized propagators, where the self-energy is kept constant. We introduce the short-hand notation $D_\Lambda = \frac{\partial}{\partial\Lambda}\Big|_\Sigma$ for this operation. Figure 4.7 shows the diagrammatic representation of fermionic and bosonic propagators. The flow of the bosonic self-energy is defined as $\frac{d}{d\Lambda}\Sigma_b(p) = \frac{d}{d\Lambda}(G_b^{-1}(p) - G_b^{-1,(0)}(p))$ with $G_b^{-1,(0)}(p) = -\frac{1}{U} + \frac{R_b(p)}{2}$.

The flow for the bosonic self-energy is then given by

$$\frac{d}{d\Lambda}\Sigma_b(p) = -g^2 \int_k D_\Lambda \left[G_f(k)G_f(-k+p)\right] + \frac{1}{4}\int_q D_\Lambda G_b(q)\Big[u + U(q-p)\Big]. \tag{4.36}$$

Bosonic mass and renormalization factors parametrizing the frequency and momentum dependence are obtained by $\frac{d}{d\Lambda}\frac{m_b^2}{2} = \frac{d}{d\Lambda}\Sigma_b(0)$ and $\frac{d}{d\Lambda}Z_b = \frac{\partial^2}{\partial p_x^2}\Big|_{p=0}\frac{d}{d\Lambda}\Sigma_b(p)$, respectively. The bosonic mass flow reads

$$\frac{d}{d\Lambda}\frac{m_b^2}{2} = -g^2 \int_k D_\Lambda \left[G_f(k)G_f(-k)\right] + \frac{1}{4}\int_q D_\Lambda G_b(q)\Big[u + U(q)\Big]. \tag{4.37}$$

Fermionic contributions reduce the bosonic mass, whereas bosonic contribution weaken this effect. The renormalization factor parametrizing the quadratic momentum and fre-

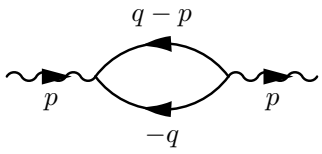

Figure 4.8: Fermionic contributions to the bosonic self-energy are given by the fermionic particle-particle bubble.

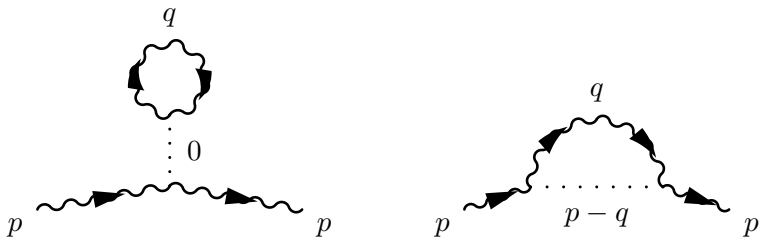

Figure 4.9: Bosonic contributions to the bosonic self-energy can be distinguished as Hartree (left) and Fock (right) term.

quency dependence is given by

$$\frac{d}{d\Lambda}Z_b = -g^2\frac{\partial^2}{\partial p_x^2}\Big|_{p=0}\left(\int_k D_\Lambda\left[G_f(k)G_f(-k+p)\right]\right) + \frac{1}{4}\frac{\partial^2}{\partial p_x^2}\Big|_{p=0}\int_q D_\Lambda G_b(q)U(q-p). \tag{4.38}$$

Finally, the linear frequency dependence of the bosonic propagator is obtained as

$$\frac{d}{d\Lambda}W = -2i\frac{\partial}{\partial p_0}\Big|_{p=0} g^2\int_k D_\Lambda\left[G_f(k)G_f(-k+p)\right] - i\int_q D_\Lambda G_b(q)Y q_0. \tag{4.39}$$

In figure 4.8 and 4.9 the relevant fermionic and bosonic 1PI diagrams contributing to the flow of the bosonic self-energy are shown. As mentioned above, the internal momentum and frequency transfer within the non-local bosonic interaction is now resolved. Solid and wiggly lines with black arrows denote fermionic and bosonic propagators, respectively. Dotted lines indicate the bosonic self-interaction and the corresponding momentum and frequency transfer. Bosonic contributions can be differentiated between a Hartree (tadpole) and a Fock (oyster) term. The fermionic contribution is given by the fermionic particle-particle bubble.

Next, we present the flow equations for the couplings parametrizing the bosonic self-

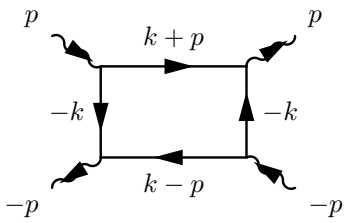

Figure 4.10: Fermionic box diagram generating the bosonic two-particle self-interaction. The external momenta are chosen in a highly symmetric way.

interaction. The flow of the (local) bosonic self-interaction reads

$$\frac{d}{d\Lambda}u = 4g^4 \int_k D_\Lambda \left[G_f(k)G_f(-k)\right]^2 - \frac{1}{4}\int_q D_\Lambda \left[G_b(q)G_b(-q)\right]\left[U(q)\right]^2 - \frac{1}{4}\int_q D_\Lambda \left[G_b(q)\right]^2\left[u + U(q)\right]^2, \tag{4.40}$$

and the flow for the non-local contribution, the Y-term

$$\begin{aligned}\frac{d}{d\Lambda}Y = {} & \frac{\partial^2}{\partial p_x^2}\Big|_{p=0}\int_k D_\Lambda \left[G_f^2(k)G_f(-k+p)G_f(-k-p)\right] \\ & - \frac{1}{4}\frac{\partial^2}{\partial p_x^2}\Big|_{p=0}\int_q D_\Lambda \left[G_b(q)G_b(-q)\right]\left[\frac{U(q-p)}{4} + \frac{U(q+p)}{4}\right]^2 \\ & - \frac{1}{2}\frac{\partial^2}{\partial p_x^2}\Big|_{p=0}\int_q D_\Lambda \left[G_b(q)G_b(q)\right]\left[\frac{U(q+p)}{4} + \frac{u}{4}\right]\left[\frac{U(q-p)}{4} + \frac{u}{4}\right] \\ & - \frac{1}{2}\frac{\partial^2}{\partial p_x^2}\Big|_{p=0}\int_q D_\Lambda \left[G_b(q+p)G_b(q-p)\right]\left[\frac{U(2p)}{4} + \frac{U(q)}{4}\right]^2.\end{aligned} \tag{4.41}$$

Both couplings are generated by expressions with four fermionic propagators.

It is again illuminating to resolve the internal momentum and frequency transfer in the 1PI diagrams for those contributions. The fermionic contribution consists of a fermionic box diagram and is shown in figure 4.10. Bosonic contributions can be classified in particle-particle, particle-hole and crossed particle-hole contributions illustrated in figures 4.11, 4.12 and 4.13. They are identical to the 1PI-diagrams contributing to the theory of the interacting Bose gas. Furthermore, they are structurally identical to 1PI fermionic diagrams contributing to the fermionic two-particle vertex, see Metzner et al. (2012). The analytical expressions can be written in a compact form due to a highly symmetric choice for the external momentum and frequency dependence of the bosonic two-particle vertex, where the total incoming momentum is zero.

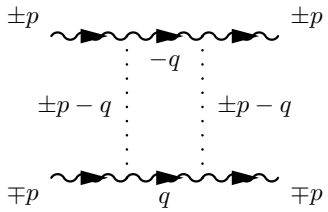

Figure 4.11: Bosonic particle-particle diagram contributing to the flow of the bosonic two-particle interaction.

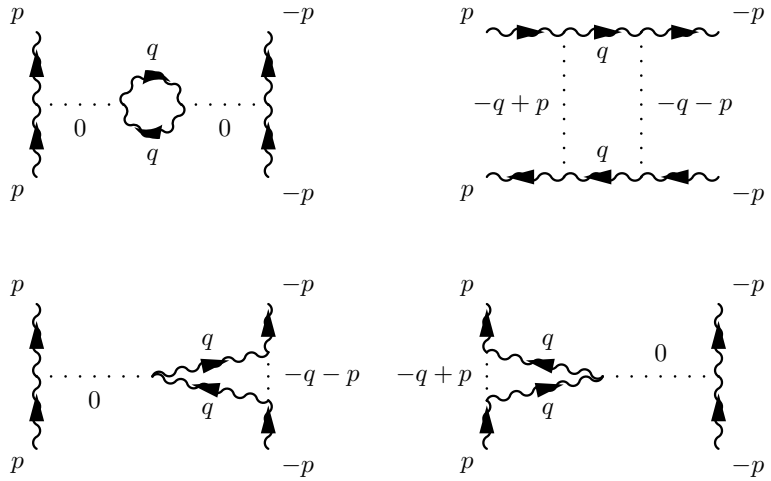

Figure 4.12: Bosonic particle-hole diagrams contributing to the flow of the bosonic two-particle interaction.

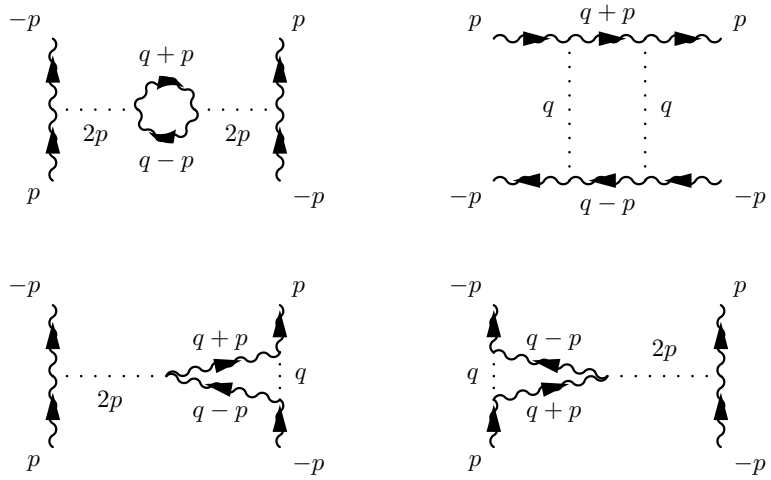

Figure 4.13: Bosonic crossed particle-hole diagrams contributing to the flow of the bosonic two-particle interaction.

4.4.2 Symmetry-broken regime: Flow equations

The symmetry-broken regime of the RG flow is characterized by the appearance of anomalous expectations values. Hence, a finite bosonic order parameter and a fermionic single-particle gap are generated. We will now present the RG equations for the couplings parametrizing the scale-dependent effective action in this regime introduced in subsection 4.3.2. As before, the RG flow of the effective action is expanded in powers of fields and gradients. Finally, coefficients are compared and the flows of the couplings are extracted. We explicitly derive the RG equations for the couplings in appendix B.

We regularize the effective action in the symmetry-broken regime with the same fermionic and bosonic regulator as in the symmetric regime. Hence, the fermionic regulator reads

$$R_f(k) = i(\Lambda \mathrm{sgn}(\mathrm{k}_0) - \mathrm{k}_0)\Theta(\Lambda - |\mathrm{k}_0|). \tag{4.42}$$

We choose an identical regulator for transverse and longitudinal bosons

$$R_\pi(q) = R_\sigma(q) = Z_\pi(\Lambda^2 - q_0^2)\Theta(\Lambda^2 - q_0^2). \tag{4.43}$$

Then, the regularized normal and anomalous fermionic propagators are given by

$$F_f(k) = \frac{\Delta}{\Delta^2 + |ik_0 - \xi_{\mathbf{k}} + R_f(k)|^2}, \tag{4.44}$$

$$G_f(k) = \frac{-ik_0 - \xi_{\mathbf{k}} - R_f(k)}{\Delta^2 + |ik_0 - \xi_{\mathbf{k}} + R_f(k)|^2}, \tag{4.45}$$

and obey the relation

$$F_f^2(k) + G_f^2(k) = \frac{F_f(k)}{\Delta}. \tag{4.46}$$

The regularized longitudinal and transverse bosonic propagators are given by

$$G_{\sigma^2}(q) = \frac{\gamma_{\pi^2}(q)}{\gamma_{\sigma^2}(q)\gamma_{\pi^2}(q) + W^2 q_0^2}, \tag{4.47}$$

$$G_{\pi^2}(q) = \frac{\gamma_{\sigma^2}(q)}{\gamma_{\sigma^2}(q)\gamma_{\pi^2}(q) + W^2 q_0^2}, \tag{4.48}$$

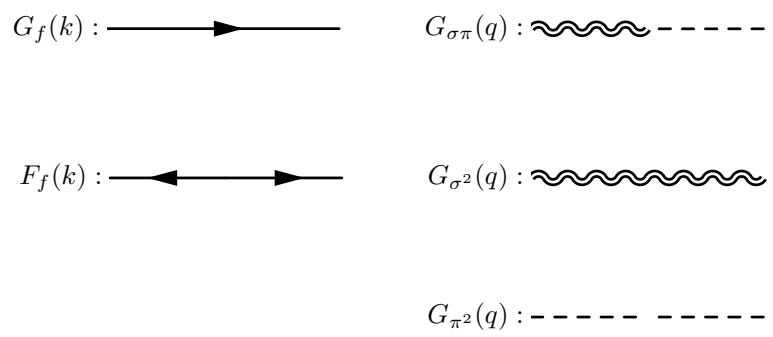

Figure 4.14: Fermionic and bosonic propagators in the symmetry-broken regime.

and the mixed bosonic propagators by

$$G_{\sigma\pi}(q) = \frac{-Wq_0}{\gamma_{\sigma^2}(q)\gamma_{\pi^2}(q) + W^2 q_0^2}, \tag{4.49}$$

$$G_{\pi\sigma}(q) = \frac{Wq_0}{\gamma_{\sigma^2}(q)\gamma_{\pi^2}(q) + W^2 q_0^2}. \tag{4.50}$$

The functions

$$\gamma_{\sigma^2}(q) = Z_\sigma(q_0^2 + \omega_{\mathbf{q}}^2) + m_\sigma^2 + R_\sigma(q), \tag{4.51}$$

$$\gamma_{\pi^2}(q) = Z_\pi(q_0^2 + \omega_{\mathbf{q}}^2) + R_\pi(q) \tag{4.52}$$

include bosonic regulators. The exact relation

$$\gamma_{\sigma^2}(q) - \gamma_{\pi^2}(q) = U(q)\alpha^2 \tag{4.53}$$

between transverse and longitudinal bosonic propagator and the function $U(q)$ holds. Both relations, Eq. (4.46) and Eq. (4.53), become relevant in the discussion of analytic results of the flow equations in section 4.5 and 4.6. Figure 4.14 shows the diagrams for fermionic and bosonic propagators in the symmetry-broken phase.

We again use the short-hand notation for the scale derivative acting only on the regulator $D_\Lambda = \frac{\partial}{\partial\Lambda}\Big|_\Sigma$, where the self-energies are kept constant. The fermionic single-scale propagators then reads

$$S_G(q) = D_\Lambda G_f(q), \quad S_F(q) = D_\Lambda F_f(q), \tag{4.54}$$

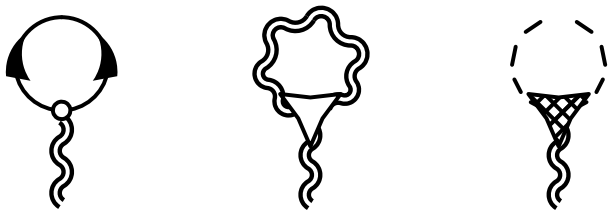

Figure 4.15: Contributions to the bosonic order parameter α.

and bosonic single-scale propagators are given by

$$S_{\sigma^2}(q) = D_\Lambda G_{\sigma^2}(q), \quad S_{\pi^2}(q) = D_\Lambda G_{\pi^2}(q), \tag{4.55}$$

$$S_{\sigma\pi}(q) = D_\Lambda G_{\sigma\pi}(q), \quad S_{\pi\sigma}(q) = D_\Lambda G_{\pi\sigma}(q). \tag{4.56}$$

The single-scale propagators are obtained by a scale derivative, where the self-energy is kept constant. For bosons the explicit expressions are given by

$$S_{\sigma^2}(q) = -\partial_\Lambda R_\pi(q) \frac{\gamma_{\pi^2}(q)^2 - W^2 q_0^2}{(\gamma_{\sigma^2}(q)\gamma_{\pi^2}(q) + W^2 q_0^2)^2}, \tag{4.57}$$

$$S_{\pi^2}(q) = -\partial_\Lambda R_\pi(q) \frac{\gamma_{\sigma^2}(q)^2 - W^2 q_0^2}{(\gamma_{\sigma^2}(q)\gamma_{\pi^2}(q) + W^2 q_0^2)^2}, \tag{4.58}$$

and

$$S_{\sigma\pi}(q) = -\partial_\Lambda R_\pi(q) \frac{-W q_0(\gamma_{\sigma^2}(q) + \gamma_{\pi^2}(q))}{(\gamma_{\sigma^2}(q)\gamma_{\pi^2}(q) + W^2 q_0^2)^2}, \tag{4.59}$$

$$S_{\pi\sigma}(q) = -\partial_\Lambda R_\pi(q) \frac{W q_0(\gamma_{\sigma^2}(q) + \gamma_{\pi^2}(q))}{(\gamma_{\sigma^2}(q)\gamma_{\pi^2}(q) + W^2 q_0^2)^2}. \tag{4.60}$$

We now present the RG equations for the couplings. The flow equation for the bosonic order parameter reads

$$\frac{d}{d\Lambda}\alpha = 2\frac{g_\sigma}{m_\sigma^2} \int_k D_\Lambda F_f(k) \tag{4.61}$$

$$- \frac{1}{2}\frac{1}{m_\sigma^2} \left[\int_q D_\Lambda G_{\sigma^2}(q) \left[2U(q) + u\right] \alpha + u\alpha \int_q D_\Lambda G_{\pi^2}(q) \right]. \tag{4.62}$$

and consists of fermionic and bosonic tadpole diagrams visualized in figure 4.15. Here we do not resolve the internal frequency and momentum dependence in the Feynman diagrams as in the symmetric regime.

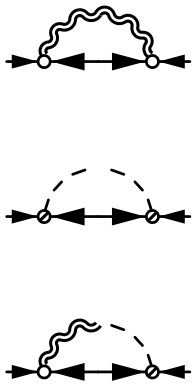

Figure 4.16: Contributions to the fermionic single-particle gap Δ.

The order parameter flow dominates the flow of the fermionic gap

$$\frac{d}{d\Lambda}\Delta = g_\sigma \frac{d}{d\Lambda}\alpha - g_\sigma^2 \int_q D_\Lambda \left[G_{\sigma^2}(q) F_f(k_f - q)\right] + g_\pi^2 \int_q D_\Lambda \left[G_{\pi^2}(q) F_f(k_f - q)\right] \\ - (i g_\sigma g_\pi) \int_q D_\Lambda \left[G_{\pi\sigma}(q) F_f(k_f - q)\right] - i g_\pi g_\sigma \int_q D_\Lambda \left[G_{\sigma\pi}(q) F_f(-q + k_f)\right], \quad (4.63)$$

due to the first term, as we will later see numerically. The variable $k_f = (0, \mathbf{k}_f)$ includes momenta on the Fermi surface. Bosonic fluctuations appear in terms of mixed fermion-boson diagrams. However, contributions with mixed bosonic propagators $G_{\sigma\pi}(q)$ vanish due to symmetry. Figure 4.16 shows the corresponding diagrammatic contributions.

Next, we present the flow equation for the bosonic self-energies. We find the following expression for the flow of the longitudinal bosonic self-energy

$$\begin{aligned} \frac{d}{d\Lambda}\Sigma_{\sigma^2}(p) = {} & \alpha(2U(p) + u)\frac{d}{d\Lambda}\alpha \\ & - g_\sigma^2 \int_k D_\Lambda \left\{ \left[G_f(k) G_f(-k + p) - F_f(k) F_f(-k + p)\right] + (p \leftrightarrow -p) \right\} \\ & + \frac{1}{2}\int_q D_\Lambda G_{\sigma^2}(q) \left[2U(q + p) + u\right] + \frac{u}{2}\int_q D_\Lambda G_{\pi^2}(q) \\ & - \frac{1}{2}\int_q D_\Lambda \left[G_{\pi^2}(q + \frac{p}{2}) G_{\pi^2}(q - \frac{p}{2})\right] \left[U(p)\right]^2 \alpha^2 \\ & - \frac{1}{2}\int_q D_\Lambda \left[G_{\sigma^2}(q + \frac{p}{2}) G_{\sigma^2}(q - \frac{p}{2})\right] \\ & \qquad \cdot \left[U(q - \frac{p}{2}) + U(q + \frac{p}{2}) + U(p)\right]^2 \alpha^2 \\ & - \int_q D_\Lambda \left[G_{\sigma\pi}(q) G_{\pi\sigma}(q + p)\right] \left[U(q) + U(q + p) + U(p)\right] U(p) \alpha^2. \end{aligned} \quad (4.64)$$

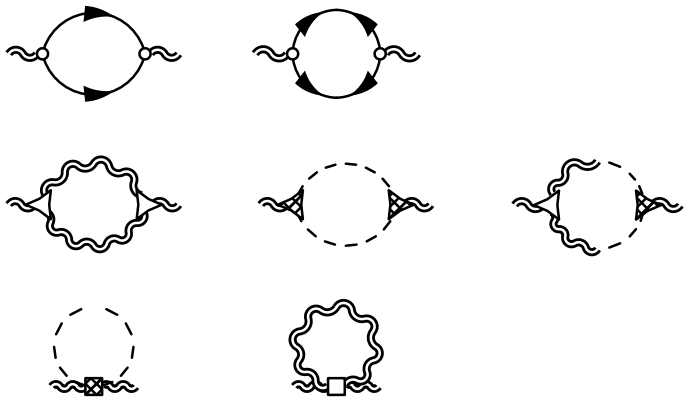

Figure 4.17: Contributions to the self-energy of the longitudinal boson $\Sigma_{\sigma^2}(q)$.

Later, we will see that the bosonic bubble with two Goldstone propagators dominates the infrared behaviour. Diagrammatic contributions to the longitudinal self-energy can be found in figure 4.17. We determine the flow for the longitudinal mass and renormalization factors by

$$\frac{d}{d\Lambda}m_\sigma = \frac{d}{d\Lambda}\Sigma_{\sigma^2}(0), \quad \frac{d}{d\Lambda}Z_\sigma = \frac{1}{2}\frac{\partial^2}{\partial p_x^2}\Big|_{p=0}\frac{d}{d\Lambda}\Sigma_{\sigma^2}(p). \tag{4.65}$$

Thus, the flow for the longitudinal mass reads

$$\begin{aligned}\frac{d}{d\Lambda}m_\sigma^2 = {} & 3u\alpha\frac{d}{d\Lambda}\alpha - 2g_{\sigma^2}\int_k D_\Lambda\left[G_f(k)G_f(-k) - {F_f}^2(k)\right] \\ & + \frac{1}{2}\int_q D_\Lambda G_{\sigma^2}(q)\Big[2U(q)+u\Big] + \frac{u}{2}\int_q D_\Lambda G_{\pi^2}(q) \\ & - \frac{u^2\alpha^2}{2}\int_q D_\Lambda\left[G_{\pi^2}(q)\right]^2 - \frac{1}{2}\int_q D_\Lambda\left[G_{\sigma^2}(q)\right]^2\left[2U(q)+u\right]^2\alpha^2 \\ & - \int_q D_\Lambda\left[G_{\sigma\pi}(q)G_{\pi\sigma}(q)\right]\left[2U(q)+u\right]u\alpha^2,\end{aligned} \tag{4.66}$$

and the flow for the longitudinal renormalization factor parametrizing momenta and fre-

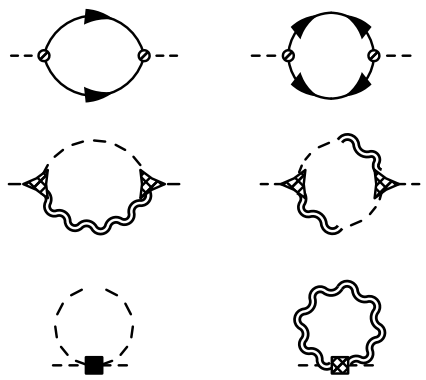

Figure 4.18: Contributions to the self-energy of the transverse boson $\Sigma_{\pi^2}(q)$.

quencies is given by

$$\begin{aligned}\frac{d}{d\Lambda}Z_\sigma = &\frac{1}{2}\frac{\partial^2}{\partial p_x^2}\Big|_{p=0}\left[2U(p)+u\right]\alpha\frac{d}{d\Lambda}\alpha + \frac{1}{2}\frac{\partial^2}{\partial p_x^2}\Big|_{p=0}\int_q D_\Lambda G_{\sigma^2}(q)U(q+p) \\ &- g_\sigma^2\frac{\partial^2}{\partial p_x^2}\Big|_{p=0}\int_k D_\Lambda\left[G_f(k)G_f(-k+p) - F_f(k)F_f(-k+p)\right] \\ &- \frac{1}{4}\frac{\partial^2}{\partial p_x^2}\Big|_{p=0}\int_q D_\Lambda\left[G_{\pi^2}(q+\frac{p}{2})G_{\pi^2}(q-\frac{p}{2})\right]\left[U(p)\right]^2\alpha^2 \\ &- \frac{1}{4}\frac{\partial^2}{\partial p_x^2}\Big|_{p=0}\int_q D_\Lambda G_{\sigma^2}(q+\frac{p}{2})G_{\sigma^2}(q-\frac{p}{2})\Big[U(q-\frac{p}{2})+U(q+\frac{p}{2})+U(p)\Big]^2\alpha^2 \\ &- \frac{1}{2}\frac{\partial^2}{\partial p_x^2}\Big|_{p=0}\int_q D_\Lambda\left[G_{\sigma\pi}(q)G_{\pi\sigma}(q+p)\right]\left[U(q)+U(q+p)+U(p)\right]\left[U(p)\right]\alpha^2.\end{aligned} \tag{4.67}$$

The flow of the transverse bosonic self-energy is given by

$$\begin{aligned}\frac{d}{d\Lambda}\Sigma_{\pi^2}(p) = &\, u\alpha\frac{d}{d\Lambda}\alpha - g_\pi^2\int_k D_\Lambda\left[G_f(k)G_f(-k+p) + F_f(k)F_f(k+p) + (p\leftrightarrow -p)\right] \\ &+ \frac{1}{2}\int_q [2U(q+p)+u]D_\Lambda G_{\pi^2}(q) + \frac{u}{2}\int_q D_\Lambda G_{\sigma^2}(q) \\ &- \int_q D_\Lambda[G_{\pi^2}(q+p)G_{\sigma^2}(q)]\left[U(q)\right]^2\alpha^2 \\ &- \int_q D_\Lambda\Big[G_{\sigma\pi}(q)G_{\sigma\pi}(q+p)\Big]\left[U(q)U(q+p)\right]\alpha^2.\end{aligned} \tag{4.68}$$

Figure 4.18 shows the corresponding contributions in terms of Feynman diagrams. The flow for the transverse mass and transverse renormalization factor are obtained by the

relations

$$\frac{d}{d\Lambda}m_\pi^2 = \frac{d}{d\Lambda}\Sigma_{\pi^2}(0), \quad \frac{d}{d\Lambda}Z_\pi = \frac{1}{2}\frac{\partial^2}{\partial p_x^2}\Big|_{p=0}\frac{d}{d\Lambda}\Sigma_{\pi^2}(p). \tag{4.69}$$

Thus, the flow equations for the transverse mass reads

$$\begin{aligned}\frac{d}{d\Lambda}m_\pi^2 = u\alpha\frac{d}{d\Lambda}\alpha - 2g_\pi^2\int_k D_\Lambda\left[G_f(k)G_f(-k)+F_f^2(k)\right]\\ + \frac{1}{2}\int_q D_\Lambda G_{\pi^2}(q)\left[2U(q)+u\right] + \frac{u}{2}\int_q D_\Lambda G_{\sigma^2}(q)\\ - \int_q D_\Lambda\left[G_{\pi^2}(q)G_{\sigma^2}(q)\right]\left[U(q)\right]^2\alpha^2 - \int_q D_\Lambda\left[G_{\sigma\pi}(q)\right]^2\left[U(q)\right]^2\alpha^2,\end{aligned} \tag{4.70}$$

and for the transverse renormalization factor

$$\begin{aligned}\frac{d}{d\Lambda}Z_\pi = -g_\pi^2\frac{\partial^2}{\partial p_x^2}\Big|_{p=0}\int_k D_\Lambda\left[G_f(k)G_f(-k+p)\right] - g_\pi^2\frac{\partial^2}{\partial p_x^2}\Big|_{p=0}\int_k D_\Lambda\left[F_f(k)F_f(k+p)\right]\\ - \frac{1}{2}\frac{\partial^2}{\partial p_x^2}\Big|_{p=0}\int_q D_\Lambda\left[G_{\pi^2}(q+p)G_{\sigma^2}(q)\right]\left[U(q)\right]^2\alpha^2\\ + \frac{1}{4}\frac{\partial^2}{\partial p_x^2}\Big|_{p=0}\int_q D_\Lambda G_{\pi^2}(q)\left[2U(q+p)+u\right]\\ - \frac{1}{2}\frac{\partial^2}{\partial p_x^2}\Big|_{p=0}\int_q D_\Lambda\left[G_{\sigma\pi}(q)G_{\sigma\pi}(q+p)\right]\left[U(q)U(q+p)\right]\alpha^2.\end{aligned} \tag{4.71}$$

Finally, the flow for the mixed bosonic self-energy is given by

$$\begin{aligned}\frac{d}{d\Lambda}\Sigma_{\sigma\pi}(p) = ig_\sigma g_\pi\Big(\int_k D_\Lambda\left[G_f(k)G_f(-p-k)\right] - \int_k D_\Lambda\left[G_f(k)G_f(p-k)\right]\Big)\\ + ig_\sigma g_\pi\int_k D_\Lambda\left[F_f(k)F_f(k+p)\right] - ig_\sigma g_\pi\int_k D_\Lambda\left[F_f(k)F_f(k-p)\right]\\ - \int_q D_\Lambda G_{\sigma\pi}(q)U(q+p)\\ - \int_q D_\Lambda\left[G_{\sigma^2}(q)G_{\sigma\pi}(q+p)\right]\left[U(q)+U(q+p)+U(p)\right]\left[U(q)\right]\alpha^2\\ - \int_q D_\Lambda\left[G_{\pi^2}(q+p)G_{\sigma\pi}(q)\right]\left[U(p)U(q)\right]\alpha^2.\end{aligned} \tag{4.72}$$

The flow for mixed bosonic mass and the linear frequency dependence is calculated by

$$\frac{d}{d\Lambda}m_{\sigma\pi} = \frac{d}{d\Lambda}\Sigma_{\sigma\pi}(0), \qquad \frac{d}{d\Lambda}W = \frac{\partial}{\partial p_0}\frac{d}{d\Lambda}\Big|_{p=0}\Sigma_{\sigma\pi}(p). \tag{4.73}$$

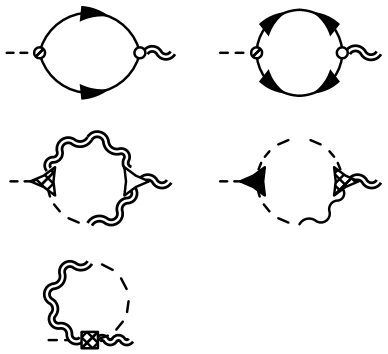

Figure 4.19: Contributions to the self-energy of the mixed bosonic self-energy $\Sigma_{\sigma\pi}(q)$.

Diagrammatic contributions to the flow of the mixed self-energy can be found in figure 4.19. It is easy to see that all contributions to the mixed mass $\frac{d}{d\Lambda}m_{\sigma\pi} = \frac{d}{d\Lambda}\Sigma_{\sigma\pi}(0)$ cancel out due to symmetry

$$\frac{d}{d\Lambda}m_{\sigma\pi}^2 = 0. \tag{4.74}$$

The flow for the linear frequency dependence reads

$$\begin{aligned}
\frac{d}{d\Lambda}W = {} & ig_\sigma g_\pi \frac{\partial}{\partial p_0}\Big|_{p=0} \int_k D_\Lambda \left[G_f(k)G_f(-k-p) - G_f(k)G_f(-k+p)\right) \\
& + ig_\sigma g_\pi \frac{\partial}{\partial p_0}\Big|_{p=0} \int_k D_\Lambda \left[F_f(k)F_f(k+p) - F_f(k)F_f(k-p)\right] \\
& + 2\int_q D_\Lambda G_{\pi\sigma}(q) Y q_0 \\
& - \frac{\partial}{\partial p_0}\Big|_{p=0} \int_q D_\Lambda \left[G_{\sigma^2}(q)G_{\sigma\pi}(q+p)\right]\left[U(q)+U(q+p)+U(p)\right]\left[U(q)\right]\alpha^2 \\
& - \frac{\partial}{\partial p_0}\Big|_{p=0} \int_q D_\Lambda \left[G_{\pi^2}(q+p)G_{\sigma\pi}(q)\right]\left[U(q)U(p)\right]\alpha^2.
\end{aligned} \tag{4.75}$$

Flows for the (local) bosonic self-interaction and the Y-term are extracted indirectly from the relations

$$\frac{d}{d\Lambda}u = \frac{d}{d\Lambda}\left(\frac{m_\sigma^2}{\alpha^2}\right), \qquad \frac{d}{d\Lambda}Y = \frac{d}{d\Lambda}\left(\frac{Z_\sigma - Z_\pi}{\alpha^2}\right). \tag{4.76}$$

Finally, the flow for the transverse Yukawa vertex, which couples fermions and bosons, is

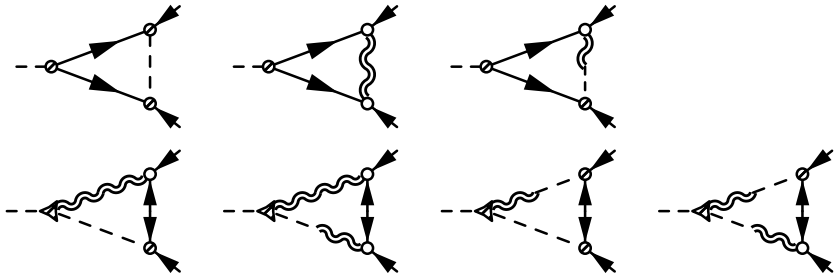

Figure 4.20: Contributions to the flow of the transverse Yukawa vertex g_π.

given by

$$\frac{d}{d\Lambda}g_\pi = g_\pi \int_q D_\Lambda \left[F_f^2(k_f - q)) + |G_f(k_f - q)|^2\right] \left[g_\sigma^2 G_{\sigma^2}(q) - g_\pi^2 G_{\pi^2}(q)\right] + 2g_\sigma g_\pi \int_q D_\Lambda \left[G_{\sigma^2}(q)G_{\pi^2}(q) + G_{\sigma\pi}(q)^2\right] F_f(k_f - q)U(q)\alpha \tag{4.77}$$

with $k_f = (0, \mathbf{k}_f)$, where we set the bosonic momenta to zero and choose the fermionic momenta on diametral positions on the Fermi surface. Figure 4.20 shows the corresponding diagrammatic contributions to the flow.[10] We do not write out the flow equation for the longitudinal Yukawa vertex g_σ, since we set it identical to the transverse Yukawa vertex $g_\sigma = g_\pi$ for reasons that will become clear in the next section.

4.5 Ward identities and Goldstone theorem

In general, truncations and other approximations of the effective action lead to a violation of conservation laws and theorems valid for the full theory. In subsection 4.5.1 we will discuss the fulfillment of Ward identities in our ansatz. We first analyze Ward identities for the purely bosonic sector and confirm that our truncation is consistent with lowest order Ward identities. Afterwards, we discuss identities for the coupled fermion-boson theory. A relation between bosonic order parameter and fermionic single-particle gap is found. Another Ward identity between two-boson-two-fermion vertex and the anomalous Yukawa vertex is presented. We prove that lowest order Ward identities are respected by our truncation of the functional RG flow. Finally, in subsection 4.5.2 we show explicitly that fermionic and bosonic contributions to the RG flow of the transverse mass cancel exactly. The relations between couplings implied by the fulfillment of the lowest order

[10] Contributions to the flow of the transverse Yukawa vertex g_π with one anomalous fermionic propagator were neglected in the previous work by Strack et al. (2008). However, they play a major role for the flow equation to respect the Ward identity between fermionic gap and order parameter.

Ward identities are thereby essential.

4.5.1 Ward identities

Ward identities connect correlation functions of different order due to the underlying symmetry of the system, see for instance Zinn-Justin (2002). A discussion of the fulfillment of local Ward identities in the fermionic functional RG flow can be found in Katanin (2004). Eberlein (2013) discusses the incompatibility between global Ward identities and the Katanin scheme. A discussion of fermion-boson RG equations in a vertex expansion and applications of Ward identities in this context can be found in Kopietz et al. (2010).

Here, we investigate the fulfillment of Ward identities, associated with the U(1)-charge symmetry, within our truncation. We show that our truncation fulfills relations derived from exact Ward identities of a linear sigma model and of a coupled boson-fermion theory. We concentrate on the broken symmetry-phase where a finite bosonic order parameter appears. The starting point for the derivation of Ward identities between bosonic correlation functions is given by

$$\int_q \phi_q \frac{\delta\Gamma}{\delta\phi_q} - \int_q \phi_q^* \frac{\delta\Gamma}{\delta\phi_q^*} = 0. \tag{4.78}$$

This equation is identical to a similar equation derived in the appendix C for a coupled fermion-boson system in absence of fermionic degrees of freedom. In transverse-longitudinal decomposition this purely bosonic identity reads

$$\int_q \left((\alpha\delta_{q,0} + \sigma_q) \frac{\delta\Gamma}{\delta\pi_q} - \pi_q \frac{\delta\Gamma}{\delta\sigma_q} \right) = 0, \tag{4.79}$$

see Amit (1984). Differentiation with respect to transverse and longitudinal fields then yields

$$\frac{\delta^2\Gamma}{\delta\sigma_p\delta\sigma_{-p}} - \frac{\delta^2\Gamma}{\delta\pi_p\delta\pi_{-p}} = \alpha \frac{\delta^3\Gamma}{\delta\pi_0\delta\pi_{-p}\delta\sigma_p}, \tag{4.80}$$

$$\frac{\partial^2}{\partial p^2}\frac{\delta^2\Gamma}{\delta\sigma_p\delta\sigma_{-p}} - \frac{\partial^2}{\partial p^2}\frac{\delta^2\Gamma}{\delta\pi_p\delta\pi_{-p}} = \alpha \frac{\partial^2}{\partial p^2}\frac{\delta^3\Gamma}{\delta\pi_0\delta\pi_{-p}\delta\sigma_p}. \tag{4.81}$$

The difference between longitudinal and transverse two-point functions is linked to the three-particle vertex $\Gamma_{\pi^2\sigma}$. The transverse and longitudinal mass are connected via Eq. (4.80). Momentum and frequency dependence of transverse and longitudinal renormalization factors are connected via Eq. (4.81). Inserting the ansatz for the scale-dependent effective

action

$$\Gamma_{\sigma\sigma} + \Gamma_{\pi\pi} = \frac{1}{2}\int_q \sigma_q (Z_\sigma(q_0^2 + \omega_{\mathbf{q}}^2) + m_\sigma^2)\sigma_{-q} + \frac{1}{2}\int_q \pi_q \left(Z_\pi(q_0^2 + \omega_{\mathbf{q}}^2) + m_\pi^2\right)\pi_{-q} \tag{4.82}$$

$$\Gamma_{\sigma\pi^2} = \frac{1}{2}\int_{q,p} U(q)\alpha\sigma_q\pi_p\pi_{-q-p} \tag{4.83}$$

in Eq. (4.80) and (4.81), we find

$$m_\sigma^2 - m_\pi^2 = u\alpha^2 \tag{4.84}$$

and

$$Y\alpha^2 = Z_\sigma - Z_\pi. \tag{4.85}$$

This totally agrees with the flow equation for the couplings parametrizing the bosonic self-interaction, see Eq. (4.76). Those flow equations were naturally obtained by inserting the transverse longitudinal decomposition Eq. (4.12) and (4.13) in the particle representation of the effective action Eq. (4.18). Hence, the bosonic sector of our ansatz satisfies lowest order Ward identities. Clearly, higher order Ward identities connecting the bosonic four-point function with the five-point function are not satisfied due to the absence of bosonic terms of order higher than four.

Ward identities for coupled fermion-boson theory:
We now discuss Ward identities between fermionic and bosonic correlation functions. We will find an identity connecting the fermionic single-particle gap with the bosonic order parameter via the transverse Yukawa vertex. Another identity couples the two-fermion-two-boson vertex to the difference between transverse and longitudinal Yukawa vertex.

The starting point for the derivation of the Ward identities for a coupled fermion-boson theory associated with $U(1)$-symmetry breaking is given by the connection

$$\int_{k\sigma} \psi_{k\sigma}\frac{\delta\Gamma}{\delta\psi_{k\sigma}} - \int_{k\sigma} \bar{\psi}_{k\sigma}\frac{\delta\Gamma}{\delta\bar{\psi}_{k\sigma}} = -2\int_q \phi_q \frac{\delta\Gamma}{\delta\phi_q} + 2\int_q \phi_q^* \frac{\delta\Gamma}{\delta\phi_q^*}. \tag{4.86}$$

An explicit derivation can be found in the appendix C or in Kopietz et al. (2010). Functional differentiation with respect to fermionic fields $\frac{\delta^2}{\delta\bar{\psi}_{p\uparrow}\delta\psi_{-p\downarrow}}$ leads to

$$\frac{\delta^2\Gamma}{\delta\bar{\psi}_{p\uparrow}\delta\bar{\psi}_{-p\downarrow}} = \alpha\frac{\delta^3\Gamma}{\delta\bar{\psi}_{p\uparrow}\delta\bar{\psi}_{-p\downarrow}\delta\phi_0} - \alpha^*\frac{\delta^3\Gamma}{\delta\bar{\psi}_{p\uparrow}\delta\bar{\psi}_{-p\downarrow}\delta\phi_0^*} \tag{4.87}$$

at $\psi = \bar{\psi} = 0$ and $\phi_q = \alpha\delta_{q,0}$. After inserting the ansatz for the quadratic anomalous fermionic term

$$\Gamma_{\psi\psi} = \int_k \left(\Delta\bar{\psi}_{k\downarrow}\bar{\psi}_{-k\uparrow} + \Delta^*\psi_{k\uparrow}\psi_{-k\downarrow}\right) \tag{4.88}$$

and the normal and anomalous Yukawa vertices

$$\begin{aligned}\Gamma_{\psi^2\phi^*} + \Gamma_{\psi^2\phi} = g\int_{k,q}\left(\bar{\psi}_{k\downarrow}\bar{\psi}_{-k+q\uparrow}\phi_q + \psi_{k\uparrow}\psi_{-k+q\downarrow}\phi_q^*\right) \\ + \tilde{g}\int_{k,q}\left(\bar{\psi}_{k\downarrow}\bar{\psi}_{-k+q\uparrow}\phi_{-q}^* + \psi_{-k\uparrow}\psi_{-k+q\downarrow}\phi_{-q}\right),\end{aligned} \tag{4.89}$$

the relation

$$\Delta = \alpha g - \alpha^*\tilde{g} \tag{4.90}$$

is immediately found. Differentiation with respect to $\frac{\delta^2}{\delta\psi_{p\uparrow}\delta\psi_{-p\downarrow}}$ leads to the complex conjugated relation. Assuming a real-valued gap and order parameter, the above relation reduces to

$$\Delta = \alpha g_\pi \tag{4.91}$$

with $g - \tilde{g} = g_\pi$. Hence, the fermionic gap is connected to the bosonic order parameter via the transverse Yukawa coupling.[11]

Next, we derive Ward identities concerning the two-boson-two-fermion vertex. Such a term was neglected in our ansatz for the effective action. We will now study the implication of this approximation on our couplings. A constraint between transverse and longitudinal Yukawa couplings will emerge.

Functional differentiation with respect to fermionic fields $\frac{\delta^2}{\delta\psi_{-p\uparrow}\delta\psi_{p\downarrow}}$ and bosonic fields $\frac{\delta}{\delta\phi_0}$ and $\frac{\delta}{\delta\phi_0^*}$ yields

$$\phi_0\frac{\delta^4\Gamma}{\delta\phi_0^*\delta\psi_{-p\uparrow}\delta\psi_{p\downarrow}\delta\phi_0} = \phi_0^*\frac{\delta^4\Gamma}{\delta\phi_0^*\delta\psi_{-p\uparrow}\delta\psi_{p\downarrow}\delta\phi_0^*}, \tag{4.92}$$

$$-2\frac{\delta^3\Gamma}{\delta\phi_0\delta\psi_{p\downarrow}\delta\psi_{-p\uparrow}} = -\phi_0\frac{\delta^4\Gamma}{\delta\phi_0\delta\psi_{-p\uparrow}\delta\psi_{p\downarrow}\delta\phi_0} + \phi_0^*\frac{\delta^4\Gamma}{\delta\phi_0\delta\psi_{-p\uparrow}\delta\psi_{p\downarrow}\delta\phi_0^*}, \tag{4.93}$$

[11] Bartosch et al. (2009) derived a similar identity between order parameter and fermionic gap. In their work both quantities were connected by a general Yukawa vertex. However, we distinguish here explicitly between the transverse and longitudinal Yukawa vertices.

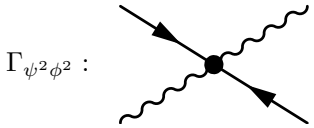

Figure 4.21: The absence of two-boson-two-fermion vertices in our truncation constrains transverse and longitudinal Yukawa vertices to be identical $g_\sigma = g_\pi$.

see appendix C for more details. In the case of a real-valued gap $\Delta = \Delta^*$ and order parameter $\alpha = \alpha^*$, these expressions reduce to

$$\alpha \frac{\delta^4 \Gamma}{\delta\phi_0^* \delta\psi_{-p\uparrow} \delta\psi_{p\downarrow} \delta\phi_0} = \alpha \frac{\delta^4 \Gamma}{\delta\phi_0^* \delta\psi_{-p\uparrow} \delta\psi_{p\downarrow} \delta\phi_0^*}, \tag{4.94}$$

$$-2 \frac{\delta^3 \Gamma}{\delta\phi_0 \delta\psi_{p\downarrow} \delta\psi_{-p\uparrow}} = -\alpha \frac{\delta^4 \Gamma}{\delta\phi_0^2 \delta\psi_{-p\uparrow} \delta\psi_{p\downarrow}} + \alpha \frac{\delta^4 \Gamma}{\delta\phi_0 \delta\psi_{-p\uparrow} \delta\psi_{p\downarrow} \delta\phi_0^*}. \tag{4.95}$$

A finite local two-boson-two-fermion vertex[12]

$$\Gamma_{\psi^2\phi^2} = \int_{k,q,q'} \lambda \left(\bar{\psi}_{k+q'\uparrow} \bar{\psi}_{-k+q\downarrow} \phi^*_{-q} \phi^*_{-q'} + \psi_{-k+q\downarrow} \psi_{k+q'\uparrow} \phi_{-q} \phi_{-q'} \right) \tag{4.96}$$

parametrized by the coupling λ, would then lead to the relation

$$g_\sigma - g_\pi = 2\tilde{g} = \alpha\lambda. \tag{4.97}$$

Figure 4.21 shows a diagram corresponding to a two-boson-two-fermion vertex. However, such a two-boson-two-fermion term was not included in our truncation

$$\Gamma_{\psi^2\phi^2} = 0. \tag{4.98}$$

Equation (4.97) thus implies the constraint

$$g_\sigma = g_\pi \tag{4.99}$$

for our truncation of the scale-dependent effective action.

In summary, the above considerations suggests constraints for our truncation, which are given by the relations

- $m_\sigma^2 = u\alpha^2$ and $Y = \frac{Z_\sigma - Z_\pi}{\alpha^2}$,

[12] A two-boson-two fermion vertex was recently implemented in a functional RG study to analyze the polaron problem, see Schmidt (2013).

- $\Delta = \alpha g_\pi$ and $g_\sigma = g_\pi$.

They determine the flow for the couplings parametrizing the bosonic self-interaction u and Y and the Yukawa vertices g_σ and g_π. Thereby, our minimal set for truncation is consistent with lowest order Ward identities. Next, we show that indeed the Ward identity $\Delta = \alpha g_\pi$ is also consistent with the explicit flow for gap, order parameter and transverse Yukawa coupling. This will play a crucial role in the fulfillment of Goldstone's theorem, implying $m_\pi^2 = 0$. We thus insert the relation $G_f(k)^2 + F_f(k)^2 = \frac{F_f(k)}{\Delta}$ into the flow equation for the transverse Yukawa vertex Eq. (4.77) and obtain

$$\frac{d}{d\Lambda} g_\pi = \frac{g_\pi}{\Delta} \int_q D_\Lambda F(k_f - q) \left[g_\sigma^2 G_{\sigma^2}(q) - g_\pi^2 G_{\pi^2}(q) \right] \tag{4.100}$$

$$+ 2 \frac{g_\sigma g_\pi}{\alpha} \int_q D_\Lambda \left[G_{\sigma^2}(q) G_{\pi^2}(q) + G_{\sigma\pi}(q)^2 \right] F(k_f - q) U(q) \alpha^2. \tag{4.101}$$

The application of the constraints $\Delta = g_\pi \alpha$, $g_\pi = g_\sigma$ and the exact identity

$$\left[G_{\sigma^2}(q) G_{\pi^2}(q) + G_{\sigma\pi}(q) G_{\sigma\pi}(q) \right] U(q) \alpha^2 = G_{\pi^2}(q) - G_{\sigma^2}(q) \tag{4.102}$$

yields

$$\frac{d}{d\Lambda} g_\pi = -\frac{g_\pi^2}{\alpha} \int_q D_\Lambda \left\{ F(k_f - q) \left[G_{\sigma^2}(q) - G_{\pi^2}(q) \right] \right\}. \tag{4.103}$$

By inserting this expression for the Yukawa vertex into the scale-derivative of the identity $\Delta = g_\pi \alpha$ we obtain

$$\frac{d}{d\Lambda} \Delta = g_\pi \frac{d}{d\Lambda} \alpha + \alpha \frac{d}{d\Lambda} g_\pi \tag{4.104}$$

$$= g_\pi \frac{d}{d\Lambda} \alpha - g_\pi^2 \int_q D_\Lambda \left\{ F_f(k_f - q) \left[G_{\sigma^2}(q) - G_{\pi^2}(q) \right] \right\}, \tag{4.105}$$

which is easily identified with the flow of the fermionic single particle-gap, see Eq. (4.63), under the constraint $g_\sigma = g_\pi$. Hence, we see that our RG equations indeed respect the lowest order Ward identities derived between fermions and bosons, Eq. (4.91). Another possible minimal truncation would be given by an ansatz where both the transverse and longitudinal Yukawa coupling are set equal one, $g_\sigma = g_\pi = 1$. Under this constraint the lowest order Ward identity remains valid only if we set the flow of the gap identical to the order parameter, $\frac{d}{d\Lambda}\Delta = \frac{d}{d\Lambda}\alpha$. Our results naturally suggest that a finite two-boson-two-fermion vertex $\Gamma_{\psi^2\phi^2} \neq 0$ implies $g_\sigma \neq g_\pi$, entailing additional contributions to the flow

equations for gap and vertices.

4.5.2 Goldstone theorem

The fulfillment of Ward identities is strongly connected to important theorems valid for the exact theory. The breaking of the global continuous $U(1)$-symmetry leads to a massless excitation, the Goldstone boson. In our truncation, the transverse bosonic mode corresponds to the Goldstone excitation in the fermionic superfluid. The so-called Goldstone theorem guarantees the disappearance of the transverse mass in an exact theory of our model. However, in general due to truncations and an ansatz for the effective action the Goldstone theorem is not respected by the flow and has to be implemented by hand, see for instance Strack et al. (2008), Bartosch et al. (2009) and Eberlein (2013). We will analyze both fermionic and bosonic contributions to the flow of the transverse mass and show that the Goldstone mass m_π^2 remains indeed zero in the symmetry-broken phase within our truncation.

The flow of the transverse mass Eq. (4.70)

$$\frac{d}{d\Lambda}m_\pi^2 = \frac{d}{d\Lambda}m_\pi^{2,fer} + \frac{d}{d\Lambda}m_\pi^{2,bos} \tag{4.106}$$

can be split into fermionic and bosonic contributions and are denoted as $m_\pi^{2,fer}$ and $m_\pi^{2,bos}$. Contributions due to the flow of the order parameter $\frac{d}{d\Lambda}\alpha^\Lambda$ can also be separated in fermionic and bosonic fluctuations, see Eq. (4.62), and are already separated in Eq. (4.106).

Fermionic contributions to the flow of the transverse mass are then obtained as

$$\begin{aligned}\frac{d}{d\Lambda}m_\pi^{2,fer} = &-2g_\pi^2\int_k D_\Lambda\left[G_f(k)G_f(-k)\right] - 2g_\pi^2\int_k D_\Lambda F_f^2(k)) \\ &+ \frac{2g_\sigma}{\alpha}\int_k D_\Lambda F_f(k).\end{aligned} \tag{4.107}$$

Using the relation Eq. (4.46) between fermionic propagators and the Ward identity Eq. (4.91) connecting gap and order parameter this expression simplifies to

$$\frac{d}{d\Lambda}m_\pi^{2,fer} = 2\left(-\frac{g_\pi^2}{\Delta}+\frac{g_\sigma}{\alpha}\right)\int_k D_\Lambda F_f(k) \tag{4.108}$$

$$= \frac{2g_\pi}{\Delta}\left(g_\sigma - g_\pi\right)\int_k D_\Lambda F_f(k). \tag{4.109}$$

Hence, only under the constraint of identical longitudinal and transverse Yukawa vertices,

see Eq. (4.99), fermionic contributions will cancel exactly out in our truncation.

Bosonic contributions to the flow of the transverse mass are given by

$$\begin{aligned}\frac{d}{d\Lambda}m_\pi^{2,bos} = &-\frac{1}{2}\int_q D_\Lambda\left[G_{\pi^2}(q)G_{\sigma^2}(q)\right]\left[U(q)\right]\left[U(q)\alpha^2 - 2G_{\sigma^2}^{-1}(q)\right] \\ &-\frac{1}{2}\int_q D_\Lambda\left[G_{\sigma^2}(q)G_{\pi^2}(q)\right]\left[U(q)\right]\left[U(q)\alpha^2 + 2G_{\pi^2}^{-1}(q)\right] \\ &-\frac{1}{2}\int_q D_\Lambda\left[G_{\sigma\pi}(q)G_{\sigma\pi}(q) + G_{\pi\sigma}(q)G_{\pi\sigma}(q)\right]\left[U(q)\right]^2\alpha^2,\end{aligned} \tag{4.110}$$

where contributions owing to the scale derivative of the order parameter are already included. Application of $G_{\sigma\pi}^2(q) = G_{\pi\sigma}^2(q)$ and the exact identity

$$\left[G_{\sigma^2}(q)G_{\pi^2}(q) + G_{\sigma\pi}(q)G_{\sigma\pi}(q)\right]U(q)\alpha^2 = G_{\pi^2}(q) - G_{\sigma^2}(q) \tag{4.111}$$

in the last line of the previous equation yields

$$\begin{aligned}\frac{d}{d\Lambda}m_\pi^{2,bos} = &-\frac{1}{2}\int_q D_\Lambda\left[G_{\pi^2}(q)G_{\sigma^2}(q)\right]\left[U(q)\right]\left[U(q)\alpha^2 - 2G_{\sigma^2}^{-1}(q)\right] \\ &-\frac{1}{2}\int_q D_\Lambda\left[G_{\sigma^2}(q)G_{\pi^2}(q)\right]\left[U(q)\right]\left[U(q)\alpha^2 + 2G_{\pi^2}^{-1}(q)\right] \\ &+\int_q D_\Lambda\left[U(q)\right]\left[G_{\sigma^2}(q) - G_{\pi^2}(q)\right] + \int_q D_\Lambda\left[U(q)\right]^2\alpha^2\left[G_{\sigma^2}(q)G_{\pi^2}(q)\right] \qquad (4.112) \\ = &\ 0, \qquad (4.113)\end{aligned}$$

where all terms obviously cancel. Thus, we obtain

$$\frac{d}{d\Lambda}m_\pi^{2,bos} = 0. \tag{4.114}$$

for the bosonic contribution to the flow of the transverse mass . Since both fermionic and bosonic contributions to the transverse mass flow vanish, the Goldstone theorem is preserved. We explicitly used the identities connecting couplings parametrizing the bosonic two-point and four-point functions, see Eq. (4.84) and (4.85). Fermionic contributions cancel out due to an implementation of the fermionic Ward identity $\Delta = \alpha g_\pi$.

In summary, we showed that fermionic contributions cancel due to the Ward identity Eq. (4.91). It is easy to see that the choice $g_\sigma \neq g_\pi$ would lead to finite contributions to the flow of the Goldstone mass, violating Goldstone's theorem in our truncation. However, we showed that the inclusion of a two-boson-two-fermion vertex naturally implies $g_\sigma \neq g_\pi$. In that case, the RG equation will experience a structural change by the appearance of

further diagrams with two-boson-two-fermion vertices. We then expect that the Goldstone theorem will again be fulfilled in a new truncation with a relation of the form $g_\sigma - g_\pi = \lambda\alpha$, where λ denotes a coupling parametrizing the local part of the two-fermion-two-boson vertex.

4.6 Behaviour in the infrared $\Lambda \to 0$

4.6.1 Asymptotic behaviour

The infrared behaviour is independent of microscopic details of the system and exhibits universal behaviour. Renormalization contributions including Goldstone modes dominate the infrared. We find that the collective excitations of our fermionic superfluid behave as an interacting Bose gas. We will reproduce the asymptotic singular behaviour for longitudinal fluctuations obtained earlier by Strack et al. (2008) within a functional RG approach.[13] We will focus on the infrared behaviour of the transverse fluctuations and couplings, extending the previous truncation. Here, we will explicitly show the finiteness of the transverse renormalization factor Z_π that ensures a finite spectral weight for the Goldstone mode.

In the infrared the flow of the longitudinal mass is dominated by a term including two Goldstone bosons

$$\frac{d}{d\Lambda} m_\sigma^2 \propto -\frac{\alpha^2 u^2}{2} \int_q D_\Lambda \left[G_{\pi^2}(q)\right]^2 \tag{4.115}$$

The infrared behaviour of the integral $\propto \Lambda^{d-4}$ together with the relation $m_\sigma^2 = u\alpha^2$ implies that the longitudinal mass m_σ^2 and the bosonic self-interaction u vanish as Λ^{3-d} in $d < 3$. Both quantities vanish logarithmically in $d = 3$.

The leading contribution to the flow of the longitudinal renormalization factors is given by

$$\frac{d}{d\Lambda} Z_\sigma \propto -\frac{1}{4} \frac{\partial^2}{\partial {p_x}^2}\Big|_{p=0} \int_q D_\Lambda G_{\pi^2}(q) G_{\pi^2}(p+q) [U(p)]^2 \alpha^2, \tag{4.116}$$

and also includes two Goldstone propagators. The scale-dependent non-local bosonic interaction $U(q)$ scales as Λ^{3-d}, the momentum differentiation as Λ^{-2}, and the integration as Λ^{d-4}. Hence, the derivative of the longitudinal renormalization $\frac{d}{d\Lambda} Z_\sigma$ scales as

[13] Singular behaviour of longitudinal fluctuations is already well-known in the literature of the interacting Bose gas, see Nepomnashchy et al. (1992), Castellani et al. (1997) and Pistolesi et al. (2004).

$\Lambda^{-2}\Lambda^{2(3-d)}\Lambda^{d-4}$ for $1 < d < 3$. The renormalization factor Z_σ shows then a Λ^{1-d} singularity in the infrared. In three dimensions $U(q)$ vanishes only logarithmically in the infrared due to the longitudinal mass. It thus entails singularities with logarithms for the longitudinal renormalization factor $\frac{d}{d\Lambda} Z_\sigma \propto |\log(\Lambda)|^{-2}\Lambda^{-3}$ and $Z_\sigma \propto |\Lambda \log(\Lambda)|^{-2}$. The non-local bosonic self-interaction parametrized by Y-term diverges as Z_σ due to the identity Eq. (4.85), if the order parameter and the transverse renormalization factors saturate.

Flows of fermionic gap and bosonic order parameter saturate in the infrared. Singularities caused by bosonic Goldstone modes are compensated by the integration. In the case of the order parameter the situation it not that clear at first glance. A prefactor given by the inverse $1/m_\sigma^2$ signals a divergence. However this is compensated due to the bosonic self-interaction $U(q)$ that scales also as m_σ^2. It is essential that the fermionic cutoff is removed fast enough, otherwise artificial divergences appear in the flow of the order parameter, see Strack et al. (2008).

In the quantities discussed above bosonic mixing terms entailed by the linear frequency dependence W and other contributions due to the Y-term do not lead to qualitatively different singularities as without those terms. Thus, the infrared scaling remains the same as in the limit $W = Y = 0$, discussed in the previous work. Finally, we discuss the infrared behaviour of those renormalization factors which strongly depend on a finite choice of both couplings $W, Y \neq 0$.

We begin with the renormalization factor for the transverse bosonic mode and show that it remains finite in the infrared. This implies a finite spectral weight and preserves the linear dispersion relation for the Goldstone boson. The leading contribution to the flow of the transverse renormalization factor is given by

$$\begin{aligned} \frac{d}{d\Lambda} Z_\pi \propto \frac{1}{2} \frac{\partial^2}{\partial p_x^2}\Big|_{p=0} \int_q D_\Lambda U(p+q) G_{\pi^2}(q) \\ - \frac{1}{2} \frac{\partial^2}{\partial p_x^2}\Big|_{p=0} \int_q [U(q)]^2 \alpha^2 D_\Lambda \left[G_{\sigma^2}(q) G_{\pi^2}(p+q)\right] + \text{finite terms} \end{aligned} \tag{4.117}$$

consisting of two divergent contributions $\propto \Lambda^{-1}$ in the infrared limit for $1 < d < 3$. Hence, a logarithmic divergence of Z_π is expected. This is true in the case of a purely local bosonic self-interaction, $Y = 0$. In this limit the tadpole contribution with only one single Goldstone propagator vanishes and the bosonic bubble consisting of one transverse and one longitudinal propagator diverges logarithmically. However, in the case of a finite Y-term, a singular tadpole term emerges, canceling the singularities of the divergent bosonic bubble. Finally, a finite transverse renormalization factor Z_π is obtained, which

preserves a finite spectral weight for the Goldstone excitation.

We prove this in the next few lines. To this end, we replace the bosonic interaction by the relation $U(q)\alpha^2 = \gamma_{\sigma^2}(q) - \gamma_{\pi^2}(q)$ and commute it with the derivative D_Λ. Neglecting subleading terms proportional to W (justified below), the equation for the transverse renormalization reduces to

$$\begin{aligned}\frac{d}{d\Lambda} Z_\pi \propto \frac{1}{2}\frac{\partial^2}{\partial p_x^2}\Big|_{p=0} \int_q D_\Lambda U(p+q) G_{\pi^2}(q) \\ - \frac{1}{2}\frac{\partial^2}{\partial p_x^2}\Big|_{p=0} \int_q U(q) D_\Lambda \Big[G_{\pi^2}(p+q) \\ - G_{\sigma^2}(q)\gamma_{\pi^2}(q) G_{\pi^2}(p+q)\Big] + \text{finite terms}.\end{aligned} \tag{4.118}$$

Here, the singular dependencies on the scale dependence cancel out exactly, while the remaining terms are finite in the limit $\Lambda \to 0$. The momentum dependence of the non-local bosonic self-interaction entails this cancellation and preserves a finite transverse renormalization factor in the infrared, $Z_\pi \to \text{const}$. Although irrelevant in power counting arguments, the Y-term proves to be important due to symmetry for the correct infrared behaviour of the Goldstone boson.

Finally, we discuss the infrared behaviour of the linear imaginary frequency dependence of the bosonic propagator parametrized by W. It is generated due to the fermionic particle-particle bubble, while in the infrared it is dominated by terms consisting of transverse fluctuations. We will show that it will vanish linearly as in the interacting Bose gas. The leading contribution to the flow of W is given by

$$\frac{d}{d\Lambda} W \propto \frac{\partial}{\partial p_0}\Big|_{p=0} \int_q D_\Lambda \left[G_{\sigma\pi}(p-q) G_{\pi^2}(q) \right] U(p) U(p-q) \alpha^2. \tag{4.119}$$

By neglecting $(Wq_0)^2$ in the denominator of the longitudinal propagator, this expression simplifies to

$$\frac{d}{d\Lambda} W \propto -u \frac{\partial}{\partial p_0}\Big|_{p=0} \int_q D_\Lambda \left[\Big(\frac{W(p_0 - q_0)}{\gamma_{\pi^2}(p-q)} - \frac{W(p_0-q_0)}{\gamma_{\sigma^2}(p-q)} \Big) G_{\pi^2}(q) \right], \tag{4.120}$$

and finally to

$$\begin{aligned}\frac{d}{d\Lambda} W &\propto -u \frac{\partial}{\partial p_0}\Big|_{p=0} \int_q D_\Lambda \left[\frac{W(p_0-q_0)}{\gamma_{\pi^2}(p-q)} \frac{1}{\gamma_{\pi^2}(q)} \right] \\ &\propto -u \frac{\partial}{\partial p_0}\Big|_{p=0} \int_q \Big[- \partial_\Lambda R_\pi(p_0-q_0) \frac{W(p_0-q_0)}{\gamma_{\pi^2}(p-q)^2 \gamma_{\pi^2}(q)} - \partial_\Lambda R_\pi(q_0) \frac{W(p_0-q_0)}{\gamma_{\pi^2}(p-q)\gamma_{\pi^2}(q)^2} \Big].\end{aligned} \tag{4.121}$$

In the next step we perform two linear transformation $q_0 \to q_0 + p_0$ and $q_0 \to -q_0$ on the first term on the right side leading to

$$\begin{aligned}\frac{dW}{d\Lambda} &\overset{q_0 \to q_0+p_0}{\propto} -u\frac{\partial}{\partial p_0}\Big|_{p=0}\int_q \Big[-\partial_\Lambda R_\pi(-q_0)\frac{W(-q_0)}{\gamma_{\pi^2}(-q)^2\gamma_{\pi^2}(q+p)} - \partial_\Lambda R_\pi(q_0)\frac{W(p_0-q_0)}{\gamma_{\pi^2}(p-q)\gamma_{\pi^2}(q)^2}\Big] \\ &\overset{q_0 \to -q_0}{\propto} -u\frac{\partial}{\partial p_0}\Big|_{p=0}\int_q \Big[-\partial_\Lambda R_\pi(q_0)\Big(\frac{Wq_0}{\gamma_{\pi^2}(q)^2\gamma_{\pi^2}(p-q)} + \frac{W(p_0-q_0)}{\gamma_{\pi^2}(p-q)\gamma_{\pi^2}(q)^2}\Big) \\ &\propto -u\frac{\partial}{\partial p_0}\Big|_{p=0}\int_q (-\partial_\Lambda R_\pi(q_0))\Big[\frac{Wp_0}{\gamma_{\pi^2}(q)^2\gamma_{\pi^2}(p-q)}\Big], \end{aligned} \tag{4.122}$$

where both terms are combined into a compact form. Finally we differentiate with respect to the external frequency $\frac{\partial}{\partial_{p_0}}$, yielding

$$\begin{aligned}\frac{dW}{d\Lambda} &\propto -u\int_q (-\partial_\Lambda R_\pi(q_0))\left[\frac{W}{\gamma_{\pi^2}(q)^2\gamma_{\pi^2}(p-q)} - \frac{Wp_0}{\gamma_{\pi^2}(q)^2\gamma_{\pi^2}(p-q)^2}\frac{\partial\gamma_{\pi\pi}(p_0-q_0)}{\partial p_0}\right]\Big|_{p=0} \\ &\propto -u\int_q (-\partial_\Lambda R_\pi(q_0))\Big[\frac{W}{\gamma_{\pi^2}(q)^3}\Big] \overset{\Lambda\to 0}{=} -\frac{uW}{2}\int_q D_\Lambda\left[G_{\pi^2}(q)G_{\pi^2}(q)\right]\Big|_{p=0}, \end{aligned} \tag{4.123}$$

where the infrared behaviour is dominated by an integral over two transverse bosonic propagators. This resembles the infrared behaviour of the longitudinal mass

$$\frac{d}{d\Lambda}m_\sigma^2 \propto -\frac{u^2}{2}\alpha^2\int_q D_\Lambda\left[G_{\pi^2}(q)G_{\pi^2}(q)\right] \tag{4.124}$$

Combining both expressions yields

$$\frac{\frac{d}{d\Lambda}m_\sigma^2}{\frac{d}{d\Lambda}W} = \frac{m_\sigma^2}{W} \tag{4.125}$$

implying a finite ratio between both quantities

$$\frac{W}{m_\sigma^2} \to C = \text{const.} \tag{4.126}$$

The linear imaginary frequency dependence W behaves as the longitudinal mass m_σ^2 in the infrared and vanishes linearly as in the interacting Bose gas, see Pistolesi et al. (2004).[14]

From the asymptotic behaviour of these renormalization factors the asymptotic form

[14] In an interacting Bose gas this ratio is proportional to a finite condensate compressibility $d\alpha^2/d\mu$, where μ denotes the chemical potential for the bosons, see Castellani et al. (1997) and Pistolesi et al. (2004).

of the propagators is given by

$$G_{\pi^2}(q) \propto \frac{1}{Z_\pi(q_0^2 + \omega_{\mathbf{q}}^2)} \tag{4.127}$$

and

$$G_{\pi\sigma}(q) \propto \frac{Cq_0}{Z_\pi(q_0^2 + \omega_{\mathbf{q}}^2)} \propto -G_{\sigma\pi}(q) \tag{4.128}$$

for small q. The longitudinal propagator $G_{\sigma^2}(q)$ shows anomalous scaling due to the divergence of Z_σ. In dimensions smaller than three, $d < 3$, we find power-law behaviour, while in three dimensions, $d = 3$, logarithmic corrections appear.

4.7 Fermionic particle-particle bubble and mean-field flow

In subsection 4.7.1 we analyze the small q-dependence of the fermionic particle-particle bubble. Regular terms justify our quadratic ansatz in frequencies and momenta. Additionally, a finite real-valued linear term appears due to the sharp cutoff. We neglected it in our truncation, since it disappears in absence of the cutoff scale Λ and does not exist at all in a momentum regularization scheme. Subsection 4.7.2 presents the mean-field flow of different cutoff schemes by neglecting bosonic fluctuations. We also study a flow including bosonic fluctuations in the symmetric regime but excluding them in the symmetry-broken phase. For both cases superfluid gaps are presented and discussed.

4.7.1 Fermionic particle-particle bubble

The fermionic particle-particle bubble is the main building block for the RPA propagator in the superconducting channel. In our work we focus on the superfluid phase of the attractive Hubbard model around quarter filling. We thus do not expect any non-analytic momentum and frequency dependence in the particle-particle bubble in presence of a cutoff Λ. However, due to the application of a sharp Litim frequency cutoff this argument is flawed for the frequency dependence. Non-analytic frequency dependencies appear in presence of a cutoff Λ, which vanish for $\Lambda \to 0$ and would disappear in presence of a momentum regulator replacing the frequency regulator. Thus, we neglect these terms in our ansatz for the scale-dependent effective action, since they are merely artificial due to the choice of a sharp frequency cutoff, and use a quadratic momentum and frequency

dependence parametrizing the bosonic self-energy.

The fermionic particle-particle bubble reads

$$\Pi(q_0, \mathbf{q}) = \int_k G_f(k) G_f(-k+q), \tag{4.129}$$

and is the central building block for the RPA propagator

$$G^{RPA}(q) = \frac{-U}{1 + U\Pi(q_0, \mathbf{q})} \tag{4.130}$$

in the superconducting channel. Instead of that expression we will study here the derivative of the regularized particle-particle bubble appearing on the right hand side of the flow equation

$$\partial_\Lambda \Pi^\Lambda(q_0, \mathbf{q}) = \int_k D_\Lambda \left[G_f(k) G_f(-k+q) \right] \tag{4.131}$$

with the regularized fermionic propagator $G_f(k) = \frac{1}{ik_0 - \xi_\mathbf{k} + R_f(k)}$ and the regulator $R_f(k) = i(-k_0 + \Lambda \mathrm{sgn}(k_0))\Theta(\Lambda - |k_0|)$. The bubble can be split into two parts with the help of the Heaviside function $\Theta_{q_0 - k_0} = \Theta(\Lambda - |q_0 - k_0|)$. In the symmetric regime in presence of a cutoff the fermionic particle-particle bubble reads

$$\begin{aligned}
\partial_\Lambda \Pi^\Lambda(q_0, \mathbf{q}) &= \int_k D_\Lambda \left[G_f(k) G_f(-k+q) \right] && (4.132) \\
&= \int_k \left(-\frac{d}{d\Lambda} R_f(k) \right) \frac{2}{(ik_0 - \xi_\mathbf{k} + R_f(k))^2 (-i(k_0 - q_0) - \xi_{\mathbf{k}-\mathbf{q}} + R_f(-k+q))} \\
&= \int_k i \cdot \mathrm{sgn}(k_0) \frac{-2\Theta_{k_0}\Theta_{k_0 - q_0}}{(i\Lambda \mathrm{sgn}(k_0) - \xi_\mathbf{k})^2 (-i\Lambda \mathrm{sgn}(\mathrm{k_0 - q_0}) - \xi_{\mathbf{k}-\mathbf{q}})} \\
&\quad + \int_k i \cdot \mathrm{sgn}(k_0) \frac{-2\Theta_{k_0}(1 - \Theta_{k_0 - q_0})}{(i\Lambda \mathrm{sgn}(k_0) - \xi_\mathbf{k})^2 (-i(k_0 - q_0) - \xi_{\mathbf{k}-\mathbf{q}})}. && (4.133)
\end{aligned}$$

The real part of the bubble is symmetric in the external frequency q_0, whereas the imaginary part is antisymmetric in q_0 in the case of zero external momenta

$$\Re\left(\Pi(q_0, 0)\right) = \Re\left(\Pi(-q_0, 0)\right), \quad \Im\left(\Pi(q_0, 0)\right) = -\Im\left(\Pi(-q_0, 0)\right). \tag{4.134}$$

It is thus sufficient to restrict our analysis to positive external frequencies $q_0 > 0$. In the next step, we accomplish a proof by cases for frequencies in the range $0 \leq q_0 \leq \Lambda$. For general functionals $f[k_0, q_0, \Theta_{k_0}, \Theta_{k_0 - q_0}]$ depending on both internal and external

frequencies, k_0 and q_0, and on the Heaviside function $\Theta_{k_0} = \Theta(\Lambda - |k_0|)$, the relations

$$\int_{-\infty}^{\infty} \frac{dk_0}{2\pi}\, \Theta_{k_0}\, \Theta_{k_0-q_0} f[k_0, q_0, \Theta_{k_0}, \Theta_{k_0-q_0}] = \int_{q_0-\Lambda}^{\Lambda} \frac{dk_0}{2\pi} f[k_0, q_0, 1, 1] \tag{4.135}$$

and

$$\int_{-\infty}^{\infty} \frac{dk_0}{2\pi}\, \Theta_{k_0}\, (1 - \Theta_{k_0-q_0})\, f[k_0, q_0, \Theta_{k_0}, \Theta_{k_0-q_0}] = \int_{-\Lambda}^{q_0-\Lambda} \frac{dk_0}{2\pi} f(k_0, q_0, 1, 0) \tag{4.136}$$

hold. These relations facilitate an analytic perfomance of the frequency integrations. Expansion in positive frequencies $q_0 > 0$ and capitalizing the symmetry relations then yields

$$\begin{aligned} \partial_\Lambda \Pi^\Lambda(q_0, 0) &= \int_k D_\Lambda \left[G_f(k) G_f(-k+q)\right] \qquad (4.137) \\ &\propto \partial_\Lambda \Pi^\Lambda(0,0) + i q_0 \left(\frac{1}{2\pi}\right) \int_{\mathbf{k}} \frac{-8\Lambda^2 \xi_{\mathbf{k}}}{(\Lambda^2 + \xi_{\mathbf{k}}^2)^3} \\ &\quad - |q_0| \left(\frac{1}{2\pi}\right) \int_{\mathbf{k}} \frac{4\Lambda(-\Lambda^2 + \xi_{\mathbf{k}}^2)}{(\xi_{\mathbf{k}}^2 + \Lambda^2)^3} \\ &\quad + q_0^2 \left(\frac{1}{2\pi}\right) \int_{\mathbf{k}} \frac{1}{(\Lambda^2 + \xi_{\mathbf{k}}^2)^2}. \qquad (4.138) \end{aligned}$$

Analogously, the expansion of the fermionic particle-particle bubble in the symmetry-broken regime with the normal fermionic propagator $G_f(k) = \frac{-ik_0 - \xi_{\mathbf{k}} - R_f(k)}{|ik_0 - \xi_{\mathbf{k}} + R_f(k)|^2 + \Delta^2}$ reads

$$\begin{aligned} \partial_\Lambda \Pi^\Lambda(q_0, 0) &\propto \partial_\Lambda \Pi^\Lambda(0,0) + i q_0 \left(\frac{1}{2\pi}\right) \int_{\mathbf{k}} \frac{-8\Lambda^2 \xi_{\mathbf{k}}}{(\Delta^2 + \Lambda^2 + \xi_{\mathbf{k}}^2)^3} \\ &\quad - |q_0| \left(\frac{1}{2\pi}\right) \int_{\mathbf{k}} \frac{4\Lambda(\Delta^2 - \Lambda^2 + \xi_{\mathbf{k}}^2)}{(\xi_{\mathbf{k}}^2 + \Delta^2 + \Lambda^2)^3} \\ &\quad + q_0^2 \left(\frac{1}{2\pi}\right) \int_{\mathbf{k}} \frac{(\Delta^2 + \Lambda^2 + \xi_{\mathbf{k}}^2)^2 - 4\Delta^2 \xi_{\mathbf{k}}^2}{(\Delta^2 + \Lambda^2 + \xi_{\mathbf{k}}^2)^4}. \qquad (4.139) \end{aligned}$$

In the limit $\Delta \to 0$ this expression reduces to the corresponding expression in the symmetric case.

The small q-dependence includes a linear imaginary frequency dependence that resembles the term $\partial_\tau \phi^* \phi$ from the interacting Bose gas. Further, a quadratic frequency dependence q_0^2 is generated. However, due to a sharp Litim cutoff an artificial real-valued linear frequency terms appears $|q_0|$. It vanishes in absence of the cutoff, $\Lambda = 0$. This indicates its artificial character owing to the presence of a sharp frequency cutoff. It is

also easy to see that this non-analytic term vanishes in presence of a momentum cutoff. We thus neglect this term in our ansatz for the scale-dependent effective action.

It is appropriate to mention that the method to determine the frequency dependence, where the frequency regulator is kept constant during the differentiation, fails here. The second frequency differentiation of the particle-particle bubble

$$\frac{\partial}{\partial q_0^2}\Big|_{q=0}\Big|_{R^\Lambda}\partial_\Lambda \Pi^\Lambda(q_0,\mathbf{q}) = \left(\frac{2\Lambda}{2\pi}\right)\int_{\mathbf{k}}\frac{-4\Lambda}{(\Lambda^2+\xi_{\mathbf{k}}^2)^3} \tag{4.140}$$

leads to a wrong sign for the prefactor. Yet, up to the sign it reproduces the structurally correct Λ-dependence. A linear frequency dependence is not generated at all in this case

$$\frac{\partial}{\partial q_0}\Big|_{q=0}\Big|_{R^\Lambda}\partial_\Lambda \Pi^\Lambda(q_0,\mathbf{q}) = 0 \tag{4.141}$$

due to symmetry. Finally, we consider the expansion for small momenta in $\mathbf{q}_x$-direction to second order

$$\partial_\Lambda \Pi^\Lambda(0,\mathbf{q}) \propto \partial_\Lambda \Pi^\Lambda(0,0) + q_x \frac{\partial}{\partial q_x}\Big|_{q=0}\partial_\Lambda \Pi^\Lambda(0,\mathbf{q}) + \frac{q_x^2}{2}\frac{\partial^2}{\partial q_x^2}\Big|_{q=0}\partial_\Lambda \Pi^\Lambda(0,\mathbf{q}) \tag{4.142}$$

It is easy to see that the term linear in q_x vanishes due to symmetry, $\frac{\partial}{\partial q_x}\Big|_{q=0}\Pi(0,\mathbf{q}) = 0$. However, the quadratic part remains finite

$$\frac{\partial^2}{\partial q_x^2}\Big|_{q=0}\partial_\Lambda \Pi^\Lambda(0,\mathbf{q}) = \left(\frac{2\Lambda}{2\pi}\right)\int_{\mathbf{k}}\frac{4\Lambda(\frac{\partial \xi_{\mathbf{k}-\mathbf{q}}}{\partial q_x})^2}{(\Lambda^2+\xi_{\mathbf{k}}^2)^3}. \tag{4.143}$$

In summary, we analyzed the small q-dependence. Regular terms appear which justify the quadratic ansatz in frequencies and momenta for the scale-dependent effective action. However a real-valued linear frequency dependence appears due to the sharp Litim frequency cutoff. In absence of a cutoff this term vanishes, we thus neglect it in our ansatz for the effective action. The ratio of the renormalization factors, which parametrize the frequency and momentum dependence, is only finite under renormalization. Since we are not interested in this ratio, we set the renormalization factors parametrizing frequency and momentum dependence equal.

4.7.2 Mean-field flow

Here, we present mean-field flows for the attractive Hubbard model in $d = 2$ at interaction strength $U = 4$. First, we show the solution of the mean-field equations. Then, we present

our results of the mean-field flow for two different regulators. Afterwards, we discuss the determination of the fermionic contributions to the renormalization factors parametrizing the frequency and momentum dependence of the bosonic self-energy. Finally, we discuss the impact of fluctuations on the critical scale and the superfluid gap in different cutoff schemes. Here, we will only allow fluctuations in the symmetric regime and neglect them in the symmetry-broken regime. The results of a full treatment of fluctuations in both regimes, the symmetric and the symmetry-broken one, are presented and discussed in the next section 4.8.

We begin with the solution of the BCS gap equation

$$\Delta = -U \int_k \frac{\Delta}{E_{\mathbf{k}}^2 + k_0^2}, \tag{4.144}$$

where $E_{\mathbf{k}} = \sqrt{\Delta^2 + \xi_{\mathbf{k}}^2}$ denotes the energy of single-particle excitations. Bosonic order parameter and fermionic gap are identical. For the mean-field value of the superfluid gap we find

$$\Delta_{BCS}^{MF} = 1.16. \tag{4.145}$$

Next, we numerically solve the functional RG equations for the symmetric regime in presence of a Litim frequency cutoff, see section 4.4, in absence of bosonic fluctuations. The flow equations then reduce to

$$\frac{d}{d\Lambda} m_b^2 = g^2 \left(\frac{2\Lambda}{2\pi}\right) \int_{\mathbf{k}} \frac{4\Lambda}{(\Lambda^2 + \xi_{\mathbf{k}}^2)^2}, \tag{4.146}$$

$$\frac{d}{d\Lambda} u = g^4 \left(\frac{2\Lambda}{2\pi}\right) \int_{\mathbf{k}} \frac{-16\Lambda}{(\Lambda^2 + \xi_{\mathbf{k}}^2)^3}, \tag{4.147}$$

where $\int_{\mathbf{k}} = \int_{-\pi}^{\pi} \int_{-\pi}^{\pi} \frac{dk_x dk_y}{(2\pi)^2}$ denotes momentum integrals over the Brillouin zone. At the critical scale symmetry breaking occurs and a fermionic gap appears. Now, we solve the mean-field flow in the symmetry-broken regime. The superfluid gap is obtained by solving the coupled differential equation system between mass and gap equation in absence of bosonic fluctuation contributions

$$\frac{d}{d\Lambda} \Delta = \frac{2}{m_\sigma^2} \left(\frac{2\Lambda}{2\pi}\right) \int_{\mathbf{k}} \frac{-2\Lambda\Delta}{(\Lambda^2 + \xi_{\mathbf{k}}^2 + \Delta^2)^2}, \tag{4.148}$$

$$\frac{d}{d\Lambda} m_\sigma^2 = \left(\frac{2\Lambda}{2\pi}\right) \int_{\mathbf{k}} \frac{-\Lambda(24\Delta^2 + 8\Lambda^2 + 8\xi_{\mathbf{k}}^2)}{(\Lambda^2 + \xi_{\mathbf{k}}^2 + \Delta^2)^3}. \tag{4.149}$$

Cutoff type (frequency)	Λ_0	Λ_c	u^{Λ_c}	$\Delta^{\mathrm{MF}}_{\mathrm{Cutoff}}$
Litim	100	1.48	0.18	0.98
Litim	1000	1.54	0.16	1.02
Multiplicative	100	0.50	0.34	0.84
Multiplicative	1000	0.47	0.33	0.86

Table 4.1: Comparison of different couplings and the superconducting gap between a multiplicative cutoff and an additive sharp Litim cutoff for a mean-field flow. The flow equations are employed for different ultraviolet cutoff scales $\Lambda_0 = (100, 1000)$.

The gap saturates in the infrared limit $\Lambda \to 0$ and we find the following mean-field values

$$\Delta^{MF}_{Litim} = 0.98 \quad (\Lambda_0 = 100), \qquad \Delta^{MF}_{Litim} = 1.02 \quad (\Lambda_0 = 1000) \tag{4.150}$$

for different ultraviolet cutoffs Λ_0.

In the case of a sharp frequency multiplicative cutoff[15] the equivalent flow equation for the symmetric regime reads

$$\frac{d}{d\Lambda} m_b^2 = g^2 \int_{\mathbf{k}} \frac{4}{2\pi} \frac{1}{(\Lambda^2 + \xi^2_{\mathbf{q}})}, \tag{4.151}$$

$$\frac{d}{d\Lambda} u = -4g^2 \int_{\mathbf{k}} \left(\frac{2}{2\pi}\right) \frac{1}{(\Lambda^2 + \xi^2_{\mathbf{k}})^2}. \tag{4.152}$$

The solution of the coupled RG equations in the broken-symmetry regime

$$\frac{d}{d\Lambda} \Delta = -\frac{2}{m_\sigma^2} \frac{2}{2\pi} \int_{\mathbf{k}} \frac{\Delta}{\Lambda^2 + \xi^2_{\mathbf{k}} + \Delta^2}, \tag{4.153}$$

$$\frac{d}{d\Lambda} m_\sigma^2 = -\frac{4}{2\pi} \int_{\mathbf{k}} \frac{4\Delta^2 + 2\Lambda^2 + 2\xi^2_{\mathbf{k}}}{(\Lambda^2 + \xi^2_{\mathbf{k}} + \Delta^2)^2} \tag{4.154}$$

yields the following mean-field values for the superconducting gap

$$\Delta^{MF}_{Multi} = 0.84 \quad (\Lambda_0 = 100), \qquad \Delta^{MF}_{Multi} = 0.86 \quad (\Lambda_0 = 1000) \tag{4.155}$$

for different choices of the ultraviolet cutoff Λ_0. Table 4.1 sums up our results for the superfluid gap for the different cutoff schemes in a compact way. The value of the bosonic self-interaction is presented at the critical scale. Different cutoff schemes lead to different mean-field gaps, see Eq. (4.150) and (4.155). Both superconducting gaps are reduced

[15] See Strack et al. (2008) for more details about the application of the sharp multiplicative cutoff in the context of a fermionic superfluid.

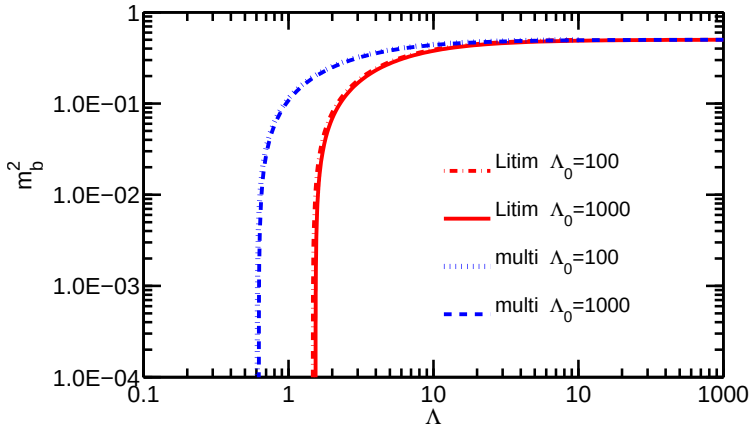

Figure 4.22: Mean-field flow (purely fermionic flow) for the bosonic mass m_b for different cutoff schemes (multiplicative and additive Litim cutoff) at different UV cutoff $\Lambda_0 = (100, 1000)$. The critical scale is reached at $m_b^2 = 0$

compared to the exact mean-field results, due to our approximation for the bosonic potential compared to the exact mean-field potential (see Strack et al. (2008) for a detailed discussion). However, a rather large difference between the cutoff schemes arises for the value of the critical scale. The critical scale in presence of a Litim cutoff is almost three times as large as the critical scale in presence of a multiplicative cutoff. This effect is nicely illustrated in the bosonic mass flow driven only by fermions, see figure 4.22. An explanation for that behaviour can be found in the technical details of both regularization schemes. The multiplicative cutoff regularizes low energy modes by simply cut them off at the scale Λ. In contrast the Litim works more subtly and does not fully exclude low energy modes, but includes them in a regularized manner. The frequency dependence ik_0 is replaced by the expression $i\Lambda \mathrm{sgn}(\mathrm{k}_0)$ in the fermionic propagator. Hence, at the scale Λ the theory with a Litim cutoff has already included more low-energy degrees of freedom compared to a theory with a multiplicative cutoff at the same scale. Thus, symmetry breaking occurs at a higher critical scale in presence of a Litim cutoff compared to a multiplicative cutoff.

Now, we discuss the determination of fermionic contributions to the flow of the renormalization factors parametrizing the frequency and momentum dependence of the bosonic self-energy. It is generally known, that a determination of the frequency dependence of renormalization factors in the presence of a frequency cutoff is a delicate procedure. Hence, for the determination of the frequency dependence often a scheme is applied, where the (frequency) regulator is kept constant during differentiation (with respect to external frequencies), see for instance the work by Strack et al. (2008). However, in our case it turned

out that unphysical values for the renormalization factor appear. Determination of the prefactor within that differentiation scheme

$$\frac{d}{d\Lambda} Z_b^\omega = \frac{1}{2} \frac{\partial^2}{\partial q_0^2}\Big|_{p=0} \Big|_R \frac{d}{d\Lambda} \Sigma_b(p), \tag{4.156}$$

leads to the result

$$\frac{d}{d\Lambda} Z_b^\omega = g^2 \left(\frac{2\Lambda}{2\pi}\right) \int_{\mathbf{k}} \frac{4\Lambda}{(\Lambda^2 + \xi_{\mathbf{k}}^2)^3} \tag{4.157}$$

implying a negative Z_b^ω factor for all scales. This is an indication that additional contributions due to the frequency dependence of the regulator have to be included to obtain the correct (positive) prefactor. The same issue occurs in presence of a multiplicative regulator, where the corresponding fermionic contribution to the flow of the frequency renormalization factors reads

$$\frac{d}{d\Lambda} Z_b^\omega = g^2 \int_{\mathbf{k}} \left(\frac{2}{2\pi}\right) \frac{-2(\xi_{\mathbf{k}}^2 - \Lambda^2)}{(\Lambda^2 + \xi_{\mathbf{k}}^2)^3}. \tag{4.158}$$

Here, the right side is positive for all scales leading to a negative Z_b^ω factor as in the case of the Litim cutoff during the RG flow. This again indicates that important contributions from frequency derivatives of the frequency regulator were neglected. A formal expansion of the particle-particle bubble for small frequencies, as discussed in the previous subsection, yields the correct sign. However, in that case a non-analytic frequency dependence appears.

In contrast to the renormalization factor parametrizing the frequency dependence, the renormalization factors parametrizing the momentum dependence of the bosonic self-energy can be easily determined. Differentiation with respect to momenta yields

$$\frac{d}{d\Lambda} Z_b = g^2 \left(\frac{2\Lambda}{2\pi}\right) \int_{\mathbf{k}} \frac{-4\Lambda(2\sin(k_x))^2}{(\Lambda^2 + \xi_{\mathbf{k}}^2)^3}, \tag{4.159}$$

in presence of a Litim cutoff and

$$\frac{d}{d\Lambda} Z_b = g^2 \int_{\mathbf{k}} \left(\frac{2}{2\pi}\right) \left[\frac{2(2\sin(q_x))^2(\xi_{\mathbf{k}}^2 - \Lambda^2)}{(\Lambda^2 + \xi_{\mathbf{k}}^2)^3} + \frac{-2\xi_{\mathbf{k}}\cos(k_x)}{(\Lambda^2 + \xi_{\mathbf{k}}^2)^2}\right], \tag{4.160}$$

in presence of a multiplicative cutoff. In figures 4.23 and 4.24 the flow for the bosonic renormalization factor is shown, which parametrizes the quadratic momentum dependence of the bosonic self-energy. Here, only the fermionic contribution to the flow of the

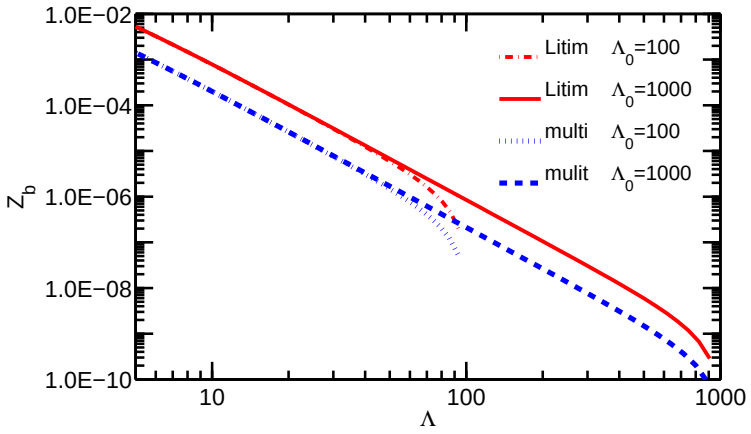

Figure 4.23: Mean-field flow (purely fermionic flow) of the renormalization factor Z_b in different cutoff schemes and different ultraviolet cutoffs Λ_0.

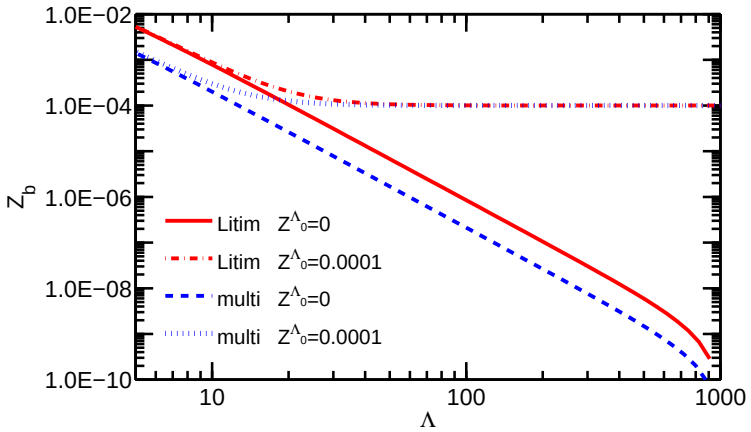

Figure 4.24: Mean-field flow (purely fermionic flow) of the renormalization factor Z_b in different cutoff schemes and different intial values.

bosonic renormalization factors is considered. The renormalization factor in presence of a multiplicative cutoff is almost a magnitude smaller than the renormalization factor in presence of the Litim cutoff. Again this reflects the technical difference in the regularization schemes between both cutoff schemes. Now, we discuss the ultraviolet behaviour of the renormalization factors. Figure 4.23 shows the flow of the renormalization factors starting all at the initial value $Z_b = 0$. In the ultraviolet jumps appear due to the numerical initialization. However, it is remarkable that below a certain scale there is no difference recognizable in the flow of the renormalization factor between different ultraviolet cutoffs for each cutoff scheme. The same effect happens by employing finite initial values, $Z_b = 0.0001$, see figure 4.24.

Finally, we discuss the effect of fluctuations in the symmetric regime in presence of

Approximations for coupled theory (Litim, $\Lambda_0 = 1000$)	Λ_c	$Z_b^{\Lambda_c}$	u^{Λ_c}	Δ_{SSB}^{MF}
Mean-Field (pure fermionic flow)	1.54	0.09	0.16	1.02
Coupled theory (full flow)	1.36	0.12	0.19	0.88
Coupled theory (full flow $\dot{Z}_b^{feedback} = 0$)	0.88	0.29	0.38	0.62
Bosons included ($W = 0, Y \neq 0$)	1.36	0.13	0.18	0.93
Bosons included ($W = 0, Y = 0$)	1.29	0.13	0.18	0.91
Bosons included ($W = 0, Y = 0, \dot{Z}_b^{feedback} = 0$)	0.70	0.48	0.53	0.51

Table 4.2: Critical scale Λ_c, bosonic self-interaction u, renormalization factor Z_b and gap Δ_{SSB}^{MF} for different approximations of the flow equation. The renormalization factor and the bosonic self-interaction are evaluated at the critical scale. The cutoff is a sharp Litim frequency cutoff and the flow starts from an UV cutoff of $\Lambda_0 = 1000$. In all cases fluctuation effects in the symmetry-broken regime are neglected, which is marked as $'SSB'$ in Δ_{SSB}^{MF}.

a sharp Litim frequency cutoff. To this end, we use the RG equations derived in section 4.4. However, in the symmetry-broken regime we still neglect bosonic fluctuations and use only the mean-field flow equations given by the coupled flow equation between bosonic mass, Eq. (4.149), and fermionic gap, Eq. (4.148). Our results are summarized in table 4.2. Results for the critical scale, the momentum renormalization factor, the bosonic self-interaction and the superconducting gap are presented. Different truncations are shown and the impact of the non-local Y-term, the linear frequency dependence W and the impact of the scale derivative of the bosonic renormalization factor $\frac{d}{d\Lambda} Z_b$, appearing in the scale derivative of the regulator $\frac{d}{d\Lambda} R_b(q)$, are illustrated. For completeness also results for the full RG flow including bosonic fluctuations in both regimes, the symmetric and the symmetry-broken regime, are shown in the table. In general bosonic fluctuations slightly reduce the critical scale compared to the pure fermionic (mean-field) flow. It turns out that the inclusion of the Y-term and the W-term leads only to a minor difference of the gap compared to the full flow. The inclusion of both W and Y tend to slow down the impact of order parameter fluctuations compared to the pure mean-field result. The most dominant impact is obtained by the inclusion of feedback effects due to the scale-derivative of the Litim cutoff. In this case bosonic fluctuation contributions in the symmetric regime are almost canceled out due to this additional term, and the results are roughly comparable to the mean-field results. Neglecting these scale derivative leads to a significant drop of the mean-field gap to almost one half. Numerical results for the total flow in the symmetric and symmetry-broken regime including all fluctuations are presented and discussed in detail in the next section.

In summary, we obtained the following results. First, different cutoff schemes lead to significant different critical scales in the mean-field flow. However, similar results for the superconducting gap were obtained. Secondly, the weakness of the frequency differentiation scheme was revealed, where the regulator is treated as a constant in presence of a frequency cutoff. Negative signs for the frequency renormalization factors appeared suggesting that important terms due to the frequency derivative of the sharp frequency cutoff were neglected. Third, a refined ansatz for the frequency and momentum dependence of the bosons including Y and W did not show a drastic impact on the superfluid gap, at least not in the case where bosonic fluctuation are neglected in the symmetry-broken regime. However, a pronounced impact on the superfluid gap was caused by the inclusion of the scale-derivative of the bosonic renormalization factors produced by the scale derivative of the regulator. This term cancels almost all bosonic fluctuation contributions in the symmetric regime.

4.8 Numerical results in $d = 2$

Here, we present numerical results for the flow equations in two dimensions in the symmetric and symmetry-broken regime. The equations were solved on a double-core CPU with the software package Matlab. On the right side of the flow equations three dimensional integrations over frequencies and momenta are performed numerically in most cases. Two dimensional integrations over the momentum space in the Brillouin zone were partly reduced to one-dimensional integrations over energy with the bosonic density of states, see appendix B. Throughout the discussion we will work with an intermediate interaction strength $U = 4$. For weaker interaction strength qualitatively the same results are obtained. The hopping is set to $t = 1$ and we start in the ultraviolet at the scale $\Lambda_0 = 1000$. We will show numerical results for the bosonic order parameter and the fermionic gap. Additionally, the flow of the transverse Yukawa vertex is shown. Afterwards, results for the longitudinal mass and renormalization factors Z_σ, Z_π and W are presented. Finally, the flow for u and Y-term parametrizing the non-local bosonic self-interaction are shown.

We begin with the results for the order parameter and the fermionic single-particle gap shown in figure 4.25. At the critical scale $\Lambda_c \approx 1.36$ spontaneous symmetry breaking occurs. Above the critical scale $\Lambda > \Lambda_c$ both quantities are identical zero. Below the critical scale they develop gradually. The order parameter is slightly reduced compared to the mean-field gap, due to bosonic fluctuations. In our truncation the result for the fermionic gap is given by $\Delta = 0.88$. The value for the gap is reduced compared to mean-field gap obtained from the solution of the BCS-gap equation due to fluctuation effects

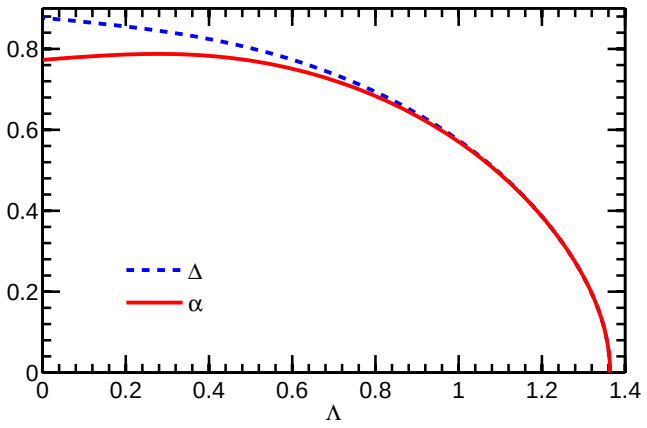

Figure 4.25: Renormalization group flow of the bosonic order parameter α and the fermionic single-particle gap Δ. Both quantities are generated at the critical scale $\Lambda = \Lambda_c$ and saturate in the infrared limit $\Lambda \to 0$.

and due to a finite truncation of our ansatz. Strack et al. (2008) pointed out that in a coupled fermion-boson mean-field flow a finite truncation of the bosonic potential will not reproduce the exact mean-field result due to missing contributions. As mentioned above, fluctuations also lead to a reduction of the superconducting gap compared to the mean-field solution even in the weak coupling limit $U \to 0$ due to particle-hole excitations, see Gorkov and Melik-Barkhudarov (1961). However, compared to previous results we obtained a rather high value for the superconducting gap. Gersch et al. (2008) and Eberlein and Metzner (2013) found that the superconducting gap was approximately half of the mean-field value at the same interaction strength in a purely fermionic functional RG approach. A similar result was obtained by Martin-Rodero et al. (1992) in a perturbative calculation. In the previous study by Strack et al. (2008) within a coupled fermion-boson RG a more drastic reduction to roughly one quarter was observed. In our case, the rather high value for the gap can be traced back to lack of particle-hole fluctuations in our truncation. It also turned out that the scale derivative of the bosonic renormalization factor $\frac{d}{d\Lambda} Z_b$, which appears in the scale derivative of the Litim regulator $\frac{d}{d\Lambda} R_b(q)$, compensates the impact of bosonic fluctuations almost totally in the symmetric regime.

In figure 4.26 the renormalization of the transverse Yukawa vertex is illustrated. In contrast to the earlier work, we find a value bigger than one that is consistent with the fermion-boson Ward identity between gap and order parameter. Vertex corrections including two bosons and one anomalous fermion propagator cause this behaviour see Eq. (4.91), which were not considered in the previous work.

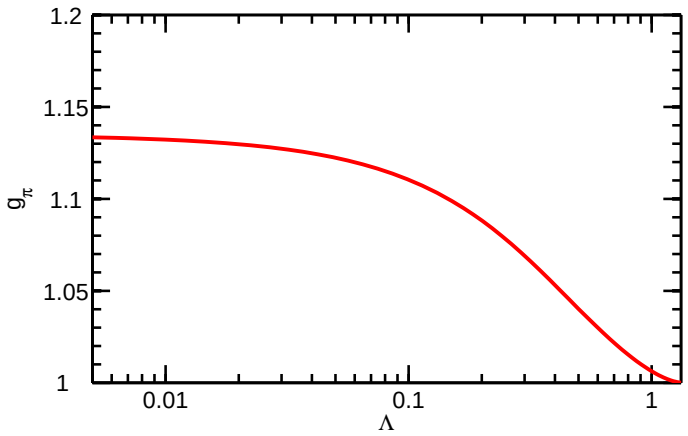

Figure 4.26: Renormalization group flow of the transverse Yukawa vertex.

Figures 4.27-4.29 show the flow of various parameters for the bosonic self-energy in our ansatz. In figure 4.27 the flow of the longitudinal bosonic mass is presented. It starts at $m_b^2 = \frac{2}{|U|}$ in the ultraviolet limit $\Lambda = \Lambda_0$ and vanishes at the critical scale $\Lambda = \Lambda_c$, signalling the pairing instability. In the symmetric regime above the critical scale bosonic fluctuations slightly compensate the drop of the longitudinal mass, leading to a lower critical scale compared to the mean field value. In the symmetry-broken regime the situation is reversed. Fermions generate a finite longitudinal mass below and bosonic Goldstone fluctuations dominate the infrared behaviour leading to a linear disappearance of the mass term $m_\sigma^2 \propto \Lambda$. The transverse mass $m_\pi = 0$ remains zero in the whole symmetry-broken phase as discussed in section 4.5.

The flow of the bosonic renormalization factor is shown in figure 4.28. In the symmetric regime the particle-particle bubble entails a smooth increase of the renormalization factors parametrizing frequency and momentum dependence of the bosonic propagator. At the critical scale we distinguish between transverse and longitudinal renormalization factors. The transverse renormalization factor slowly grows due to fermionic contributions. But then it saturates due to cancellations between logarithmically diverging bosonic contributions, see section 4.6. This preserves the linearly dispersing Goldstone mode in our theory and leads to a finite spectral weight of the Goldstone excitation. Finally, the longitudinal renormalization factor diverges in the infrared, $Z_\sigma \propto \frac{1}{\Lambda}$. This signals the existence of an incoherent continuum for the longitudinal excitations. Weichmann (1988) and Zwerger (2004) found a similar behaviour for the longitudinal renormalization factor in a different physical context.

On intermediate scales the value for Z_π is higher as Z_σ which is consistent with

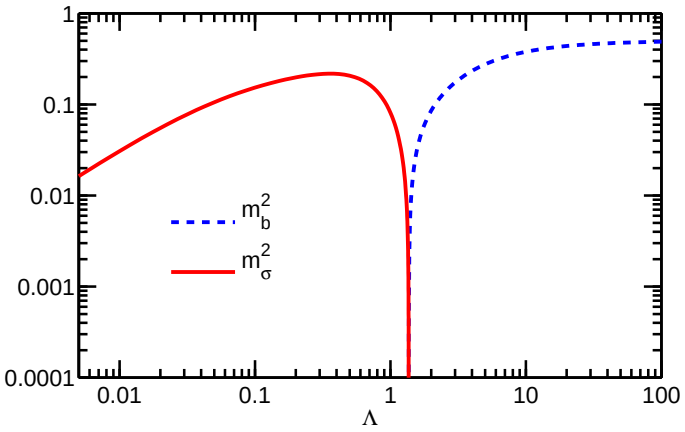

Figure 4.27: Renormalization group flow of the bosonic mass m_b^2 in the symmetric regime and of the longitudinal bosonic mass in the symmetry-broken regime. The bosonic mass m_b^2 starts at the inverse interaction strength and vanishes at the critical scale, while the lonigitudinal mass emerges at the critical scale, but vanishes linearly in the infrared limit $\Lambda \to 0$.

the flow of the higher gradient term Y displayed in figure 4.30. The linear frequency dependence parametrized by W is plotted in 4.29. In the symmetric regime it evolves gradually from zero and vanishes linearly as the longitudinal mass in the infrared limit due to Goldstone fluctuations $W \propto \Lambda$. The ratio between W and the bosonic mass was determined as $C = \frac{W}{m_\sigma^2} = 0.25$. In the context of the interacting Bose gas, this quantity ensures a finite condensate compressibility (Castellani et al. (1997) and Pistolesi et al. (2004)).

Finally, in figure 4.30 we discuss the flow of the bosonic self-interaction parametrized by the local term u, and the Y-term inducing non-locality. The local interaction shown in figure 4.30 is generated in the symmetric regime but vanishes linearly in the infrared $u \propto \Lambda$ triggered by the behaviour of the longitudinal mass and the saturation of the order parameter. In contrast, the Y-term diverges in the infrared as a power law $Y \propto \frac{1}{\Lambda}$ dictated by the behaviour of the longitudinal renormalization factor Z_σ. From the beginning of the flow down to a scale Λ^* below the critical scale, the Y-term is negative, since the transverse renormalization factor is larger compared to the longitudinal one in that regime.

The behaviour of the discussed quantities is in full agreement with the behaviour of a weakly interacting Bose gas in two dimensions (Castellani et al. (1997) and Pistolesi et al. (2004), Sinner et al. (2009, 2010) and Dupuis (2009)).

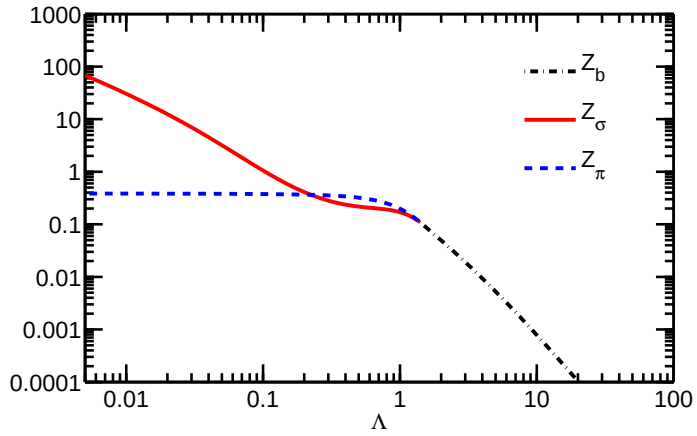

Figure 4.28: Renormalization group flow of bosonic renormalization factors. Z_b denotes the flow of the bosonic momentum and frequency dependence in the symmetric regime above the critical scale. In the symmetry-broken phase $\Lambda < \Lambda_c$ transverse and longitudinal renormalization factors Z_π and Z_σ are distinguished.

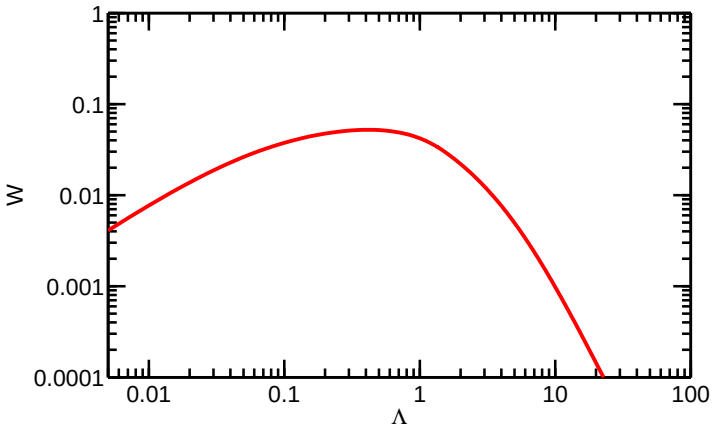

Figure 4.29: Renormalization group flow of the linear imaginary frequency dependence coefficient W.

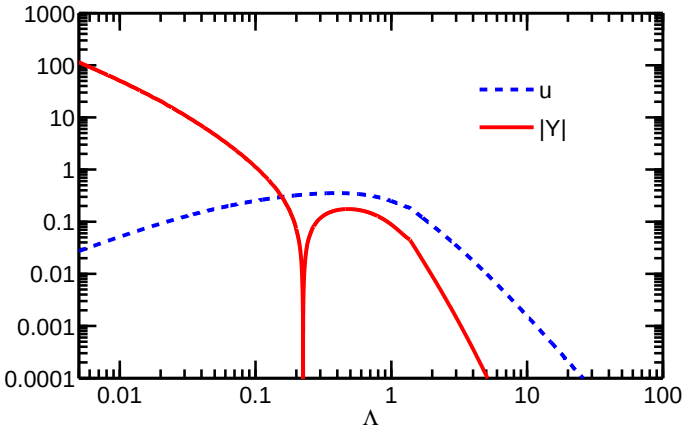

Figure 4.30: Renormalization group flow for the couplings parmetrizing the bosonic self-interaction. u corresponds to the local bosonic self-interaction and Y denotes the non-local quadratic frequency and momentum dependence of the bosonic self-interaction.

4.9 Conclusion

In this chapter we have analyzed the attractive Hubbard model as a prototype model for a fermionic superfluid. Order parameter fluctuations and their interplay with fermions were studied within a coupled fermion-boson functional RG analysis. The fermionic two-particle interaction was decoupled by a Hubbard-Stratonovich transformation in the particle-particle s-wave singlet channel. A previous truncation was extended in several directions. The introduction of the so-called Y-term, implying a non-local bosonic self-interaction, was necessary to preserve the $U(1)$-symmetry, when longitudinal and transverse fluctuations are distinguished in the symmetry-broken regime of the flow. An imaginary linear frequency dependence of the bosonic propagator entails mixed transverse-longitudinal bosonic propagators. During the flow the $U(1)$-symmetric potential develops a Mexican-hat-like structure at the critical scale, signalling symmetry breaking. A finite order parameter and a fermionic single-particle gap emerges. In the superfluid regime bosonic fluctuations were decomposed in transverse and longitudinal components around the order parameter. Transverse modes correspond to phase fluctuations and longitudinal modes to amplitude fluctuations.

We consistently described the fermion-boson theory within a relatively simple truncation of the RG equations. Our truncation preserves the Goldstone theorem and a finite spectral weight for the Goldstone mode in spite of infrared divergencies. Lowest order Ward identities are found to be respected by the ansatz. The collective excitations be-

have as an interacting Bose gas. The correct asymptotic behaviour for the fluctuation propagators are reproduced within our theory. Our study may serve as a reference for future truncations requiring a fulfillment of Ward identities.

CHAPTER 5

Summary and Outlook

In this work we investigated two different models of interacting fermions exhibiting s-wave superfluidity within the framework of the coupled fermion-boson functional renormalization group method. We studied the mutual interplay between order parameter fluctuations and fermions in both systems.

5.1 Superfluid-semimetallic quantum phase transition

5.1.1 Summary

We analyzed the quantum phase transition between a semimetal and a superfluid in the Dirac cone model. We were interested in the impact of critical fluctuations close to and at the quantum critical point and their interplay with fermionic degrees of freedom. Hence, bosonic fields were introduced in the s-wave singlet channel through a Hubbard-Stratonovich transformation decoupling the fermionic two-particle interaction of the Dirac cone model. In contrast to the standard approach of quantum criticality by Hertz and Millis, we did not integrate out the fermions to derive a purely bosonic action. Instead we analyzed the coupled fermion-boson theory with the functional renormalization group.

The Dirac cone model was introduced and first analyzed by Strack et al. (2010). An ansatz for the scale-dependent effective action was employed in powers of fields and in a gradient expansion. They investigated the quantum critical point starting from the semimetallic phase at zero temperature and found non-Fermi-liquid and non-Gaussian

behaviour at the quantum critical point. Compared to the mean-field result the ordered phase shrank due to bosonic order parameter fluctuations. We extended this previous truncation of the functional RG flow in several directions. The fermionic two-particle interaction led to an opening of a fermionic band gap. Thus, a finite counterterm was added to the action and was tuned in such a way that the fermionic band gap was kept closed during the RG flow, especially in the infrared limit preserving thus the semimetallic phase. The fermionic renormalization factors parametrizing the frequency and momentum dependence of the fermionic self-energy were distinguished. The renormalization factor parametrizing the frequency dependence diverges, whereas the renormalization factor parametrizing the momentum dependence remains constant at the quantum critical point. In contrast to the previous work, this behaviour leads to a vanishing Fermi velocity at the quantum critical point. Furthermore, a fermionic anomalous dimension appears, implying a breakdown of the Fermi liquid concept at the quantum critical point. We could also confirm the result of a vanishing spectral weight of the fermionic quasi-particles. The renormalization factors parametrizing the frequency and momentum dependence of the bosonic self-energy diverge at the quantum critical point, leading to bosonic anomalous dimensions implying non-Gaussian behaviour. The fermionic and bosonic anomalous exponents obey several scaling laws. At the quantum critical point the pairing susceptibility, the correlation time and the correlation length are infinite.

Surprisingly, in the semimetallic ground state, away from the quantum critical point, both correlation length and correlation time were found to be infinite, too, whereas the pairing susceptibility remained finite there. The origin of this unexpected behaviour could be traced back to non-analytic linear frequency and momentum dependencies of the fermionic particle-particle bubble at zero temperature, leading to a power law decay in space and time, respectively. At finite temperature or in presence of an infrared cutoff only a regular frequency and momentum dependence appears in the particle-particle bubble. At finite temperatures, above the quantum critical point, a finite susceptibility, correlation length, and correlation time were found which all show a power law behaviour, as expected. The corresponding critical exponents obey classical scaling laws and the anomalous dynamical critical exponents for bosons and fermions were determined. We summarize the central results in a list:

1. RG analysis of a quantum phase transition between a superfluid and a semimetal
2. non-Fermi liquid behaviour and non-Gaussian behaviour at the quantum critical point
3. vanishing Fermi velocity and spectral weight of fermionic quasi-particles at the quantum critical point
4. correlation length, correlation time and susceptibility infinite at the quantum critical point
5. scaling laws for critical exponents at zero and finite temperature
6. divergent correlation length in the entire semimetallic ground state

5.1.2 Outlook

The simplicity of the Dirac cone model naturally suggests it as a textbook model for non-Gaussian criticality and non-Fermi liquid behaviour, illustrating the application of the functional RG framework in a simple case study. Here an interesting quantum phase transition close to s-wave superfluidity was investigated in our work. In an era, where Dirac cones in graphene and in topological materials are intensively studied in condensed matter physics, such a prototypical study between fermionic s-wave superfluidity and a semimetallic phase consisting of one Dirac cone is timely.

Extensions towards more realistic models of topological insulators and superconductors, graphene or relativistic QED_{2+1} models are conceivable. In this case the structure of the fermionic degrees of freedom has to be adapted to capture the correct entanglement between spin and the momentum. In the case of graphene one should include the internal spinor structure to include the second Dirac cone and an adapted kinetic term. Furthermore, the concept of exciton-condensation in bilayer graphene could also be studied in such a simplified framework.

The work may serve as a guide line for studies of the concept of quantum criticality at zero and finite temperatures by the fermion-boson functional RG studies. Other intriguing problems to analyze would be magnetic and nematic quantum phase transitions in itinerant electronic systems.

5.2 Low-energy singularities in fermionic superfluidity

5.2.1 Summary

In this second project, the mutual interplay between fermions and bosonic order parameter fluctuations in the ground state of a charge-neutral fermionic s-wave superfluid was investigated. The attractive Hubbard model served as a prototype model for fermionic superfluidity in the numerical analysis of the problem. Massless Goldstone fluctuations emerge due to spontaneous symmetry breaking of the global U(1)-symmetry, which dramatically influence the behaviour of the system. This is already visible in plain perturbation theory, where they lead to severe divergences. Our goal was to capture the correct infrared behaviour within a minimal truncation of the fermion-boson functional RG flow. Furthermore, we intended to study the mutual interplay between fermions and order parameter fluctuations, especially the dramatic impact of Goldstone fluctuations.

To this end, the fermionic two-particle interaction of the model was decoupled by a Hubbard-Stratonovich transformation in the s-wave singlet channel, and the resulting coupled fermion-boson theory was investigated with the functional renormalization group method in its 1PI version. In this approach the interplay between fermions and bosonic fluctuations, especially Goldstone fluctuations, can be captured already in a one-loop truncation of the RG flow. Fermions dominate the RG flow at high energies, whereas bosonic fluctuations dominate the RG flow in the infrared limit, where the Goldstone mode has a drastic impact.

We extended a previous truncation of a coupled fermion-boson functional RG flow by Strack et al. (2008) in several directions. They distinguished already between the fermionic single-particle gap and the bosonic order parameter. Further, longitudinal and transverse fluctuations of the bosonic order parameter fluctuations were distinguished in their study. The impact of Goldstone fluctuations on the longitudinal excitations was proved, which behaved similarly as an interacting Bose gas (Castellani et al. (1997) and Pistolesi et al. (2005)). However, in our work we additionally included a renormalization factor parametrizing the linear imaginary frequency dependence of the bosonic self-energy, which was neglected in this previous work. Such a term is generated by fermionic diagrams and leads to a mixing between transverse and longitudinal order parameter fluctuations. Furthermore, a non-local bosonic self-interaction is taken into account, parametrized by the so-called Y-term. This term is irrelevant in power counting, but turned out to be important due to symmetry. Only a finite Y-term was consistent with distinguished renormalization factors between the longitudinal and transverse fluctuations

in the symmetry-broken phase, because of the $U(1)$-symmetry of the model.

In the following, we explain our main results. The fermionic single-particle gap was reduced due to fluctuations compared to the mean-field result, as expected. However, compared to a purely fermionic RG flow our gap was much larger, which could be traced back to the lack of particle-hole fluctuations in our truncation. In two dimensions, the renormalization factor parametrizing the linear imaginary frequency dependence of the bosonic self-energy vanishes linearly in the infrared just as the longitudinal bosonic mass and the local bosonic self-interaction. The renormalization factor parametrizing the quadratic frequency and momentum dependence of the longitudinal bosonic self-energy diverged as the inverse of the cutoff scale, caused by Goldstone fluctuations, just as the Y-term. In three dimensions logarithmic behaviour in the infrared limit was found. This infrared behaviour is in full agreement with the behaviour of an interacting Bose gas.

Our simple truncation satisfies Ward identities of lowest order. Especially, we showed that our truncation is consistent with a bosonic Ward identity, connecting the longitudinal and transverse bosonic self-energies to the non-local bosonic self-interaction. Furthermore, we derived two fermion-boson Ward identities. The first identity linked the fermionic single-particle gap and the bosonic order parameter via the transverse Yukawa vertex. Another fermion-boson Ward identity appeared that coupled the two-boson-two-fermion vertex to the anomalous Yukawa coupling. In absence of a finite two-boson-two-fermion vertex, as in our truncation, this identity constrained the transverse and longitudinal Yukawa coupling to be identical.

Afterwards, we investigated the implications of these lowest order Ward identities. First, we could explicitly show that all bosonic fluctuations contributing to the flow of the Goldstone mass cancel out, due to the bosonic Ward identity. Here, the non-locality of the bosonic self-interaction played a crucial role. Second, we showed that the fermion-boson Ward identities led to a cancellation between fermionic contributions to the flow of the Goldstone mass. Finally, we also proved that in the infrared limit two singular contributions to the spectral weight of the Goldstone mode canceled out exactly. Goldstone fluctuations caused this singular behaviour of both contributions and the non-local bosonic self-interaction was again crucial for this cancellation process. Hence, in our truncation the Goldstone theorem was satisfied and a finite spectral weight for the Goldstone mode was obtained. We also pointed out that the introduction of a finite two-boson-two-fermion vertex in our theory would imply naturally differing longitudinal and transverse Yukawa couplings. We proved analytically that the RG equations for the couplings in our truncation were consistent with the Ward identity linking the fermionic gap and the bosonic order parameter via the transverse Yukawa coupling.

We summarize the central results in a list:

1. RG analysis of the ground state of a fermionic s-wave superfluid
2. transverse and longitudinal fluctuations were distinguished
3. mixing between transverse and longitudinal bosonic modes was taken into account
4. fermionic gap and bosonic order parameter were distinguished
5. gap was reduced compared to the mean-field result.
6. non-local bosonic self-interaction is important due to symmetry
7. collective excitations behaved as an interacting Bose gas
8. (lowest order) Ward identities were fulfilled in the truncation
9. massless linearly dispersing Goldstone mode was preserved in the truncation

5.2.2 Outlook

In this project, we presented a minimal truncation for the boson-fermion functional RG flow describing a fermionic superfluid in a consistent way. Since we use an ansatz for the effective action in powers of fields and gradients, new developments and extensions may follow in that direction. As mentioned above, the impact of particle-hole fluctuations (Flörchinger et al. (2007)) was not considered in our work. Hence, fluctuation contributions that are important for the size of the fermionic single-particle gap were neglected. This drawback could be addressed by the application of the dynamical bosonization in our RG scheme, where the regenerated fermionic two-particle interaction is dynamically decoupled during the RG flow (Gies et al. (2002, 2004) and Flörchinger et al. (2009)). Another improvement towards a quantitative result for the fermionic gap is given by a fully functional flow for the frequency and momentum dependence instead of a gradient ansatz. This was implemented recently in a purely fermionic RG approach (Eberlein and Metzner (2013)). The combination of the advantages of both improvements together with our achievements would lead to an accurate result for the fermionic single-particle gap, besides the correct infrared asymptotic of the collective low-energy excitations. Furthermore, it would also be interesting to investigate under what circumstances and conditions a roton

minimum appears in the spectrum of the transverse excitations, which is well-known to occur in superfluid Bose systems.

In our truncation, we neglected a two-boson-two-fermion term, which is also generated in the RG flow. As we pointed out, a finite two-boson-two-fermion vertex is connected to the anomalous Yukawa vertex through a Ward identity. The inclusion of such a term allows the distinction between transverse and longitudinal Yukawa vertices. The introduction of such a term would lead to a structural change of the RG equations. We expect that the linearly dispersing massless Goldstone mode would still be preserved within such a truncation.

In the context of ultra-cold atoms, our minimal ansatz would be an ideal basis to revisit the BCS-BEC crossover within a truncation that consistently treats the fermion-boson sector. Further RG studies of continuum models of interacting fermions in three dimensions or the attractive Hubbard model in two dimensions could be employed to investigate the crossover. For the description of the crossover, the particle number has to be fixed, which could be implemented by allowing a flow of the chemical potential. In that situation, the Goldstone fluctuations would have a more drastic impact leading to quasi-long-range order (Goldenfeld (1992)). At finite temperature, one would expect a Kosterlitz-Thouless transition in two dimensions. A BCS-BEC-like crossover is also conjectured to exist in excitonic insulators (Phan et al. (2010)), which provides a new playground for experimental and theoretical research. Here, the condensed pairs consist of electron-hole pairs instead of electron-electron pairs.

Our truncation may serve as a standard for future fermion-boson functional RG studies, where a fulfillment of Ward identities is desired.

APPENDIX A

Derivation of RG equations: Symmetric regime

In this section, we derive explicit flow equations for the couplings, which parametrize the scale-dependent effective action in the symmetric regime of the fermionic superfluid investigated in chapter 4. The flow of the couplings is extracted by successively applying functional field derivatives to the right hand side of the RG equation of the effective action. We also show that these flow equations, describing the fermionic superfluid, reduce to the flow equations investigated in the context of the Dirac cone model in chapter 3.

This appendix is structured as follows: In section A.1 the ansatz for the scale-dependent effective action is presented. Section A.2 shows the matrix representation of fermionic and bosonic propagators. Amputated vertices connecting the propagator lines and expressions for the couplings extracted from the effective action can be found in section A.3. Finally, section A.4 presents the RG flow of the couplings. The reduction of these RG equations to equations describing the quantum phase transition in the Dirac cone model is discussed in section A.5.

A.1 Ansatz for the effective action

We briefly repeat the ansatz of the scale-dependent effective action that we use for our analysis of the fermionic superfluid. The ansatz for the scale-dependent effective action

reads

$$\Gamma = \Gamma_{\bar{\psi}\psi} + \Gamma_{\phi^*\phi} + \Gamma_{\phi^4} + \Gamma_{\psi^2\phi^*}, \tag{A.1}$$

where the quadratic part in fermionic fields is given by

$$\Gamma_{\bar{\psi}\psi} = \int_{k\sigma} \bar{\psi}_{k\sigma}(ik_0 - \xi_{\mathbf{k}})\psi_{k\sigma} \tag{A.2}$$

and in bosonic fields by

$$\Gamma_{\phi^*\phi} = \frac{1}{2}\int_q \phi_q^* \left(-iWq_0 + Z_b(q_0^2 + \omega_{\mathbf{q}}^2) + m_b^2\right)\phi_q. \tag{A.3}$$

The local and non-local parts of the bosonic self-interaction

$$\Gamma_{\phi^4} = \frac{1}{8}\int_{k,k',q} U(q)\phi_k\phi^*_{k-q}\phi_{k'}\phi^*_{k'+q} \tag{A.4}$$

are parametrized by the couplings u and Y in the function $U(q) = u + Y(q_0^2 + \omega_{\mathbf{q}}^2)$. In the symmetric regime, only a normal Yukawa coupling occurs

$$\Gamma_{\psi^2\phi^*} = g\int_{k,q} \left(\bar{\psi}_{-k+q/2\downarrow}\bar{\psi}_{k+q/2\uparrow}\phi_q + \psi_{k+q/2\uparrow}\psi_{-k+q/2\downarrow}\phi_q^*\right), \tag{A.5}$$

due to the decoupling of the fermionic two-particle interaction by the Hubbard-Stratonovich transformation in the particle-particle channel.

A.2 Matrix representation of the fermionic and bosonic propagator

Here, we present the fermionic and bosonic propagator in a matrix representation. This representation will be useful for the evaluation of the RG equations in section A.4. We work in the bosonic basis $(\phi_Q) = (\phi_q, \phi_q^*)$. The functional field derivative of the scale-dependent effective action Eq. (A.1) with respect to bosonic fields is defined as

$$\frac{\delta^2\Gamma}{\delta\phi^2} \equiv \left(\frac{\delta^2\Gamma}{\delta\phi_{Q'}\delta\phi_{Q''}}\right) \equiv \begin{pmatrix} \frac{\delta^2\Gamma}{\delta\phi_{q'}\delta\phi_{q''}} & \frac{\delta^2\Gamma}{\delta\phi_{q'}\delta\phi^*_{q''}} \\ \frac{\delta^2\Gamma}{\delta\phi^*_{q'}\delta\phi_{q''}} & \frac{\delta^2\Gamma}{\delta\phi^*_{q'}\delta\phi^*_{q''}} \end{pmatrix}.$$

Inserting our ansatz yields

$$\frac{\delta^2\Gamma}{\delta\phi^2} = \begin{pmatrix} 0 & -i\frac{W}{2}q_0' + \frac{Z_b}{2}(q_0'^2 + \omega_{\mathbf{q}'}^2) + \frac{m_b^2}{2} \\ -i\frac{W}{2}q_0' + \frac{Z_b}{2}(q_0'^2 + \omega_{\mathbf{q}'}^2) + \frac{m_b^2}{2} & 0 \end{pmatrix} \delta_{q',q''} \tag{A.6}$$

in the limit of vanishing fields $\phi = \psi = 0$. In the next step, we introduce the regularized effective action as

$$\tilde{\Gamma} = \Gamma + \frac{1}{2}\int_{Q,Q'} \phi_Q \mathcal{R}_b(Q,Q')\phi_{Q'} + \frac{1}{2}\int_{K,K'} \psi_K \mathcal{R}_f(K,K')\psi_{K'}, \tag{A.7}$$

where $\mathcal{R}_b(Q,Q')$ and $\mathcal{R}_f(Q,Q')$ denote bosonic and fermionic regulators which suppress low energy modes in the effective action Γ. In matrix representation the bosonic regulator reads

$$\mathcal{R}_b(q,q') \equiv \begin{pmatrix} 0 & R_b(q)\delta_{q,q'} \\ R_b(q)\delta_{q,q'} & 0 \end{pmatrix}. \tag{A.8}$$

The matrix representation of the fermionic regulator will be shown below, when we discuss the fermionic sector of the theory.

We define the inverse of the second derivative of the regularized effective action with respect to bosonic fields as

$$\mathcal{B} \equiv \Big[\frac{\delta^2\tilde{\Gamma}}{\delta\phi^2} + \mathcal{R}_b\Big]^{-1} \equiv \Big(\mathcal{B}(\phi_{Q'},\phi_{Q''})\Big) \equiv \begin{pmatrix} \mathcal{B}(\phi_{q'},\phi_{q''}) & \mathcal{B}(\phi_{q'},\phi_{q''}^*) \\ \mathcal{B}(\phi_{q'}^*,\phi_{q''}) & \mathcal{B}(\phi_{q'}^*,\phi_{q''}^*) \end{pmatrix}. \tag{A.9}$$

Inserting our ansatz for the effective action yields the bosonic propagator in matrix representation

$$\mathcal{G}_b \equiv \mathcal{B} = \begin{pmatrix} 0 & G_b(q')\delta_{q',q''} \\ G_b(q')\delta_{q',q''} & 0 \end{pmatrix} \tag{A.10}$$

with the regularized bosonic propagator

$$G_b(q) = \frac{2}{-iWq_0 + Z_b(q_0^2 + \omega_{\mathbf{q}}^2) + m_b^2 + R_b(q)}. \tag{A.11}$$

The bosonic single-scale propagator

$$\mathcal{S}_b \equiv \frac{\partial}{\partial\Lambda}\Big|_\Sigma \mathcal{G}_b \equiv \Big(\mathcal{S}_b(\phi_{Q'},\phi_{Q''})\Big) \equiv \begin{pmatrix} 0 & S_b(q')\delta_{q',q''} \\ S_b(q')\delta_{q',q''} & 0 \end{pmatrix} \tag{A.12}$$

is defined as the first scale-derivative of the bosonic propagator, where the self-energy is kept constant.

In the fermionic case, we choose the basis $(\psi_K) = (\psi_{k\uparrow}, \psi_{k\downarrow}, \bar{\psi}_{k\uparrow}, \bar{\psi}_{k\downarrow})$, where K collects spin, charge, momentum and Matsubara frequencies. The second derivative of the effective action Eq. (A.1) with respect to fermionic fields is defined as

$$\frac{\delta^2\Gamma}{\delta\psi^2} \equiv \left(\frac{\delta^2\Gamma}{\delta\psi_{K'}\delta\psi_{K''}}\right) \equiv \begin{pmatrix} \frac{\delta^2\Gamma}{\delta\psi_{k'\uparrow}\delta\psi_{k''\uparrow}} & \frac{\delta^2\Gamma}{\delta\psi_{k'\uparrow}\delta\psi_{k''\downarrow}} & \frac{\delta^2\Gamma}{\delta\psi_{k'\uparrow}\delta\bar{\psi}_{k''\uparrow}} & \frac{\delta^2\Gamma}{\delta\psi_{k'\uparrow}\delta\bar{\psi}_{k''\downarrow}} \\ \frac{\delta^2\Gamma}{\delta\psi_{k'\downarrow}\delta\psi_{k''\uparrow}} & \frac{\delta^2\Gamma}{\delta\psi_{k'\downarrow}\delta\psi_{k''\downarrow}} & \frac{\delta^2\Gamma}{\delta\psi_{k'\downarrow}\delta\bar{\psi}_{k''\uparrow}} & \frac{\delta^2\Gamma}{\delta\psi_{k'\downarrow}\delta\bar{\psi}_{k''\downarrow}} \\ \frac{\delta^2\Gamma}{\delta\bar{\psi}_{k'\uparrow}\delta\psi_{k''\uparrow}} & \frac{\delta^2\Gamma}{\delta\bar{\psi}_{k'\uparrow}\delta\psi_{k''\downarrow}} & \frac{\delta^2\Gamma}{\delta\bar{\psi}_{k'\uparrow}\delta\bar{\psi}_{k''\uparrow}} & \frac{\delta^2\Gamma}{\delta\bar{\psi}_{k'\uparrow}\delta\bar{\psi}_{k''\downarrow}} \\ \frac{\delta^2\Gamma}{\delta\bar{\psi}_{k'\downarrow}\delta\psi_{k''\uparrow}} & \frac{\delta^2\Gamma}{\delta\bar{\psi}_{k'\downarrow}\delta\psi_{k''\downarrow}} & \frac{\delta^2\Gamma}{\delta\bar{\psi}_{k'\downarrow}\delta\bar{\psi}_{k''\uparrow}} & \frac{\delta^2\Gamma}{\delta\bar{\psi}_{k'\downarrow}\delta\bar{\psi}_{k''\downarrow}} \end{pmatrix}.$$

Inserting our ansatz yields

$$\frac{\delta^2\Gamma}{\delta\psi^2} = \begin{pmatrix} 0 & 0 & ik_0' - \xi_{\mathbf{k}'} & 0 \\ 0 & 0 & 0 & ik_0' - \xi_{\mathbf{k}'} \\ -(ik_0' - \xi_{\mathbf{k}'}) & 0 & 0 & 0 \\ 0 & -(ik_0' - \xi_{\mathbf{k}'}) & 0 & 0 \end{pmatrix} \delta_{k',k''} \tag{A.13}$$

in the limit of vanishing fields $\psi = \phi = 0$.

The inverse of the second functional derivative of the regularized effective action with respect to fermionic fields is defined as

$$\mathcal{F} \equiv \left(\mathcal{F}(\psi_{K'}, \psi_{K''})\right) \equiv \left[\frac{\delta^2\Gamma}{\delta\psi^2} - \mathcal{R}_f\right]^{-1} \tag{A.14}$$

$$\equiv \begin{pmatrix} \mathcal{F}(\psi_{k'\uparrow}, \psi_{k''\uparrow}) & \mathcal{F}(\psi_{k'\uparrow}, \psi_{k''\downarrow}) & \mathcal{F}(\psi_{k'\uparrow}, \bar{\psi}_{k''\uparrow}) & \mathcal{F}(\psi_{k'\uparrow}, \bar{\psi}_{k''\downarrow}) \\ \mathcal{F}(\psi_{k'\downarrow}, \psi_{k''\uparrow}) & \mathcal{F}(\psi_{k'\downarrow}, \psi_{k''\downarrow}) & \mathcal{F}(\psi_{k'\downarrow}, \bar{\psi}_{k''\uparrow}) & \mathcal{F}(\psi_{k'\downarrow}, \bar{\psi}_{k''\downarrow}) \\ \mathcal{F}(\bar{\psi}_{k'\uparrow}, \psi_{k''\uparrow}) & \mathcal{F}(\bar{\psi}_{k'\uparrow}, \psi_{k''\downarrow}) & \mathcal{F}(\bar{\psi}_{k'\uparrow}, \bar{\psi}_{k''\uparrow}) & \mathcal{F}(\bar{\psi}_{k',\uparrow}, \bar{\psi}_{k''\downarrow}) \\ \mathcal{F}(\bar{\psi}_{k'\downarrow}, \psi_{k''\uparrow}) & \mathcal{F}(\bar{\psi}_{k'\downarrow}, \psi_{k''\downarrow}) & \mathcal{F}(\bar{\psi}_{k'\downarrow}, \bar{\psi}_{k''\uparrow}) & \mathcal{F}(\bar{\psi}_{k'\downarrow}, \bar{\psi}_{k''\downarrow}) \end{pmatrix}, \tag{A.15}$$

where the matrix representation of the fermionic regulator is given by

$$\mathcal{R}_f \equiv \Big(\mathcal{R}_f(\psi_{K'}, \psi_{K''})\Big) \tag{A.16}$$

$$\equiv \begin{pmatrix} 0 & 0 & -R_f(k')\delta_{k',k''} & 0 \\ 0 & 0 & 0 & -R_f(k')\delta_{k',k''} \\ R_f(k')\delta_{k',k''} & 0 & 0 & 0 \\ 0 & R_f(k')\delta_{k',k''} & 0 & 0 \end{pmatrix}. \tag{A.17}$$

Inserting our ansatz yields

$$\mathcal{F} \equiv \begin{pmatrix} 0 & 0 & -G_f(k') & 0 \\ 0 & 0 & 0 & -G_f(k') \\ G_f(k') & 0 & 0 & 0 \\ 0 & G_f(k') & 0 & 0 \end{pmatrix} \delta_{k',k''} \tag{A.18}$$

with the regularized fermionic propagators

$$G_f(k) = \frac{1}{ik_0 - \xi_{\mathbf{k}} + R_f(k)}. \tag{A.19}$$

In contrast to the bosons, the fermionic propagator is defined as the negative inverse of the second derivative of the effective action with respect to fermionic fields

$$\mathcal{G}_f \equiv \Big(\mathcal{G}_f(\psi_{K'}, \psi_{K''})\Big) \equiv -\mathcal{F}(\psi_{K'}, \psi_{K''}) \tag{A.20}$$

$$\equiv \begin{pmatrix} 0 & 0 & G_f(k') & 0 \\ 0 & 0 & 0 & G_f(k') \\ -G_f(k') & 0 & 0 & 0 \\ 0 & -G_f(k') & 0 & 0 \end{pmatrix} \delta_{k',k''}.$$

The fermionic single-scale propagator

$$\mathcal{S}_f \equiv \Big(\mathcal{S}_f(\psi_{K'}, \psi_{K''})\Big) \equiv \frac{d}{d\Lambda}\Big|_\Sigma \mathcal{G}_f \tag{A.21}$$

$$\equiv \begin{pmatrix} 0 & 0 & S_f(k') & 0 \\ 0 & 0 & 0 & S_f(k') \\ -S_f(k') & 0 & 0 & 0 \\ 0 & -S_f(k') & 0 & 0 \end{pmatrix} \delta_{k',k''}. \tag{A.22}$$

is again given by the scale-derivative of the fermionic propagator.

During the evaluation of the RG equations in the next sections, we will use the shorthand notation

$$\mathcal{F} = \left[\frac{\delta^2\tilde{\Gamma}}{\delta\psi^2}\right]^{-1} = \left[\frac{\delta^2\Gamma}{\delta\psi^2} - \mathcal{R}_f\right]^{-1}, \quad \mathcal{S}_f = \frac{\partial}{\partial\Lambda}\Big|_\Sigma \mathcal{G}_f = -\frac{\partial}{\partial\Lambda}\Big|_\Sigma \mathcal{F} = -\mathcal{F}\partial_\Lambda \mathcal{R}_f \mathcal{F}, \tag{A.23}$$

$$\mathcal{B} = \left[\frac{\delta^2\tilde{\Gamma}}{\delta\phi^2}\right]^{-1} = \left[\frac{\delta^2\Gamma}{\delta\phi^2} + \mathcal{R}_b\right]^{-1}, \quad \mathcal{S}_b = \frac{\partial}{\partial\Lambda}\Big|_\Sigma \mathcal{G}_b = \frac{\partial}{\partial\Lambda}\Big|_\Sigma \mathcal{B} = -\mathcal{B}\partial_\Lambda \mathcal{R}_b \mathcal{B}. \tag{A.24}$$

The abbreviations $\mathcal{S}_f$ and $\mathcal{S}_b$ denote the matrix representation for the fermionic and bosonic single-scale propagators, whereas $\mathcal{F}$ and $\mathcal{B}$ denote the matrix representation of the inverse of the second functional derivative of the effective action for fermions and bosons. Fermionic and bosonic regulators $R_f(k)$ and $R_b(q)$ are not specified here, but are chosen in such a way that they regularize low energy modes in the effective action with the cutoff scale Λ.

A.3 Interaction vertices and couplings

The contributions to the RG flow are given in terms of one-particle-irreducible contributions consisting of propagator lines connected by vertices. First, we present the amputated form of the interaction vertices, which are required to evaluate the functional RG equations. Second, we show how the flow of the couplings is extracted from the RG flow of the effective action.

In our truncation bosonic propagators lines are connected to each other only by the

bosonic self-interaction Eq. (A.4), which are given in its amputated form by

$$\begin{aligned}\frac{\delta^4\Gamma}{\delta\phi_d^*\delta\phi_c\delta\phi_b^*\delta\phi_a} &= \frac{1}{4}\left(U(b-a)+U(b-c)\right)\delta_{a+c-b-d} \\ &= \left(\frac{u}{2}+\frac{Y}{4}((b-a)^2+(b-c)^2)\right)\delta_{a+c-b-d},\end{aligned} \tag{A.25}$$

where $a=(a_0,\mathbf{a})$, $b=(b_0,\mathbf{b})$, $c=(c_0,\mathbf{c})$ and $d=(d_0,\mathbf{d})$ collect Matsubara frequencies and bosonic momenta. Fermions and bosons interact through the normal Yukawa coupling Eq. (A.5), that in its amputated form reads as

$$\frac{\delta^3\Gamma}{\delta\psi_{k'\uparrow}\delta\psi_{k''\downarrow}\delta\phi_q^*} = -g\delta_{k''+k'-q}, \quad \frac{\delta^3\Gamma}{\delta\bar{\psi}_{k'\uparrow}\delta\bar{\psi}_{k''\downarrow}\delta\phi_q} = g\delta_{k''+k'-q}. \tag{A.26}$$

The variables $k'=(k_0',\mathbf{k}')$ and $k''=(k_0'',\mathbf{k}'')$ denote fermionic momenta and Matsubara frequencies, and $q=(q_0,\mathbf{q})$ bosonic momenta and Matsubara frequencies. In both expressions the delta functions conserve frequencies and momenta of the ingoing and outgoing fields.

The couplings parametrizing the ansatz of the scale-dependent action are accessed by functional field differentiation of the effective action with respect to fermion and boson fields and subsequent frequency or momentum differentiation, respectively. Hence, the flow of these couplings is obtained in the same way. The flow of the fermionic and bosonic self-energies are calculated by

$$\frac{d}{d\Lambda}\Sigma_f(k) = \frac{\delta^2}{\delta\psi_{k\uparrow}\delta\bar{\psi}_{k\uparrow}}\frac{d}{d\Lambda}\Gamma, \quad \frac{d}{d\Lambda}\Sigma_b(p) = \frac{\delta^2}{\delta\phi_p^*\delta\phi_p}\frac{d}{d\Lambda}\Gamma \tag{A.27}$$

at zero fields. Consequently, the renormalization constants parametrizing the frequency and momentum dependence of the fermionic and bosonic self-energy can be easily extracted from these expressions by additional frequency and momentum derivatives

$$\frac{d}{d\Lambda}Z_f = \frac{\partial}{\partial ik_0}\Big|_{k=0}\frac{d}{d\Lambda}\Sigma_f(k), \quad \frac{d}{d\Lambda}A_f = \frac{\partial^2}{\partial k_x^2}\Big|_{k=0}\frac{d}{d\Lambda}\Sigma_f(k), \tag{A.28}$$

and

$$\frac{d}{d\Lambda}Z_b^\omega = \frac{\partial^2}{\partial p_0^2}\Big|_{p=0}\frac{d}{d\Lambda}\Sigma_b(p), \quad \frac{d}{d\Lambda}Z_b = \frac{\partial^2}{\partial p_x^2}\Big|_{p=0}\frac{d}{d\Lambda}\Sigma_b(p), \tag{A.29}$$

$$\frac{d}{d\Lambda}W = 2i\frac{\partial}{\partial p_0}\Big|_{p=0}\frac{d}{d\Lambda}\Sigma_b(p). \tag{A.30}$$

Next, the flow of the bosonic self-interaction u and the Y-term is given by

$$\frac{d}{d\Lambda}\frac{u}{2} = \frac{\delta^4}{\delta\phi_0^*\delta\phi_0\delta\phi_0^*\delta\phi_0}\frac{d}{d\Lambda}\Gamma, \quad \frac{d}{d\Lambda}Y = \frac{1}{2}\frac{\partial^2}{\partial p_x^2}\frac{\delta^4}{\delta\phi_p^*\delta\phi_p\delta\phi_{-p}^*\delta\phi_{-p}}\frac{d}{d\Lambda}\Gamma. \tag{A.31}$$

We use a highly symmetric choice for the ingoing and outgoing frequencies and momenta for extracting the flow of Y. At last, the flow of the Yukawa coupling is determined from

$$\frac{d}{d\Lambda}g = \frac{\delta^3}{\delta\bar{\psi}_{k\uparrow}\delta\bar{\psi}_{-k\downarrow}\delta\phi_0}\frac{d}{d\Lambda}\Gamma. \tag{A.32}$$

A.4 RG equations for couplings

Here, we will derive the explicit flow equations for the couplings parametrizing the ansatz for the scale-dependent effective action Eq. (A.1). To this end, the ansatz is plugged into the renormalization group equation for the effective action Eq. (2.33). Afterwards, the couplings are extracted by functional field differentiation on the right and left hand side of the flow equation.

The section is structured as follows. First, we discuss the general form and properties of the renormalization equation for the effective action Γ, which will be also relevant for the discussion of the RG flow in the symmmetry-broken regime of the fermionic superfluid in appendix B. Second, we explicitly derive formal expressions for the couplings. The renormalization group equations for the bosonic self-energy Eq. (A.42) and the bosonic self-interaction Eq. (A.52) and (A.53) form the central results of this chapter.

We first analyze the structure of the renormalization group equation Eq. (2.33) for the scale-dependent effective action. The expression for the flow of the scale-dependent effective action reads

$$\begin{aligned}\frac{d}{d\Lambda}\Gamma &= \frac{1}{2}\mathrm{Tr}\left[\partial_\Lambda\mathcal{R}_b\left(\frac{\delta^2\tilde{\Gamma}}{\delta\phi^2}\right)^{-1}\left(1-\frac{\delta^2\tilde{\Gamma}}{\delta\phi\delta\psi}\left(\frac{\delta^2\tilde{\Gamma}}{\delta\psi^2}\right)^{-1}\left(\frac{\delta^2\tilde{\Gamma}}{\delta\psi\delta\phi}\right)\left(\frac{\delta^2\tilde{\Gamma}}{\delta\phi^2}\right)^{-1}\right)^{-1}\right] \\ &\quad + \frac{1}{2}\mathrm{Tr}\left[\partial_\Lambda\mathcal{R}_f\left(\frac{\delta^2\tilde{\Gamma}}{\delta\psi^2}\right)^{-1}\left(1-\frac{\delta^2\tilde{\Gamma}}{\delta\psi\delta\phi}\left(\frac{\delta^2\tilde{\Gamma}}{\delta\phi^2}\right)^{-1}\left(\frac{\delta^2\tilde{\Gamma}}{\delta\phi\delta\psi}\right)\left(\frac{\delta^2\tilde{\Gamma}}{\delta\psi^2}\right)^{-1}\right)^{-1}\right]. \\ &= \frac{1}{2}\mathrm{Tr}\left[\partial_\Lambda\mathcal{R}_b\left(\frac{\delta^2\tilde{\Gamma}}{\delta\phi^2}\right)^{-1}\Big(1-E_1\Big)^{-1}\right] + \frac{1}{2}\mathrm{Tr}\left[\partial_\Lambda\mathcal{R}_b\left(\frac{\delta^2\tilde{\Gamma}}{\delta\psi^2}\right)^{-1}\Big(1-E_2\Big)^{-1}\right],\end{aligned} \tag{A.33}$$

where Γ denotes the unregularized and $\tilde{\Gamma}$ the regularized effective action. It consists of

two main internal building blocks

$$E_1 \equiv \left(\frac{\delta^2\tilde{\Gamma}}{\delta\phi\delta\psi}\right)\left(\frac{\delta^2\tilde{\Gamma}}{\delta\psi^2}\right)^{-1}\left(\frac{\delta^2\tilde{\Gamma}}{\delta\psi\delta\phi}\right)\left(\frac{\delta^2\tilde{\Gamma}}{\delta\phi^2}\right)^{-1}, \tag{A.34}$$

$$E_2 \equiv \left(\frac{\delta^2\tilde{\Gamma}}{\delta\psi\delta\phi}\right)\left(\frac{\delta^2\tilde{\Gamma}}{\delta\phi^2}\right)^{-1}\left(\frac{\delta^2\tilde{\Gamma}}{\delta\phi\delta\psi}\right)\left(\frac{\delta^2\tilde{\Gamma}}{\delta\psi^2}\right)^{-1}. \tag{A.35}$$

This structure naturally suggests an expansion of the RG equations in a geometric series in E_1 and E_2, for instance $(1-E_1)^{-1} = \sum_{n=0}^{\infty}(E_1)^n$.[1]

Functional differentiation with respect to bosonic fields

$$\frac{\delta^n}{\delta\phi^n}E_1\Big|_{\psi,\phi=0} = \frac{\delta^n}{\delta\phi^n}E_2\Big|_{\psi,\phi=0} = 0, \tag{A.36}$$

does not give any contributions from E_1 and E_2 with $n \geq 0$ in the limit of vanishing fields, since no vertex

$$\frac{\delta^n\Gamma}{\delta\phi^n\delta\psi}\Big|_{\psi,\phi=0} = 0 \tag{A.37}$$

with merely one single fermion field derivative exists. Hence, if we are only interested in the renormalization of bosonic quantities, the reduced version

$$\frac{d}{d\Lambda}\Gamma = \frac{1}{2}\mathrm{Tr}\left(\partial_\Lambda\mathcal{R}_\mathrm{b}\left(\frac{\delta^2\tilde{\Gamma}}{\delta\phi^2}\right)^{-1}\right) + \frac{1}{2}\mathrm{Tr}\left(\partial_\Lambda\mathcal{R}_\mathrm{f}\left(\frac{\delta^2\tilde{\Gamma}}{\delta\psi^2}\right)^{-1}\right) \tag{A.38}$$

of (A.33) is sufficient for the analysis.

However, the terms E_1 and E_2 become relevant as soon as fermionic field derivatives come into play. For instance, the second derivative of E_1 with respect to fermionic fields yields two finite contributions of the form

$$\begin{aligned}\frac{\delta^2 E_1}{\delta\psi_b\delta\psi_a} = &\left(\frac{\delta^3\tilde{\Gamma}}{\delta\psi_a\delta\phi\delta\psi}\right)\left(\frac{\delta^2\tilde{\Gamma}}{\delta\psi^2}\right)^{-1}\left(\frac{\delta^3\tilde{\Gamma}}{\delta\psi_b\delta\psi\delta\phi}\right)\left(\frac{\delta^2\tilde{\Gamma}}{\delta\phi^2}\right)^{-1}\\ &-\left(\frac{\delta^3\tilde{\Gamma}}{\delta\psi_b\delta\phi\delta\psi}\right)\left(\frac{\delta^2\tilde{\Gamma}}{\delta\psi^2}\right)^{-1}\left(\frac{\delta^3\tilde{\Gamma}}{\delta\psi_a\delta\psi\delta\phi}\right)\left(\frac{\delta^2\tilde{\Gamma}}{\delta\phi^2}\right)^{-1}\end{aligned} \tag{A.39}$$

[1] To evaluate the functional differentiation of the RG flow equation with respect to fermionic and bosonic fields, the relations $\frac{\delta}{\delta\phi}(A)^{-1} = -A^{-1}\frac{\delta}{\delta\phi}AA^{-1}$ and $\frac{\delta}{\delta\psi}(A)^{-1} = -A^{-1}\frac{\delta}{\delta\psi}AA^{-1}$ are helpful, where A denotes a general (functional) matrix.

in the limit of vanishing fermionic and bosonic fields due to the Yukawa coupling.

Thus, we conclude that the terms E_1 and E_2 are relevant for the RG flow of the fermionic self-energy, that means for fermionic renormalization factors and for the fermionic single-particle gap. They also give a finite contribution to the renormalization of the Yukawa vertex $\Gamma_{\phi^*\psi^2}$ and the renormalization of the two-boson two-fermion vertex $\Gamma_{\phi^2\psi^2}$. In this case, the full flow equation Eq. (A.33) for the effective action is required to capture all contributions.

After the above discussion concerning the structure of the functional RG equation of the effective action, we will now calculate the flow equations for the couplings, which parametrize our gradient ansatz of the scale-dependent effective action. We apply functional field derivatives to the right hand side of the flow equation to extract the flow of couplings. First, we present the derivation of the RG flow of the bosonic self-energy, where we need the second functional derivative of the effective action with respect to the bosonic fields

$$\begin{aligned}\frac{\delta^2}{\delta\phi_b^*\delta\phi_a}\frac{d}{d\Lambda}\Gamma = \frac{1}{2}\mathrm{Tr}\left(\mathcal{S}_b\frac{\delta^4\tilde{\Gamma}}{\delta\phi_b^*\delta\phi_a\delta\phi^2}\right) \\ -\frac{1}{2}\mathrm{Tr}\left(\mathcal{S}_f\frac{\delta^3\tilde{\Gamma}}{\delta\phi_b^*\delta\psi^2}\mathcal{F}\frac{\delta^3\tilde{\Gamma}}{\delta\phi_a\delta\psi^2}\right) - \frac{1}{2}\mathrm{Tr}\left(\mathcal{S}_f\frac{\delta^3\tilde{\Gamma}}{\delta\phi_a\delta\psi^2}\mathcal{F}\frac{\delta^3\tilde{\Gamma}}{\delta\phi_b^*\delta\psi^2}\right).\end{aligned} \tag{A.40}$$

Now, we evaluate the columns and the rows of the matrix representation for the propagators $\mathcal{F}$, $\mathcal{B}$, $\mathcal{S}_f$ and $\mathcal{S}_b$, see Eq. (A.23) and Eq. (A.24). Further, we consider only the processes which are allowed due to the vertices Eq. (A.25) and (A.26). This yields

$$\begin{aligned}\frac{\delta^2}{\delta\phi_b^*\delta\phi_a}\frac{d}{d\Lambda}\Gamma = \frac{1}{2}\mathrm{Tr}\left(\mathcal{S}_\mathrm{b}(\phi_\mathrm{c}^*,\phi_\mathrm{d})\frac{\delta^4\tilde{\Gamma}}{\delta\phi_\mathrm{b}^*\delta\phi_\mathrm{a}\delta\phi_\mathrm{d}\delta\phi_\mathrm{c}^*}\right) \\ +\frac{1}{2}\mathrm{Tr}\left(\mathcal{S}_\mathrm{b}(\phi_\mathrm{c},\phi_\mathrm{d}^*)\frac{\delta^4\tilde{\Gamma}}{\delta\phi_\mathrm{b}^*\delta\phi_\mathrm{a}\delta\phi_\mathrm{d}^*\delta\phi_\mathrm{c}}\right) \\ -\frac{1}{2}\mathrm{Tr}\left(\mathcal{S}_\mathrm{f}(\bar{\psi}_\mathrm{x},\psi_\mathrm{y})\frac{\delta^3\tilde{\Gamma}}{\delta\phi_\mathrm{b}^*\delta\psi_\mathrm{y}\delta\psi_\mathrm{z}}\mathcal{F}(\psi_\mathrm{z},\bar{\psi}_\mathrm{w})\frac{\delta^3\tilde{\Gamma}}{\delta\phi_\mathrm{a}\delta\bar{\psi}_\mathrm{w}\delta\bar{\psi}_\mathrm{x}}\right) \\ -\frac{1}{2}\mathrm{Tr}\left(\mathcal{S}_\mathrm{f}(\psi_\mathrm{x},\bar{\psi}_\mathrm{y})\frac{\delta^3\tilde{\Gamma}}{\delta\phi_\mathrm{a}\delta\bar{\psi}_\mathrm{y}\delta\bar{\psi}_\mathrm{z}}\mathcal{F}(\bar{\psi}_\mathrm{z},\psi_\mathrm{w})\frac{\delta^3\tilde{\Gamma}}{\delta\phi_\mathrm{b}^*\delta\psi_\mathrm{w}\delta\psi_\mathrm{x}}\right).\end{aligned} \tag{A.41}$$

Here, the trace integrates over the remaining degrees of freedom.[2] In the next step we

[2] In the first two lines of the equation, we use the abbreviation $\mathrm{Tr} \mathrel{\hat{=}} \int_{\mathrm{c,d}}$, whereas and in the last two lines the relation $\mathrm{Tr} \mathrel{\hat{=}} \int_{\mathrm{y,z,w}}$ holds. We will apply this compact notation throughout the rest of the work.

insert both amputated vertices Eq. (A.25) and (A.26) and evaluate the integration over the Dirac delta functions and sums over the fermionic spin σ index and set $a = b = p$. Then, the flow of the bosonic self-energy is obtained as

$$\frac{d}{d\Lambda}\Sigma_b(p) = \frac{\delta^2}{\delta\phi_p^*\delta\phi_p}\frac{d}{d\Lambda}\Gamma = \int_q D_\Lambda G_b(q)\left(\frac{u}{2} + \frac{Y}{4}\Big((q_0-p_0)^2 + \omega^2_{\mathbf{q}-\mathbf{p}}\Big)\right) - g^2\int_k D_\Lambda\left[G_f(k)G_f(-k+p)\right] \tag{A.42}$$

Finally, the flow for the renormalization factors parametrizing the bosonic self-energy can be calculated by

$$\frac{d}{d\Lambda}\frac{m_b^2}{2} = \int_q D_\Lambda G_b(q)\left(\frac{u}{2} + \frac{Y}{4}\Big(q_0^2 + \omega^2_{\mathbf{q}}\Big)\right) - g^2\int_k D_\Lambda\left[G_f(k)G_f(-k)\right], \tag{A.43}$$

$$\frac{d}{d\Lambda}Z_b^\omega = -g^2\frac{\partial^2}{\partial p_0^2}\Big|_{p=0}\int_k D_\Lambda\left[G_f(k)G_f(-k+p)\right] + \frac{\partial^2}{\partial p_0^2}\Big|_{p=0}\int_q D_\Lambda G_b(q)\Big(\frac{Y}{4}(q_0-p_0)^2\Big), \tag{A.44}$$

$$\frac{d}{d\Lambda}Z_b = -g^2\frac{\partial^2}{\partial p_x^2}\Big|_{p=0}\int_k D_\Lambda\left[G_f(k)G_f(-k+p)\right] + \frac{\partial^2}{\partial p_x^2}\Big|_{p=0}\int_q D_\Lambda G_b(q)\Big(\frac{Y}{4}\omega^2_{\mathbf{q}-\mathbf{p}}\Big), \tag{A.45}$$

$$\frac{d}{d\Lambda}W = -2i\frac{\partial}{\partial p_0}\Big|_{p=0}g^2\int_k D_\Lambda\left[G_f(k)G_f(-k+q)\right] - i\int_q D_\Lambda G_b(q)Yq_0. \tag{A.46}$$

The regularized bosonic and fermionic propagators are defined as

$$G_b(q) = \frac{2}{-iWq_0 + Z_b(q_0^2+\omega^2_{\mathbf{q}}) + m_b^2 + R_b(q)}, \tag{A.47}$$

$$G_f(k) = \frac{1}{ik_0 - \xi_{\mathbf{k}} + R_f(k)}. \tag{A.48}$$

Second, we evaluate the contributions which determine the flow of the non-local bosonic self-interaction. We will first discuss fermionic contributions to the flow and then bosonic contributions to the flow of the bosonic self-interaction. Functional differentiation of the effective action with respect to bosonic fields yields

$$\frac{\delta^4}{\delta\phi_d^*\delta\phi_c\delta\phi_b^*\delta\phi_a}\frac{d}{d\Lambda}\Gamma = I_1 + I_2 \tag{A.49}$$

a fermionic and a bosonic contribution to the flow. The fermionic contribution reads

$$
\begin{aligned}
I_1 = &-\frac{1}{2}\mathrm{Tr}\left(\mathcal{S}_\mathrm{f}\frac{\delta^3\tilde{\Gamma}}{\delta\phi_\mathrm{a}\delta\bar{\psi}^2}\mathcal{F}\frac{\delta^3\tilde{\Gamma}}{\delta\phi_\mathrm{b}^*\delta\psi^2}\mathcal{F}\frac{\delta^3\tilde{\Gamma}}{\delta\phi_\mathrm{c}\delta\bar{\psi}^2}\mathcal{F}\frac{\delta^3\tilde{\Gamma}}{\delta\phi_\mathrm{d}^*\delta\psi^2}\right)\\
&-\frac{1}{2}\mathrm{Tr}\left(\mathcal{S}_\mathrm{f}\frac{\delta^3\tilde{\Gamma}}{\delta\phi_\mathrm{a}\delta\bar{\psi}^2}\mathcal{F}\frac{\delta^3\tilde{\Gamma}}{\delta\phi_\mathrm{d}^*\delta\psi^2}\mathcal{F}\frac{\delta^3\tilde{\Gamma}}{\delta\phi_\mathrm{c}\delta\bar{\psi}^2}\mathcal{F}\frac{\delta^3\tilde{\Gamma}}{\delta\phi_\mathrm{b}^*\delta\psi^2}\right)\\
&-\frac{1}{2}\mathrm{Tr}\left(\mathcal{S}_\mathrm{f}\frac{\delta^3\tilde{\Gamma}}{\delta\phi_\mathrm{c}\delta\bar{\psi}^2}\mathcal{F}\frac{\delta^3\tilde{\Gamma}}{\delta\phi_\mathrm{b}^*\delta\psi^2}\mathcal{F}\frac{\delta^3\tilde{\Gamma}}{\delta\phi_\mathrm{a}\delta\bar{\psi}^2}\mathcal{F}\frac{\delta^3\tilde{\Gamma}}{\delta\phi_\mathrm{d}^*\delta\psi^2}\right)\\
&-\frac{1}{2}\mathrm{Tr}\left(\mathcal{S}_\mathrm{f}\frac{\delta^3\tilde{\Gamma}}{\delta\phi_\mathrm{c}\delta\bar{\psi}^2}\mathcal{F}\frac{\delta^3\tilde{\Gamma}}{\delta\phi_\mathrm{d}^*\delta\psi^2}\mathcal{F}\frac{\delta^3\tilde{\Gamma}}{\delta\phi_\mathrm{a}\delta\bar{\psi}^2}\mathcal{F}\frac{\delta^3\tilde{\Gamma}}{\delta\phi_\mathrm{b}^*\delta\psi^2}\right)\\
&-\frac{1}{2}\mathrm{Tr}\left(\mathcal{S}_\mathrm{f}\frac{\delta^3\tilde{\Gamma}}{\delta\phi_\mathrm{b}^*\delta\psi^2}\mathcal{F}\frac{\delta^3\tilde{\Gamma}}{\delta\phi_\mathrm{a}\delta\bar{\psi}^2}\mathcal{F}\frac{\delta^3\tilde{\Gamma}}{\delta\phi_\mathrm{d}^*\delta\psi^2}\mathcal{F}\frac{\delta^3\tilde{\Gamma}}{\delta\phi_\mathrm{c}\delta\bar{\psi}^2}\right)\\
&-\frac{1}{2}\mathrm{Tr}\left(\mathcal{S}_\mathrm{f}\frac{\delta^3\tilde{\Gamma}}{\delta\phi_\mathrm{b}^*\delta\psi^2}\mathcal{F}\frac{\delta^3\tilde{\Gamma}}{\delta\phi_\mathrm{c}\delta\bar{\psi}^2}\mathcal{F}\frac{\delta^3\tilde{\Gamma}}{\delta\phi_\mathrm{d}^*\delta\psi^2}\mathcal{F}\frac{\delta^3\tilde{\Gamma}}{\delta\phi_\mathrm{a}\delta\bar{\psi}^2}\right)\\
&-\frac{1}{2}\mathrm{Tr}\left(\mathcal{S}_\mathrm{f}\frac{\delta^3\tilde{\Gamma}}{\delta\phi_\mathrm{d}^*\delta\psi^2}\mathcal{F}\frac{\delta^3\tilde{\Gamma}}{\delta\phi_\mathrm{a}\delta\bar{\psi}^2}\mathcal{F}\frac{\delta^3\tilde{\Gamma}}{\delta\phi_\mathrm{b}^*\delta\psi^2}\mathcal{F}\frac{\delta^3\tilde{\Gamma}}{\delta\phi_\mathrm{c}\delta\bar{\psi}^2}\right)\\
&-\frac{1}{2}\mathrm{Tr}\left(\mathcal{S}_\mathrm{f}\frac{\delta^3\tilde{\Gamma}}{\delta\phi_\mathrm{d}^*\delta\psi^2}\mathcal{F}\frac{\delta^3\tilde{\Gamma}}{\delta\phi_\mathrm{c}\delta\bar{\psi}^2}\mathcal{F}\frac{\delta^3\tilde{\Gamma}}{\delta\phi_\mathrm{b}^*\delta\psi^2}\mathcal{F}\frac{\delta^3\tilde{\Gamma}}{\delta\phi_\mathrm{a}\delta\bar{\psi}^2}\right).
\end{aligned}
$$

For clarity reasons, we will now explicitly write out the sums over spins in the first contribution to I_1:

$$
\begin{aligned}
&-\frac{1}{2}\mathrm{Tr}\left(\mathcal{S}_\mathrm{f}\frac{\delta^3\tilde{\Gamma}}{\delta\phi_\mathrm{a}\delta\bar{\psi}^2}\mathcal{F}\frac{\delta^3\tilde{\Gamma}}{\delta\phi_\mathrm{b}^*\delta\psi^2}\mathcal{F}\frac{\delta^3\tilde{\Gamma}}{\delta\phi_\mathrm{c}\delta\bar{\psi}^2}\mathcal{F}\frac{\delta^3\tilde{\Gamma}}{\delta\phi_\mathrm{d}^*\delta\psi^2}\right)\\
&\quad=-\frac{1}{2}\mathrm{Tr}\left(\mathcal{S}_\mathrm{f}(\psi_{\mathrm{x}\uparrow},\bar{\psi}_{\mathrm{y}\uparrow})\frac{\delta^3\tilde{\Gamma}}{\delta\phi_\mathrm{a}\delta\bar{\psi}_{\mathrm{y}\uparrow}\delta\bar{\psi}_{\mathrm{z}\downarrow}}\mathcal{F}(\bar{\psi}_{\mathrm{z}\downarrow},\psi_{\mathrm{s}\downarrow})\frac{\delta^3\tilde{\Gamma}}{\delta\phi_\mathrm{b}^*\delta\psi_{\mathrm{s}\downarrow}\delta\psi_{\mathrm{t}\uparrow}}\right.\\
&\qquad\left.\cdot\,\mathcal{F}(\psi_{t\uparrow},\bar{\psi}_{u\uparrow})\frac{\delta^3\tilde{\Gamma}}{\delta\phi_c\delta\bar{\psi}_{u\uparrow}\delta\bar{\psi}_{v\downarrow}}\mathcal{F}(\bar{\psi}_{v\downarrow},\psi_{w\downarrow})\frac{\delta^3\tilde{\Gamma}}{\delta\phi_d^*\delta\psi_{w\downarrow}\delta\psi_{x\uparrow}}\right)\\
&\quad\quad-\frac{1}{2}\mathrm{Tr}\left(\mathcal{S}_\mathrm{f}(\psi_{\mathrm{x}\downarrow},\bar{\psi}_{\mathrm{y}\downarrow})\frac{\delta^3\tilde{\Gamma}}{\delta\phi_\mathrm{a}\delta\bar{\psi}_{\mathrm{y}\downarrow}\delta\bar{\psi}_{\mathrm{z}\uparrow}}\mathcal{F}(\bar{\psi}_{\mathrm{z}\uparrow},\psi_{\mathrm{s}\uparrow})\frac{\delta^3\tilde{\Gamma}}{\delta\phi_\mathrm{b}^*\delta\psi_{\mathrm{s}\uparrow}\delta\psi_{\mathrm{t}\downarrow}}\right.\\
&\qquad\left.\cdot\,\mathcal{F}(\psi_{t\downarrow},\bar{\psi}_{u\downarrow})\frac{\delta^3\tilde{\Gamma}}{\delta\phi_c\delta\bar{\psi}_{u\downarrow}\delta\bar{\psi}_{v\uparrow}}\mathcal{F}(\bar{\psi}_{v\uparrow},\psi_{w\uparrow})\frac{\delta^3\tilde{\Gamma}}{\delta\phi_d^*\delta\psi_{w\uparrow}\delta\psi_{x\downarrow}}\right).
\end{aligned}
\tag{A.50}
$$

We see that due to the normal Yukawa vertex Eq. (A.26), for each contribution only two different spin configurations are possible which lead to a doubling of fermionic contribu-

tions to the flow of the non-local bosonic self-interaction. Finally, the bosonic contributions to the flow of the non-local bosonic self-interaction are obtained as

$$\begin{aligned} I_2 = &-\frac{1}{2}\mathrm{Tr}\left(\mathcal{S}_b \frac{\delta^4\tilde{\Gamma}}{\delta\phi_c\delta\phi_a\delta\phi^2}\mathcal{B}\frac{\delta^4\tilde{\Gamma}}{\delta\phi_d^*\delta\phi_b^*\delta\phi^2}\right) - \frac{1}{2}\mathrm{Tr}\left(\mathcal{S}_b \frac{\delta^4\tilde{\Gamma}}{\delta\phi_d^*\delta\phi_b^*\delta\phi^2}\mathcal{B}\frac{\delta^4\tilde{\Gamma}}{\delta\phi_c\delta\phi_a\delta\phi^2}\right) \\ &-\frac{1}{2}\mathrm{Tr}\left(\mathcal{S}_b \frac{\delta^4\tilde{\Gamma}}{\delta\phi_b^*\delta\phi_a\delta\phi^2}\mathcal{B}\frac{\delta^4\tilde{\Gamma}}{\delta\phi_d^*\delta\phi_c\delta^2\phi}\right) - \frac{1}{2}\mathrm{Tr}\left(\mathcal{S}_b \frac{\delta^4\tilde{\Gamma}}{\delta\phi_d^*\delta\phi_c\delta\phi^2}\mathcal{B}\frac{\delta^4\tilde{\Gamma}}{\delta\phi_b^*\delta\phi_a\delta\phi^2}\right). \\ &-\frac{1}{2}\mathrm{Tr}\left(\mathcal{S}_b \frac{\delta^4\tilde{\Gamma}}{\delta\phi_d^*\delta\phi_a\delta\phi^2}\mathcal{B}\frac{\delta^4\tilde{\Gamma}}{\delta\phi_c\delta\phi_b^*\delta^2\phi}\right) - \frac{1}{2}\mathrm{Tr}\left(\mathcal{S}_b \frac{\delta^4\tilde{\Gamma}}{\delta\phi_c\delta\phi_b^*\delta\phi^2}\mathcal{B}\frac{\delta^4\tilde{\Gamma}}{\delta\phi_d^*\delta\phi_a\delta\phi^2}\right), \end{aligned}$$

where we used that no bosonic three particle interaction term exists in the symmetric phase. Evaluation of the bosonic c-index yields

$$\begin{aligned} I_2 = &-\frac{1}{2}\mathrm{Tr}\left(D_\Lambda\Big[\mathcal{B}(\phi_x,\phi_y^*)\frac{\delta^4\tilde{\Gamma}}{\delta\phi_c\delta\phi_a\delta\phi_y^*\delta\phi_z^*}\mathcal{B}(\phi_z^*,\phi_w)\frac{\delta^4\tilde{\Gamma}}{\delta\phi_d^*\delta\phi_b^*\delta\phi_w\delta\phi_x}\Big]\right) \\ &-\frac{1}{2}\mathrm{Tr}\left(D_\Lambda\Big[\mathcal{B}(\phi_x^*,\phi_y)\frac{\delta^4\tilde{\Gamma}}{\delta\phi_b^*\delta\phi_a\delta\phi_y\delta\phi_z^*}\mathcal{B}(\phi_z^*,\phi_w)\frac{\delta^4\tilde{\Gamma}}{\delta\phi_d^*\delta\phi_c\delta\phi_w\delta\phi_x^*}\Big]\right) \\ &-\frac{1}{2}\mathrm{Tr}\left(D_\Lambda\Big[\mathcal{B}(\phi_x,\phi_y^*)\frac{\delta^4\tilde{\Gamma}}{\delta\phi_b^*\delta\phi_a\delta\phi_y^*\delta\phi_z}\mathcal{B}(\phi_z,\phi_w^*)\frac{\delta^4\tilde{\Gamma}}{\delta\phi_d^*\delta\phi_c\delta\phi_w^*\delta\phi_x}\Big]\right) \\ &-\frac{1}{2}\mathrm{Tr}\left(D_\Lambda\Big[\mathcal{B}(\phi_x^*,\phi_y)\frac{\delta^4\tilde{\Gamma}}{\delta\phi_d^*\delta\phi_a\delta\phi_y\delta\phi_z^*}\mathcal{B}(\phi_z^*,\phi_w)\frac{\delta^4\tilde{\Gamma}}{\delta\phi_c\delta\phi_b^*\delta\phi_w\delta\phi_x^*}\Big]\right) \\ &-\frac{1}{2}\mathrm{Tr}\left(D_\Lambda\Big[\mathcal{B}(\phi_x,\phi_y^*)\frac{\delta^4\tilde{\Gamma}}{\delta\phi_d^*\delta\phi_a\delta\phi_y^*\delta\phi_z}\mathcal{B}(\phi_z,\phi_w^*)\frac{\delta^4\tilde{\Gamma}}{\delta\phi_c\delta\phi_b^*\delta\phi_w^*\delta\phi_x}\Big]\right), \end{aligned} \tag{A.51}$$

where we already used the internal symmetry of the bosonic self-interaction to write the expression in a compact way. The flow of the (local) bosonic self-interaction

$$\begin{aligned} \frac{d}{d\Lambda}u = &4g^4\int_k \frac{d}{d\Lambda}\left[G_f(k)G_f(-k)\right]^2 - \int_q D_\Lambda\left[G_b(q)G_b(-q)\right]\left(\frac{u}{2}+\frac{Y}{2}(q_0^2+\omega_{\mathbf{q}}^2)\right)^2 \\ &-4\int_q D_\Lambda\left[G_b(q)\right]^2\left(\frac{u}{2}+\frac{Y}{4}(q_0^2+\omega_{\mathbf{q}}^2)\right)^2. \end{aligned} \tag{A.52}$$

is obtained by setting all external frequencies and momenta to zero $a,b,c,d=0$. The RG

flow of the Y-term is given by

$$\begin{aligned}\frac{d}{d\Lambda}Y=&\frac{1}{2}\frac{\partial^2}{\partial p_x^2}\Big|_{p=0}\int_k D_\Lambda[G_f^2(k)G_f(-k+p)G_f(-k-p)] \\ &+\frac{1}{2}\frac{\partial^2}{\partial p_x^2}\Big|_{p=0}\int_k D_\Lambda\left[G_f(k-p)G_f(k+p)G_f(-k)^2\right] \\ &-\frac{1}{4}\frac{\partial^2}{\partial p_x^2}\Big|_{p=0}\int_q D_\Lambda\left[G_b(q)G_b(-q)\right]\left(\frac{Y}{4}\left((q-p)^2+(q+p)^2\right)+\frac{u}{2}\right)^2 \\ &-\frac{1}{2}\frac{\partial^2}{\partial p_x^2}\Big|_{p=0}\int_q D_\Lambda\left[G_b(q)G_b(q)\right]\left(\frac{Y}{4}(q+p)^2+\frac{u}{2}\right)\left(\frac{Y}{4}(q-p)^2+\frac{u}{2}\right) \\ &-\frac{1}{2}\frac{\partial^2}{\partial p_x^2}\Big|_{p=0}\int_q D_\Lambda\left[G_b(q+p)G_b(q-p)\right]\left(\frac{Y}{4}(4p^2+q^2)+\frac{u}{2}\right)^2,\end{aligned} \tag{A.53}$$

where we choose the external frequencies and momenta in a highly symmetric way, $a = -c = p$ and $b = -d = p$.

The equations Eq. (A.52) and (A.53), describing the RG flow of the non-local bosonic self-interaction, and the RG equation for the bosonic self-energy Eq. (A.42) are the central results of this chapter.

A.5 RG equations for the Dirac cone model

Here, we present the functional RG equations describing the quantum phase transition between a superfluid and a semimetal in the Dirac cone model in chapter 3. The equations governing the RG flow for the attractive Hubbard model and the Dirac cone model in the symmetric regime are similar, since the fermionic two-particle interaction is decoupled by a Hubbard-Stratonovich transformation in the particle-particle channel in both systems. Thus, the one-particle-irreducible contributions to the RG flow are identical in both cases and differ only in the explicit form of the propagators. However, the Dirac cone model includes an internal band index α parametrizing the upper and lower Dirac cone, which has to be considered additionally.

We start from the functional RG equations Eq. (A.42) and (A.52), which describe the flow of the bosonic self-energy and self-interaction in the symmetric regime in the attractive Hubbard model. In the limit of a vanishing Y-Term and a vanishing linear frequency dependence in the bosonic propagator, $W = Y = 0$, this set of equations

reduces to

$$\frac{d}{d\Lambda}\Sigma_b(p) = \frac{u}{2}\int_q D_\Lambda G_b(q) - g^2\int_k D_\Lambda\left[G_f(k)G_f(-k+p)\right] \tag{A.54}$$

$$\frac{d}{d\Lambda}u = 4g^4\int_k D_\Lambda\left[G_f(k)G_f(-k)\right]^2 - \frac{5}{4}u^2\int_q D_\Lambda\left[G_b(q)\right]^2 \tag{A.55}$$

and therefore the flow equations for the couplings reads

$$\frac{d}{d\Lambda}\frac{m_b^2}{2} = \frac{u}{2}\int_q D_\Lambda G_b(q) - g^2\int_k D_\Lambda\left[G_f(k)G_f(-k)\right], \tag{A.56}$$

$$\frac{d}{d\Lambda}Z_b = -g^2\frac{\partial^2}{\partial q_0^2}\Big|_{q=0}\int_k D_\Lambda\left[G_f(k)G_f(-k+q)\right], \tag{A.57}$$

$$\frac{d}{d\Lambda}A_b = -g^2\frac{\partial^2}{\partial q_x^2}\Big|_{q=0}\int_k D_\Lambda\left[G_f(k)G_f(-k+q)\right], \tag{A.58}$$

$$\frac{d}{d\Lambda}u = 4g^4\int_k D_\Lambda\left[G_f(k)G_f(-k)\right]^2 - \frac{5}{4}u^2\int_q D_\Lambda\left[G_b(q)\right]^2, \tag{A.59}$$

$$\frac{d}{d\Lambda}g = 0. \tag{A.60}$$

We used the following definition for the regularized fermionic and bosonic propagator

$$G_b(q) = \frac{2}{Z_b q_0^2 + A_b\omega_{\mathbf{q}}^2 + m_b^2 + R_b(q)}, \tag{A.61}$$

$$G_f(k) = \frac{1}{iZ_f k_0 - A_f\xi_{\mathbf{k}} + R_f(k)}, \tag{A.62}$$

where Z_b and A_b denote bosonic frequency and momentum renormalization factors and Z_f and A_f fermionic frequency and momentum renormalization factors. Both regulators are regularized by a sharp Litim cutoff

$$R_b(q) = Z_b(\Lambda^2 - q_0^2)\Theta(\Lambda^2 - q_0^2) \tag{A.63}$$

$$R_f(k) = Z_f(i\Lambda\mathrm{sgn}(k_0) - ik_0)\Theta(\Lambda^2 - k_0^2). \tag{A.64}$$

An internal sign change in the definition of the fermionic and bosonic regulator, $R_f(k) \to -R_f(k)$ and $R_b(q) \to -R_b(q)$, is compensated by the scale-derivative of the regulator and hence does not affect the form of the flow equations. However, a sign change in the definition of the bosonic propagator has a more drastic impact: The sign structure of the prefactors changes throughout the flow equations. Substituting the bosonic propagator

$G_b(q) \to -\bar{G}(q)$ with

$$\bar{G}_b(q) = \frac{-1}{Z_b q_0^2 + A_b \omega_{\mathbf{q}}^2 + m_b^2 - R_b(q)} \tag{A.65}$$

the equations Eq. (A.54) and (A.55) transform to

$$\frac{d}{d\Lambda}\bar{G}_b^{-1}(p) = \frac{u}{2}\int_q D_\Lambda \bar{G}_b(q) + g^2 \int_k D_\Lambda \left[G_f(k)G_f(-k+p)\right] \tag{A.66}$$

$$\frac{d}{d\Lambda}u = 4g^4 \int_k D_\Lambda \left[G_f(k)G_f(-k)\right]^2 - \frac{5}{4}u^2 \int_q D_\Lambda \left[\bar{G}_b(q)\right]^2. \tag{A.67}$$

It is easy to check that the prefactors and the signs of this flow equations are identical to those of the Dirac cone model. However, the RG equations of both systems still differ. Until now the band structure reflecting interactions of fermions in the two Dirac cones is not included. A diligent examination of the contributions to the flow leads to additional summations over the band index α, which only affect fermionic contributions. In total, the renormalization group equations for the Dirac cone model are then obtained as

$$\frac{d}{d\Lambda}\bar{G}_b^{-1}(p) = g^2 \int_{k\alpha} D_\Lambda \left[G_{f\alpha}(k)G_{f\alpha}(-k+p)\right] + \frac{u}{2}\int_q D_\Lambda \bar{G}_b(q) \tag{A.68}$$

$$\frac{d}{d\Lambda}u = 4g^4 \int_{k\alpha} D_\Lambda \left[G_{f\alpha}(-k)\right]^2 \left[G_{f\alpha}(k)\right]^2 - \frac{5}{4}u^2 \int_q D_\Lambda \left[\bar{G}_b(q)\right]^2. \tag{A.69}$$

Finally, we obtain the central result of this section, the flow equations describing the RG flow in the symmetric phase of the Dirac cone model:

$$\frac{d}{d\Lambda}m_b^2 = -g^2 \int_{k\alpha} D_\Lambda \left[G_{f\alpha}(k)G_{f\alpha}(-k)\right] - \frac{u}{2}\int_q D_\Lambda \bar{G}_b(q) \tag{A.70}$$

$$\frac{d}{d\Lambda}Z_b = -\frac{1}{2}\frac{\partial^2}{\partial p_0^2}\Big|_{p=0} g^2 \int_{k\alpha} D_\Lambda \left[G_{f\alpha}(k+p)G_{f\alpha}(-k)\right] \tag{A.71}$$

$$\frac{d}{d\Lambda}A_b = -\frac{1}{2}\frac{\partial^2}{\partial p_x^2}\Big|_{p=0} g^2 \int_{k\alpha} D_\Lambda \left[G_{f\alpha}(k+p)G_{f\alpha}(-k)\right] \tag{A.72}$$

$$\frac{d}{d\Lambda}u = 4g^4 \int_{k\alpha} D_\Lambda \left[G_{f\alpha}(-k)\right]^2 \left[G_{f\alpha}(k)\right]^2 - \frac{5}{4}u^2 \int_q D_\Lambda \left[\bar{G}_b(q)\right]^2 \tag{A.73}$$

$$\frac{d}{d\Lambda}g = 0. \tag{A.74}$$

with the abbreviation $D_\Lambda = \frac{d}{d\Lambda}\Big|_{\Sigma^\Lambda} = \sum_{s=f,b} (\partial_\Lambda R_s)\partial_{R_s}$. The regularized fermionic and

bosonic propagators are now defined as

$$G_{f\alpha}(k) = \frac{1}{iZ_f k_0 - A_f \xi_{\mathbf{k}\alpha} + R_f(k)}, \quad \bar{G}_b(q) = \frac{-1}{Z_b q_0^2 + A_b \omega_{\mathbf{q}}^2 + m_b^2 - R_b(q)}. \tag{A.75}$$

The propagators are regularized by a Litim momentum cutoff

$$R_b(q) = A_b \left(\Lambda^2 - \omega_{\mathbf{q}}^2\right) \Theta(\Lambda^2 - \mathbf{q}^2) \tag{A.76}$$

$$R_{f\alpha}(q) = A_f(\xi_{\mathbf{k}\alpha} - \Lambda \mathrm{sgn}(\xi_{\mathbf{k}\alpha}))\Theta(\Lambda - |\xi_{\mathbf{k}\alpha}|). \tag{A.77}$$

instead of a sharp Litim frequency cutoff. The RG flow for the fermionic renormalization factors Z_f and A_f can be derived in a similar way, but is not explicitly shown here. The renormalization group equations Eq. (A.70)-(A.74) are identical to the equations derived by Strack et al. (2010) in a diagrammatic approach.

APPENDIX B

Derivation of RG equations: SSB regime

In this chapter, we derive RG equations for the couplings parametrizing the ansatz of the scale-dependent effective action in the symmetry-broken phase. We use a coupled fermion-boson ansatz to describe the RG flow in the symmetry-broken regime of a fermionic superfluid. After the introduction of the explicit ansatz containing fermionic and bosonic degrees of freedom in transverse and longitudinal decomposition, fermionic and bosonic propagators are shown. In the symmetry-broken phase, also anomalous fermionic propagators exist. A non-local bosonic self-interaction and a linear frequency dependence in the bosonic propagator are generated during the flow. They lead to additional contributions to the flow, compared to the previous work by Strack et al. (2008). The central result of this chapter is given by the RG flow equations for the fermionic gap, Eq. (B.73), for the transverse Yukawa coupling, Eq. (B.78), for the bosonic order parameter, Eq. (B.82) and finally for the bosonic self-energies, Eq. (B.87), (B.91) and (B.95). The chapter is divided into five parts. It begins with section B.1 introducing the ansatz of the scale-dependent effective action. In section B.2 we present the matrix representation for fermionic and bosonic propagators. Section B.3 shows amputated vertices and a calculation of the couplings from the theory. Finally, in section B.4 the RG flow for the couplings can be found. The chapter closes with section B.5 presenting the bosonic densities of states, which are employed for the numerical solution of the RG flow.

B.1 Ansatz for the effective action

Here, we present the ansatz of the scale-dependent effective action for the symmetry-broken phase in the attractive Hubbard model. The ansatz is parametrized by several couplings, whose RG flows are calculated in section B.4. The total ansatz for the effective action

$$\begin{aligned}\Gamma = \Gamma_{\bar{\psi}\psi} + \Gamma_{\psi\psi} + \Gamma_{\sigma^2} + \Gamma_{\pi^2} + \Gamma_{\pi\sigma} \\ + \Gamma_{\sigma^3} + \Gamma_{\sigma\pi^2} + \Gamma_{\sigma^4} + \Gamma_{\sigma^2\pi^2} + \Gamma_{\pi^4} + \Gamma_{\psi^2\sigma} + \Gamma_{\psi^2\pi}\end{aligned} \tag{B.1}$$

consists of several terms, which will be explained in the following. The normal quadratic part in fermionic fields reads

$$\Gamma_{\bar{\psi}\psi} = \int_{k\sigma} \bar{\psi}_{k\sigma} \left(ik_0 - \xi_{\mathbf{k}}\right) \psi_{k\sigma} \tag{B.2}$$

and includes no renormalization factors parametrizing the fermionic self-energy. The anomalous self-energy term

$$\Gamma_{\psi\psi} = \int_k \left(\Delta\bar{\psi}_{-k\downarrow}\bar{\psi}_{k\uparrow} + \Delta^*\psi_{k\uparrow}\psi_{-k\downarrow}\right) \tag{B.3}$$

is parametrized by Δ, which represents the fermionic single-particle gap in our theory. The quadratic part in bosonic fields reads

$$\Gamma_{\pi^2} = \frac{1}{2}\int_q \pi_q \left(Z_\pi(q_0^2 + \omega_{\mathbf{q}}^2) + m_\pi^2\right) \pi_{-q}, \tag{B.4}$$

$$\Gamma_{\sigma^2} = \frac{1}{2}\int_q \sigma_q \left(Z_\sigma(q_0^2 + \omega_{\mathbf{q}}^2) + m_\sigma^2\right) \sigma_{-q}, \tag{B.5}$$

$$\Gamma_{\pi\sigma} = \int_q \pi_q(m_{\sigma\pi}^2 + W q_0)\sigma_{-q}. \tag{B.6}$$

Here, Z_σ and Z_π parametrize the frequency and momentum dependence of the longitudinal and transverse modes. Bosonic mass terms are represented by m_σ^2, m_π^2 and $m_{\sigma\pi}^2$ and the linear frequency dependence is parametrized by W. In transverse and longitudinal

representation the non-local bosonic self-interaction splits into several interaction parts

$$\Gamma_{\sigma^3} = \frac{1}{2}\int_{q,p} U(q)\alpha\sigma_p\sigma_{-q-p}\sigma_q, \tag{B.7}$$

$$\Gamma_{\sigma^4} = \frac{1}{8}\int_{q,p',p} U(q)\sigma_p\sigma_{q-p}\sigma_{p'}\sigma_{-q-p'}, \tag{B.8}$$

$$\Gamma_{\pi^4} = \frac{1}{8}\int_{q,p',p} U(q)\pi_p\pi_{q-p}\pi_{p'}\pi_{-q-p'}, \tag{B.9}$$

$$\Gamma_{\sigma^2\pi^2} = \frac{1}{4}\int_{q,p',p} U(q)\sigma_p\sigma_{q-p}\pi_{p'}\pi_{-q-p'}, \tag{B.10}$$

$$\Gamma_{\sigma\pi^2} = \frac{1}{2}\int_{q,p} U(q)\alpha\sigma_q\pi_p\pi_{-p-q} \tag{B.11}$$

with the function $U(q) = Y(q_0^2 + \omega_{\mathbf{q}}^2) + u$. Finally, the Yukawa coupling connects the fermionic and the bosonic sector of the theory. In the symmetry-broken phase, besides the normal Yukawa coupling

$$\Gamma_{\psi^2\phi^*} = g\int_{k,q}\left(\bar{\psi}_{-k+q\downarrow}\bar{\psi}_{k\uparrow}\phi_q + \psi_{k\uparrow}\psi_{-k+q\downarrow}\phi_q^*\right) \tag{B.12}$$

also an anomalous Yukawa coupling

$$\Gamma_{\psi^2\phi} = \tilde{g}\int_{k,q}\left(\bar{\psi}_{-k+q\downarrow}\bar{\psi}_{k\uparrow}\phi_{-q}^* + \psi_{k\uparrow}\psi_{-k+q\downarrow}\phi_{-q}\right) \tag{B.13}$$

is generated. In σ-π representation the longitudinal and transverse Yukawa vertex then reads

$$\Gamma_{\psi^2\sigma} = g_\sigma\int_{k,q}\left(\bar{\psi}_{-k+q/2\downarrow}\bar{\psi}_{k+q/2\uparrow}\sigma_q + \psi_{k+q/2\uparrow}\psi_{-k+q/2\downarrow}\sigma_{-q}\right), \tag{B.14}$$

$$\Gamma_{\psi^2\pi} = ig_\pi\int_{k,q}\left(\bar{\psi}_{-k+q/2\downarrow}\bar{\psi}_{k+q/2\uparrow}\pi_q - \psi_{k+q/2\uparrow}\psi_{-k+q/2\downarrow}\pi_{-q}\right). \tag{B.15}$$

with the relations $2g = g_\sigma + g_\pi$ and $2\tilde{g} = g_\sigma - g_\pi$.

B.2 Matrix representation of the fermionic and bosonic propagators

Before we present the RG equations, we introduce the matrix representation of the fermionic and the bosonic propagators. Due to the anomalous fermionic term also anoma-

lous fermionic propagators appear. Further, the linear imaginary dependence of the bosonic propagator leads to a mixing between transverse and longitudinal fluctuations.

We begin with the discussion of the fermionic propagator. For the fermions we choose the basis $(\psi_K) = (\psi_{k\uparrow}, \psi_{k\downarrow}, \bar{\psi}_{k\uparrow}, \bar{\psi}_{k\downarrow})$. The second functional derivative of the effective action Eq. (B.1) with respect to fermionic fields in matrix representation reads

$$\frac{\delta^2\Gamma}{\delta\psi^2} \equiv \left(\frac{\delta^2\Gamma}{\delta\psi_{K'}\delta\psi_{K''}}\right) \equiv \begin{pmatrix} \frac{\delta^2\Gamma}{\delta\psi_{k'\uparrow}\delta\psi_{k''\uparrow}} & \frac{\delta^2\Gamma}{\delta\psi_{k'\uparrow}\delta\psi_{k''\downarrow}} & \frac{\delta^2\Gamma}{\delta\psi_{k'\uparrow}\delta\bar{\psi}_{k''\uparrow}} & \frac{\delta^2\Gamma}{\delta\psi_{k'\uparrow}\delta\bar{\psi}_{k''\downarrow}} \\ \frac{\delta^2\Gamma}{\delta\psi_{k'\downarrow}\delta\psi_{k''\uparrow}} & \frac{\delta^2\Gamma}{\delta\psi_{k'\downarrow}\delta\psi_{k''\downarrow}} & \frac{\delta^2\Gamma}{\delta\psi_{k'\downarrow}\delta\bar{\psi}_{k''\uparrow}} & \frac{\delta^2\Gamma}{\delta\psi_{k'\downarrow}\delta\bar{\psi}_{k''\downarrow}} \\ \frac{\delta^2\Gamma}{\delta\bar{\psi}_{k'\uparrow}\delta\psi_{k''\uparrow}} & \frac{\delta^2\Gamma}{\delta\bar{\psi}_{k'\uparrow}\delta\psi_{k''\downarrow}} & \frac{\delta^2\Gamma}{\delta\bar{\psi}_{k'\uparrow}\delta\bar{\psi}_{k''\uparrow}} & \frac{\delta^2\Gamma}{\delta\bar{\psi}_{k'\uparrow}\delta\bar{\psi}_{k''\downarrow}} \\ \frac{\delta^2\Gamma}{\delta\bar{\psi}_{k'\downarrow}\delta\psi_{k''\uparrow}} & \frac{\delta^2\Gamma}{\delta\bar{\psi}_{k'\downarrow}\delta\psi_{k''\downarrow}} & \frac{\delta^2\Gamma}{\delta\bar{\psi}_{k'\downarrow}\delta\bar{\psi}_{k''\uparrow}} & \frac{\delta^2\Gamma}{\delta\bar{\psi}_{k'\downarrow}\delta\bar{\psi}_{k''\downarrow}} \end{pmatrix},$$

and leads to

$$\frac{\delta^2\Gamma}{\delta\psi^2} = \begin{pmatrix} 0 & -\Delta^*\delta_{k',-k''} & (ik'_0 - \xi_{\mathbf{k}'})\delta_{k,k'} & 0 \\ \Delta^*\delta_{k',-k''} & 0 & 0 & (ik'_0 - \xi_{\mathbf{k}'})\delta_{k',k''} \\ -(ik'_0 - \xi_{\mathbf{k}'})\delta_{k',k''} & 0 & 0 & \Delta\delta_{k',-k''} \\ 0 & -(ik'_0 - \xi_{\mathbf{k}'})\delta_{k',k''} & -\Delta\delta_{k',-k''} & 0 \end{pmatrix} \tag{B.16}$$

in the limit of vanishing fermionic and bosonic fields.

In matrix representation the fermionic regulator reads

$$\mathcal{R}_f \equiv \Big(\mathcal{R}_f(\psi_{K'}, \psi_{K''})\Big) \tag{B.17}$$

$$\equiv \begin{pmatrix} 0 & 0 & -R_f(k')\delta_{k',k''} & 0 \\ 0 & 0 & 0 & -R_f(k')\delta_{k',k''} \\ R_f(k')\delta_{k',k''} & 0 & 0 & 0 \\ 0 & R_f(k')\delta_{k',k''} & 0 & 0 \end{pmatrix}, \tag{B.18}$$

and regularizes low energy excitations in the absence of a fermionic single-particle gap. We discuss here only the case of an additive cutoff. The regularized effective action can then be defined as

$$\tilde{\Gamma} = \Gamma + \frac{1}{2}\int_{K,K'} \psi_K \mathcal{R}_f(\psi_K, \psi_{K'})\psi_{K'} + \frac{1}{2}\int_{Q,Q'} \phi_Q \mathcal{R}_b(\phi_Q, \phi_{Q'})\phi_{Q'}, \tag{B.19}$$

where we will introduce the bosonic regulator $\mathcal{R}_b$ below, when we discuss the bosonic sector of the theory. The second derivative of the regularized effective action with respect

to fermionic fields is given by

$$\frac{\delta^2\tilde{\Gamma}}{\delta\psi_{K'}\delta\psi_{K''}} = \frac{\delta^2\Gamma}{\delta\psi_{K'}\delta\psi_{K''}} - \mathcal{R}_f(K',K''), \tag{B.20}$$

where the regulator is chosen in such a way that the low energy modes become regularized in $\tilde{\Gamma}$ by the cutoff scale Λ. We then define the inverse of the second derivative of the regularized effective action as

$$\mathcal{F} \equiv \left[\frac{\delta^2\tilde{\Gamma}}{\delta\psi^2}\right]^{-1} \tag{B.21}$$

$$\equiv \begin{pmatrix} \mathcal{F}(\psi_{k'\uparrow},\psi_{k''\uparrow}) & \mathcal{F}(\psi_{k'\uparrow},\psi_{k''\downarrow}) & \mathcal{F}(\psi_{k'\uparrow},\bar{\psi}_{k''\uparrow}) & \mathcal{F}(\psi_{k'\uparrow},\bar{\psi}_{k''\downarrow}) \\ \mathcal{F}(\psi_{k'\downarrow},\psi_{k''\uparrow}) & \mathcal{F}(\psi_{k'\downarrow},\psi_{k''\downarrow}) & \mathcal{F}(\psi_{k'\downarrow},\bar{\psi}_{k''\uparrow}) & \mathcal{F}(\psi_{k'\downarrow},\bar{\psi}_{k''\downarrow}) \\ \mathcal{F}(\bar{\psi}_{k'\uparrow},\psi_{k''\uparrow}) & \mathcal{F}(\bar{\psi}_{k'\uparrow},\psi_{k''\downarrow}) & \mathcal{F}(\bar{\psi}_{k'\uparrow},\bar{\psi}_{k''\uparrow}) & \mathcal{F}(\bar{\psi}_{k',\uparrow},\bar{\psi}_{k''\downarrow}) \\ \mathcal{F}(\bar{\psi}_{k'\downarrow},\psi_{k''\uparrow}) & \mathcal{F}(\bar{\psi}_{k'\downarrow},\psi_{k''\downarrow}) & \mathcal{F}(\bar{\psi}_{k'\downarrow},\bar{\psi}_{k''\uparrow}) & \mathcal{F}(\bar{\psi}_{k'\downarrow},\bar{\psi}_{k''\downarrow}) \end{pmatrix}. \tag{B.22}$$

In the next step, we insert our ansatz for the regularized effective action into this definition and obtain

$$\mathcal{F}= \begin{pmatrix} 0 & F_f(k',k'') & -G_f(k,k'') & 0 \\ -F_f(k',k'') & 0 & 0 & -G_f(k',k'') \\ G_f(k',k'') & 0 & 0 & -\bar{F}_f(k,k'') \\ 0 & G_f(k,k'') & \bar{F}_f(k,k'') & 0 \end{pmatrix} \tag{B.23}$$

in the limit of vanishing fields. The matrix entries are given by the functions

$$F_f(k',k'') \equiv F_f(k')\delta_{k',-k''}, \tag{B.24}$$

$$\bar{F}_f(k',k'') \equiv \bar{F}_f(k')\delta_{k',-k''}, \tag{B.25}$$

$$G_f(k',k'') \equiv G_f(k')\delta_{k',k''}, \tag{B.26}$$

which consists of (regularized) normal and anomalous fermionic propagators

$$F_f(k) \equiv \frac{\Delta}{|\Delta|^2 + |ik_0 - \xi_{\mathbf{k}} + R_f(k)|^2}, \tag{B.27}$$

$$\bar{F}_f(k) \equiv \frac{\Delta^*}{|\Delta|^2 + |ik_0 - \xi_{\mathbf{k}} + R_f(k)|^2}, \tag{B.28}$$

$$G_f(k) \equiv \frac{-ik_0 - \xi_{\mathbf{k}} + R_f(-k)}{|\Delta|^2 + |ik_0 - \xi_{\mathbf{k}} + R_f(k)|^2}. \tag{B.29}$$

The regularized fermionic propagator in matrix representation is given by the negative

inverse

$$\mathcal{G}_f = -\mathcal{F} = -\left[\frac{\delta^2\Gamma}{\delta\psi^2} - \mathcal{R}_f\right]^{-1}. \tag{B.30}$$

In the matrix formulation the fermionic propagator reads

$$\mathcal{G}_f = \Big(\mathcal{G}_f(\psi_{K'}, \psi_{K''})\Big) \tag{B.31}$$

$$= \begin{pmatrix} 0 & -F_f(k',k'') & G_f(k,k'') & 0 \\ F_f(k',k'') & 0 & 0 & G_f(k',k'') \\ -G_f(k',k'') & 0 & 0 & \bar{F}_f(k,k'') \\ 0 & -G_f(k,k'') & -\bar{F}_f(k,k'') & 0 \end{pmatrix}. \tag{B.32}$$

The fermionic single-scale propagator can then be defined as the scale-derivative of the regularized fermionic propagator Eq. (B.30)

$$\mathcal{S}_f \equiv \frac{\partial}{\partial\Lambda}\Big|_\Sigma \mathcal{G}_f = -\frac{\partial}{\partial\Lambda}\Big|_\Sigma \Big[\frac{\delta^2\Gamma}{\delta\psi^2} - \mathcal{R}_f\Big]^{-1} \tag{B.33}$$

$$= -\Big[\frac{\delta^2\Gamma}{\delta\psi^2} - \mathcal{R}_f\Big]^{-1} \partial_\Lambda \mathcal{R}_f \Big[\frac{\delta^2\Gamma}{\delta\psi^2} - \mathcal{R}_f\Big]^{-1} \tag{B.34}$$

$$= -\mathcal{G}_f \partial_\Lambda \mathcal{R}_f \mathcal{G}_f, \tag{B.35}$$

where the self-energy Σ is kept constant. The single-scale propagator reads

$$\mathcal{S}_f = \begin{pmatrix} 0 & -S_F(k',k'') & S_G(k',k'') & 0 \\ S_F(k',k'') & 0 & 0 & S_G(k',k'') \\ -S_G(k',k'') & 0 & 0 & S_{\bar{F}}(k',k'') \\ 0 & -S_G(k',k'') & -S_{\bar{F}}(k',k'') & 0 \end{pmatrix} \tag{B.36}$$

with the matrix entries

$$S_F(k',k'') = S_F(k')\delta_{k',-k''}, \quad S_{\bar{F}}(k',k'') = S_{\bar{F}}(k')\delta_{k',-k''}, \quad S_G(k',k'') = S_G(k')\delta_{k',k''} \tag{B.37}$$

The anomalous and normal fermionic single-scale propagators are then given by

$$S_F(k) = \frac{\partial}{\partial\Lambda}\Big|_\Sigma F_f(k), \qquad S_{\bar{F}}(k) = \frac{\partial}{\partial\Lambda}\Big|_\Sigma \bar{F}_f(k), \qquad S_G(k) = \frac{\partial}{\partial\Lambda}\Big|_\Sigma G_f(k). \tag{B.38}$$

These quantities appear on the right hand side of the RG flow equation for the couplings, when evaluating the RG flow of the effective action in section B.4.

In the next step, we derive bosonic propagators from the ansatz of the effective action Eq. (B.1). We choose the bosonic basis $(\phi_Q) = (\sigma_q, \pi_q)$. The second derivative of the scale-dependent effective action with respect to bosonic fields yields

$$\frac{\delta^2\Gamma}{\delta\phi^2} \equiv \left(\frac{\delta^2\Gamma}{\delta\phi_Q\delta\phi_{Q'}}\right) \equiv \begin{pmatrix} \frac{\delta\Gamma}{\delta\sigma_q\delta\sigma_{q'}} & \frac{\delta\Gamma}{\delta\sigma_q\delta\pi_{q'}} \\ \frac{\delta\Gamma}{\delta\pi_q\delta\sigma_{q'}} & \frac{\delta\Gamma}{\delta\pi_q\delta\pi_{q'}} \end{pmatrix}. \tag{B.39}$$

We insert now the ansatz for the effective action and obtain in the limit of vanishing fermionic and bosonic fields the result

$$\frac{\delta^2\Gamma}{\delta\phi^2} = \begin{pmatrix} Z_\sigma(q_0^2+\omega_{\mathbf{q}}^2)+m_\sigma^2 & -Wq_0 \\ Wq_0 & Z_\pi(q_0^2+\omega_{\mathbf{q}}^2)+m_\pi^2 \end{pmatrix} \delta_{q,-q'}. \tag{B.40}$$

The regularized effective action was introduced above. Here, we present now the bosonic regulator in matrix representation [1] as

$$\mathcal{R}_b(q,q') \equiv \begin{pmatrix} R_\pi(q)\delta_{q,-q'} & 0 \\ 0 & R_\pi(q)\delta_{q,-q'} \end{pmatrix}. \tag{B.41}$$

Now, we define the inverse of the regularized effective action as

$$\mathcal{B} \equiv \left[\frac{\delta^2\tilde{\Gamma}}{\delta\phi^2}\right]^{-1} \equiv \Big(\mathcal{B}(\phi_Q,\phi_{Q'})\Big) \equiv \begin{pmatrix} \mathcal{B}(\sigma_q,\sigma_{q'}) & \mathcal{B}(\sigma_q,\pi_{q'}) \\ \mathcal{B}(\pi_q,\sigma_{q'}) & \mathcal{B}(\pi_q,\pi_{q'}) \end{pmatrix}. \tag{B.42}$$

After inserting our ansatz for the regularized effective action, we obtain

$$\mathcal{B} = \frac{1}{\gamma_{\sigma^2}(q)\gamma_{\pi^2}(q)+W^2q_0^2} \begin{pmatrix} \gamma_{\pi^2}(q) & -Wq_0 \\ Wq_0 & \gamma_{\sigma^2}(q) \end{pmatrix} \delta_{q,-q}, \tag{B.43}$$

with the functions $\gamma_{\sigma^2}(q) = Z_\sigma(q_0^2+\omega_{\mathbf{q}}^2)+m_\sigma^2+R_\pi(q)$ and $\gamma_{\pi^2}(q) = Z_\pi(q_0^2+\omega_{\mathbf{q}}^2)+m_\pi^2+R_\pi(q)$. The linear frequency dependence of the bosonic propagator leads to a rich structure in the bosonic propagators. Besides diagonal elements now also off-diagonal elements appear, associated to a mixing between transverse and longitudinal fluctuations.

The regularized bosonic propagator (matrix) is then defined as

$$\mathcal{G}_b \equiv \mathcal{B} \equiv \begin{pmatrix} G_{\sigma^2}(q) & G_{\sigma\pi}(q) \\ G_{\pi\sigma}(q) & G_{\pi^2}(q) \end{pmatrix} \delta_{q,-q'}.$$

[1] We choose the same regulator for longitudinal and transverse modes in order to preserve the underlying symmetry of the model, hence $R_\sigma(q) = R_\pi(q)$.

In total the transverse, longitudinal and mixed bosonic propagators read

$$G_{\sigma^2}(q) = \frac{\gamma_{\pi^2}(q)}{\gamma_{\pi^2}(q)\gamma_{\sigma^2}(q) + W^2 q_0^2}, \quad G_{\pi^2}(q) = \frac{\gamma_{\sigma^2}(q)}{\gamma_{\pi^2}(q)\gamma_{\sigma^2}(q) + W^2 q_0^2}, \tag{B.44}$$

$$G_{\sigma\pi}(q) = \frac{-W q_0}{\gamma_{\pi^2}(q)\gamma_{\sigma^2}(q) + W^2 q_0^2}, \quad G_{\pi\sigma}(q) = \frac{W q_0}{\gamma_{\pi^2}(q)\gamma_{\sigma^2}(q) + W^2 q_0^2}. \tag{B.45}$$

The corresponding single-scale propagators are obtained as the first scale-derivative of the bosonic propagator

$$\mathcal{S}_b \equiv \frac{\partial}{\partial \Lambda}\Big|_{\Sigma} \mathcal{G}_b, \tag{B.46}$$

where the self-energy Σ is kept constant.

The longitudinal, transverse and mixed bosonic single-scale propagators then read

$$S_{\sigma^2}(q) = -\partial_\Lambda R_\pi(q) \frac{\gamma_{\pi^2}^2(q) - W^2 q_0^2}{(\gamma_{\sigma^2}(q)\gamma_{\pi^2}(q) + W^2 q_0^2)^2}, \quad S_{\pi^2}(q) = -\partial_\Lambda R_\pi(q) \frac{\gamma_{\sigma^2}^2(q) - W^2 q_0^2}{(\gamma_{\sigma^2}(q)\gamma_{\pi^2}(q) - W^2 q_0^2)^2},$$

$$S_{\sigma\pi}(q) = -\partial_\Lambda R_\pi(q) \frac{-W q_0(\gamma_{\sigma^2}(q) + \gamma_{\pi^2}(q))}{(\gamma_{\sigma^2}(q)\gamma_{\pi^2}(q) + W^2 q_0^2)^2}, \quad S_{\pi\sigma}(q) = -S_{\sigma\pi}(q). \tag{B.47}$$

B.3 Interaction vertices and couplings

The contributions to the RG flow of the couplings are given by 1PI Feynman diagrams. The diagrams consist of the previously derived fermionic and bosonic propagators and vertices connecting those propagators. Here, we present an amputated form of those vertices, which are required to evaluate the flow equation in the next section. Afterwards, we show how the flow of the RG couplings is calculated from the flow equation of the effective action. For this purpose, derivatives with respect to fermionic and bosonic fields are applied to extract self-energies and couplings.

In the longitudinal-transverse representation several interaction processes between bosonic fields exist, see Eq. (B.7)-(B.11). The field-amputated form of these bosonic

interaction vertices reads

$$\frac{\delta^4\Gamma_{\sigma^4}}{\delta\sigma_{k''}\delta\sigma_{k'}\delta\sigma_{q''}\delta\sigma_{q'}} = \left[U(q'+q'')+U(k'+q')+U(k'+q'')\right]\delta_{0,q'+q''+k'+k''}, \tag{B.48}$$

$$\frac{\delta^4\Gamma_{\sigma^2\pi^2}}{\delta\sigma_{k''}\delta\sigma_{k'}\delta\pi_{q''}\delta\pi_{q'}} = U(q'+q'')\delta_{0,k'+k''+q'+q''}, \tag{B.49}$$

$$\frac{\delta^3\Gamma_{\sigma^3}}{\delta\sigma_{k'}\delta\sigma_{q''}\delta\sigma_{q'}} = \alpha\left[U(q')+U(q'')+U(q'+q'')\right]\delta_{0,k'+q'+q''}, \tag{B.50}$$

$$\frac{\delta^4\Gamma_{\sigma^2\pi^2}}{\delta\pi_{k''}\delta\pi_{k'}\delta\sigma_{q''}\delta\sigma_{q'}} = U(q'+q'')\delta_{0,k''+k'+q'+q''}, \tag{B.51}$$

$$\frac{\delta^4\Gamma_{\pi^4}}{\delta\pi_{k''}\delta\pi_{k'}\delta\pi_{q''}\delta\pi_{q'}} = \left[U(q'+q'')+U(k'+q')+U(k'+q'')\right]\delta_{0,q'+q''+k'+k''}, \tag{B.52}$$

$$\frac{\delta^3\Gamma_{\sigma\pi^2}}{\delta\pi_{k'}\delta\sigma_{q''}\delta\pi_{q'}} = \alpha U(q'')\delta_{0,k'+q'+q''} \tag{B.53}$$

with $U(q) = Y(q_0^2+\omega_{\mathbf{q}}^2)+u$ and the variables $q=(q_0,\mathbf{q})$ and $k=(k_0,\mathbf{k})$ collecting bosonic frequencies and momenta. Vertices between the fermionic and bosonic sector are given by the normal and anomalous Yukawa couplings Eq. (B.14) and (B.15). Amputating the external fields yields

$$\frac{\delta^3\Gamma_{\psi^2\sigma}}{\delta\psi_{k''-\sigma'}\delta\psi_{k'\sigma'}\delta\sigma_{q'}} = g_\sigma\delta_{0,k'+k''+q'}\left(\delta_{\sigma',\uparrow}-\delta_{\sigma',\downarrow}\right), \tag{B.54}$$

$$\frac{\delta^3\Gamma_{\psi^2\sigma}}{\delta\bar\psi_{k''-\sigma'}\delta\bar\psi_{k'\sigma'}\delta\sigma_{q'}} = -g_\sigma\delta_{0,k'+k''-q'}\left(\delta_{\sigma',\uparrow}-\delta_{\sigma',\downarrow}\right), \tag{B.55}$$

$$\frac{\delta^3\Gamma_{\psi^2\pi}}{\delta\psi_{k''-\sigma'}\delta\psi_{k'\sigma'}\delta\pi_{q'}} = -ig_\pi\delta_{0,k'+k''+q'}\left(\delta_{\sigma',\uparrow}-\delta_{\sigma',\downarrow}\right), \tag{B.56}$$

$$\frac{\delta^3\Gamma_{\psi^2\pi}}{\delta\bar\psi_{k''-\sigma'}\delta\bar\psi_{k'\sigma'}\delta\pi_{q'}} = -ig_\pi\delta_{0,k'+k''-q'}\left(\delta_{\sigma',\uparrow}-\delta_{\sigma',\downarrow}\right). \tag{B.57}$$

Now we show how the RG flow of the couplings is determined from the flow of the scale-dependent effective action. As usual, we apply functional field derivatives with respect to bosonic and fermionic fields to the flow of the scale-dependent effective action. The flow of the fermionic single-particle gap is obtained from

$$\frac{d}{d\Lambda}\Delta = \frac{\delta^2}{\delta\bar\psi_{k_f\uparrow}\delta\bar\psi_{-k_f\downarrow}}\frac{d}{d\Lambda}\Gamma. \tag{B.58}$$

The bosonic order parameter is obtained from

$$\frac{d}{d\Lambda}\alpha = -\frac{1}{m_\sigma^2}\frac{\delta}{\delta\sigma_0}\frac{d}{d\Lambda}\Gamma, \tag{B.59}$$

by a shift of the bosonic field in the effective action, which was discussed in chapter 2 in section 2.3.

Further, the flow of the bosonic self-energies is given by

$$\frac{d}{d\Lambda}\Sigma_{\sigma^2}(p) = \frac{\delta^2}{\delta\sigma_p\delta\sigma_{-p}}\frac{d}{d\Lambda}\Gamma, \quad \frac{d}{d\Lambda}\Sigma_{\pi^2}(p) = \frac{\delta^2}{\delta\pi_p\delta\pi_{-p}}\frac{d}{d\Lambda}\Gamma, \tag{B.60}$$

$$\frac{d}{d\Lambda}\Sigma_{\sigma\pi}(p) = \frac{\delta^2}{\delta\pi_p\delta\sigma_{-p}}\frac{d}{d\Lambda}\Gamma. \tag{B.61}$$

Couplings parametrizing the bosonic self-energy are obtained by taking frequency and momentum derivatives. For the longitudinal bosonic mode we find

$$\frac{d}{d\Lambda}Z_\sigma^\omega = \frac{1}{2}\frac{\partial^2}{\partial p_0^2}\Big|_{p=0}\frac{d}{d\Lambda}\Sigma_{\sigma^2}(p), \quad \frac{d}{d\Lambda}Z_\sigma = \frac{1}{2}\frac{\partial^2}{\partial p_x^2}\Big|_{p=0}\frac{d}{d\Lambda}\Sigma_{\sigma^2}(p), \tag{B.62}$$

$$\frac{d}{d\Lambda}m_\sigma^2 = \frac{d}{d\Lambda}\Sigma_{\sigma^2}(0), \tag{B.63}$$

and for the transverse bosonic mode we find

$$\frac{d}{d\Lambda}Z_\pi^\omega = \frac{1}{2}\frac{\partial^2}{\partial p_0^2}\Big|_{p=0}\frac{d}{d\Lambda}\Sigma_{\pi^2}(p), \quad \frac{d}{d\Lambda}Z_\pi = \frac{1}{2}\frac{\partial^2}{\partial p_x^2}\Big|_{p=0}\frac{d}{d\Lambda}\Sigma_{\pi^2}(p), \tag{B.64}$$

$$\frac{d}{d\Lambda}m_\pi^2 = \frac{d}{d\Lambda}\Sigma_{\pi^2}(0). \tag{B.65}$$

The linear frequency dependence of the bosonic propagator is obtained as

$$\frac{d}{d\Lambda}W = \frac{\partial}{\partial p_0}\Big|_{p=0}\frac{\delta^2}{\delta\sigma_{-p}\delta\pi_p}\frac{d}{d\Lambda}\Gamma. \tag{B.66}$$

The RG flow of the bosonic self-interactions is extracted indirectly by the relations

$$\frac{d}{d\Lambda}u = \frac{d}{d\Lambda}\left(\frac{m_\sigma^2}{\alpha^2}\right), \quad \frac{d}{d\Lambda}Y = \frac{d}{d\Lambda}\left(\frac{Z_\sigma - Z_\pi}{\alpha^2}\right). \tag{B.67}$$

B.4 RG equations of the couplings

In this section, we derive the RG flow equations for the couplings parametrizing the scale-dependent effective action Eq. (B.1). To this end, our ansatz for the scale-dependent effective action is inserted into the RG equation for the effective action see Eq. (2.48).[2]

[2]Note that the quantity $\tilde{\Gamma}$ appearing on the right hand side of the flow equation denotes the regularized effective action. In contrast, the quantity Γ appearing on the left hand side of the flow equation denotes the non-regularized effective action from which the flow of self-energies and couplings are extracted by

By successively applying functional derivatives with respect to fermionic and bosonic fields, the flow for the fermionic and bosonic self-energies, Yukawa coupling and bosonic self-interactions are extracted. The flow of the couplings parametrizing the self-energies are obtained by additional frequency and momentum derivatives. We will derive explicitly the RG flow for the fermionic single-particle gap, Eq. (B.73), for the Yukawa coupling, Eq. (B.78), for the order parameter, Eq. (B.82), the bosonic self-energies, Eq. (B.87), (B.91) and (B.95), and the bosonic self-interaction, Eq. (B.99). These are the central results of this chapter. In the case of the fermionic gap and the Yukawa vertex the full flow equation has to be taken into account due to contributions with both fermions and bosons, see the discussion in the appendix A.

We begin with the derivation of the flow equation for the fermionic single-particle gap. The second functional derivative with respect to fermionic fields yields

$$\begin{aligned}\frac{\delta^2}{\delta\bar{\psi}_{k'\uparrow}\bar{\psi}_{k\downarrow}}\frac{d}{d\Lambda}\Gamma = \frac{\delta^3\Gamma}{\delta\bar{\psi}_{k'\uparrow}\delta\bar{\psi}_{k\downarrow}\delta\sigma_0}\frac{d}{d\Lambda}\alpha \\ - \frac{1}{2}\mathrm{Tr}\left(\mathcal{S}_b\frac{\delta^2\tilde{\Gamma}}{\delta\bar{\psi}_{k\downarrow}\delta\phi\delta\psi}\mathcal{F}\frac{\delta^2\tilde{\Gamma}}{\delta\bar{\psi}_{k'\uparrow}\delta\psi\delta\phi}\right) \\ + \frac{1}{2}\mathrm{Tr}\left(\mathcal{S}_b\frac{\delta^2\tilde{\Gamma}}{\delta\bar{\psi}_{k'\uparrow}\delta\phi\delta\psi}\mathcal{F}\frac{\delta^2\tilde{\Gamma}}{\delta\bar{\psi}_{k\downarrow}\delta\psi\delta\phi}\right) \\ - \frac{1}{2}\mathrm{Tr}\left(\mathcal{S}_f\frac{\delta^2\tilde{\Gamma}}{\delta\bar{\psi}_{k\downarrow}\delta\psi\delta\phi}\mathcal{B}\frac{\delta^2\tilde{\Gamma}}{\delta\bar{\psi}_{k'\uparrow}\delta\phi\delta\psi}\right) \\ + \frac{1}{2}\mathrm{Tr}\left(\mathcal{S}_f\frac{\delta^2\tilde{\Gamma}}{\delta\bar{\psi}_{k'\uparrow}\delta\psi\delta\phi}\mathcal{B}\frac{\delta^2\tilde{\Gamma}}{\delta\bar{\psi}_{k\downarrow}\delta\phi\delta\psi}\right).\end{aligned} \tag{B.68}$$

In the next step, we insert the matrix representation and evaluate the trace over the spin and charge index. We then obtain

$$\frac{\delta^2}{\delta\bar{\psi}_{k'\uparrow}\delta\bar{\psi}_{k\downarrow}}\frac{d}{d\Lambda}\Gamma = \frac{\delta^3\Gamma}{\delta\bar{\psi}_{k'\uparrow}\delta\bar{\psi}_{k\downarrow}\delta\sigma_0}\frac{d}{d\Lambda}\alpha + \frac{d}{d\Lambda}A_1 + \frac{d}{d\Lambda}A_2, \tag{B.69}$$

where we distinguish between the contributions A_1 and A_2. The first contribution is given

functional differentiation with respect to fermionic and bosonic fields.

by

$$\begin{aligned}\frac{d}{d\Lambda}A_1 = &-\frac{1}{2}\mathrm{Tr}\left(\mathcal{S}_\mathrm{b}(\pi_\mathrm{a},\sigma_\mathrm{b})\frac{\delta^3\tilde{\Gamma}}{\delta\bar{\psi}_{\mathrm{k}\downarrow}\delta\sigma_\mathrm{b}\delta\bar{\psi}_{\mathrm{x}\uparrow}}\mathcal{F}(\bar{\psi}_{\mathrm{x}\uparrow},\bar{\psi}_{\mathrm{y}\downarrow})\frac{\delta^3\tilde{\Gamma}}{\delta\bar{\psi}_{\mathrm{k}'\uparrow}\delta\bar{\psi}_{\mathrm{y}\downarrow}\delta\pi_\mathrm{a}}\right)\\
&-\frac{1}{2}\mathrm{Tr}\left(\mathcal{S}_\mathrm{b}(\sigma_\mathrm{a},\pi_\mathrm{b})\frac{\delta^3\tilde{\Gamma}}{\delta\bar{\psi}_{\mathrm{k}\downarrow}\delta\pi_\mathrm{b}\delta\bar{\psi}_{\mathrm{x}\uparrow}}\mathcal{F}(\bar{\psi}_{\mathrm{x}\uparrow},\bar{\psi}_{\mathrm{y}\downarrow})\frac{\delta^3\tilde{\Gamma}}{\delta\bar{\psi}_{\mathrm{k}'\uparrow}\delta\bar{\psi}_{\mathrm{y}\downarrow}\delta\sigma_\mathrm{a}}\right)\\
&+\frac{1}{2}\mathrm{Tr}\left(\mathcal{S}_\mathrm{b}(\pi_\mathrm{a},\sigma_\mathrm{b})\frac{\delta^3\tilde{\Gamma}}{\delta\bar{\psi}_{\mathrm{k}'\uparrow}\delta\sigma_\mathrm{b}\delta\bar{\psi}_{\mathrm{x}\downarrow}}\mathcal{F}(\bar{\psi}_{\mathrm{x}\downarrow},\bar{\psi}_{\mathrm{y}\uparrow})\frac{\delta^3\tilde{\Gamma}}{\delta\bar{\psi}_{\mathrm{k}\downarrow}\delta\bar{\psi}_{\mathrm{y}\uparrow}\delta\pi_\mathrm{a}}\right)\\
&+\frac{1}{2}\mathrm{Tr}\left(\mathcal{S}_\mathrm{b}(\sigma_\mathrm{a},\pi_\mathrm{b})\frac{\delta^3\tilde{\Gamma}}{\delta\bar{\psi}_{\mathrm{k}'\uparrow}\delta\pi_\mathrm{b}\delta\bar{\psi}_{\mathrm{x}\downarrow}}\mathcal{F}(\bar{\psi}_{\mathrm{x}\downarrow},\bar{\psi}_{\mathrm{y}\uparrow})\frac{\delta^3\tilde{\Gamma}}{\delta\bar{\psi}_{\mathrm{k}\downarrow}\delta\bar{\psi}_{\mathrm{y}\uparrow}\delta\sigma_\mathrm{a}}\right)\\
&-\frac{1}{2}\mathrm{Tr}\left(\mathcal{S}_\mathrm{f}(\bar{\psi}_{\mathrm{x}\downarrow},\bar{\psi}_{\mathrm{y}\uparrow})\frac{\delta^3\tilde{\Gamma}}{\delta\bar{\psi}_{\mathrm{k}\downarrow}\delta\sigma_\mathrm{a}\delta\bar{\psi}_{\mathrm{y}\uparrow}}\mathcal{B}(\sigma_\mathrm{a},\pi_\mathrm{b})\frac{\delta^3\tilde{\Gamma}}{\delta\bar{\psi}_{\mathrm{k}'\uparrow}\delta\bar{\psi}_{\mathrm{x}\downarrow}\delta\pi_\mathrm{b}}\right)\\
&-\frac{1}{2}\mathrm{Tr}\left(\mathcal{S}_\mathrm{f}(\bar{\psi}_{\mathrm{x}\downarrow},\bar{\psi}_{\mathrm{y}\uparrow})\frac{\delta^3\tilde{\Gamma}}{\delta\bar{\psi}_{\mathrm{k}\downarrow}\delta\pi_\mathrm{a}\delta\bar{\psi}_{\mathrm{y}\uparrow}}\mathcal{B}(\pi_\mathrm{a},\sigma_\mathrm{b})\frac{\delta^3\tilde{\Gamma}}{\delta\bar{\psi}_{\mathrm{k}'\uparrow}\delta\bar{\psi}_{\mathrm{x}\downarrow}\delta\sigma_\mathrm{b}}\right)\\
&+\frac{1}{2}\mathrm{Tr}\left(\mathcal{S}_\mathrm{f}(\bar{\psi}_{\mathrm{x}\uparrow},\bar{\psi}_{\mathrm{y}\downarrow})\frac{\delta^3\tilde{\Gamma}}{\delta\bar{\psi}_{\mathrm{k}'\uparrow}\delta\sigma_\mathrm{a}\delta\bar{\psi}_{\mathrm{y}\downarrow}}\mathcal{B}(\sigma_\mathrm{a},\pi_\mathrm{b})\frac{\delta^3\tilde{\Gamma}}{\delta\bar{\psi}_{\mathrm{k}\downarrow}\delta\bar{\psi}_{\mathrm{x}\uparrow}\delta\pi_\mathrm{b}}\right)\\
&+\frac{1}{2}\mathrm{Tr}\left(\mathcal{S}_\mathrm{f}(\bar{\psi}_{\mathrm{x}\uparrow},\bar{\psi}_{\mathrm{y}\downarrow})\frac{\delta^3\tilde{\Gamma}}{\delta\bar{\psi}_{\mathrm{k}'\uparrow}\delta\pi_\mathrm{a}\delta\bar{\psi}_{\mathrm{y}\downarrow}}\mathcal{B}(\pi_\mathrm{a},\sigma_\mathrm{b})\frac{\delta^3\tilde{\Gamma}}{\delta\bar{\psi}_{\mathrm{k}\downarrow}\delta\bar{\psi}_{\mathrm{x}\uparrow}\delta\sigma_\mathrm{b}}\right),\end{aligned} \tag{B.70}$$

and includes mixed bosonic propagators. The second contribution is given by

$$\begin{aligned}\frac{d}{d\Lambda}A_2 = &-\frac{1}{2}\mathrm{Tr}\left(\mathcal{S}_{\mathrm{b}}(\sigma_{\mathrm{a}},\sigma_{\mathrm{b}})\frac{\delta^3\tilde{\Gamma}}{\delta\bar{\psi}_{\mathrm{k}\downarrow}\delta\sigma_{\mathrm{b}}\delta\bar{\psi}_{\mathrm{x}\uparrow}}\mathcal{F}(\bar{\psi}_{\mathrm{x}\uparrow},\bar{\psi}_{\mathrm{y}\downarrow})\frac{\delta^3\tilde{\Gamma}}{\delta\bar{\psi}_{\mathrm{k}'\uparrow}\delta\bar{\psi}_{\mathrm{y}\downarrow}\delta\sigma_{\mathrm{a}}}\right)\\
&-\frac{1}{2}\mathrm{Tr}\left(\mathcal{S}_{\mathrm{b}}(\pi_{\mathrm{a}},\pi_{\mathrm{b}})\frac{\delta^3\tilde{\Gamma}}{\delta\bar{\psi}_{\mathrm{k}\downarrow}\delta\pi_{\mathrm{b}}\delta\bar{\psi}_{\mathrm{x}\uparrow}}\mathcal{F}(\bar{\psi}_{\mathrm{x}\uparrow},\bar{\psi}_{\mathrm{y}\downarrow})\frac{\delta^3\tilde{\Gamma}}{\delta\bar{\psi}_{\mathrm{k}'\uparrow}\delta\bar{\psi}_{\mathrm{y}\downarrow}\delta\pi_{\mathrm{a}}}\right)\\
&+\frac{1}{2}\mathrm{Tr}\left(\mathcal{S}_{\mathrm{b}}(\sigma_{\mathrm{a}},\sigma_{\mathrm{b}})\frac{\delta^3\tilde{\Gamma}}{\delta\bar{\psi}_{\mathrm{k}'\uparrow}\delta\sigma_{\mathrm{b}}\delta\bar{\psi}_{\mathrm{x}\downarrow}}\mathcal{F}(\bar{\psi}_{\mathrm{x}\downarrow},\bar{\psi}_{\mathrm{y}\uparrow})\frac{\delta^3\tilde{\Gamma}}{\delta\bar{\psi}_{\mathrm{k}\downarrow}\delta\bar{\psi}_{\mathrm{y}\uparrow}\delta\sigma_{\mathrm{a}}}\right)\\
&+\frac{1}{2}\mathrm{Tr}\left(\mathcal{S}_{\mathrm{b}}(\pi_{\mathrm{a}},\pi_{\mathrm{b}})\frac{\delta^3\tilde{\Gamma}}{\delta\bar{\psi}_{\mathrm{k}'\uparrow}\delta\pi_{\mathrm{b}}\delta\bar{\psi}_{\mathrm{x}\downarrow}}\mathcal{F}(\bar{\psi}_{\mathrm{x}\downarrow},\bar{\psi}_{\mathrm{y}\uparrow})\frac{\delta^3\tilde{\Gamma}}{\delta\bar{\psi}_{\mathrm{k}\downarrow}\delta\bar{\psi}_{\mathrm{y}\uparrow}\delta\pi_{\mathrm{a}}}\right)\\
&-\frac{1}{2}\mathrm{Tr}\left(\mathcal{S}_{\mathrm{f}}(\bar{\psi}_{\mathrm{x}\downarrow},\bar{\psi}_{\mathrm{y}\uparrow})\frac{\delta^3\tilde{\Gamma}}{\delta\bar{\psi}_{\mathrm{k}\downarrow}\delta\sigma_{\mathrm{a}}\delta\bar{\psi}_{\mathrm{y}\uparrow}}\mathcal{B}(\sigma_{\mathrm{a}},\sigma_{\mathrm{b}})\frac{\delta^3\tilde{\Gamma}}{\delta\bar{\psi}_{\mathrm{k}'\uparrow}\delta\bar{\psi}_{\mathrm{x}\downarrow}\delta\sigma_{\mathrm{b}}}\right)\\
&-\frac{1}{2}\mathrm{Tr}\left(\mathcal{S}_{\mathrm{f}}(\bar{\psi}_{\mathrm{x}\downarrow},\bar{\psi}_{\mathrm{y}\uparrow})\frac{\delta^3\tilde{\Gamma}}{\delta\bar{\psi}_{\mathrm{k}\downarrow}\delta\pi_{\mathrm{a}}\delta\bar{\psi}_{\mathrm{y}\uparrow}}\mathcal{B}(\pi_{\mathrm{a}},\pi_{\mathrm{b}})\frac{\delta^3\tilde{\Gamma}}{\delta\bar{\psi}_{\mathrm{k}'\uparrow}\delta\bar{\psi}_{\mathrm{x}\downarrow}\delta\pi_{\mathrm{b}}}\right)\\
&+\frac{1}{2}\mathrm{Tr}\left(\mathcal{S}_{\mathrm{f}}(\bar{\psi}_{\mathrm{x}\uparrow},\bar{\psi}_{\mathrm{y}\downarrow})\frac{\delta^3\tilde{\Gamma}}{\delta\bar{\psi}_{\mathrm{k}'\uparrow}\delta\sigma_{\mathrm{a}}\delta\bar{\psi}_{\mathrm{y}\downarrow}}\mathcal{B}(\sigma_{\mathrm{a}},\sigma_{\mathrm{b}})\frac{\delta^3\tilde{\Gamma}}{\delta\bar{\psi}_{\mathrm{k}\downarrow}\delta\bar{\psi}_{\mathrm{x}\uparrow}\delta\sigma_{\mathrm{b}}}\right)\\
&+\frac{1}{2}\mathrm{Tr}\left(\mathcal{S}_{\mathrm{f}}(\bar{\psi}_{\mathrm{x}\uparrow},\bar{\psi}_{\mathrm{y}\downarrow})\frac{\delta^3\tilde{\Gamma}}{\delta\bar{\psi}_{\mathrm{k}'\uparrow}\delta\pi_{\mathrm{a}}\delta\bar{\psi}_{\mathrm{y}\downarrow}}\mathcal{B}(\pi_{\mathrm{a}},\pi_{\mathrm{b}})\frac{\delta^3\tilde{\Gamma}}{\delta\bar{\psi}_{\mathrm{k}\downarrow}\delta\bar{\psi}_{\mathrm{x}\uparrow}\delta\pi_{\mathrm{b}}}\right)\end{aligned} \tag{B.71}$$

and includes transverse and longitudinal bosonic propagators. To calculate the flow for the gap

$$\frac{d}{d\Lambda}\Delta = \frac{\delta^2}{\delta\bar{\psi}_{k_f\uparrow}\delta\bar{\psi}_{-k_f\downarrow}}\frac{d}{d\Lambda}\Gamma, \tag{B.72}$$

the external momenta and frequencies are evaluated on the Fermi surface, $k = -k' = k_f = (0, \mathbf{k}_f)$. Furthermore, the amputated Yukawa vertices Eq. (B.54)-(B.57) and the propagators from Eq. (B.23) and (B.43) are inserted in the above expressions. Finally, the integrals over the remaining delta functions are performed. The flow for the gap then

reads

$$\begin{aligned}\frac{d}{d\Lambda}\Delta = g_\sigma \frac{d}{d\Lambda}\alpha \\ &- \frac{1}{2}g_\sigma^2 \int_q D_\Lambda \left[G_{\sigma^2}(q)F_f(-q+k_f)\right] + \frac{1}{2}g_\pi^2 \int_q D_\Lambda \left[G_{\pi^2}(k)F_f(-q+k_f)\right] \\ &- \frac{1}{2}(ig_\sigma g_\pi) \int_q D_\Lambda \left[G_{\pi\sigma}(q)F_f(-q+k_f) + G_{\sigma\pi}(q)F_f(-q+k_f)\right] \\ &+ (k_f \leftrightarrow -k_f),\end{aligned} \tag{B.73}$$

where we introduced the shorthand notation $D_\Lambda = \frac{d}{d\Lambda}\Big|_\Sigma$ for scale derivatives, where the self-energy Σ is kept constant. The fermionic and bosonic single-scale operators are then defined as $S_f(k) = D_\Lambda F_f(k)$, $S_f(k) = D_\Lambda G_f(k)$, $S_{\sigma^2}(q) = D_\Lambda G_{\sigma^2}(q)$, $S_{\pi^2}(q) = D_\Lambda G_{\pi^2}(q)$. We set $\bar{F}_f(k) = F_f(k)$, since we choose a real-valued gap and order parameter. Contributions with mixed bosonic propagators vanish due to symmetry.

Next, we will derive the flow equation for the transverse Yukawa coupling. The derivation for the longitudinal Yukawa vertex works analogously but will not be presented here. The flow equation for the transverse Yukawa vertex is extracted by applying two fermionic and one bosonic functional field derivative to the effective action

$$\begin{aligned}\frac{\delta^3}{\delta\phi_q\delta\bar{\psi}_{k'\uparrow}\delta\bar{\psi}_{k\downarrow}}\frac{d}{d\Lambda}\Gamma = \frac{\delta^4\Gamma}{\delta\phi_q\delta\sigma_0\delta\bar{\psi}_{k'\uparrow}\delta\bar{\psi}_{k\downarrow}}\frac{d}{d\Lambda}\alpha \\ &+ \Big[\frac{1}{2}\mathrm{Tr}\left(\mathcal{B}\frac{\delta^3\tilde{\Gamma}}{\delta\phi^2\phi_\mathrm{q}}\mathcal{S}_\mathrm{b}\frac{\delta^3\tilde{\Gamma}}{\delta\bar{\psi}_{\mathrm{k}\downarrow}\delta\phi\delta\psi}\mathcal{F}\frac{\delta^3\tilde{\Gamma}}{\delta\bar{\psi}_{\mathrm{k}'\uparrow}\delta\psi\delta\phi}\right) \\ &+ \frac{1}{2}\mathrm{Tr}\left(\mathcal{S}_\mathrm{b}\frac{\delta^3\tilde{\Gamma}}{\delta\phi_\mathrm{q}\delta\phi\delta\phi}\mathcal{B}\frac{\delta^3\tilde{\Gamma}}{\delta\bar{\psi}_{\mathrm{k}\downarrow}\delta\phi\delta\psi}\mathcal{F}\frac{\delta^3\tilde{\Gamma}}{\delta\bar{\psi}_{\mathrm{k}'\uparrow}\delta\psi\delta\phi}\right) \\ &+ \frac{1}{2}\mathrm{Tr}\left(\mathcal{S}_\mathrm{b}\frac{\delta^3\tilde{\Gamma}}{\delta\bar{\psi}_{\mathrm{k}\downarrow}\delta\phi\delta\psi}\mathcal{F}\frac{\delta^3\tilde{\Gamma}}{\delta\phi_\mathrm{q}\delta\psi^2}\mathcal{F}\frac{\delta^3\tilde{\Gamma}}{\delta\bar{\psi}_{\mathrm{k}'\uparrow}\delta\psi\delta\phi}\right) \\ &+ \frac{1}{2}\mathrm{Tr}\left(\mathcal{F}\frac{\delta^3\tilde{\Gamma}}{\delta\phi_\mathrm{q}\delta\psi^2}\mathcal{S}_\mathrm{f}\frac{\delta^3\tilde{\Gamma}}{\delta\psi_{\mathrm{k}\downarrow}\delta\psi\delta\phi}\mathcal{B}\frac{\delta^3\tilde{\Gamma}}{\delta\bar{\psi}_{\mathrm{k}'\uparrow}\delta\phi\delta\psi}\right) \\ &+ \frac{1}{2}\mathrm{Tr}\left(\mathcal{S}_\mathrm{f}\frac{\delta^3\tilde{\Gamma}}{\delta\phi_\mathrm{q}\delta\psi^2}\mathcal{F}\frac{\delta^3\tilde{\Gamma}}{\delta\bar{\psi}_{\mathrm{k}\downarrow}\delta\psi\delta\phi}\mathcal{B}\frac{\delta^3\tilde{\Gamma}}{\delta\bar{\psi}_{\mathrm{k}'\uparrow}\delta\phi\delta\psi}\right) \\ &+ \frac{1}{2}\mathrm{Tr}\left(\mathcal{S}_\mathrm{f}\frac{\delta^3\tilde{\Gamma}}{\delta\bar{\psi}_{\mathrm{k}\downarrow}\delta\psi\delta\phi}\mathcal{B}\frac{\delta^3\tilde{\Gamma}}{\delta\phi_\mathrm{q}\delta\phi^2}\mathcal{B}\frac{\delta^3\tilde{\Gamma}}{\delta\bar{\psi}_{\mathrm{k}'\uparrow}\delta\phi\delta\psi}\right) \\ &- \left(\bar{\psi}_{k'\uparrow} \leftrightarrow \bar{\psi}_{k\downarrow}\right)\Big].\end{aligned} \tag{B.74}$$

We can rewrite this expression

$$\frac{\delta^3}{\delta\pi_q\delta\bar{\psi}_{k'\uparrow}\delta\bar{\psi}_{k\downarrow}}\frac{d}{d\Lambda}\Gamma = \frac{\delta^4\Gamma}{\delta\pi_q\delta\sigma_0\delta\bar{\psi}_{k'\uparrow}\delta\bar{\psi}_{k\downarrow}}\frac{d}{d\Lambda}\alpha + \frac{d}{d\Lambda}A_3 + \frac{d}{d\Lambda}A_4 \tag{B.75}$$

with the contributions

$$\begin{aligned}
\frac{d}{d\Lambda}A_3 = {}& \frac{\tilde{D}_\Lambda}{2}\mathrm{Tr}\left(\mathcal{G}_\mathrm{b}(\sigma_\mathrm{a},\sigma_\mathrm{b})\frac{\delta^3\tilde{\Gamma}}{\delta\sigma_\mathrm{b}\delta\pi_\mathrm{c}\delta\pi_\mathrm{q}}\mathcal{G}_\mathrm{b}(\pi_\mathrm{c},\pi_\mathrm{d})\frac{\delta^3\tilde{\Gamma}}{\delta\bar{\psi}_{\mathrm{k}\downarrow}\delta\bar{\psi}_{\mathrm{x}\uparrow}\delta\pi_\mathrm{d}}\mathcal{F}(\bar{\psi}_{\mathrm{x}\uparrow},\bar{\psi}_{\mathrm{y}\downarrow})\frac{\delta^3\tilde{\Gamma}}{\delta\bar{\psi}_{\mathrm{k}'\uparrow}\delta\bar{\psi}_{\mathrm{y}\downarrow}\delta\sigma_\mathrm{a}}\right) \\
&+ \frac{\tilde{D}_\Lambda}{2}\mathrm{Tr}\left(\mathcal{G}_\mathrm{b}(\pi_\mathrm{a},\pi_\mathrm{b})\frac{\delta^3\tilde{\Gamma}}{\delta\pi_\mathrm{b}\delta\sigma_\mathrm{c}\delta\pi_\mathrm{q}}\mathcal{G}_\mathrm{b}(\sigma_\mathrm{c},\sigma_\mathrm{d})\frac{\delta^3\tilde{\Gamma}}{\delta\bar{\psi}_{\mathrm{k}\downarrow}\delta\bar{\psi}_{\mathrm{x}\uparrow}\delta\sigma_\mathrm{d}}\mathcal{F}(\bar{\psi}_{\mathrm{x}\uparrow},\bar{\psi}_{\mathrm{y}\downarrow})\frac{\delta^3\tilde{\Gamma}}{\delta\bar{\psi}_{\mathrm{k}'\uparrow}\delta\bar{\psi}_{\mathrm{y}\downarrow}\delta\pi_\mathrm{a}}\right) \\
&+ \frac{\tilde{D}_\Lambda}{2}\mathrm{Tr}\left(\mathcal{G}_\mathrm{b}(\sigma_\mathrm{a},\pi_\mathrm{b})\frac{\delta^3\tilde{\Gamma}}{\delta\pi_\mathrm{q}\delta\pi_\mathrm{b}\delta\sigma_\mathrm{c}}\mathcal{G}_\mathrm{b}(\sigma_\mathrm{c},\pi_\mathrm{d})\frac{\delta\tilde{\Gamma}}{\delta\bar{\psi}_{\mathrm{k}\downarrow}\delta\pi_\mathrm{d}\delta\bar{\psi}_{\mathrm{x}\uparrow}}\mathcal{F}(\bar{\psi}_{\mathrm{x}\uparrow},\bar{\psi}_{\mathrm{y}\downarrow})\frac{\delta^3\tilde{\Gamma}}{\delta\bar{\psi}_{\mathrm{k}'\uparrow}\delta\bar{\psi}_{\mathrm{y}\downarrow}\delta\sigma_\mathrm{a}}\right) \\
&+ \frac{\tilde{D}_\Lambda}{2}\mathrm{Tr}\left(\mathcal{G}_\mathrm{b}(\pi_\mathrm{a},\sigma_\mathrm{b})\frac{\delta^3\tilde{\Gamma}}{\delta\pi_\mathrm{q}\delta\sigma_\mathrm{b}\delta\pi_\mathrm{c}}\mathcal{G}_\mathrm{b}(\pi_\mathrm{c},\sigma_\mathrm{d})\frac{\delta\tilde{\Gamma}}{\delta\bar{\psi}_{\mathrm{k}\downarrow}\delta\sigma_\mathrm{d}\delta\bar{\psi}_{\mathrm{x}\uparrow}}\mathcal{F}(\bar{\psi}_{\mathrm{x}\uparrow},\bar{\psi}_{\mathrm{y}\downarrow})\frac{\delta^3\tilde{\Gamma}}{\delta\bar{\psi}_{\mathrm{k}'\uparrow}\delta\bar{\psi}_{\mathrm{y}\downarrow}\delta\pi_\mathrm{a}}\right) \\
&- \left(\bar{\psi}_{k'\uparrow}\leftrightarrow\bar{\psi}_{k\downarrow}\right)
\end{aligned} \tag{B.76}$$

and

$$\begin{aligned}
\frac{d}{d\Lambda}A_4 = {}& \frac{\tilde{D}_\Lambda}{2}\mathrm{Tr}\left(\mathcal{G}_\mathrm{b}(\pi_\mathrm{a},\pi_\mathrm{b})\frac{\delta^3\tilde{\Gamma}}{\delta\bar{\psi}_{\mathrm{k}\downarrow}\delta\pi_\mathrm{b}\delta\bar{\psi}_{\mathrm{x}\uparrow}}\mathcal{F}(\bar{\psi}_{\mathrm{x}\uparrow},\bar{\psi}_{\mathrm{y}\downarrow})\frac{\delta^3\tilde{\Gamma}}{\delta\pi_\mathrm{q}\delta\bar{\psi}_{\mathrm{y}\downarrow}\delta\bar{\psi}_{\mathrm{z}\uparrow}}\mathcal{F}(\bar{\psi}_{\mathrm{z}\uparrow},\bar{\psi}_{\mathrm{w}\downarrow})\frac{\delta^3\tilde{\Gamma}}{\delta\bar{\psi}_{\mathrm{k}'\uparrow}\delta\bar{\psi}_{\mathrm{w}\downarrow}\delta\pi_\mathrm{a}}\right) \\
&+ \frac{\tilde{D}_\Lambda}{2}\mathrm{Tr}\left(\mathcal{G}_\mathrm{b}(\pi_\mathrm{a},\pi_\mathrm{b})\frac{\delta^3\tilde{\Gamma}}{\delta\bar{\psi}_{\mathrm{k}\downarrow}\delta\pi_\mathrm{b}\delta\bar{\psi}_{\mathrm{x}\uparrow}}\mathcal{F}(\bar{\psi}_{\mathrm{x}\uparrow},\psi_{\mathrm{y}\uparrow})\frac{\delta^3\tilde{\Gamma}}{\delta\pi_\mathrm{q}\delta\psi_{\mathrm{y}\uparrow}\delta\psi_{\mathrm{z}\downarrow}}\mathcal{F}(\psi_{\mathrm{z}\downarrow},\bar{\psi}_{\mathrm{w}\downarrow})\frac{\delta^3\tilde{\Gamma}}{\delta\bar{\psi}_{\mathrm{k}'\uparrow}\delta\bar{\psi}_{\mathrm{w}\downarrow}\delta\pi_\mathrm{a}}\right) \\
&+ \frac{\tilde{D}_\Lambda}{2}\mathrm{Tr}\left(\mathcal{G}_\mathrm{b}(\sigma_\mathrm{a},\sigma_\mathrm{b})\frac{\delta^3\tilde{\Gamma}}{\delta\bar{\psi}_{\mathrm{k}\downarrow}\delta\sigma_\mathrm{b}\delta\bar{\psi}_{\mathrm{x}\uparrow}}\mathcal{F}(\bar{\psi}_{\mathrm{x}\uparrow},\bar{\psi}_{\mathrm{y}\downarrow})\frac{\delta^3\tilde{\Gamma}}{\delta\pi_\mathrm{q}\delta\bar{\psi}_{\mathrm{y}\downarrow}\bar{\psi}_{\mathrm{z}\uparrow}}\mathcal{F}(\bar{\psi}_{\mathrm{z}\uparrow},\bar{\psi}_{\mathrm{w}\downarrow})\frac{\delta^3\tilde{\Gamma}}{\delta\bar{\psi}_{\mathrm{k}'\uparrow}\delta\bar{\psi}_{\mathrm{w}\downarrow}\delta\sigma_\mathrm{a}}\right) \\
&+ \frac{\tilde{D}_\Lambda}{2}\mathrm{Tr}\left(\mathcal{G}_\mathrm{b}(\sigma_\mathrm{a},\sigma_\mathrm{b})\frac{\delta^3\tilde{\Gamma}}{\delta\bar{\psi}_{\mathrm{k}\downarrow}\delta\sigma_\mathrm{b}\delta\bar{\psi}_{\mathrm{x}\uparrow}}\mathcal{F}(\bar{\psi}_{\mathrm{x}\uparrow},\psi_{\mathrm{y}\uparrow})\frac{\delta^3\tilde{\Gamma}}{\delta\pi_\mathrm{q}\delta\psi_{\mathrm{y}\uparrow}\psi_{\mathrm{z}\downarrow}}\mathcal{F}(\psi_{\mathrm{z}\downarrow},\bar{\psi}_{\mathrm{w}\downarrow})\frac{\delta^3\tilde{\Gamma}}{\delta\bar{\psi}_{\mathrm{k}'\uparrow}\delta\bar{\psi}_{\mathrm{w}\downarrow}\delta\sigma_\mathrm{a}}\right) \\
&- \left(\bar{\psi}_{k'\uparrow}\leftrightarrow\bar{\psi}_{k\downarrow}\right),
\end{aligned} \tag{B.77}$$

where we defined a new operator $\tilde{D}_\Lambda$ which acts similarly as D_Λ for a compact notation.[3] The spin degree of freedom in contributions with two fermionic propagators leads to a doubling of each term. Integrals over terms with only one mixed bosonic propagator $G_{\sigma\pi}(q)$ and two fermionic propagator vanish due to the antisymmetric frequency depen-

[3]The operator $\tilde{D}_\Lambda$ is identical to $D_\Lambda = \frac{\partial}{\partial\Lambda}\Big|_\Sigma$ if it acts on bosonic propagators. However, it will induce an additional minus sign if it is applied to fermionic propagators. Hence, for instance $\tilde{D}_\Lambda G_\sigma(q) = D_\Lambda G_\sigma(q)$, but $\tilde{D}_\Lambda F(q) = -D_\Lambda F(q)$

dence of the bosonic propagator. We discarded them already in the above equation. After setting bosonic external frequencies and momenta to zero, and fermionic frequencies and momenta onto the Fermi surface, we find

$$\begin{aligned}\frac{d}{d\Lambda}g_\pi = g_\pi \int_q D_\Lambda \left[F_f^2(k_f-q)) + |G_f(k_f-q)|^2\right]\left[g_\sigma^2 G_{\sigma^2}(q) - g_\pi^2 G_{\pi^2}(q)\right] \\ + 2g_\sigma g_\pi \int_q D_\Lambda \left[G_{\sigma^2}(q)G_{\pi^2}(q) + G_{\sigma\pi}(q)^2\right] F(k_f-q)U(q)\alpha. \end{aligned} \tag{B.78}$$

Now, we will calculate the RG flow for the bosonic order parameter. The flow equation for the order parameter in general reads

$$\frac{d}{d\Lambda}\alpha = -\left(\frac{\delta^2\Gamma}{\delta\sigma_0\delta\sigma_0}\right)^{-1}\frac{\delta}{\delta\sigma_0}\frac{d}{d\Lambda}\Gamma \tag{B.79}$$

with $\frac{\delta^2\Gamma}{\delta\sigma_0\delta\sigma_0} = m_\sigma^2$. A derivation can be found in section 2.3 of chapter 2. Hence, we need the first derivative of the effective action with respect to a longitudinal bosonic field that is given by

$$\frac{\delta}{\delta\sigma_0}\frac{\partial}{\partial\Lambda}\Gamma = \frac{1}{2}\mathrm{Tr}\left(\mathcal{S}_\mathrm{b}\frac{\delta^3\tilde{\Gamma}}{\delta\sigma_0\delta\phi^2}\right) + \frac{1}{2}\mathrm{Tr}\left(\mathcal{S}_\mathrm{f}\frac{\delta^3\tilde{\Gamma}}{\delta\sigma_0\delta\psi^2}\right). \tag{B.80}$$

In the next step, we evaluate the columns and rows of the matrix representation and obtain

$$\begin{aligned}\frac{\partial}{\partial\Lambda}\frac{\delta\Gamma}{\delta\sigma_0} = \frac{1}{2}\mathrm{Tr}\left(\mathcal{S}_\mathrm{b}(\pi_\mathrm{a},\pi_\mathrm{b})\frac{\delta^3\tilde{\Gamma}}{\delta\sigma_0\delta\pi_\mathrm{b}\delta\pi_\mathrm{a}}\right) + \frac{1}{2}\mathrm{Tr}\left(\mathcal{S}_\mathrm{b}(\sigma_\mathrm{a},\sigma_\mathrm{b})\frac{\delta^3\tilde{\Gamma}}{\delta\sigma_0\delta\sigma_\mathrm{b}\delta\sigma_\mathrm{a}}\right) \\ + \frac{1}{2}\mathrm{Tr}\left(\mathcal{S}_\mathrm{f}(\bar{\psi}_{\mathrm{x}\downarrow},\bar{\psi}_{\mathrm{y}\uparrow})\frac{\delta^3\tilde{\Gamma}}{\delta\sigma_0\delta\bar{\psi}_{\mathrm{y}\uparrow}\delta\bar{\psi}_{\mathrm{x}\downarrow}}\right) + \frac{1}{2}\mathrm{Tr}\left(\mathcal{S}_\mathrm{f}(\psi_{\mathrm{x}\downarrow},\psi_{\mathrm{y}\uparrow})\frac{\delta^3\tilde{\Gamma}}{\delta\sigma_0\delta\psi_{\mathrm{y}\uparrow}\delta\psi_{\mathrm{x}\downarrow}}\right) \\ + \frac{1}{2}\mathrm{Tr}\left(\mathcal{S}_\mathrm{f}(\bar{\psi}_{\mathrm{x}\uparrow},\bar{\psi}_{\mathrm{y}\downarrow})\frac{\delta^3\tilde{\Gamma}}{\delta\sigma_0\delta\bar{\psi}_{\mathrm{y}\downarrow}\delta\bar{\psi}_{\mathrm{x}\uparrow}}\right) + \frac{1}{2}\mathrm{Tr}\left(\mathcal{S}_\mathrm{f}(\psi_{\mathrm{x}\uparrow},\psi_{\mathrm{y}\downarrow})\frac{\delta^3\tilde{\Gamma}}{\delta\sigma_0\delta\psi_{\mathrm{y}\downarrow}\delta\psi_{\mathrm{x}\uparrow}}\right). \end{aligned} \tag{B.81}$$

Finally, the RG flow for the bosonic order parameter is given by

$$\begin{aligned}\frac{d}{d\Lambda}\alpha = -\frac{u\alpha}{2m_\sigma^2}\int_q D_\Lambda G_{\pi^2}(q) - \frac{1}{2m_\sigma^2}\int_q D_\Lambda G_{\sigma^2}(q)\left[2U(q)+u\right]\alpha \\ + \frac{2g_\sigma}{m_\sigma^2}\int_k D_\Lambda F_f(k), \end{aligned} \tag{B.82}$$

which we obtain after inserting the amputated Yukawa vertices and bosonic interactions

from Eq. (B.54)-(B.57) and Eq. (B.7)-(B.11).

Now, we derive the explicit flow equations of the bosonic self-energies, see Eq. (B.60) and (B.61). We first present an expression for the functional field derivatives with respect to general bosonic fields

$$\begin{aligned}\frac{\delta^2}{\delta\phi_Q\delta\phi_{Q'}}\frac{d}{d\Lambda}\Gamma = \frac{\delta^3\Gamma}{\delta\phi_Q\delta\phi_{Q'}\delta\sigma_0}\frac{d}{d\Lambda}\alpha \\ - \frac{1}{2}\mathrm{Tr}\left(\mathcal{S}_\mathrm{f}\frac{\delta^3\tilde{\Gamma}}{\delta\phi_\mathrm{Q}\delta\psi^2}\mathcal{F}\frac{\delta^3\tilde{\Gamma}}{\delta\phi_{\mathrm{Q}'}\delta\psi^2} + (\phi_\mathrm{Q}\leftrightarrow\phi_{\mathrm{Q}'})\right) \\ + \frac{1}{2}\mathrm{Tr}\left(\mathcal{S}_\mathrm{b}\frac{\delta^4\tilde{\Gamma}}{\delta\phi_\mathrm{Q}\delta\phi_{\mathrm{Q}'}\delta\phi^2}\right) \\ - \frac{1}{2}\mathrm{Tr}\left(\mathcal{S}_\mathrm{b}\frac{\delta^3\tilde{\Gamma}}{\delta\phi_\mathrm{Q}\delta\phi^2}\mathcal{B}\frac{\delta^3\tilde{\Gamma}}{\delta\phi_{\mathrm{Q}'}\delta\phi^2} + (\phi_\mathrm{Q}\leftrightarrow\phi_{\mathrm{Q}'})\right).\end{aligned} \tag{B.83}$$

Next, we specify these general bosonic fields of the transverse and longitudinal fields and obtain the RG equations for the transverse, longitudinal and mixed bosonic self-energy.

We begin with the longitudinal bosonic self-energy specifying the general bosonic fields in terms of longitudinal fields $\phi_Q, \phi_{Q'} \to \sigma_q, \sigma_{q'}$. The flow for the second derivative of the effective action with respect to longitudinal fields reads

$$\frac{\delta^2}{\delta\sigma_q\delta\sigma_{q'}}\frac{d}{d\Lambda}\Gamma = \frac{\delta^3\Gamma}{\delta\sigma_q\delta\sigma_{q'}\delta\sigma_0}\frac{d}{d\Lambda}\alpha + \frac{d}{d\Lambda}A_5 + \frac{d}{d\Lambda}A_6, \tag{B.84}$$

and can be split in two contributions A_5 and A_6. The first term

$$\begin{aligned}\frac{d}{d\Lambda}A_5 = &-\frac{1}{2}\mathrm{Tr}\left(\mathcal{S}_\mathrm{f}(\psi_{\mathrm{l}''\uparrow},\bar{\psi}_{\mathrm{k}'\uparrow})\frac{\delta^3\tilde{\Gamma}}{\delta\sigma_\mathrm{q}\delta\bar{\psi}_{\mathrm{k}'\uparrow}\delta\bar{\psi}_{\mathrm{k}''\downarrow}}\mathcal{F}(\bar{\psi}_{\mathrm{k}''\downarrow},\psi_{\mathrm{l}'\downarrow})\frac{\delta^3\tilde{\Gamma}}{\delta\sigma_{\mathrm{q}'}\delta\psi_{\mathrm{l}'\downarrow}\delta\psi_{\mathrm{l}''\uparrow}}\right)\\
&-\frac{1}{2}\mathrm{Tr}\left(\mathcal{S}_\mathrm{f}(\bar{\psi}_{\mathrm{l}''\downarrow},\bar{\psi}_{\mathrm{k}'\uparrow})\frac{\delta^3\tilde{\Gamma}}{\delta\sigma_\mathrm{q}\delta\bar{\psi}_{\mathrm{k}'\uparrow}\delta\bar{\psi}_{\mathrm{k}''\downarrow}}\mathcal{F}(\bar{\psi}_{\mathrm{k}''\downarrow},\bar{\psi}_{\mathrm{l}'\uparrow})\frac{\delta^3\tilde{\Gamma}}{\delta\sigma_{\mathrm{q}'}\delta\bar{\psi}_{\mathrm{l}'\uparrow}\delta\bar{\psi}_{\mathrm{l}''\downarrow}}\right)\\
&-\frac{1}{2}\mathrm{Tr}\left(\mathcal{S}_\mathrm{f}(\psi_{\mathrm{l}''\downarrow},\bar{\psi}_{\mathrm{k}'\downarrow})\frac{\delta^3\tilde{\Gamma}}{\delta\sigma_\mathrm{q}\delta\bar{\psi}_{\mathrm{k}'\downarrow}\delta\bar{\psi}_{\mathrm{k}''\uparrow}}\mathcal{F}(\bar{\psi}_{\mathrm{k}''\uparrow},\psi_{\mathrm{l}'\uparrow})\frac{\delta^3\tilde{\Gamma}}{\delta\sigma_{\mathrm{q}'}\delta\psi_{\mathrm{l}'\uparrow}\delta\psi_{\mathrm{l}''\downarrow}}\right)\\
&-\frac{1}{2}\mathrm{Tr}\left(\mathcal{S}_\mathrm{f}(\bar{\psi}_{\mathrm{l}''\uparrow},\bar{\psi}_{\mathrm{k}'\downarrow})\frac{\delta^3\tilde{\Gamma}}{\delta\sigma_\mathrm{q}\delta\bar{\psi}_{\mathrm{k}'\downarrow}\delta\bar{\psi}_{\mathrm{k}''\uparrow}}\mathcal{F}(\bar{\psi}_{\mathrm{k}''\uparrow},\bar{\psi}_{\mathrm{l}'\downarrow})\frac{\delta^3\tilde{\Gamma}}{\delta\sigma_{\mathrm{q}'}\delta\bar{\psi}_{\mathrm{l}'\downarrow}\delta\bar{\psi}_{\mathrm{l}''\uparrow}}\right)\\
&-\frac{1}{2}\mathrm{Tr}\left(\mathcal{S}_\mathrm{f}(\bar{\psi}_{\mathrm{l}''\uparrow},\psi_{\mathrm{k}'\uparrow})\frac{\delta^3\tilde{\Gamma}}{\delta\sigma_\mathrm{q}\delta\psi_{\mathrm{k}'\uparrow}\delta\psi_{\mathrm{k}''\downarrow}}\mathcal{F}(\psi_{\mathrm{k}''\downarrow},\bar{\psi}_{\mathrm{l}'\downarrow})\frac{\delta^3\tilde{\Gamma}}{\delta\sigma_{\mathrm{q}'}\delta\bar{\psi}_{\mathrm{l}'\downarrow}\delta\bar{\psi}_{\mathrm{l}''\uparrow}}\right)\\
&-\frac{1}{2}\mathrm{Tr}\left(\mathcal{S}_\mathrm{f}(\psi_{\mathrm{l}''\downarrow},\psi_{\mathrm{k}'\uparrow})\frac{\delta^3\tilde{\Gamma}}{\delta\sigma_\mathrm{q}\delta\psi_{\mathrm{k}'\uparrow}\delta\psi_{\mathrm{k}''\downarrow}}\mathcal{F}(\psi_{\mathrm{k}''\downarrow},\psi_{\mathrm{l}'\uparrow})\frac{\delta^3\tilde{\Gamma}}{\delta\sigma_{\mathrm{q}'}\delta\psi_{\mathrm{l}'\uparrow}\delta\psi_{\mathrm{l}''\downarrow}}\right)\\
&-\frac{1}{2}\mathrm{Tr}\left(\mathcal{S}_\mathrm{f}(\bar{\psi}_{\mathrm{l}''\downarrow},\psi_{\mathrm{k}'\downarrow})\frac{\delta^3\tilde{\Gamma}}{\delta\sigma_\mathrm{q}\delta\psi_{\mathrm{k}'\downarrow}\delta\psi_{\mathrm{k}''\uparrow}}\mathcal{F}(\psi_{\mathrm{k}''\uparrow},\bar{\psi}_{\mathrm{l}'\uparrow})\frac{\delta^3\tilde{\Gamma}}{\delta\sigma_{\mathrm{q}'}\delta\bar{\psi}_{\mathrm{l}'\uparrow}\delta\bar{\psi}_{\mathrm{l}''\downarrow}}\right)\\
&-\frac{1}{2}\mathrm{Tr}\left(\mathcal{S}_\mathrm{f}(\psi_{\mathrm{l}''\uparrow},\psi_{\mathrm{k}'\downarrow})\frac{\delta^3\tilde{\Gamma}}{\delta\sigma_\mathrm{q}\delta\psi_{\mathrm{k}'\downarrow}\delta\psi_{\mathrm{k}''\uparrow}}\mathcal{F}(\psi_{\mathrm{k}''\uparrow},\psi_{\mathrm{l}'\downarrow})\frac{\delta^3\tilde{\Gamma}}{\delta\sigma_{\mathrm{q}'}\delta\psi_{\mathrm{l}'\downarrow}\delta\psi_{\mathrm{l}''\uparrow}}\right)\\
&+(\sigma_q\leftrightarrow\sigma_{q'})\end{aligned}\tag{B.85}$$

includes fermionic contributions to the flow, whereas the second term

$$\begin{aligned}\frac{d}{d\Lambda}A_6 = &\frac{1}{2}\mathrm{Tr}\left(\mathcal{S}_\mathrm{b}(\sigma_\mathrm{a},\sigma_\mathrm{b})\frac{\delta^4\tilde{\Gamma}}{\delta\sigma_{\mathrm{q}'}\delta\sigma_\mathrm{q}\delta\sigma_\mathrm{b}\delta\sigma_\mathrm{a}}\right)+\frac{1}{2}\mathrm{Tr}\left(\mathcal{S}_\mathrm{b}(\pi_\mathrm{a},\pi_\mathrm{b})\frac{\delta^4\tilde{\Gamma}}{\delta\sigma_{\mathrm{q}'}\delta\sigma_\mathrm{q}\delta\pi_\mathrm{b}\delta\pi_\mathrm{a}}\right)\\
&+\Bigg[-\frac{1}{2}\mathrm{Tr}\left(\mathcal{S}_\mathrm{b}(\sigma_\mathrm{a},\sigma_\mathrm{b})\frac{\delta^3\tilde{\Gamma}}{\delta\sigma_\mathrm{q}\delta\sigma_\mathrm{b}\delta\sigma_\mathrm{c}}\mathcal{B}(\sigma_\mathrm{c},\sigma_\mathrm{d})\frac{\delta^3\tilde{\Gamma}}{\delta\sigma_{\mathrm{q}'}\delta\sigma_\mathrm{d}\delta\sigma_\mathrm{a}}\right)\\
&-\frac{1}{2}\mathrm{Tr}\left(\mathcal{S}_\mathrm{b}(\pi_\mathrm{a},\pi_\mathrm{b})\frac{\delta^3\tilde{\Gamma}}{\delta\sigma_\mathrm{q}\delta\pi_\mathrm{b}\delta\pi_\mathrm{c}}\mathcal{B}(\pi_\mathrm{c},\pi_\mathrm{d})\frac{\delta^3\tilde{\Gamma}}{\delta\sigma_{\mathrm{q}'}\delta\pi_\mathrm{d}\delta\pi_\mathrm{a}}\right)\\
&-\frac{1}{2}\mathrm{Tr}\left(\mathcal{S}_\mathrm{b}(\sigma_\mathrm{a},\pi_\mathrm{b})\frac{\delta^3\tilde{\Gamma}}{\delta\sigma_\mathrm{q}\delta\pi_\mathrm{b}\delta\pi_\mathrm{c}}\mathcal{B}(\pi_\mathrm{c},\sigma_\mathrm{d})\frac{\delta^3\tilde{\Gamma}}{\delta\sigma_{\mathrm{q}'}\delta\sigma_\mathrm{d}\delta\sigma_\mathrm{a}}\right)\\
&-\frac{1}{2}\mathrm{Tr}\left(\mathcal{S}_\mathrm{b}(\pi_\mathrm{a},\sigma_\mathrm{b})\frac{\delta^3\tilde{\Gamma}}{\delta\sigma_\mathrm{q}\delta\sigma_\mathrm{b}\delta\sigma_\mathrm{c}}\mathcal{B}(\sigma_\mathrm{c},\pi_\mathrm{d})\frac{\delta^3\tilde{\Gamma}}{\delta\sigma_{\mathrm{q}'}\delta\pi_\mathrm{d}\delta\pi_\mathrm{a}}\right)+\left(\sigma_\mathrm{q}\leftrightarrow\sigma_{\mathrm{q}'}\right)\Bigg]\end{aligned}\tag{B.86}$$

includes bosonic fluctuations. To determine the flow of the longitudinal bosonic self-

energy, we insert again the expressions for the amputated Yukawa vertices Eq. (B.54)-(B.57) and the matrix representation of fermionic and bosonic propagators Eq. (B.23) and (B.43) into the above expression. Setting external momenta $q = -q' = p$ we obtain the RG flow for the longitudinal bosonic self-energy

$$\begin{aligned}\frac{d}{d\Lambda}\Sigma_{\sigma^2}(p) = {} & \alpha(2U(p)+u)\frac{d}{d\Lambda}\alpha \\ & - g_\sigma^2 \int_k D_\Lambda \left\{[G_f(k)G_f(-k+p) - F_f(k)F_f(k+p)] + (p \leftrightarrow -p)\right\} \\ & + \frac{1}{2}\int_q D_\Lambda G_{\sigma^2}(q)\left[2U(q+p)+u\right] + \frac{u}{2}\int_q D_\Lambda G_{\pi^2}(q) \\ & - \frac{1}{2}\int_q D_\Lambda \left[G_{\pi^2}(q+\frac{p}{2})G_{\pi^2}(q-\frac{p}{2})\right]\left[U(p)\right]^2\alpha^2 \\ & - \frac{1}{2}\int_q D_\Lambda \left[G_{\sigma^2}(q+\frac{p}{2})G_{\sigma^2}(q-\frac{p}{2})\right] \\ & \qquad \cdot \left[U(q-\frac{p}{2}) + U(q+\frac{p}{2}) + U(p)\right]^2\alpha^2 \\ & - \int_q D_\Lambda \left[G_{\sigma\pi}(q)G_{\pi\sigma}(q+p)\right]\left[U(q)+U(q+p)+U(p)\right]U(p)\alpha^2.\end{aligned} \tag{B.87}$$

Secondly, we derive the flow equation for the transverse bosonic self-energy. We now need the second derivative of the effective action with respect to transverse bosonic fields and choose $\phi_Q, \phi_{Q'} \to \pi_q, \pi_{q'}$. The flow equation then reads

$$\frac{\delta^2}{\delta\pi_q\delta\pi_{q'}}\frac{d}{d\Lambda}\Gamma = \frac{\delta^3\Gamma}{\delta\pi_q\delta\pi_{q'}\delta\sigma_0}\frac{d\alpha}{d\Lambda} + \frac{d}{d\Lambda}A_7 + \frac{d}{d\Lambda}A_8 \tag{B.88}$$

consisting of two contributions A_7 and A_8. The first term

$$
\begin{aligned}
\frac{d}{d\Lambda}A_7 = &-\frac{1}{2}\mathrm{Tr}\left(\mathcal{S}_\mathrm{f}(\psi_{\mathrm{l}''\uparrow},\bar{\psi}_{\mathrm{k}'\uparrow})\frac{\delta^3\tilde{\Gamma}}{\delta\pi_\mathrm{q}\delta\bar{\psi}_{\mathrm{k}'\uparrow}\delta\bar{\psi}_{\mathrm{k}''\downarrow}}\mathcal{F}(\bar{\psi}_{\mathrm{k}''\downarrow},\psi_{\mathrm{l}'\downarrow})\frac{\delta^3\tilde{\Gamma}}{\delta\pi_{\mathrm{q}'}\delta\psi_{\mathrm{l}'\downarrow}\delta\psi_{\mathrm{l}''\uparrow}}\right)\\
&-\frac{1}{2}\mathrm{Tr}\left(\mathcal{S}_\mathrm{f}(\bar{\psi}_{\mathrm{l}''\downarrow},\bar{\psi}_{\mathrm{k}'\uparrow})\frac{\delta^3\tilde{\Gamma}}{\delta\pi_\mathrm{q}\delta\bar{\psi}_{\mathrm{k}'\uparrow}\delta\bar{\psi}_{\mathrm{k}''\downarrow}}\mathcal{F}(\bar{\psi}_{\mathrm{k}''\downarrow},\bar{\psi}_{\mathrm{l}'\uparrow})\frac{\delta^3\tilde{\Gamma}}{\delta\pi_{\mathrm{q}'}\delta\bar{\psi}_{\mathrm{l}'\uparrow}\delta\bar{\psi}_{\mathrm{l}''\downarrow}}\right)\\
&-\frac{1}{2}\mathrm{Tr}\left(\mathcal{S}_\mathrm{f}(\psi_{\mathrm{l}''\downarrow},\bar{\psi}_{\mathrm{k}'\downarrow})\frac{\delta^3\tilde{\Gamma}}{\delta\pi_\mathrm{q}\delta\bar{\psi}_{\mathrm{k}'\downarrow}\delta\bar{\psi}_{\mathrm{k}''\uparrow}}\mathcal{F}(\bar{\psi}_{\mathrm{k}''\uparrow},\psi_{\mathrm{l}'\uparrow})\frac{\delta^3\tilde{\Gamma}}{\delta\pi_{\mathrm{q}'}\delta\psi_{\mathrm{l}'\uparrow}\delta\psi_{\mathrm{l}''\downarrow}}\right)\\
&-\frac{1}{2}\mathrm{Tr}\left(\mathcal{S}_\mathrm{f}(\bar{\psi}_{\mathrm{l}''\uparrow},\bar{\psi}_{\mathrm{k}'\downarrow})\frac{\delta^3\tilde{\Gamma}}{\delta\pi_\mathrm{q}\delta\bar{\psi}_{\mathrm{k}'\downarrow}\delta\bar{\psi}_{\mathrm{k}''\uparrow}}\mathcal{F}(\bar{\psi}_{\mathrm{k}''\uparrow},\bar{\psi}_{\mathrm{l}'\downarrow})\frac{\delta^3\tilde{\Gamma}}{\delta\pi_{\mathrm{q}'}\delta\bar{\psi}_{\mathrm{l}'\downarrow}\delta\bar{\psi}_{\mathrm{l}''\uparrow}}\right)\\
&-\frac{1}{2}\mathrm{Tr}\left(\mathcal{S}_\mathrm{f}(\bar{\psi}_{\mathrm{l}''\uparrow},\psi_{\mathrm{k}'\uparrow})\frac{\delta^3\tilde{\Gamma}}{\delta\pi_\mathrm{q}\delta\psi_{\mathrm{k}'\uparrow}\delta\psi_{\mathrm{k}''\downarrow}}\mathcal{F}(\psi_{\mathrm{k}''\downarrow},\bar{\psi}_{\mathrm{l}'\downarrow})\frac{\delta^3\tilde{\Gamma}}{\delta\pi_{\mathrm{q}'}\delta\bar{\psi}_{\mathrm{l}'\downarrow}\delta\bar{\psi}_{\mathrm{l}''\uparrow}}\right)\\
&-\frac{1}{2}\mathrm{Tr}\left(\mathcal{S}_\mathrm{f}(\psi_{\mathrm{l}''\downarrow},\psi_{\mathrm{k}'\uparrow})\frac{\delta^3\tilde{\Gamma}}{\delta\pi_\mathrm{q}\delta\psi_{\mathrm{k}'\uparrow}\delta\psi_{\mathrm{k}''\downarrow}}\mathcal{F}(\psi_{\mathrm{k}''\downarrow},\psi_{\mathrm{l}'\uparrow})\frac{\delta^3\tilde{\Gamma}}{\delta\pi_{\mathrm{q}'}\delta\psi_{\mathrm{l}'\uparrow}\delta\psi_{\mathrm{l}''\downarrow}}\right)\\
&-\frac{1}{2}\mathrm{Tr}\left(\mathcal{S}_\mathrm{f}(\bar{\psi}_{\mathrm{l}''\downarrow},\psi_{\mathrm{k}'\downarrow})\frac{\delta^3\tilde{\Gamma}}{\delta\pi_\mathrm{q}\delta\psi_{\mathrm{k}'\downarrow}\delta\psi_{\mathrm{k}''\uparrow}}\mathcal{F}(\psi_{\mathrm{k}''\uparrow},\bar{\psi}_{\mathrm{l}'\uparrow})\frac{\delta^3\tilde{\Gamma}}{\delta\pi_{\mathrm{q}'}\delta\bar{\psi}_{\mathrm{l}'\uparrow}\delta\bar{\psi}_{\mathrm{l}''\downarrow}}\right)\\
&-\frac{1}{2}\mathrm{Tr}\left(\mathcal{S}_\mathrm{f}(\psi_{\mathrm{l}''\uparrow},\psi_{\mathrm{k}'\downarrow})\frac{\delta^3\tilde{\Gamma}}{\delta\pi_\mathrm{q}\delta\psi_{\mathrm{k}'\downarrow}\delta\psi_{\mathrm{k}''\uparrow}}\mathcal{F}(\psi_{\mathrm{k}''\uparrow},\psi_{\mathrm{l}'\downarrow})\frac{\delta^3\tilde{\Gamma}}{\delta\pi_{\mathrm{q}'}\delta\psi_{\mathrm{l}'\downarrow}\delta\psi_{\mathrm{l}''\uparrow}}\right)\\
&+(\pi_q\leftrightarrow\pi_{q'})
\end{aligned}
\tag{B.89}
$$

describes fermionic contributions to the flow, whereas the latter

$$
\begin{aligned}
\frac{d}{d\Lambda}A_8 = &\frac{1}{2}\mathrm{Tr}\left(\mathcal{S}_\mathrm{b}(\sigma_\mathrm{a},\sigma_\mathrm{b})\frac{\delta^4\tilde{\Gamma}}{\delta\pi_{\mathrm{q}'}\delta\pi_\mathrm{q}\delta\sigma_\mathrm{b}\delta\sigma_\mathrm{a}}\right)+\frac{1}{2}\mathrm{Tr}\left(\mathcal{S}_\mathrm{b}(\pi_\mathrm{a},\pi_\mathrm{b})\frac{\delta^4\tilde{\Gamma}}{\delta\pi_{\mathrm{q}'}\delta\pi_\mathrm{q}\delta\pi_\mathrm{b}\delta\pi_\mathrm{a}}\right)\\
&+\Bigg[-\frac{1}{2}\mathrm{Tr}\left(\mathcal{S}_\mathrm{b}(\sigma_\mathrm{a},\sigma_\mathrm{b})\frac{\delta^3\tilde{\Gamma}}{\delta\pi_\mathrm{q}\delta\sigma_\mathrm{b}\delta\pi_\mathrm{c}}\mathcal{B}(\pi_\mathrm{c},\pi_\mathrm{d})\frac{\delta^3\tilde{\Gamma}}{\delta\pi_{\mathrm{q}'}\delta\pi_\mathrm{d}\delta\sigma_\mathrm{a}}\right)\\
&-\frac{1}{2}\mathrm{Tr}\left(\mathcal{S}_\mathrm{b}(\sigma_\mathrm{a},\pi_\mathrm{b})\frac{\delta^3\tilde{\Gamma}}{\delta\pi_\mathrm{q}\delta\pi_\mathrm{b}\delta\sigma_\mathrm{c}}\mathcal{B}(\sigma_\mathrm{c},\pi_\mathrm{d})\frac{\delta^3\tilde{\Gamma}}{\delta\pi_{\mathrm{q}'}\delta\pi_\mathrm{d}\delta\sigma_\mathrm{a}}\right)\\
&-\frac{1}{2}\mathrm{Tr}\left(\mathcal{S}_\mathrm{b}(\pi_\mathrm{a},\sigma_\mathrm{b})\frac{\delta^3\tilde{\Gamma}}{\delta\pi_\mathrm{q}\delta\sigma_\mathrm{b}\delta\pi_\mathrm{c}}\mathcal{B}(\pi_\mathrm{c},\sigma_\mathrm{d})\frac{\delta^3\tilde{\Gamma}}{\delta\pi_{\mathrm{q}'}\delta\sigma_\mathrm{d}\delta\pi_\mathrm{a}}\right)\\
&-\frac{1}{2}\mathrm{Tr}\left(\mathcal{S}_\mathrm{b}(\pi_\mathrm{a},\pi_\mathrm{b})\frac{\delta^3\tilde{\Gamma}}{\delta\pi_\mathrm{q}\delta\pi_\mathrm{b}\delta\sigma_\mathrm{c}}\mathcal{B}(\sigma_\mathrm{c},\sigma_\mathrm{d})\frac{\delta^3\tilde{\Gamma}}{\delta\pi_{\mathrm{q}'}\delta\sigma_\mathrm{d}\delta\pi_\mathrm{a}}\right)+(\pi_\mathrm{q}\leftrightarrow\pi_{\mathrm{q}'})\Bigg]
\end{aligned}
\tag{B.90}
$$

includes bosonic fluctuations. Again we insert the Yukawa couplings Eq. (B.54)-(B.57) and

bosonic interactions Eq. (B.7)-(B.11) into the above expressions and perform the internal integrations over the delta functions. We set the external momenta and frequencies to $q = -q' = p$. The RG flow equations for the transverse self-energy then reads

$$\begin{aligned}\frac{d}{d\Lambda}\Sigma_{\pi^2}(p) = u\alpha\frac{d}{d\Lambda}\alpha - g_\pi^2\int_k D_\Lambda\left[G_f(k)G_f(-k+p) + F_f(k)F_f(k+p) + (p\leftrightarrow -p)\right] \\ - \int_q D_\Lambda[G_{\pi^2}(q+p)G_{\sigma^2}(q)]\left[U(q)\right]^2\alpha^2 \\ + \frac{1}{2}\int_q [2U(q+p)+u]D_\Lambda G_{\pi^2}(q) + \frac{u}{2}\int_q D_\Lambda G_{\sigma^2}(q) \\ - \int_q D_\Lambda\Big[G_{\sigma\pi}(q)G_{\sigma\pi}(q+p)\Big]\left[U(q)U(q+p)\right]\alpha^2. \end{aligned} \tag{B.91}$$

At last we derive the flow equations for the mixed bosonic self-energy $\Sigma_{\sigma\pi}(p)$. Here, we require the second derivative of the effective action with respect to transverse and longitudinal bosonic fields

$$\frac{\delta^2}{\delta\sigma_{q'}\delta\pi_q}\frac{d}{d\Lambda}\Gamma = \frac{d}{d\Lambda}A_9 + \frac{d}{d\Lambda}A_{10}, \tag{B.92}$$

which we split into two parts A_9 and A_{10}. The first part describes fermionic contributions

to the flow

$$\begin{aligned}\frac{d}{d\Lambda}A_9 = &-\frac{1}{2}\mathrm{Tr}\left(\mathcal{S}_\mathrm{f}(\psi_{\mathrm{l}''\uparrow},\bar{\psi}_{\mathrm{k}'\uparrow})\frac{\delta^3\tilde{\Gamma}}{\delta\pi_\mathrm{q}\delta\bar{\psi}_{\mathrm{k}'\uparrow}\delta\bar{\psi}_{\mathrm{k}''\downarrow}}\mathcal{F}(\bar{\psi}_{\mathrm{k}''\downarrow},\psi_{\mathrm{l}'\downarrow})\frac{\delta^3\tilde{\Gamma}}{\delta\sigma_{\mathrm{q}'}\delta\psi_{\mathrm{l}'\downarrow}\delta\psi_{\mathrm{l}''\uparrow}}\right)\\
&-\frac{1}{2}\mathrm{Tr}\left(\mathcal{S}_\mathrm{f}(\bar{\psi}_{\mathrm{l}''\downarrow},\bar{\psi}_{\mathrm{k}'\uparrow})\frac{\delta^3\tilde{\Gamma}}{\delta\pi_\mathrm{q}\delta\bar{\psi}_{\mathrm{k}'\uparrow}\delta\bar{\psi}_{\mathrm{k}''\downarrow}}\mathcal{F}(\bar{\psi}_{\mathrm{k}''\downarrow},\bar{\psi}_{\mathrm{l}'\uparrow})\frac{\delta^3\tilde{\Gamma}}{\delta\sigma_{\mathrm{q}'}\delta\bar{\psi}_{\mathrm{l}'\uparrow}\delta\bar{\psi}_{\mathrm{l}''\downarrow}}\right)\\
&-\frac{1}{2}\mathrm{Tr}\left(\mathcal{S}_\mathrm{f}(\psi_{\mathrm{l}''\downarrow},\bar{\psi}_{\mathrm{k}'\downarrow})\frac{\delta^3\tilde{\Gamma}}{\delta\pi_\mathrm{q}\delta\bar{\psi}_{\mathrm{k}'\downarrow}\delta\bar{\psi}_{\mathrm{k}''\uparrow}}\mathcal{F}(\bar{\psi}_{\mathrm{k}''\uparrow},\psi_{\mathrm{l}'\uparrow})\frac{\delta^3\tilde{\Gamma}}{\delta\sigma_{\mathrm{q}'}\delta\psi_{\mathrm{l}'\uparrow}\delta\psi_{\mathrm{l}''\downarrow}}\right)\\
&-\frac{1}{2}\mathrm{Tr}\left(\mathcal{S}_\mathrm{f}(\bar{\psi}_{\mathrm{l}''\uparrow},\bar{\psi}_{\mathrm{k}'\downarrow})\frac{\delta^3\tilde{\Gamma}}{\delta\pi_\mathrm{q}\delta\bar{\psi}_{\mathrm{k}'\downarrow}\delta\bar{\psi}_{\mathrm{k}''\uparrow}}\mathcal{F}(\bar{\psi}_{\mathrm{k}''\uparrow},\bar{\psi}_{\mathrm{l}'\downarrow})\frac{\delta^3\tilde{\Gamma}}{\delta\sigma_{\mathrm{q}'}\delta\bar{\psi}_{\mathrm{l}'\downarrow}\delta\bar{\psi}_{\mathrm{l}''\uparrow}}\right)\\
&-\frac{1}{2}\mathrm{Tr}\left(\mathcal{S}_\mathrm{f}(\bar{\psi}_{\mathrm{l}''\uparrow},\psi_{\mathrm{k}'\uparrow})\frac{\delta^3\tilde{\Gamma}}{\delta\pi_\mathrm{q}\delta\psi_{\mathrm{k}'\uparrow}\delta\psi_{\mathrm{k}''\downarrow}}\mathcal{F}(\psi_{\mathrm{k}''\downarrow},\bar{\psi}_{\mathrm{l}'\downarrow})\frac{\delta^3\tilde{\Gamma}}{\delta\sigma_{\mathrm{q}'}\delta\bar{\psi}_{\mathrm{l}'\downarrow}\delta\bar{\psi}_{\mathrm{l}''\uparrow}}\right)\\
&-\frac{1}{2}\mathrm{Tr}\left(\mathcal{S}_\mathrm{f}(\psi_{\mathrm{l}''\downarrow},\psi_{\mathrm{k}'\uparrow})\frac{\delta^3\tilde{\Gamma}}{\delta\pi_\mathrm{q}\delta\psi_{\mathrm{k}'\uparrow}\delta\psi_{\mathrm{k}''\downarrow}}\mathcal{F}(\psi_{\mathrm{k}''\downarrow},\psi_{\mathrm{l}'\uparrow})\frac{\delta^3\tilde{\Gamma}}{\delta\sigma_{\mathrm{q}'}\delta\psi_{\mathrm{l}'\uparrow}\delta\psi_{\mathrm{l}''\downarrow}}\right)\\
&-\frac{1}{2}\mathrm{Tr}\left(\mathcal{S}_\mathrm{f}(\bar{\psi}_{\mathrm{l}''\downarrow},\psi_{\mathrm{k}'\downarrow})\frac{\delta^3\tilde{\Gamma}}{\delta\pi_\mathrm{q}\delta\psi_{\mathrm{k}'\downarrow}\delta\psi_{\mathrm{k}''\uparrow}}\mathcal{F}(\psi_{\mathrm{k}''\uparrow},\bar{\psi}_{\mathrm{l}'\uparrow})\frac{\delta^3\tilde{\Gamma}}{\delta\sigma_{\mathrm{q}'}\delta\bar{\psi}_{\mathrm{l}'\uparrow}\delta\bar{\psi}_{\mathrm{l}''\downarrow}}\right)\\
&-\frac{1}{2}\mathrm{Tr}\left(\mathcal{S}_\mathrm{f}(\psi_{\mathrm{l}''\uparrow},\psi_{\mathrm{k}'\downarrow})\frac{\delta^3\tilde{\Gamma}}{\delta\pi_\mathrm{q}\delta\psi_{\mathrm{k}'\downarrow}\delta\psi_{\mathrm{k}''\uparrow}}\mathcal{F}(\psi_{\mathrm{k}''\uparrow},\psi_{\mathrm{l}'\downarrow})\frac{\delta^3\tilde{\Gamma}}{\delta\sigma_{\mathrm{q}'}\delta\psi_{\mathrm{l}'\downarrow}\delta\psi_{\mathrm{l}''\uparrow}}\right)\\
&+(\pi_q\leftrightarrow\sigma_{q'}),\end{aligned}\tag{B.93}$$

and the second part includes bosonic contributions

$$\begin{aligned}\frac{d}{d\Lambda}A_{10}=&\frac{1}{2}\mathrm{Tr}\left(\mathcal{S}_{\mathrm{b}}(\sigma_{\mathrm{a}},\pi_{\mathrm{b}})\frac{\delta^4\tilde{\Gamma}}{\delta\sigma_{\mathrm{q}'}\delta\pi_{\mathrm{q}}\delta\pi_{\mathrm{b}}\delta\sigma_{\mathrm{a}}}\right)+\frac{1}{2}\mathrm{Tr}\left(\mathcal{S}_{\mathrm{b}}(\pi_{\mathrm{a}},\sigma_{\mathrm{b}})\frac{\delta^4\tilde{\Gamma}}{\delta\sigma_{\mathrm{q}'}\delta\pi_{\mathrm{q}}\delta\sigma_{\mathrm{b}}\delta\pi_{\mathrm{a}}}\right)\\
&-\frac{1}{2}\mathrm{Tr}\left(\mathcal{S}_{\mathrm{b}}(\sigma_{\mathrm{a}},\sigma_{\mathrm{b}})\frac{\delta^3\tilde{\Gamma}}{\delta\sigma_{\mathrm{q}'}\delta\sigma_{\mathrm{b}}\delta\sigma_{\mathrm{c}}}\mathcal{B}(\sigma_{\mathrm{c}},\pi_{\mathrm{d}})\frac{\delta^3\tilde{\Gamma}}{\delta\pi_{\mathrm{q}}\delta\pi_{\mathrm{d}}\delta\sigma_{\mathrm{a}}}\right)\\
&-\frac{1}{2}\mathrm{Tr}\left(\mathcal{S}_{\mathrm{b}}(\sigma_{\mathrm{a}},\pi_{\mathrm{b}})\frac{\delta^3\tilde{\Gamma}}{\delta\sigma_{\mathrm{q}'}\delta\pi_{\mathrm{b}}\delta\pi_{\mathrm{c}}}\mathcal{B}(\pi_{\mathrm{c}},\pi_{\mathrm{d}})\frac{\delta^3\tilde{\Gamma}}{\delta\pi_{\mathrm{q}}\delta\pi_{\mathrm{d}}\delta\sigma_{\mathrm{a}}}\right)\\
&-\frac{1}{2}\mathrm{Tr}\left(\mathcal{S}_{\mathrm{b}}(\pi_{\mathrm{a}},\sigma_{\mathrm{b}})\frac{\delta^3\tilde{\Gamma}}{\delta\sigma_{\mathrm{q}'}\delta\sigma_{\mathrm{b}}\delta\sigma_{\mathrm{c}}}\mathcal{B}(\sigma_{\mathrm{c}},\sigma_{\mathrm{d}})\frac{\delta^3\tilde{\Gamma}}{\delta\pi_{\mathrm{q}}\delta\sigma_{\mathrm{d}}\delta\pi_{\mathrm{a}}}\right)\\
&-\frac{1}{2}\mathrm{Tr}\left(\mathcal{S}_{\mathrm{b}}(\pi_{\mathrm{a}},\pi_{\mathrm{b}})\frac{\delta^3\tilde{\Gamma}}{\delta\sigma_{\mathrm{q}'}\delta\pi_{\mathrm{b}}\delta\pi_{\mathrm{c}}}\mathcal{B}(\pi_{\mathrm{c}},\sigma_{\mathrm{d}})\frac{\delta^3\tilde{\Gamma}}{\delta\pi_{\mathrm{q}}\delta\sigma_{\mathrm{d}}\delta\pi_{\mathrm{a}}}\right)\\
&-\frac{1}{2}\mathrm{Tr}\left(\mathcal{S}_{\mathrm{b}}(\sigma_{\mathrm{a}},\sigma_{\mathrm{b}})\frac{\delta^3\tilde{\Gamma}}{\delta\pi_{\mathrm{q}}\delta\sigma_{\mathrm{b}}\delta\pi_{\mathrm{c}}}\mathcal{B}(\pi_{\mathrm{c}},\sigma_{\mathrm{d}})\frac{\delta^3\tilde{\Gamma}}{\delta\sigma_{\mathrm{q}'}\delta\sigma_{\mathrm{d}}\delta\sigma_{\mathrm{a}}}\right)\\
&-\frac{1}{2}\mathrm{Tr}\left(\mathcal{S}_{\mathrm{b}}(\sigma_{\mathrm{a}},\pi_{\mathrm{b}})\frac{\delta^3\tilde{\Gamma}}{\delta\pi_{\mathrm{q}}\delta\pi_{\mathrm{b}}\delta\sigma_{\mathrm{c}}}\mathcal{B}(\sigma_{\mathrm{c}},\sigma_{\mathrm{d}})\frac{\delta^3\tilde{\Gamma}}{\delta\sigma_{\mathrm{q}'}\delta\sigma_{\mathrm{d}}\delta\sigma_{\mathrm{a}}}\right)\\
&-\frac{1}{2}\mathrm{Tr}\left(\mathcal{S}_{\mathrm{b}}(\pi_{\mathrm{a}},\sigma_{\mathrm{b}})\frac{\delta^3\tilde{\Gamma}}{\delta\pi_{\mathrm{q}}\delta\sigma_{\mathrm{b}}\delta\pi_{\mathrm{c}}}\mathcal{B}(\pi_{\mathrm{c}},\pi_{\mathrm{d}})\frac{\delta^3\tilde{\Gamma}}{\delta\sigma_{\mathrm{q}'}\delta\pi_{\mathrm{d}}\delta\pi_{\mathrm{a}}}\right)\\
&-\frac{1}{2}\mathrm{Tr}\left(\mathcal{S}_{\mathrm{b}}(\pi_{\mathrm{a}},\pi_{\mathrm{b}})\frac{\delta^3\tilde{\Gamma}}{\delta\pi_{\mathrm{q}}\delta\pi_{\mathrm{b}}\delta\sigma_{\mathrm{c}}}\mathcal{B}(\sigma_{\mathrm{c}},\pi_{\mathrm{d}})\frac{\delta^3\tilde{\Gamma}}{\delta\sigma_{\mathrm{q}'}\delta\pi_{\mathrm{d}}\delta\pi_{\mathrm{a}}}\right).\end{aligned}\tag{B.94}$$

For the determination of the mixed bosonic self-energy, we again insert the amputated Yukawa vertices and bosonic couplings. Finally, we perform the integrations over all internal indices and delta functions and set the external momentum and frequency dependence $q=-q'=p$. The RG flow for the mixed bosonic self-energy finally reads

$$\begin{aligned}\frac{d}{d\Lambda}\Sigma_{\sigma\pi}(p)=&\quad ig_\sigma g_\pi\Big(\int_k D_\Lambda\left[G_f(k)G_f(-p-k)\right]-\int_k D_\Lambda\left[G_f(k)G_f(p-k)\right]\Big)\\
&+ig_\sigma g_\pi\int_k D_\Lambda\left[F_f(k)F_f(k+p)\right]-ig_\sigma g_\pi\int_k D_\Lambda\left[F_f(k)F_f(k-p)\right]\\
&-\int_q D_\Lambda\left[G_{\sigma^2}(q)G_{\sigma\pi}(q+p)\right]\left[U(q)+U(q+p)+U(p)\right]\left[U(q)\right]\alpha^2\\
&-\int_q D_\Lambda\left[G_{\pi^2}(q+p)G_{\sigma\pi}(q)\right]\left[U(p)U(q)\right]\alpha^2\\
&-\int_q D_\Lambda G_{\sigma\pi}(q)U(q+p).\end{aligned}\tag{B.95}$$

The RG flows for the bosonic self-energies $\Sigma_{\sigma^2}(p)$, $\Sigma_{\pi^2}(p)$ and $\Sigma_{\sigma\pi}(p)$ determine the flow of the bosonic masses

$$\frac{d}{d\Lambda}m_\sigma^2 = \frac{d}{d\Lambda}\Sigma_{\sigma^2}(0), \quad \frac{d}{d\Lambda}m_\pi^2 = \frac{d}{d\Lambda}\Sigma_{\pi^2}(0), \quad \frac{d}{d\Lambda}m_{\sigma\pi}^2 = \frac{d}{d\Lambda}\Sigma_{\sigma\pi}(0). \tag{B.96}$$

Furthermore, they determine the RG flow for the renormalization factors

$$\frac{d}{d\Lambda}Z_\sigma = \frac{1}{2}\frac{\partial^2}{\partial p_x^2}\Big|_{p=0}\frac{d}{d\Lambda}\Sigma_{\sigma^2}(p), \quad \frac{d}{d\Lambda}Z_\pi = \frac{1}{2}\frac{\partial}{\partial p_x^2}\Big|_{p=0}\frac{d}{d\Lambda}\Sigma_{\pi^2}(p) \tag{B.97}$$

$$\frac{d}{d\Lambda}W = \frac{\partial}{\partial p_0}\Big|_{p0=0}\frac{d}{d\Lambda}\Sigma_{\sigma\pi}(p). \tag{B.98}$$

The values for the mass and gradient term of the bosonic self-interaction u and Y are determined by

$$Y = \frac{Z_\sigma - Z_\pi}{\alpha^2}, \quad u = \frac{m_\sigma^2}{\alpha^2}. \tag{B.99}$$

B.5 Density of states for bosonic dispersion relation

In this section we present expressions for bosonic densities of states for our bosonic dispersion of the attractive Hubbard model. A detailed derivation can be found in Pesz and Munn (1986), who discuss the density of state of anisotropic tight binding models. Our bosonic dispersion relation

$$\omega_{\mathbf{q}}^2 = 4 - 2\cos q_x - 2\cos q_y \tag{B.100}$$

is a special case of the general version discussed there. For this simple dispersion relation several density of state-like functions can be defined as

$$N(E) = \int_{-\pi}^{\pi}\int_{-\pi}^{\pi} dq_x dq_y \delta(E - \omega_{\mathbf{q}}^2) = 2g\left(\frac{E-4}{2}\right), \tag{B.101}$$

$$N_{\cos}(E) = \int_{-\pi}^{\pi}\int_{-\pi}^{\pi} dq_x dq_y \delta(E - \omega_{\mathbf{q}}^2)\cos q_x = 2g_{\cos}\left(\frac{E-4}{2}\right), \tag{B.102}$$

$$N_{\sin^2}(E) = \int_{-\pi}^{\pi}\int_{-\pi}^{\pi} dq_x dq_y \delta(E - \omega_{\mathbf{q}}^2)\sin^2 q_x = 2g_{\sin^2}\left(\frac{E-4}{2}\right), \tag{B.103}$$

and can be written in terms of the functions $g(\epsilon)$, $g_{\cos}(\epsilon)$ and $g_{\sin^2}(\epsilon)$ with the shifted argument $\epsilon = \frac{E-4}{2}$.[4] These functions are defined as

$$g(\epsilon) = \begin{cases} \int_{-1}^{1-\epsilon} \frac{dx}{\sqrt{1-x^2}\sqrt{1-(x+\epsilon)^2}} & \text{if} \quad 0 < \epsilon < 2, \\ \int_{-1-\epsilon}^{1} \frac{dx}{\sqrt{1-x^2}\sqrt{1-(x+\epsilon)^2}} & \text{if} \quad -2 < \epsilon < 0, \\ 0 & \text{else,} \end{cases} \tag{B.104}$$

$$g_{\cos}(\epsilon) = \begin{cases} \int_{-1}^{1-\epsilon} dx \frac{x}{\sqrt{1-x^2}\sqrt{1-(x+\epsilon)^2}} & \text{if} \quad 0 < \epsilon < 2, \\ \int_{-1-\epsilon}^{1} dx \frac{x}{\sqrt{1-x^2}\sqrt{1-(x+\epsilon)^2}} & \text{if} \quad -2 < \epsilon < 0, \\ 0 & \text{else,} \end{cases} \tag{B.105}$$

$$g_{\sin^2}(\epsilon) = \begin{cases} \int_{-1}^{1-\epsilon} dx \frac{\sqrt{1-x^2}}{\sqrt{1-(x+\epsilon)^2}} & \text{if} \quad 0 < \epsilon < 2, \\ \int_{-1-\epsilon}^{1} dx \frac{\sqrt{1-x^2}}{\sqrt{1-(x+\epsilon)^2}} & \text{if} \quad -2 < \epsilon < 0, \\ 0 & \text{else.} \end{cases} \tag{B.106}$$

Hence, double integrals over the two-dimensional momentum space can be reduced to one-dimensional integrals over energies via the above density of states. After we replace the density of states by their analytic expressions from Eq. (B.101), (B.102) and (B.103), we obtain the relations

$$\begin{aligned} \int_{-\Lambda}^{\Lambda}\int_{-\pi}^{\pi}\int_{-\pi}^{\pi} \frac{dq_0 dq_x dq_y}{(2\pi)^3} F[\omega_{\mathbf{q}}^2, q_0] &= 2\int_{-\Lambda}^{\Lambda}\int_{0}^{8} \frac{dq_0 dE}{(2\pi)^3} g(\frac{E-4}{2}) F[E, q_0], \\ \int_{-\Lambda}^{\Lambda}\int_{-\pi}^{\pi}\int_{-\pi}^{\pi} \frac{dq_0 dq_x dq_y}{(2\pi)^3} \cos q_x F[\omega_{\mathbf{q}}^2, q_0] &= 2\int_{-\Lambda}^{\Lambda}\int_{0}^{8} \frac{dq_0 dE}{(2\pi)^3} g_{\cos}(\frac{E-4}{2}) F[E, q_0], \\ \int_{-\Lambda}^{\Lambda}\int_{-\pi}^{\pi}\int_{-\pi}^{\pi} \frac{dq_0 dq_x dq_y}{(2\pi)^3} \sin^2 q_x F[\omega_{\mathbf{q}}^2, q_0] &= 2\int_{-\Lambda}^{\Lambda}\int_{0}^{8} \frac{dq_0 dE}{(2\pi)^3} g_{\sin^2}(\frac{E-4}{2}) F[E, q_0]. \end{aligned} \tag{B.107}$$

for an arbitrary test-function $F[\omega_{\mathbf{q}}^2, q_0]$. We will apply these expressions to numerically evaluate the RG flow equations for the fermionic superfluid. Three-dimensional integrations over the two-dimensional Brillouin zone and frequencies are thereby reduced to two-dimensional integrations over energy and frequency, leading to a reduction of computing time.

[4] Note that the variable E does not denote the physical energy here, but the square root of the energy.

APPENDIX C

Ward identities

In this chapter we derive the Ward identities for a coupled fermion-boson system. We follow arguments similar to Kopietz et al. (2010), Zinn-Justin (2002) and Amit (1984). First, we derive a general connection valid for the effective action due to the underlying $U(1)$-symmetry. Afterwards, Ward identities between different correlation functions are obtained by functional differentiation with respect to fermionic and bosonic fields.

C.1 Ward identities for coupled fermion-boson theory

The starting point is given by a purely fermionic microscopic action of the form

$$S[\psi,\bar{\psi}] = \int_{k\sigma} \bar{\psi}_{k\sigma}(ik_0 - \xi_{\mathbf{k}})\psi_{k\sigma} + U\sum_i \bar{\psi}_{i\uparrow}\psi_{i\uparrow}\bar{\psi}_{i\downarrow}\psi_{i\downarrow}, \tag{C.1}$$

which obeys the global $U(1)$-symmetry

$$\psi_{k\sigma} \to \psi_{k\sigma}\exp(i\alpha_\sigma), \tag{C.2}$$

$$\bar{\psi}_{k\sigma} \to \bar{\psi}_{k\sigma}\exp(-i\alpha_\sigma), \tag{C.3}$$

with phase factor α_σ for each spin configuration $\sigma = \uparrow, \downarrow$. After decoupling of the two-particle interaction by a Hubbard-Stratonovich transformation in the particle-particle

channel, we obtain the coupled fermion-boson theory, which is described by

$$S[\bar{\psi},\psi,\phi^*,\phi] = \int_{k\sigma} \bar{\psi}_{k\sigma}\left(ik_0 - \xi_{\mathbf{k}}\right)\psi_{k\sigma} - \int_q \frac{1}{U}\phi_q^*\phi_q + \int_{k,q}\left(\bar{\psi}_{-k+q\downarrow}\bar{\psi}_{k\uparrow}\phi_q + \psi_{k\uparrow}\psi_{-k+q\downarrow}\phi_q^*\right), \tag{C.4}$$

where ϕ_q and ϕ_q^* denote bosonic fields, which are conjugated to fermionic bilinears in the particle-particle channel. The $U(1)$-symmetry of the microscopic theory translates directly to transformations for the bosonic fields

$$\phi_q \to \phi_q \exp(i(\alpha_\uparrow + \alpha_\downarrow)), \tag{C.5}$$

$$\phi_q^* \to \phi_q^* \exp(-i(\alpha_\uparrow + \alpha_\downarrow)). \tag{C.6}$$

We introduce now the shorthand variables K and Q collecting fermion and bosonic frequency and momentum dependence, an index over conjugated fermionic and bosonic fields, and a spin index for fermionic fields. The fermionic and bosonic fields are then given by

$$(\psi_K) = \left(\psi_{k\uparrow}, \psi_{k\downarrow}, \bar{\psi}_{k\uparrow}, \bar{\psi}_{k\downarrow}\right), \qquad \phi_Q = (\phi_q, \phi_q^*) \tag{C.7}$$

and the corresponding external source fields are given by

$$(\eta_K) = \left(\eta_{k\uparrow}, \eta_{k\downarrow}, \bar{\eta}_{k\uparrow}, \bar{\eta}_{k\downarrow}\right), \qquad J_Q = (J_q, J_q^*). \tag{C.8}$$

The transformations for fermionic and bosonic fields then read

$$\psi_K \to \psi_K \exp(i\alpha_K^F), \tag{C.9}$$

$$\phi_Q \to \phi_Q \exp(i\alpha_Q^B), \tag{C.10}$$

with the phases

$$\alpha_K^F = \left(\alpha_\uparrow, \alpha_\downarrow, -\alpha_\uparrow, -\alpha_\downarrow\right), \quad \alpha_Q^B = \left(\alpha_\uparrow + \alpha_\downarrow, -(\alpha_\uparrow + \alpha_\downarrow)\right). \tag{C.11}$$

The partition function with external source fields is given by

$$Z[J_Q, \eta_K] = \int D\tilde{\psi} D\tilde{\phi} e^{-S[\tilde{\phi},\tilde{\psi}] - \Delta S[\tilde{\phi},\tilde{\psi}] + \int_Q J_Q \tilde{\phi}_Q + \int_K \eta_K \tilde{\psi}_K}. \tag{C.12}$$

$$\tag{C.13}$$

The invariance of the theory with respect to the $U(1)$-symmetry for fermionic and bosonic fields leads to

$$Z[J_Q, \eta_K] \overset{U(1)}{=} Z[J_Q e^{-i\alpha_Q^B}, \eta_K e^{-i\alpha_K^F}], \tag{C.14}$$

which implies transformation laws for the external source fields. In the next step we linearize the partition function to first order in the bosonic and fermionic phases α_Q^B and α_K^F. This yields

$$Z[J_Q e^{-i\alpha_Q^B}, \eta_K e^{-i\alpha_K^F}] = \int D\tilde{\psi} D\tilde{\phi} e^{-S[\tilde{\phi},\tilde{\psi}] - \Delta S[\tilde{\phi},\tilde{\psi}] + \int_Q J_Q e^{-i\alpha_Q^B} \tilde{\phi}_Q + \int_K \eta_K e^{-i\alpha_K^F} \tilde{\psi}_K} \tag{C.15}$$

$$\overset{lin}{=} Z[J_Q, \eta_K] + \mathcal{O}(\alpha_B^2, \alpha_F^2, \alpha_F \alpha_B) \tag{C.16}$$

$$- \int D\tilde{\psi} D\tilde{\phi} \Big(\int_Q \alpha_Q^B J_Q \tilde{\phi}_Q + \int_K \alpha_K^F \eta_K \tilde{\psi}_K \Big) \cdot e^{-S[\tilde{\phi},\tilde{\psi}] - \Delta S[\tilde{\phi},\tilde{\psi}] + \int_Q J_Q \tilde{\phi}_Q + \int_K \eta_K \tilde{\psi}_K}$$

$$= Z[J_Q, \eta_K] + \mathcal{O}(\alpha_B^2, \alpha_F^2, \alpha_F \alpha_B) - \Big(\int_Q \alpha_Q^B J_Q \frac{\delta}{\delta J_Q} + \int_K \alpha_K^F \eta_K \frac{\delta}{\eta_K} \Big) Z[J_Q, \eta_K] \tag{C.17}$$

Comparison of coefficients in the fermionic and bosonic phases of the same order yields

$$0 = \frac{1}{W} \left(\int_Q \alpha_Q^B J_Q \frac{\delta}{\delta J_Q} + \int_K \alpha_K^F \eta_K \frac{\delta}{\eta_K} \right) W[J_Q, \eta_K], \tag{C.18}$$

where the partition $Z[J, \eta] = \ln(W[J, \eta])$ was replaced by the generating functional for connected Green's functions $W[J, \eta]$. Next, we switch to the representation with average bosonic and fermionic fields by the Legendre transformations

$$\psi_K = \langle \tilde{\psi}_K \rangle = \frac{\delta W}{\delta \eta_K}, \quad \phi_Q = \langle \tilde{\phi}_Q \rangle = \frac{\delta W}{\delta J_Q}, \quad -\eta_K = \frac{\delta \Gamma}{\delta \psi_K}, \quad J_Q = \frac{\delta \Gamma}{\delta \phi_Q}, \tag{C.19}$$

where we use $W = W[J, \eta]$ and $\Gamma = \Gamma[\psi, \phi]$. We thus obtain

$$0 = \frac{1}{W} \left(\int_Q \alpha_Q^B \phi_Q \frac{\delta \Gamma}{\delta \phi_Q} + \int_K \alpha_K^F \psi_K \frac{\delta \Gamma}{\psi_K} \right). \tag{C.20}$$

Now, we write out the explicit spin dependence of the fermionic fields and distinguish

between conjugated bosonic and fermionic fields. The equation then reads

$$0 = \int_q (\alpha_\uparrow + \alpha_\downarrow)\phi_q \frac{\delta\Gamma}{\delta\phi_q} - \int_q (\alpha_\uparrow + \alpha_\downarrow)\phi_q^* \frac{\delta\Gamma}{\delta\phi_q^*} + \int_k \left(\alpha_\uparrow \psi_{k\uparrow} \frac{\delta\Gamma}{\delta\psi_{k\uparrow}} + \alpha_\downarrow \psi_{k\downarrow} \frac{\delta\Gamma}{\delta\psi_{k\downarrow}} - \alpha_\uparrow \bar{\psi}_{k\uparrow} \frac{\delta\Gamma}{\delta\bar{\psi}_{k\uparrow}} - \alpha_\downarrow \bar{\psi}_{k\downarrow} \frac{\delta\Gamma}{\delta\bar{\psi}_{k\downarrow}} \right). \tag{C.21}$$

In the case of charge conservation of each spin configuration separately, the above relation splits up into two equations

$$\int_q \left(-\phi_q \frac{\delta\Gamma}{\delta\phi_q} + \frac{\delta\Gamma}{\delta\phi_q^*}\phi_q^* \right) = \int_k \left(\psi_{k\uparrow} \frac{\delta\Gamma}{\delta\psi_{k\uparrow}} - \bar{\psi}_\uparrow \frac{\delta\Gamma}{\delta\bar{\psi}_{k\uparrow}} \right), \tag{C.22}$$

$$\int_q \left(-\phi_q \frac{\delta\Gamma}{\delta\phi_q} + \frac{\delta\Gamma}{\delta\phi_q^*}\phi_q^* \right) = \int_k \left(\psi_{k\downarrow} \frac{\delta\Gamma}{\delta\psi_{k\downarrow}} - \bar{\psi}_\downarrow \frac{\delta\Gamma}{\delta\bar{\psi}_{k\downarrow}} \right), \tag{C.23}$$

for the spin up phase $\alpha_\uparrow$ and spin down phase $\alpha_\downarrow$.[1] In the case of total charge conservation, both equations can be subsumed to

$$2\int_q \left(-\phi_q \frac{\delta\Gamma}{\delta\phi_q} + \frac{\delta\Gamma}{\delta\phi_q^*}\phi_q^* \right) = \int_{k\sigma} \left(\psi_{k\sigma} \frac{\delta\Gamma}{\delta\psi_{k\sigma}} - \bar{\psi}_{k\sigma} \frac{\delta\Gamma}{\delta\bar{\psi}_{k\sigma}} \right). \tag{C.24}$$

C.2 Ward identities in the symmetry-broken phase

In this section, we derive the explicit Ward identity between the fermionic gap, bosonic order parameter and the transverse Yukawa vertex. Furthermore, we present another identity between transverse and longitudinal Yukawa vertices and the two-boson-two-fermion vertex. The starting point is given by Eq. (C.24)

Differentiation with respect to fermionic fields $\frac{\delta^2}{\delta\bar{\psi}_{y\downarrow}\delta\bar{\psi}_{x\uparrow}}$ and $\frac{\delta^2}{\delta\psi_{y\downarrow}\delta\psi_{x\uparrow}}$ leads to the relations

$$-\frac{\delta^2\Gamma}{\delta\bar{\psi}_{y\downarrow}\delta\bar{\psi}_{x\uparrow}} = -\int_q \phi_q \frac{\delta^3\Gamma}{\delta\bar{\psi}_{y\downarrow}\delta\bar{\psi}_{x\uparrow}\delta\phi_q} + \int_q \phi_q^* \frac{\delta^3\Gamma}{\delta\bar{\psi}_{y\downarrow}\delta\bar{\psi}_{x\uparrow}\delta\phi_q^*}, \tag{C.25}$$

$$-\frac{\delta^2\Gamma}{\delta\psi_{x\uparrow}\delta\psi_{y\downarrow}} = -\int_q \phi_q \frac{\delta^3\Gamma}{\delta\psi_{y\downarrow}\delta\psi_{x\uparrow}\delta\phi_q} + \int_q \phi_q^* \frac{\delta^3\Gamma}{\delta\psi_{y\downarrow}\delta\psi_{x\uparrow}\delta\phi_q^*}, \tag{C.26}$$

between gap and Yukawa vertices at vanishing fermionic fields $\psi = 0$. We will now insert

[1] This result is identical to the result obtained by Kopietz et al. (2010).

the explicit ansatz for the anomalous quadratic fermionic part of the action

$$\Gamma_{\psi\psi} = \int_k \Big(\Delta \bar{\psi}_{k\downarrow} \bar{\psi}_{-k\uparrow} + \Delta^* \psi_{k\uparrow} \psi_{-k\downarrow} \Big), \tag{C.27}$$

and the ansatz for the Yukawa vertices in the particle representation

$$\begin{aligned} \Gamma_{\psi^2\phi^* + \psi^2\phi} = g \int_{k,q} \big(\bar{\psi}_{-k+q\downarrow} \bar{\psi}_{k\uparrow} (\phi_q - \alpha \delta_{q,0}) + \psi_{k\uparrow} \psi_{-k+q\downarrow} (\phi_q^* - \alpha^* \delta_{q,0}) \big) \\ + \tilde{g} \int_{k,q} \big(\bar{\psi}_{-k+q\downarrow} \bar{\psi}_{k\uparrow} (\phi_{-q}^* - \alpha^* \delta_{q,0}) + \psi_{k\uparrow} \psi_{-k+q\downarrow} (\phi_{-q} - \alpha \delta_{q,0}) \big) . \end{aligned} \tag{C.28}$$

The relations $g + \tilde{g} = g_\sigma$ and $g - \tilde{g} = g_\pi$ connect the couplings for the normal and anomalous Yukawa vertices with the couplings for the longitudinal and transverse Yukawa vertices. Bosonic fluctuations are decomposed into transverse and longitudinal direction $\phi_q = \alpha \delta_{q,0} + \sigma_q + i\pi_q$ and $\phi_q^* = \alpha \delta_{q,0} + \sigma_{-q} - i\pi_{-q}$. Inserting the ansätze Eq. (C.27) and Eq. (C.28) into Eq. (C.25) and (C.26) and setting $y = -x = -p$, we obtain the relations

$$\Delta = \alpha g - \alpha^* \tilde{g}, \tag{C.29}$$

$$\Delta^* = g\alpha^* - \tilde{g}\alpha. \tag{C.30}$$

reflecting the underlying Ward identities within our ansatz for the effective action. In the case of a real-valued gap $\Delta = \Delta^*$ and order parameter $\alpha = \alpha^*$, these equations reduce to

$$\Delta = \alpha g_\pi, \tag{C.31}$$

connecting the fermionic single-particle gap and the bosonic order parameter via the transverse Yukawa coupling.

Next, we determine Ward identities between the anomalous and normal Yukawa coupling and the two-boson-two-fermion vertex. Differentiation with respect to fermionic fields $\frac{\delta^2}{\delta\psi_{x\uparrow}\delta\psi_{y\downarrow}}$ and bosonic field $\frac{\delta}{\delta\phi_a}$ and $\frac{\delta}{\delta\phi_a^*}$, respectively, yields

$$\int_q \phi_q \frac{\delta^4\Gamma}{\delta\phi_a^*\delta\psi_{x\uparrow}\delta\psi_{y\downarrow}\delta\phi_q} = \int_q \phi_q^* \frac{\delta^4\Gamma}{\delta\phi_a^*\delta\psi_{x\uparrow}\delta\psi_{y\downarrow}\delta\phi_q^*}, \tag{C.32}$$

$$-2\frac{\delta^3\Gamma}{\delta\phi_a\delta\psi_{y\downarrow}\delta\psi_{x\uparrow}} = -\int_q \phi_q \frac{\delta^4\Gamma}{\delta\phi_a\delta\psi_{x\uparrow}\delta\psi_{y\downarrow}\delta\phi_q} + \int_q \phi_q^* \frac{\delta^4\Gamma}{\delta\phi_a\delta\psi_{x\uparrow}\delta\psi_{y\downarrow}\delta\phi_q^*}, \tag{C.33}$$

and differentiation with respect to $\frac{\delta^2}{\delta\bar{\psi}_{x\uparrow}\delta\bar{\psi}_{y\downarrow}}$, and $\frac{\delta}{\delta\phi_a}$ and $\frac{\delta}{\delta\phi_a^*}$ yields

$$\int_q \phi_q \frac{\delta^4\Gamma}{\delta\phi_a\delta\bar{\psi}_{x\uparrow}\delta\bar{\psi}_{y\downarrow}\delta\phi_q} = \int_q \phi_q^* \frac{\delta^4\Gamma}{\delta\phi_a\delta\bar{\psi}_{x\uparrow}\delta\bar{\psi}_{y\downarrow}\delta\phi_q^*}, \tag{C.34}$$

$$-2\frac{\delta^3\Gamma}{\delta\phi_a^*\delta\bar{\psi}_{y\downarrow}\delta\bar{\psi}_{x\uparrow}} = \int_q \phi_q \frac{\delta^4\Gamma}{\delta\phi_a^*\delta\bar{\psi}_{x\uparrow}\delta\bar{\psi}_{y\downarrow}\delta\phi_q} - \int_q \phi_q^* \frac{\delta^4\Gamma}{\delta\phi_a^*\delta\bar{\psi}_{x\uparrow}\delta\bar{\psi}_{y\downarrow}\delta\phi_q^*}. \tag{C.35}$$

Setting the external fermionic frequencies and momenta to $y = -x = p$ and the external bosonic frequencies and momenta to $a = 0$, we obtain

$$\phi_0 \frac{\delta^4\Gamma}{\delta\phi_0^*\delta\psi_{-p\uparrow}\delta\psi_{p\downarrow}\delta\phi_0} = \phi_0^* \frac{\delta^4\Gamma}{\delta\phi_0^*\delta\psi_{-p\uparrow}\delta\psi_{p\downarrow}\delta\phi_0^*}, \tag{C.36}$$

$$-2\frac{\delta^3\Gamma}{\delta\phi_0\delta\psi_{p\downarrow}\delta\psi_{-p\uparrow}} = -\phi_0 \frac{\delta^4\Gamma}{\delta\phi_0\delta\psi_{-p\uparrow}\delta\psi_{p\downarrow}\delta\phi_0} + \phi_0^* \frac{\delta^4\Gamma}{\delta\phi_0\delta\psi_{-p\uparrow}\delta\psi_{p\downarrow}\delta\phi_0^*}, \tag{C.37}$$

$$\phi_0 \frac{\delta^4\Gamma}{\delta\phi_0\delta\bar{\psi}_{-p\uparrow}\delta\bar{\psi}_{p\downarrow}\delta\phi_0} = \phi_0^* \frac{\delta^4\Gamma}{\delta\phi_0\delta\bar{\psi}_{-p\uparrow}\delta\bar{\psi}_{p\downarrow}\delta\phi_0^*}, \tag{C.38}$$

$$-2\frac{\delta^3\Gamma}{\delta\phi_0^*\delta\bar{\psi}_{p\downarrow}\delta\bar{\psi}_{-p\uparrow}} = \phi_0 \frac{\delta^4\Gamma}{\delta\phi_0^*\delta\bar{\psi}_{-p\uparrow}\delta\bar{\psi}_{p\downarrow}\delta\phi_0} - \phi_0^* \frac{\delta^4\Gamma}{\delta\phi_0^*\delta\bar{\psi}_{-p\uparrow}\delta\bar{\psi}_{p\downarrow}\delta\phi_0^*}, \tag{C.39}$$

due to momentum and and energy conservation at each vertex. In the case of a real gap $\Delta = \Delta^*$ and order parameter $\alpha = \alpha^*$ these equations reduce to

$$\alpha \frac{\delta^4\Gamma}{\delta\phi_0^*\delta\psi_{-p\uparrow}\delta\psi_{p\downarrow}\delta\phi_0} = \alpha \frac{\delta^4\Gamma}{\delta\phi_0^*\delta\psi_{-p\uparrow}\delta\psi_{p\downarrow}\delta\phi_0^*} \tag{C.40}$$

$$-2\frac{\delta^3\Gamma}{\delta\phi_0\delta\psi_{p\downarrow}\delta\psi_{-p\uparrow}} = -\alpha \frac{\delta^4\Gamma}{\delta\phi_0^2\delta\psi_{-p\uparrow}\delta\psi_{p\downarrow}} + \alpha \frac{\delta^4\Gamma}{\delta\phi_0\delta\psi_{-p\uparrow}\delta\psi_{p\downarrow}\delta\phi_0^*} \tag{C.41}$$

and the corresponding complex conjugated equations. As an example, we now assume a local ansatz for the two-boson-two-fermion vertex of the form

$$\Gamma_{\psi^2\phi^2} = \int_{k,k',q} \lambda\psi_{k\downarrow}\psi_{k'\uparrow}\phi_{-k-q}\phi_{-k'+q} + \int_{k,k',q} \lambda\bar{\psi}_{k'\uparrow}\bar{\psi}_{k\downarrow}\phi^*_{-k-q}\phi^*_{-k'+q} \tag{C.42}$$

consistent with the identities Eq. (C.36)-(C.39), and obtain then

$$2\tilde{g} = g_\sigma - g_\pi = \alpha\lambda. \tag{C.43}$$

This identity connects the anomalous Yukawa vertex, which is given by the difference of transverse and longitudinal Yukawa vertices, with the couplings parametrizing the two-boson-two-fermion vertex. In absence of a two-boson-two-fermion vertex, $\Gamma_{\psi^2\phi^2} = 0$, the

Ward identity Eq. (C.41) implies

$$2\tilde{g} = 0 \quad \Rightarrow \quad g_\sigma = g_\pi. \tag{C.44}$$

In that case the couplings parametrizing the transverse and longitudinal Yukawa vertices are enforced to be identical. Higher order Ward identities can be derived in a similar way.

Deutsche Zusammenfassung

In dieser Promotionsschrift werden moderne Renormierungsgruppenstrategien angewandt, um Fluktuationseffekte des Ordnungsparameters in wechselwirkenden fermionischen Systemen zu studieren. Es werden zwei Systeme untersucht, die in einem gewissen Parameterbereich Suprafluidiät zeigen. Im ersten Projekt wird ein Quantenphasenübergang zwischen Halbmetall und Supraflüssigkeit untersucht, in dem masselose kritische Fluktuationen das Geschehen am quantenkritischen Punkt bestimmen. Im zweiten Projekt wird der Grundzustand einer fermionischen Supraflüssigkeit untersucht, in dem masselose Goldstone-Fluktuationen einen dramatischen Einfluss auf das Verhalten des Systems haben. Um das vielfältige Wechselspiel zwischen Fermionen und Ordnungsparameterfluktuationen zu untersuchen, werden durch eine Hubbard-Stratonovich-Transformation bosonische Felder zur adäquaten Beschreibung der Ordnungsparameterfluktuationen eingeführt. Die gekoppelte fermionisch-bosonische Theorie wird mit Hilfe der funktionalen Renormierungsgruppenmethode untersucht.

Die Arbeit besteht aus fünf Hauptkapiteln und beginnt in Kapitel 1 mit der Einleitung, welche einen kurzen historischen Abriss über die Renormierungsgruppe (RG) gibt. Anschließend werden die zwei Forschungsprojekte eingeführt. In Kapitel 2 wird die funktionale Renormierungsgruppe diskutiert und die Flussgleichung für die skalenabhängige effektive Wirkung abgeleitet. Die nachfolgenden Kapitel 3 und 4 bilden den zentralen Kern dieser Arbeit. Dort werden die beiden Forschungsprojekte, sowie deren Resultate im Detail vorgestellt. In Kapitel 5 werden die zentralen Ergebnisse beider Projekte zusammengefasst. Außerdem wird ein Ausblick auf zukünftige mögliche Forschungsvorhaben gegeben. In den Anhängen A und B werden die expliziten Flussgleichungen für die Kopplungskonstanten, welche den Ansatz für die effektive Wirkung in der symmetrischen

und symmetriegebrochenen Phase parametrisieren, abgeleitet. Schließlich werden in Anhang C Ward-Identitäten für gemischte fermionisch-bosonische Systeme, die eine $U(1)$-Symmetrie besitzen, abgeleitet. Im Folgenden wird die Renormierungsgruppenmethode knapp skizziert. Anschliessend werden die beide Forschungsthemen im Einzelnen präsentiert.

Die funktionale Renormierungsgruppe ist eine Weiterentwicklung der Wilsonschen RG und ist ein ideales Werkzeug zur Analyse von Fluktuationseffekten in wechselwirkenden Fermi-Systemen (vgl. Review von Metzner et al. (2012)). Das Herzstück der funktionalen RG bildet eine exakte Flussgleichung für die skalenabhängige effektive Wirkung, welche die mikroskopische Wirkung und die volle effektive Wirkung durch einen Renormierungsgruppenfluss verknüpft. Die volle effektive Wirkung entspricht dem generierenden Funktional für einteilchenirreduzibele Vertexfunktionen. Aus ihr lassen sich sowohl beliebige Korrelationsfunktionen, als auch die Thermodynamik des Systems ableiten. Die Skalenabhängigkeit der effektiven Wirkung wird durch eine Regulatorfunktion implementiert. Bei endlichen Skalen unterdrückt der Regulator niederenergetische Moden in der Theorie und führt zu einer Regularisierung singulärer Terme. Im Infrarotlimes des Renormierungsgruppenflusses wird der Regulator vollständig entfernt, und man erhält die volle effektive Wirkung.

Im ersten Projekt wurde ein Quantenphasenübergang zwischen einem Halbmetall und einer Supraflüssigkeit untersucht. Beide Phasen sind durch einen quantenkritischen Punkt getrennt. Die Dispersion der Halbmetallphase ist durch einen Dirac-Kegel gegeben, dessen Fermi-Fläche bei entsprechender Wahl des chemischen Potentials aus nur einem einzigen Punkt besteht. Das System wurde ursprünglich von Strack et al. (2010) eingeführt, um Nicht-Fermi-Flüssigkeitsverhalten und Nicht-Gaußsches-Verhalten an einem quantenkritischen Punkt anhand eines simplen Modellsystems zu studieren. In der damaligen Arbeit wurde das kritische Verhalten des Systems am und in der Nähe des quantenkritischen Punktes am absoluten Nullpunkt untersucht. Die Beschreibung erfolgte im Rahmen einer gekoppelten fermionisch-bosonischen Theorie, die mit der funktionalen Renormierungsgruppe untersucht wurde. Dazu wurde ein Ansatz für die skalenabhängige effektive Wirkung in Feld- und Gradientenentwicklung verwendet. Die Frequenz- und Impulsabhängigkeit der fermionischen und bosonischen Selbstenergie wurde mit identischen Renormierungsfaktoren vereinfacht beschrieben. Der fermionische Renormierungsfaktor charakterisiert dabei das Verhalten der Quasiteilchen am quantenkritischen Punkt. Fermionen und bosonische Fluktuationen sind über einen Yukawa-Vertex verknüpft. Die Kopplungskonstante für den Yukawa-Vertex ist zu Beginn des Flusses eins und erfährt keine Renormierung. Innerhalb dieser Trunkierung wurde ein Nicht-Fermi-Flüssigkeitsver-

halten, insbesondere ein verschwindendes Quasiteilchen-Gewicht, sowie ein Nicht-Gaussches-Verhalten der Ordnungsparameterfluktuationen gefunden. Die Fermi-Geschwindigkeit blieb unverändert während der Renormierungsprozedur. Am absoluten Nullpunkt zeigte die Paarsuszeptibilität ein Potenzgesetz-Verhalten mit kritischem Exponenten in der Nähe des quantenkritischen Punktes. Der kritische Exponent der Korrelationslänge wurde indirekt durch eine Skalenrelation bestimmt.

Diese Resultate warfen folgende neue Fragen und Problemstellungen auf und inspirierten weitere Forschungstätigkeiten über das Dirac-Cone-Modell:

- Bleibt die Fermi-Geschwindigkeit auch in einem verfeinerten Ansatz für die fermionische Selbstenergie unverändert?
- Lässt sich der kritische Exponent der Korrelationslänge am absoluten Nullpunkt ebenfalls wie der kritische Exponent der Suszeptibilität direkt aus dem RG-Fluss bestimmen?
- Wie verhalten sich Suszeptibilität, Korrelationslänge und die verschiedenen Renormierungsfaktoren der fermionischen und bosonischen Selbstenergie im endlichen Temperaturbereich oberhalb des quantenkritischen Punktes?
- Sind die kritischen Exponenten und anomalen Dimensionen über Skalenrelationen miteinander verknüpft?

Ausgehend von diesen Fragestellungen wurde in der vorliegenden Arbeit die Renormierung des Dirac-Cone-Modells in verschiedene Richtungen erweitert. Dazu wurde die Trunkierung der effektiven Wirkung verbessert. Für die Frequenz- und Impulsabhängigkeit von fermionischer und bosonischer Selbstenergie wurden unterschiedliche Renormierungsfaktoren verwendet. Außerdem wurde ein endlicher und von Hand eingestellter Masseterm zur mikroskopischen Wirkung hinzugefügt. Dieser verhindert das Auftreten einer Bandlücke, welche ansonsten durch die fermionische Wechselwirkung generiert würde. Die Methode der Gegenterme garantiert dann einen masselosen Dirac-Kegel in der Halbmetallphase. Das Verhalten des RG-Flusses wurde innerhalb dieser verbesserten Trunkierung nicht nur am absoluten Nullpunkt in der Halbmetallphase und am quantenkritischen Punkt untersucht, sondern auch im endlichen Temperaturbereich oberhalb des quantenkritischen Punktes.

Im Folgenden werden wir nun die zentralen Ergebnisse unserer Renormierungsgruppenanalyse zusammengefasst darlegen. Am kritischen Punkt divergieren Korrelationslänge, Korrelationszeit und die Paarsuszeptibilität. Die Renormierungsfaktoren für die

Frequenzabhängigkeit der fermionischen Selbstenergie, sowie die Renormierungsfaktoren für die Frequenz- und Impulsabhängigkeit der bosonischen Selbstenergie sind ebenfalls divergent und zeigen dort ein Potenzgesetz-Verhalten in der Abschneideskala des Regulators, was dem Auftreten von anomalen fermionischen und bosonischen Dimensionen entspricht. Dies impliziert ein Nicht-Fermi-Flüssigkeitsverhalten, insbesondere ein Verschwinden des Quasiteilchen-Gewichts, sowie ein Nicht-Gaußsches-Verhalten der Ordnungsparameterfluktuationen. Überraschenderweise renormiert die Impulsabhängigkeit der fermionischen Selbstenergie nicht. Zusammen mit der Divergenz der Frequenzabhängigkeit der fermionischen Selbstenergie führt dies zu einer verschwindenden Fermi-Geschwindigkeit am kritischen Punkt.

Die Paarsuszeptibilität zeigt in der Halbmetallphase am absoluten Nullpunkt ein Potenzgesetz-Verhalten mit kritischen Exponenten. Für die Korrelationslänge und Korrelationszeit wurde wider Erwarten kein solches Potenzgesetz-Verhalten am absoluten Nullpunkt gefunden. Stattdessen implizierte unsere RG-Analyse eine unendliche Korrelationslänge und Korrelationszeit in der gesamten Halbmetallphase auch abseits des quantenkritischen Punktes. Dies konnte durch eine Analyse des fermionischen Teilchen-Teilchen-Diagramms, das eine nicht-analytische Frequenz- und Impulsabhängigkeit zeigt, bestätigt werden. Diese Nicht-Analytizitäten führen im Realraum und in der Realzeit zu einem Abfall von räumlichen und zeitlichen Korrelationen in Form von Potenzgesetzen, was unser RG-Ergebnis bestätigte.

Im endlichen Temperaturbereich oberhalb des quantenkritischen Punktes zeigte sich, dass sowohl die Korrelationslänge als auch die Paarsuszeptibilität in der Nähe des kritischen Punktes einem Potenzgesetz als Funktion der Temperatur gehorchen. Die dazugehörigen kritischen Exponenten konnten numerisch bestimmt werden. Es stellte sich heraus, dass die kritischen Exponenten und die anomalen Dimensionen mehrere Skalengesetze erfüllen. Die zentralen Resultate lassen sich in Form einer Liste zusammenfassen:

- RG-Studie über einen Quantenphasenübergang zwischen Halbmetall und Supraflüssigkeit
- Nicht-Fermi-Flüssigkeitsverhalten sowie Nicht-Gaußsches-Verhalten am quantenkritischen Punkt
- Verschwindende Fermi-Geschwindigkeit und verschwindendes Quasiteilchen-Gewicht am quantenkritischen Punkt
- Potenzgesetz-Verhalten mit kritischen Exponenten in der Nähe des kritischen Punktes für verschiedene Größen am absoluten Nullpunkt sowie bei endlichen Tempera-

turen.

- Divergente Korrelationslänge im Grundzustand in der gesamten Halbmetallphase auch abseits des quantenkritischen Punktes

Das zweite Projekt dieser Dissertation beschäftigte sich mit dem Grundzustand von fermionischen Supraflüssigkeiten. Dabei sollte das Wechselspiel zwischen Fermionen und bosonischen Ordnungsparameterfluktuationen untersucht werden. Aufgrund der spontanen Symmetriebrechung der kontinuierlichen U(1)-Symmetrie treten masselose kollektive Anregungen, die Goldstone-Bosonen, auf. Diese Goldstonefluktuationen verursachen Divergenzen innerhalb der Theorie und machen eine Renormierungsgruppenanalyse notwendig. Wie oben angedeutet, wird in dieser Arbeit der Grundzustand einer fermionischen Supraflüssigkeit analysiert. Mittlerweile lassen sich solche Supraflüssigkeiten in optischen Gittern mit ultrakalten Atomen experimentell realisieren (vgl. Review von Bloch et al. (2008)). Im Rahmen der funktionalen Renormierungsgruppe wurden schon mehrere Studien zu fermionischen Supraflüssigkeiten unternommen. Innerhalb einer rein fermionischen funktionalen RG-Studie untersuchten Gersch et al. (2005) und Eberlein und Metzner (2013) das attraktive Hubbard-Modell, welches häufig als Prototyp-Modell für fermionische Supraflüssigkeiten verwendet wird. Dabei konnten quantitative Ergebnisse für die fermionische Energielücke erzielt werden, die gut mit Werten aus der Literatur übereinstimmen. Es zeigte sich jedoch, dass Ordnungsparameterfluktuationen nur teilweise innerhalb der Ein-Loop-Näherung berücksichtigt sind und wichtige Beiträge fehlen, die für das korrekte Infrarot-Verhalten notwendig sind. Eine andere Möglichkeit, das Wechselspiel zwischen Fermionen und Ordnungsparameterfluktuationen zu studieren, ist durch die Analyse einer gekoppelten fermionisch-bosonischen Theorie mit Renormierungsgruppen-Techniken gegeben. Birse et al. (2005) untersuchte als erster den BEC-BCS-Crossover in einer einfachen Trunkierung. Weitere Trunkierungen des funktionalen RG-Flusses zu fermionischen Supraflüssigkeiten folgten von Krippa (2007) und Diehl et al. (2007). Bartosch et al. (2010) studierte eine Kombination von Schwinger-Dyson-Gleichungen und der funktionalen Renormierungsgruppe. In dieser Arbeit wurden die fermionische Energielücke und der bosonische Ordnungsparameter unterschieden.

Dieselbe Unterscheidung zwischen Energielücke und Ordnungsparameter wurde bereits zwei Jahre früher von Strack et al. (2008) in einer gemischten fermionisch-bosonischen funktionalen RG-Studie vorgenommen. Zusätzlich wurden in dieser Arbeit die Ordnungsparameterfluktuationen in transversale und longitudinale Fluktuationsbeiträge aufgespalten. Es konnte gezeigt werden, dass die transversalen Goldstonefluktuationen zu Singularitäten in den longitudinalen Freiheitsgraden führen, die zur erwarteten Infrarot-

Asymptotik der longitudinalen kollektiven Anregungen führt. In dieser Trunkierung wurden jedoch die Tatsache, dass die Goldstone-Masse verschwindet, sowie ein endliches Quasiteilchen-Gewicht der Goldstone-Bosonen von Hand implementiert. Außerdem wurde hier eine lineare Frequenzabhängigkeit in der bosonischen Selbstenergie vernachlässigt, welche einen Mischterm zwischen longitudinalen und transversalen Ordnungsparameterfluktuationen verursacht. Weiter wurde nur eine lokale bosonische Selbstwechselwirkung behandelt. Somit wurden neue Fragestellungen aufgeworfen, die zu weiterführenden Untersuchungen animieren:

- Gibt es eine einfache Verbindung zwischen fermionischer Energielücke und bosonischem Ordnungsparameter?
- Wie beeinflusst das Mischen von transversalen und longitudinalen Moden das Verhalten des Renormierungsgruppenflusses?
- Beschreibt eine lokale bosonische Selbstwechselwirkung das Verhalten des Systems adäquat?
- Was lässt sich allgemein über die Erfüllung von Ward-Identitäten aussagen?
- Wie sieht eine konsistente Trunkierung der fermionisch-bosonischen Flussgleichungen aus, welche die korrekte Infrarot-Asymptotik des Systems wiedergibt?

Diese Fragen und Problemstellungen wurden durch das zweite Forschungsprojekt dieser Dissertation geklärt. Dazu wurde die Trunkierung von Strack et al. in mehrere Richtungen erweitert. Zusätzlich zur früheren Trunkierung wurde ein linearer Frequenzterm eingeführt, der zu einer Mischung zwischen transversalen und longitudinalen Ordnungsparameterfluktuationen führt. Außerdem wurde eine nicht-lokale bosonische Selbstwechselwirkung eingeführt (Y-Term).

Die Resultate von Strack et al. bezüglich des Infrarot-Verhaltens der longitudinalen Moden bzw. der fermionischen Energielücke und Ordnungsparameters konnten sowohl innerhalb einer analytischen als auch numerischen Analyse bestätigt werden. In zwei Dimensionen verschwindet die longitudinale Masse und damit auch die lokale bosonische Wechselwirkung linear mit der Abschneideskala. Der Renormierungsfaktor, welcher die Frequenz und Impulsabhängigkeit der longitudinalen Fluktuationen parametrisiert, divergiert wie die inverse Abschneideskala. Dieses Verhalten ist konsistent mit dem Verhalten eines wechselwirkenden Bosegases (Castellani et al. (1997) und Pistolesi et al. (2004)). Sowohl der Fluss des bosonischen Ordnungsparameters als auch die fermionische Energielücke sättigen, wobei der Ordnungsparameter einen kleineren Wert annimmt

als die Energielücke. Der lineare Frequenzterm verschwindet linear mit der Skala und die Mischung zwischen longitudinalen und transversalen Moden führt zu keiner qualitativen Änderung der Infrarot-Asymptotik. Innerhalb unserer Trunkierung konnten wir zeigen, dass der Y-Term entscheidend ist um die ursprüngliche U(1)-Symmetrie des Modells zu erhalten, wenn zwischen longitudinalen und transversalen Fluktuationen in der symmetriegebrochenen Phase unterschieden wird.

Wir konnten zeigen, dass bosonische Ward-Identitäten in unserer Trunkierung erfüllt sind. Die bosonische Ward-Identität verknüpft dabei die transversale und longitudinale Selbstenergie mit der nicht-lokalen bosonischen Wechselwirkung. Außerdem wurden zwei weitere gemischte Ward-Identitäten abgeleitet, welche fermionische und bosonische Korrelationsfunktionen verknüpfen. Zum einen fanden wir eine Identität, die den bosonischen Ordnungsparameter mit der fermionischen Energielücke über den transversalen Yukawa-Vertex verbindet. Wir konnten explizit zeigen, dass diese Identität konsistent ist mit den expliziten Flussgleichungen. Zum anderen wurde eine Identität gefunden, welche den Zwei-Boson-Zwei-Fermion-Vertex mit dem transversalen und longitudinalen Yukawa-Vertex verbindet. Ein verschwindender Zwei-Boson-Zwei-Fermion-Vertex, wie in unserem Falle, erzwingt dann eine identische Kopplungskonstante zwischen transversalem und longitudinalem Yukawa-Vertex.

Die Auswirkung der Ward-Identitäten wird vor allem im Verhalten der Asymptotik der Goldstone-Bosonen sichtbar. Wir konnten explizit zeigen, dass die bosonische Ward-Identität zur gegenseitigen Aufhebung von bosonischen Fluktuationsbeiträgen zur Goldstone-Masse führt. Der Y-Term spielte dabei eine entscheidende Rolle. Durch Anwendung der fermionischen Ward-Identitäten konnte auch gezeigt werden, dass sich fermionische Beiträge zur Goldstone-Masse gegenseitig wegheben, und dass das Goldstonetheorem innerhalb unserer Trunkierung erfüllt ist. Bezüglich der Infrarot-Asymptotik des transversalen Quasiteilchen-Gewichtes konnte analytisch sowie numerisch gezeigt werden, dass sich zwei singuläre Beiträge gegenseitig wegheben. Auch hier spielte der Y-Term eine entscheidende Rolle.

Demnach konnten wir zeigen, dass innerhalb unserer Trunkierung der RG-Flussgleichung sowohl die longitudinale Mode als auch die Goldstone-Mode konsistent behandelt werden. In dieser Arbeit wurde zum ersten Mal die fermionisch-bosonische Theorie des Grundzustandes der fermionischen Supraflüssigkeit konsistent in einer Trunkierung behandelt und analysiert. Die Arbeit kann als Richtlinie für zukünftige Arbeiten dienen, bei denen innerhalb einer Trunkierung des fermionisch-bosonischen Flusses auch Ward-Identitäten erfüllt sein sollen. Wir fassen die zentralen Ergebnisse des zweiten Projekts in Form einer kompakten Auflistung zusammen:

- RG-Studie von Fluktuationen im Grundzustand fermionischer Supraflüssigkeiten
- Unterscheidung von bosonischem Ordnungsparameter und fermionischer Energielücke
- Unterscheidung transversaler und longitudinaler Ordnungsparameterfluktuationen
- Berücksichtigung einer nicht-lokalen bosonischen Wechselwirkung
- Berücksichtigung der Mischung zwischen transversalen und longitudinalen bosonischen Fluktuationen
- Nachweis, dass sich kollektive Moden wie ein wechselwirkendes Bosegas verhalten
- Erfüllung von Ward-Identitäten
- Konsistente Beschreibung masseloser Goldstone-Moden innerhalb der Trunkierung

Curriculum vitae

Personal Data

Name	Benjamin Obert
Date of birth	16.02.1984
Place of birth	Bad Saulgau, Germany
Nationality	German

Education

1990-1994	Primary School: Grundschule Marbach, Herbertingen-Marbach
1994-2003	Störck-Gymnasium, Bad Saulgau
2003	Abitur

University education

2003-2009	Study of Physics, Universität Ulm
2008-2009	Diploma thesis under supervision of Prof. Dr. J. Ankerhold *"Superconducting atomic and molecular point contacts"*
2009	Diploma in physics
2009-2014	Doctoral thesis under supervision of Prof. Dr. W. Metzner, Max-Planck-Institut Stuttgart *"Renormalization group analysis of order parameter fluctuations in fermionic superfluids"*

Acknowledgements

Here, I would like to thank all the people who were involved in the preparation and realization of the thesis in this form: First of all I thank Prof. Metzner for giving me the opportunity to be part of his working group at the Max Planck institute in Stuttgart. The challenging projects and his excellent supervision together with his profound knowledge gave me the chance to deepen my knowledge in modern renormalization group techniques and condensed matter theory. During my time in Stuttgart he sharpened my approach towards challenging problems and scientific work and served as a role model of an excellent scientific researcher. For co-examining this thesis, I want to thank Prof. Muramatsu. I also thank Gernot Stollhoff for being a part of my PhD committee. For huge support through administrative issues I thank Jeanette Schüller-Knapp. I am especially grateful towards my former collaborators So Takei and Christoph Husemann, who both inspired me and were always timely available for discussions concerning details about my scientific work. For reading parts of the thesis and giving me useful comments I thank Tobias Holder, Andreas Eberlein, Nils Hasselmann and Tobias Denig. I also thank Pawel Jakubczyk, Philipp Strack, Hiroyuki Yamase, Peter Horsch, Roland Zeyher, Dirk Manske and Andreas Schnyder for additional comments and discussions concerning parts of the thesis. I would also like to thank all the people I met at the campus in Büsnau and downtown in Stuttgart for their friendship, thus facilitating a great time during my stay. Finally, I thank my parents and my sister for their constant, huge support throughout my PhD.

Bibliography

[1] Abanov, A. and A.V. Chubukov, *Spin-fermion model near the quantum critical point: One-loop renormalization group results* , Phys. Rev. Lett. **84**, 5608 (2000).

[2] Abanov, A., A.V. Chubukov and J. Schmalian, *Quantum-critical theory of the spin fermion model and its application to cuprates normal state analysis*, Adv. in Phys. **52**, 119 (2003).

[3] Abanov, A. and A.V. Chubukov, *Anomalous scaling at the quantum critical point in itinerant antiferromagnets*, Phys. Rev. Lett **93**, 255702 (2004).

[4] Altland, A. and B. D. Simons, *Condensed Matter Field Theory*, (Cambridge University Press, UK, 2010).

[5] Altshuler, B. L., L. B. Ioffe and A. J. Millis, *Low energy properties of fermions with singular interactions* Phys. Rev. B **50**, 14048 (1994).

[6] Altshuler, B. L., L. B. Ioffe and A. J. Millis, *Critical behavior of the $T = 0$ $2k_f$ density-wave phase transition in a two-dimensional Fermi liquid*, Phys. Rev. B **52**, 5563 (1995).

[7] Amit, D. J., *Field Theory: The Renormalization Group and Critical Phenomena*, (World Scientific, 1984).

[8] Anderson, P. W., *Random-phase approximation in the theory of superconductivity*, Phys. Rev. **112**, 1900 (1958).

[9] Anderson, P. W., *Plasmons, gauge invariance, and mass* Phys. Rev. **130**, 439 (1963).

[10] Baier, T., E. Bick and C. Wetterich, *Temperature dependence of antiferromagnetic order in the Hubbard model*, Phys. Rev. B **70**, 125111 (2004).

[11] Bartosch L., P. Kopietz and A. Ferraz, *Renormalization of the BCS-BEC crossover by order parameter fluctuations*, Phys. Rev. B **80**, 104514 (2009).

[12] Belitz, D., T.R. Kirkpatrick, M.T. Mercaldo and S.L. Sessions, *Local field theory for disordered itinerant quantum ferromagnets: logarithmic corrections to scaling*, Phys. Rev. B **63**, 174427 (2001a).

[13] Belitz, D., T.R. Kirkpatrick, M.T. Mercaldo and S.L. Sessions, *Quantum critical behaviour in disordered itinerant ferromagnets: Logarithmic corrections to scaling*, Phys. Rev. B **63**, 174428, (2001b).

[14] Belitz, D., T.R. Kirkpatrick and T. Vojta, *How generic scale invariance influences quantum and classical phase transitions*, Rev. Mod. Phys. **77**, 579 (2005).

[15] Berges, J., N. Tetradis and C. Wetterich, *Non-perturbative renormalization flow in quantum field theory and statistical physics*, Phys. Rep. **363**, 223 (2002).

[16] Birse, M.C., B. Krippa, J.A. McGovern and N.R. Walet, *Pairing in many-fermion systems: an exact renormalization group treatment*, Phys. Lett. B **605**, 287 (2005).

[17] Bloch, I., J. Dalibard and W. Zwerger, *Many-body physics with ultra-cold gases*, Rev. Mod. Phys. **80**, 885 (2008).

[18] Cardy, J., *Scaling and Renormalization in Statistical Physics*, (Cambridge Lecture Notes in Physics **5**, University Cambridge Press UK, 1996).

[19] Castellani, C., C. Di Castro, F. Pistolsi and G.C. Strinati, *Infrared behavior of interacting bosons at zero temperature*, Phys. Rev. Lett. **78**, 1612 (1997).

[20] Chin, J. K., D. E. Miller, Y. Liu, C. Stan, W. Setiawan, C. Sanner, K. Xu and W. Ketterle, *Evidence for superfluidity of ultra-cold fermions in an optical lattice*, Nature **443**, 961 (2006).

[21] Dell'Anna, L. and W. Metzner, *Fermi surface fluctuations and single electron excitations near Pomeranchuk instability in two dimensions*, Phys. Rev. B **73**, 045127 (2006).

[22] Diehl, S., S. Flörchinger, H. Gies, J.M. Pawlowkski and C. Wetterich, *Functional renormalization group approach to the BCS-BEC crossover*, Ann. d. Phys. Vol. **522**, Issue 9, 615 (2010).

[23] Diehl, S., H. Gies, J.M. Pawlowski and C. Wetterich, *Flow equations for the BCS-BEC crossover*, Phys. Rev. A **76**, 021602(R) (2007).

[24] Diehl, S., H.C. Krahl and M. Scherer, *Three-body scattering from non-perturbative flow equations*, Phys. Rev. C **78**, 034001 (2008).

[25] Diener, R.B., R. Sensarma and M. Randeria, *Quantum fluctuations in the superfluid state of the BCS-BEC crossover*, Phys. Rev. A **77**, 023626 (2008).

[26] Dupuis, N., *Unified picture of superfluidity: From Bogoliubov's approximations to Popov's hydrodynamics theory*, Phys. Rev. Lett. **102**, 190401 (2009).

[27] Eberlein, A., *Renormalization group analysis of fluctuations in fermionic superfluids*, PhD Thesis (2013), Universität of Stuttgart.

[28] Eberlein, A. and W. Metzner, *Effective interactions and fluctuation effects in spin-singlet superfluids*, Phys. Rev. B **87**, 174523 (2013).

[29] Englert, F. and R. Brout, *Broken symmetry and the mass of gauge vector mesons*, Phys. Rev. Lett. **13**, 321 (1964).

[30] Feldman, J., J. Magnen, V. Rivasseau and E. Trubowitz, *Ward identities and a perturbative analysis of a U(1) Goldstone boson in a many fermion system*, Helv. Phys. Acta **66**, 498 (1993).

[31] Flörchinger, S., M. Scherer, S. Diehl and C. Wetterich, *Particle-hole fluctuations in BCS-BEC crossover*, Phys. Rev. B **78**, 174528 (2008).

[32] Flörchinger, S., M. M. Scherer and C. Wetterich, *Modified Fermi sphere, pairing gap, and critical temperature for the BCS-BEC crossover*, Phys. Rev. A **81**, 063619 (2010).

[33] Flörchinger, S. and C. Wetterich, *Functional renormalization for Bose-Einstein condensation*, Phys. Rev. A **77**, 053603 (2008).

[34] Flörchinger, S. and C. Wetterich, *Exact flow equation for composite operators*, Phys. Lett. B **680** 371 (2009).

[35] Flörchinger, S. and C. Wetterich, *Superfluid Bose gas in two dimensions*, Phys. Rev A **79**, 013601 (2009).

[36] Friederich, S., H. C. Krahl, C. Wetterich, *Functional renormalization for spontaneous symmetry breaking in the Hubbard model*, Phys. Rev. B **83**, 155125 (2011).

[37] Fritz, L., J. Schmalian, M. Müller and S. Sachdev, *Quantum critical transport in clean graphene*, Phys. Rev. B **78**, 085416 (2008).

[38] Gersch, R., C. Honerkamp, D. Rohe and W. Metzner, *Fermionic renormalization group flow into phases with broken discrete symmetry: charge-density wave mean-field model*, Eur Phys. J. B. **48**, 349 (2005).

[39] Gersch, R., C. Honerkamp and W. Metzner, *Superconductivity in the attractive Hubbard model: functional renormalization group analysis*, New J. Phys. **10**, 045003 (2008).

[40] Gersch, R., J. Reiss and C. Honerkamp, *Fermionic functional renormalization-group for first-order phase transitions: a mean-field model*, New J. Phys. **8**, 320 (2006).

[41] Gies, H. and J. Jaeckel, *Renormalization flow of QED*, Phys. Rev. Lett. **93**, 110405 (2004).

[42] Gies, H., F. Synatschke, and A. Wipf, *Supersymmetry breaking as a quantum phase transition*, Phys. Rev. D **80**, 101701 (2009).

[43] Gies, H. and C. Wetterich, *Renormalization flow of bound states*, Phys. Rev. D **65**, 065001 (2002).

[44] Gies, H. and C. Wetterich, *Universality of spontaneous chiral symmetry breaking in gauge theories*, Phys. Rev. D **69**, 025001 (2004).

[45] Goldenfeld, N., *Lectures on Phase Transition and The Renormalization Group*, (Westview Press, Frontiers in Physics, Boulder 1992).

[46] Gorkov, L. P. and T. K. Melik-Barkhudarov, *Contribution to the theory of superfluidity in an imperfect Fermi gas*, Sov. Phys. JETP **13**, 1018 (1961).

[47] Gradshteyn, I.S., and I. M. Ryzhik, *Table of Integrals, Series and Products*, (Academic Press, Walthan 1965).

[48] Griffin, A., D. Snoke and S. Stringari, *Bose-Einstein Condensation*, (Cambridge University Press, Cambridge 1995).

[49] Halboth, C. J., and W. Metzner, *Renormalization-group analysis of the two-dimensional Hubbard model*, Phys. Rev. B **61**, 7364 (2000).

[50] Hertz, J. A., *Quantum critical phenomena*, Phys. Rev. B **14**, 1165 (1976).

[51] Higgs, P. W., *Broken symmetries and the masses of gauge bosons*, Phys. Rev. Lett. **13**, 508 (1964).

[52] Höfling, F., C. Nowak and C. Wetterich, *Phase transition and critical behavior of the $d = 3$ Gross-Neveu model*, Phys. Rev. B **66**, 205111 (2002).

[53] Hofstetter, W., J. I. Cirac, P. Zoller, E. Demler and M. D. Lukin, *High-temperature superfluidity of fermionic atoms in optical lattices*, Phys. Rev. Lett. **89**, 220407 (2002).

[54] Honerkamp, C., D. Rohe, S. Andergassen and T. Enss, *Interaction flow method for many-fermion systems*, Phys. Rev. B **70**, 235115 (2004).

[55] Honerkamp, C., M. Salmhofer, N. Furukawa, and T. M. Rice, *Breakdown of the Landau-liquid in two dimensions due to Umklapp scattering*, Phys. Rev. B **63**, 035109 (2001a).

[56] Honerkamp, C. and M. Salmhofer, *Temperature-flow renormalization group and the competition between superconductivity and ferromagnetism*, Phys. Rev. B **64**, 184516, (2001b).

[57] Huh, Y. and S. Sachdev, *Renormalization group theory of nematic ordering in d-wave superconductors*, Phys. Rev. B **78**, 064512 (2008).

[58] Husemann, C. and M. Salmhofer, *Efficient parametrization of the vertex function, omega-scheme, and the (t,t")-Hubbard model at Van Hove filling"*, Phys. Rev. B **79**, 195125 (2009).

[59] Jaksch, D. and P. Zoller, *The cold atom Hubbard toolbox*, Ann. Phys. **315**, 52 (2005).

[60] Jakubczyk, P., W. Metzner and H. Yamase, *Turning a first order quantum phase transition continuous by fluctuations: General flow equations and application to d-wave Pomeranchuk instability*, Phys. Rev. Lett. **103**, 220602 (2009).

[61] Katanin, A. A., *Fulfillment of Ward identities in the functional renormalization group*, Phys. Rev. B **70**, 115109 (2004).

[62] Kaul, R.K. and S. Sachdev, *Quantum criticality of U(1) gauge theories with fermionic and bosonic matter in two spatial dimensions*, Phys. Rev. B **77**, 155105 (2008).

[63] Keller, M., W. Metzner and U. Schoellwoeck, *Thermodynamics of a superconductor with strongly bound Cooper pairs*, Phys. Rev. B **60**, 3499 (1999).

[64] Keller, M., W. Metzner and U. Schoellwoeck, *Dynamical mean-field theory for pairing and spin gap in the attractive Hubbard model*, Phys. Rev. Lett **86**, 4612 (2001).

[65] Kopietz, P., L. Bartosch and F. Schütz, *Introduction to the Functional Renormalization Group*, (Lecture Notes in Physics (book 798), Springer Verlag Germany, (2010)).

[66] Kosterlitz, J. M., *The critical properties of the two-dimensional xy model*, J. Phys. C **7**, 1046 (1974).

[67] Kosterlitz, J. M. and D. J. Thouless, *Ordering, metastability and phase transitions in two-dimensional systems*, J. Phys. C **6**, 1181 (1973).

[68] Krahl, H.C. and C. Wetterich, *Functional renormalization group for d-wave superconductivity*, Phys. Lett. A **367**, 263 (2007).

[69] Krippa, B., *Superfluidity in many fermion systems: Exact renormalization group treatment*, Eur. Phys. J. A **31**, 734 (2007).

[70] Litim, D. F., *Optimized renormalization group flows*, Phys. Rev. D **64**, 105007 (2001).

[71] Löhneysen, H. v., A. Rosch, M. Vojta and P. Wölfle, *Fermi-liquid instabilities at magnetic quantum phase transitions*, Rev. Mod. Phys. **79**, 1015 (2007).

[72] Martín-Rodero, A. and F. Flores, *Solution for the U-negative Hubbard superconductor including second-order correlation effects*, Phys. Rev. B **45** 13008 (1992).

[73] Meng, Z. Y., T. C. Lang, S. Wessel, F. F. Assaad, A. Muramatsu, *Quantum spin liquid emerging in two-dimensional correlated Dirac fermions*, Nature **464**, 847 (2010).

[74] Metzner W., *Functional renormalization group approach to correlated electron systems*, AIP Conference Proceedings **846**, 130 (2006).

[75] Metzner, W., D. Rohe and S. Andergassen, *Soft Fermi Surfaces and Breakdown of Fermi-Liquid Behavior*, Phys. Rev. Lett. **91**, 066402 (2003).

[76] Metzner, W., M. Salmhofer, C. Honerkamp, V. Meden and K. Schönhammer, *Functional renormalization group approach to correlated fermion systems*, Rev. Mod. Phys. **84**, (2012).

[77] Micnas, R., J. Ranninger and S. Robaszkiewicz, *Superconductivity in narrow-band systems with local non-retarded attractive interactions*, Rev. Mod. Phys. **62**, 113 (1990).

[78] Millis, A.J., *Effect of a nonzero temperature on quantum critical points in itinerant fermion systems*, Phys. Rev. B **48**, 7183 (1993).

[79] Montorsi A., *The Hubbard Model*, (World Scientific, Singapore, 1992).

[80] Moon, E. G. and S. Sachdev, *Quantum critical point shifts under superconductivity: the pnictides and the cuprates*, Phys. Rev. B **82**, 104516 (2010).

[81] Negele, J. W. and H. Orland, *Quantum Many Particle Systems*, (Advanced Book Classics, Perseus 1998).

[82] Nepomnyashchy, Y. A., *Nature of excitations in liquid He-4*, Phys. Rev. B **46**, 6611 (1992).

[83] Obert, B., C. Husemann and W. Metzner, *Low energy singularities in the ground state of fermionic superfluids*, Phys. Rev. B **88**, 144508 (2013).

[84] Obert, B., S. Takei and W. Metzner, *Anomalous criticality near semimetal-to-superfluid quantum phase transition in a two-dimensional Dirac cone model*, Ann. Phys. (Berlin) **523**, No. 8-9, 621 (2011).

[85] Pawlowski, J. M., D. F. Litim, S. Nedelko and L. v. Smekal, *Infrared behavior and fixed points in Landau-gauge QCD*, Phys. Rev. Lett. **93**, 152002 (2004).

[86] Peskin, M. E. and D. V. Schroeder, *An Introduction to Quantum Field Theory*, (Addison-Wesley, New York 1984).

[87] Pesz, K. and R. W. Munn, *Densities of states and anisotropy in tight-binding models*, J. Phys. C: Solid State Phys. **19**, 2499 (1986).

[88] Phan, V.-N., K. W. Becker and H. Fehske, *Spectral signatures of the BCS-BEC crossover in the excitonic insulator phase of the extended Falicov-Kimball mode*, Phys. Rev. B **81**, 205117 (2010).

[89] Pistolesi, F., C. Castellani, C. D. Castro and G. C. Strinati, *Renormalization-group approach to the infrared behavior of a zero-temperature Bose system*, Phys. Rev. B **69**, 024513 (2004).

[90] Polchinski, J., *Renormalization and effective lagrangians*, Nuclear Physics B **231**, 269 (1984).

[91] Polchinski, J., *Proceedings of 1993 Theoretical Advanced Studies Institute in Elementary Particle Physics* (edited by J. Harvey and J. Polchinski, World Scientific, Singapore, 1993).

[92] Popov, V. N., *Functional Integrals and Collective Excitations*, (Cambridge Monographs on Mathematical Physics, Cambridge University Press (1987)).

[93] Rech, J., C. Pepin and A.V. Chubukov, *Quantum critical behavior in itinerant electron systems: Eliashberg theory and instability of a ferromagnetic quantum critical point*, Phys. Rev. B **74**, 195126 (2006).

[94] Reiss, J., D. Rohe and W. Metzner, *Renormalized mean-field analysis of antiferromagnetism and d-wave superconductivity in the two-dimensional Hubbard model*, Phys. Rev. B **75**, 075110 (2007).

[95] Rosa, L., P. Vitale and C. Wetterich, *Critical exponents of the Gross-Neveu model from the effective average action*, Phys. Rev. Lett. **86**, 958 (2001).

[96] Ryckayzen, G., *Green's Functions and Condensed Matter*, (Techniques of Physics 5, Academic Press Limited, UK, 1980).

[97] Sachdev, S., *Quantum Phase Transitions*, (Cambridge University Press, UK 2011).

[98] Salmhofer, M., C. Honerkamp, W. Metzner and O. Lauscher, *Renormalization group flows into phases with broken symmetry*, Prog. Theor Phys. **112**, No. 6 943 (2004).

[99] Scherer, D. D., J. Braun and H. Gies, *Many-flavor phase diagram of the* $(2+1)d$ *Gross-Neveu model at finite temperature*, J. Phys. A **46**, 285002 (2013).

[100] Scherer M. M., S. Flörchinger and H. Gies, *Functional renormalization for the Bardeen-Cooper-Schrieffer to Bose-Einstein condensation crossover*, Phil. Trans. R Soc. A **369**, 2779 (2011).

[101] Scherer, M. M., S. Flörchinger and C. Wetterich, *Functional renormalization for the BCS-BEC crossover* , arXiv:1010.2890 [cond-mat.quant-gas] (2010).

[102] Schmidt, R., *From few- to many-body physics with ultra-cold gases*, PhD Thesis (2013), Technische Universität München.

[103] Schütz, F., L., Bartosch and P. Kopietz, *Collective fields in the functional renormalization group for fermions, Ward identities, and the exact solution of the Tomonaga-Luttinger model*, Phys. Rev. B **72**, 035107 (2005).

[104] Schütz, F. and P. Kopietz, *Functional renormalization group with vacuum expectation values and spontaneous symmetry breaking*, J. Phys. A **39**, 8205 (2006).

[105] Shankar, R., *Renormalization group for interacting fermions in $d > 1$*, Physica A **177**, 530 (1991).

[106] Shankar, R., *Renormalization-group approach to interacting fermions*, Rev. Mod. Phys. **66**, 129 (1994).

[107] Sheehy, D.E. and J. Schmalian, *Quantum critical scaling in graphene*, Phys. Rev. Lett. **99**, 226803 (2007).

[108] Si, Q. and F. Steglich, *Heavy Fermions and Quantum Phase Transitions*, Science **329** (5996), 1161 (2010).

[109] Sinner, A., N. Hasselmann and P. Kopietz, *Spectral function and quasiparticle damping of interacting bosons in two dimensions*, Phys. Rev. Lett. **102**, 120601 (2009).

[110] Sinner, A., N. Hasselmann and P. Kopietz, *Functional renormalization-group approach to interacting bosons at zero temperature*, Phys. Rev. A **82**, 063632 (2010).

[111] Strack, P., *Renormalization group theory for fermions and order parameter fluctuations in interacting Fermi systems* PhD thesis, Universität Stuttgart (2009).

[112] Strack, P., R. Gersch and W. Metzner, *Renormalization group flow for fermionic superfluids at zero temperature*, Phys. Rev. B **78**, 014522 (2008).

[113] Strack, P., S. Takei and W. Metzner, *Anomalous scaling of fermions and order parameter fluctuations at quantum criticality*, Phys. Rev. B **81**, 125103 (2010).

[114] Tetradis, N. and C. Wetterich, *Critical exponents from the effective average action*, Nucl. Phys. B **422**, 541 (1994).

[115] Vojta, M., Y. Zhang and S. Sachdev, *Quantum phase transition in d-wave superconductors*, Phys. Rev. Lett. **85**, 4940 (2000a).

[116] Vojta, M., Y. Zhang and S. Sachdev, *Renormalization group analysis of quantum critical points in d-wave superconductors*, Int. J. Mod. Phys. B **14**, 3719 (2000b).

[117] Vollhardt, D. and P. Wölfle, *The Superfluid Phases of Helium 3*, (Taylor and Francis Ltd, 1990).

[118] Wegner, F. J. and A. Houghton, *Renormalization group equation for critical phenomena*, Phys. Rev. A **8**, 401 (1973).

[119] Weichman, P. B., *Crossover scaling in a dilute bose superfluid near zero temperature*, Phys. Rev. B **38**, 8739 (1988).

[120] Wetterich, C., *Exact evolution equation for the effective potential*, Phys. Lett. B **301**, 90 (1993).

[121] Wieczerkowski, C., *Symanzik's improved actions from the viewpoint of the renormalization group*, Comm. Math. Phys. **120**, 149 (1988).

[122] Zanchi, D. and H. J. Schulz, *Weakly correlated electrons on a square lattice: A renormalization group theory*, Europhys. Lett. **44**, 235 (1998).

[123] Zanchi, D. and H. J. Schulz, *Weakly correlated electrons on a square lattice: Renormalization-group theory*, Phys. Rev. B **61**, 13609 (2000).

[124] Zinn-Justin J., *Quantum Field Theory and Critical Phenomena*, (International Series of Monographs on Physics (book 113), Oxford University Press, UK 2002).

[125] Zwerger W., *Anomalous fluctuations in phases with a broken continuous symmetry*, Phys. Rev. Lett. **92**, 027203 (2004).